Soil Moisture Accounting in Distributed Hydrologic Modelling

by

Shari M. Carlaw

A thesis
presented to the University of Waterloo
in fulfillment of the
thesis requirement for the degree of
Master of Applied Science
in
Civil Engineering

Waterloo, Ontario, Canada 2000

I hereby declare that I am the sole author of this thesis.

I authorize the University of Waterloo to lend this thesis to other institutions or individuals for the purpose of scholarly research.

I further authorize the University of Waterloo to reproduce this thesis by photocopying or by other means, in total or in part, at the request of other institutions or individuals for the purpose of scholarly research.

SUMMARY

This thesis evaluates the ability of the WATFLOOD distributed hydrologic model to accurately estimate the soil moisture in the active upper zone in three different study regions during both short term (3 month) and long term (3 year) simulations. This evaluation is made by comparing the upper zone storage (UZS) calculated by WATFLOOD with the water contents measured at various monitoring sites within the study regions. Evaluation of internal components is crucial in testing distributed hydrologic models as different process descriptions often lead to very similar outflow hydrographs, without identifying specific problem sources in the simulations (Western et al. 1999).

The standard method for measuring soil moisture is the Gravimetric method. Time Domain Reflectometers (TDRs) and Neutron Probes are popular field measurement devices, but only offer measurements at a point. Remote sensing techniques such as high-resolution radar systems and microwave radiometers allow for a wide range of spatial and temporal coverage even in remote regions, however, the processing required to obtain meaningful soil moisture measurements from raw images is still in the research stage.

WATFLOOD is a physically based, fully distributed model of the hydrologic budget of a watershed. It incorporates only those physical processes that have a prominent effect on runoff and resulting streamflows. WATFLOOD is unique in that the user can specify up to 16 different land classes (called Grouped Response Units, or GRUs), each having its own set of user-defined parameter values. The advantage of GRUs is that there is no need for a given model grid square to be homogeneous, and the pixels of each GRU need not be contiguous as the routing of runoff is not significantly affected by their position in any given grid square (Kouwen et al. 1993).

Hydrologic simulations were run using WATFLOOD and soil moisture data from 3 major scientific projects: MAP, BOREAS, and FIFE. Although the three projects had different objectives, each had a significant hydrological component that involved streamflow modelling and soil moisture data collection.

Comparison results between measured and modelled water contents for MAP and BOREAS were excellent. The modelled plots matched the measured traces with only minor discrepancies in the saturated Old Black Spruce site in the South Study Area of BOREAS. The active upper zone was typically between 200 mm and 300 mm for BOREAS, and slightly shallower (150 mm) for MAP, as indicated by both the measured and modelled water contents. Hydrograph results were acceptable, however, improvements could possibly be made by further calibrating model parameters not related to the upper zone storage. Results for FIFE were inconclusive as preliminary plots revealed fundamental problems with the data set, so further modelling was not performed.

It is recommended that a wetland routing utility be integrated into WATFLOOD to allow for correct modelling in saturated areas. As well, the use of remotely sensed soil moisture data for model calibration should be investigated as research in that area advances.

ACKNOWLEDGEMENTS

I would like to gratefully acknowledge the unwavering support of my supervisors, Dr. Nick Kouwen and Dr. Ric Soulis, who helped me through courses and thesis work, and were there to lend a helping hand on a moment's notice. Your patience and understanding were very much appreciated. Extra special thanks goes to Nick for all the modelling assistance, inspirational talks, and for understanding my 'grad student' habits…it's been 2 great years!

Many thanks and lots of love goes out to my parents, Donna Carlaw and Dainis Baltkalns, for everything they have done and continue to do for me. You are always there, always solid, and always the same, and it is that consistency that has helped me more than you know. Big hugs and love also to my brother John and my doggies – Cassie and Sam – who tolerated me during all the good, bad, and financially-busted times.

A thesis can't be completed without the help of friends, especially fellow grad students and classmates! Thanks to Sharla and Jennifer (you go girls!), and a huge thanks goes to Patrick and Clint for all the fun and encouragement during the wee hours of many assignments, and for being the great food connoisseurs that you are. Long live Grand China! ☺

A very special thank-you goes to Erika Klyszejko for her invaluable assistance with the final formatting and graphing. Best of luck with both your engineering and horse careers…I look forward to keeping in touch with you and seeing a wonderful 'Amber' baby!

Thanks also goes to my best friend Sherry, my roomie Tricia, my wonderful riding coach Alex, and my 'barn buddies': Don & Fancee, Jan & Billy, and Charlotte & Salem. You guys have always been there when I needed to 'get away' from it all, and know that I'll always be there for you if you need an escape!

And lastly, to my past equine companions, Cisco and Maj, and my current companion and best friend Willow – who, unbeknownst to them, are the reasons for my pursuit of a graduate degree. Their gentleness, strength, kindness, and unconditional love are foundations in my life. "There is nothing so strong as gentleness; there is nothing so gentle as real strength."

Funding for this research was generously provided through an NSERC PGS-A Scholarship.

TABLE OF CONTENTS

LIST OF FIGURES

LIST OF TABLES

1.0 INTRODUCTION

Floods have always been of great concern for civilizations and scientists and engineers are constantly searching for better methods to protect humans from their often-devastating effects. One such method is to use hydrological models designed to predict streamflows in a watershed given various types of meteorological and physiological inputs.

As technology improves, scientists and engineers have been able to build more sophisticated models that are capable of forecasting over larger areas and longer durations with greater success. As these models expand and improve, the notion of having real-time flood forecasts available over widespread areas in Canada and throughout the world becomes more realistic.

The major problem in hydrological modelling is that it is impossible to measure and simulate every single interaction between air, water, and land, whether by limitations in science or in finance. Thus, models become estimations of real world conditions based on information that is feasible to obtain. The models must be comprehensive enough to accurately represent real-life conditions, but they must also be simple enough to run within a suitable time frame on standard computing resources. It is this balance between accuracy and simplicity that modelers are constantly trying to maintain.

WATFLOOD is a physically based distributed hydrological model designed by Dr. Nicholas Kouwen of the University of Waterloo. First started in 1972, WATFLOOD has grown and expanded to become the leading hydrological model in Canada and the first to implement the Grouped Response Unit (GRU) technique for diversified land cover. The mandate used to design WATFLOOD is to develop a model that can accurately predict the physical facets of the hydrologic cycle but that is not so scientifically intense that it requires data or computing resources that are not available to the majority of the intended users.

1.1 Objectives

The objectives of this thesis are:

1. To evaluate WATFLOOD's ability to accurately estimate water content in the active upper zone of the soil profile while maintaining reasonable estimations of streamflow using both short-term (3 month) and long-term (3 year) simulations; and
2. To estimate the depth of the active upper zone in various watershed regions by examining both the measured and modelled water contents.

Three project data sets have been chosen for modelling. The first is from the Mesoscale Alpine Programme (MAP) in Europe; the second is from the Boreal Ecosystem-Atmosphere Study (BOREAS) in Manitoba and Saskatchewan; and the third is from the First ISLSCP (International Satellite Land Surface Climatology Project) Field Experiment in the Konza Prairie, Kansas. All three projects measured soil moisture values at numerous sites and have provided excellent comparison data to combine with the WATFLOOD output.

MAP is a multi-disciplinary project involving hydrologists and atmospheric scientists from Europe, Canada, and the USA. The project's overall aims are to further the basic understanding and forecasting capabilities of the physical and dynamical processes that govern precipitation over major complex topography, including hydrological aspects, and determine three-dimensional circulation patterns in the vicinity of large mountain ranges. Because flooding is a significant problem in the MAP alpine regions, one portion of MAP focussed on developing reliable real-time flood forecasts using hydrological models coupled with advanced mesoscale atmospheric prediction models.

The Boreal Ecosystem-Atmosphere Study (BOREAS) was initiated in 1990 to investigate the interactions between the boreal forest biome and the atmosphere. Surface, airborne, and satellite-based observations were collected and used for developing techniques to measure biological and physical processes and conditions that govern the exchanges of energy, water, heat, carbon, and trace gases between boreal forest ecosystems and the atmosphere, particularly those processes that may be sensitive to global change. Remote-sensing techniques, along with field measurements, were used for developing and testing models and algorithms to transfer the understanding of processes from the local scale to the regional scale (BOREAS 2000). Two different study areas were selected for data collection: the Northern Study Area (NSA) and the Southern Study Area (SSA). The NSA is an area of 8000 km^2, located between Thompson, Manitoba and Nelson House, Manitoba, and the SSA covers a total area of 11 170 km^2 over the area of Prince Albert National Park through to Candle Lake, Saskatchewan.

FIFE (First International Satellite Land Surface Climatology Project Field Experiment) was conducted in 1987 to 1989, with a "follow-on" campaign from 1989 to 1993. FIFE was designed to improve the understanding of the carbon and water cycles, coordinate data collection by satellites, aircraft, and ground measurements, and use satellite remote sensing systems to measure these cycles. It is an important part of NASA's plan to develop physically based approaches to using satellite remote sensing systems (FIFE 2000). FIFE was conducted on the Konza Prairie in central Kansas.

1.2 Scope

This thesis has five main sections: a comprehensive literature review, a discussion of the three study regions, a description of the model setup for each region, the results of the modelled and measured water content comparisons, and conclusions and recommendations. The literature review covers the basic equations and principles of soil moisture and its relationship to streamflow, soil moisture measurement techniques, current modeling methods for soil moisture, and an outline of WATFLOOD and model processes which involve soil moisture. The study regions section outlines the purpose of each project as well as location, soil moisture measurement instrumentation, and data collection periods. The modelling section will summarize the characteristics for each study area as applied in the WATFLOOD model, and outline land classifications, model grid sizes, and parameter values used for modelling. The results will summarize the findings of both the water content and upper zone storage comparisons, as well as measured and simulated streamflow comparisons for each of the three study regions. Initial values, timing, recession curves, and parameter optimization will be discussed. The final section will outline the conclusions made from the model runs, and make recommendations for the improvement of future modelling.

2.0 LITERATURE REVIEW

2.1 Soil Moisture and the Hydrologic Cycle

Soil moisture is defined simply as the amount of water in a unit volume of soil. As water can only exist in the void space of a soil sample, the measured soil moisture can theoretically range from a minimum value of 0 (dry soil) to a maximum value of the porosity (all void space filled with water) for the given soil sample. In actual field conditions, this range is less as soils do not often dry completely but can reach full saturation.

Soil moisture is commonly expressed as a volumetric water content (θ):

$$\theta = V_w / V_s$$

where V_w = volume of water and V_s = volume of soil (Dingman 1994). Another similar expression for soil moisture is degree of saturation (S) , which is the proportion of pore space that contains water:

$$S = V_w /(V_a + V_w) = \theta / \phi$$

where V_a = volume of air and ϕ = porosity (Dingman 1994). By knowing the porosity of the sample, conversions can easily be made between S and θ.

Soil moisture is a key variable in the hydrologic cycle as it is directly related to infiltration and evapotranspiration. Thus, both the amount and variation of soil moisture play important roles in the amount of runoff and evaporation during a precipitation event.

2.1.1 Soil Moisture and Infiltration

Soil moisture is directly related to hydraulic conductivity (K_h) and soil water pressure head (Ψ). As the moisture content increases, K_h increases non-linearly from 0 at low to moderate soil moistures up to the saturated hydraulic conductivity (K_{hsat}) at θ = saturation (Figure 2.1). Although Figure 2.1 shows a typical curve, values of K_h at different soil moistures can vary by several orders of magnitude depending on the soil type and texture, and for a given soil, can increase by several orders of magnitude over the range of S values (Figure 2.2) (Dingman 1994).

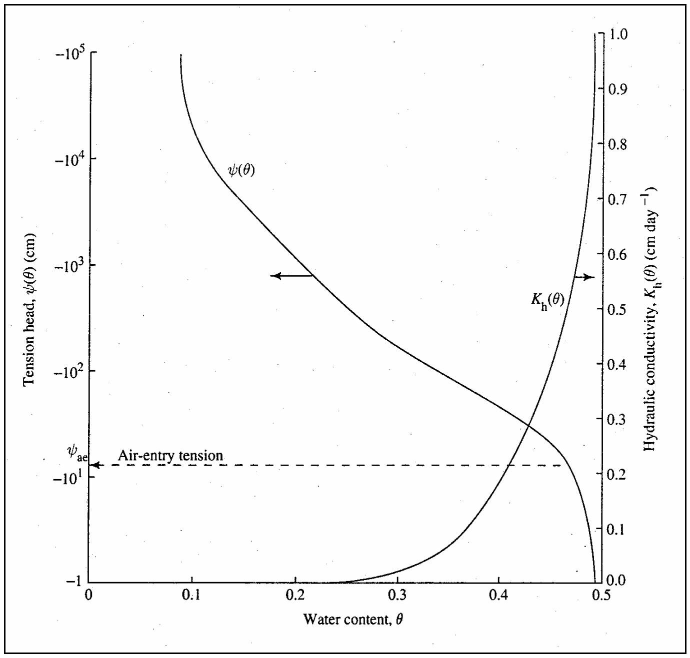

Figure 2.1: Typical forms of hydraulic relations $\Psi(\theta)$ - θ and $K_h(\theta)$ - θ for unsaturated soils (after Dingman 1994)

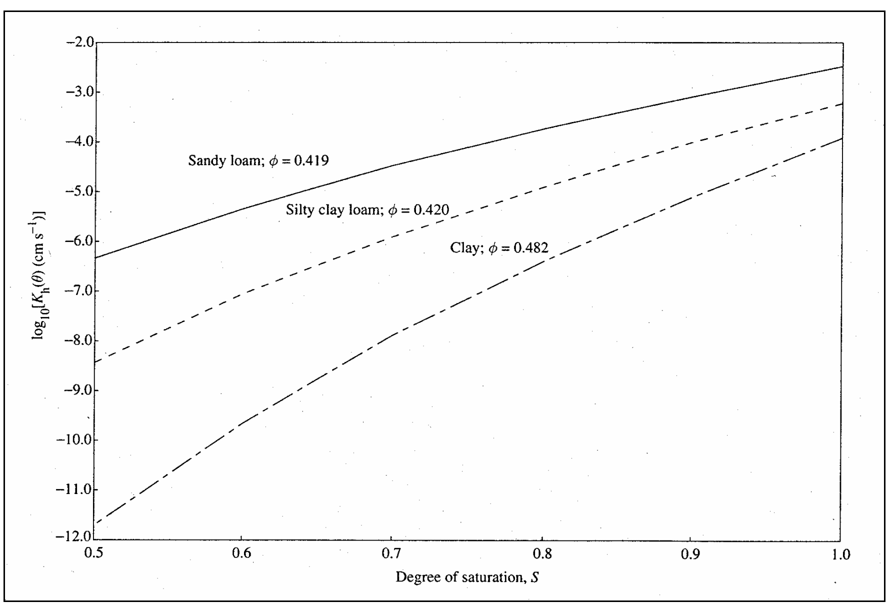

Figure 2.2: Hydraulic conductivity (K_h) vs. degree of saturation (S) for three different soil types (after Dingman 1994)

Similarly, Figure 2.1 shows that the soil water tension head (hence the negative values) at low to moderate moisture values is very high, and decreases non-linearly with increasing moisture contents. The dotted line represents the air-entry tension head (Ψ_{ae}), which is the soil moisture value at which significant amounts of air begin to fill the void space in the soil column. The absolute value of the air-entry tension head is also the height of the capillary fringe. Water is most tightly held at lower moisture contents and less so at values near saturation. Figure 2.3 shows the variation of Ψ with S for three different soil types, and similar to Figure 2.2, values of Ψ at different soil moistures can vary by several orders of magnitude depending on the soil type and texture, and for a given soil, can decrease by several orders of magnitude over the range of S values.

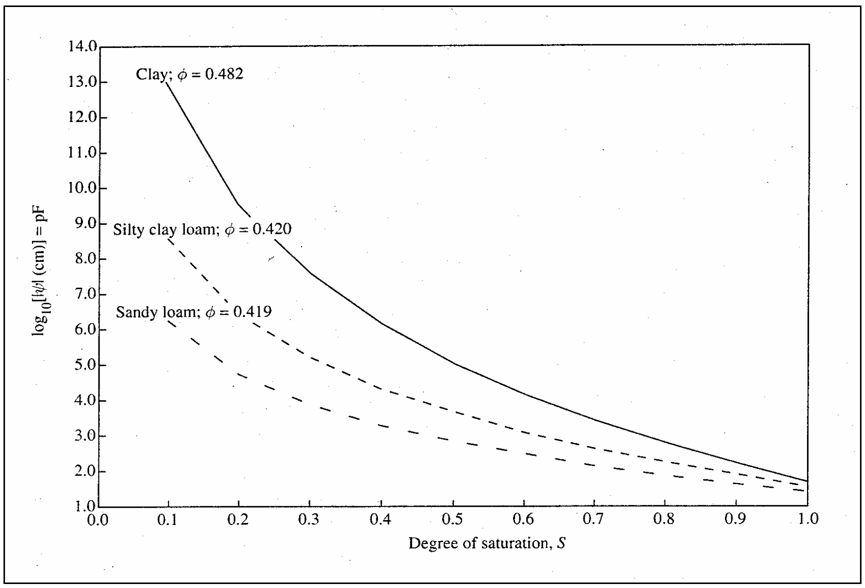

Figure 2.3: Soil water tension head (Ψ) vs. degree of saturation (S) for three different soil types (after Dingman 1994)

In real soils, the value of Ψ at a given value of θ is not unique, but depends on the soil's history of wetting and drying (Dingman 1994). (The same is true for the K_h-θ relationship, however the effect is much less pronounced and is usually neglected.) This hysteresis effect (Figure 2.4) is extremely difficult to model mathematically, so analytical approximations have been developed to allow the Ψ-θ and K_h-θ relationships to be incorporated into hydrologic models.

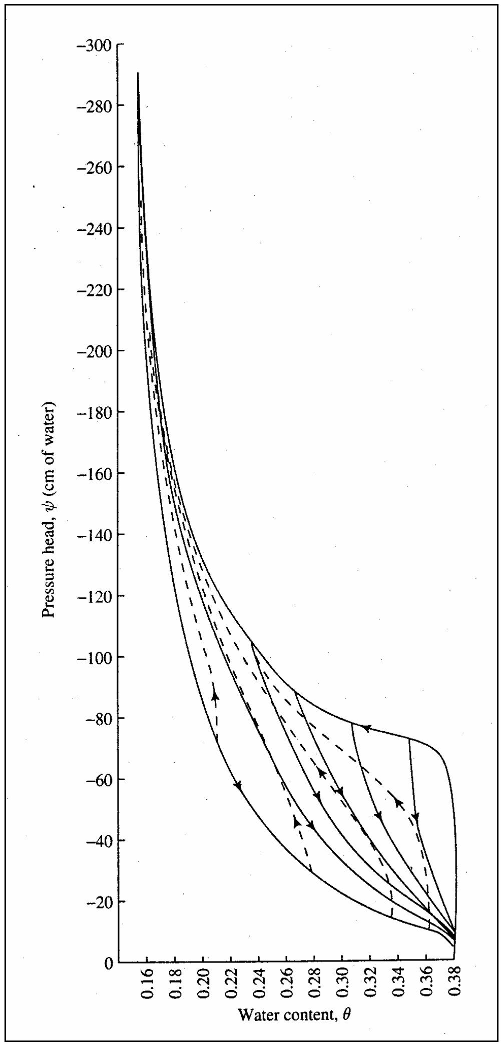

Figure 2.4: Hysteresis effect in a sandy loam (after Dingman 1994)

Clapp and Hornberger (1978) approximated these relations by power laws (Dingman 1994):

$$|\Psi(S)| = |\Psi_s|S^{-b}$$

and

$$K_h(S) = K_{hsat}S^c$$

Similarly, these expressions can be converted into terms of θ (Dingman 1994):

$$|\Psi(\theta)| = |\Psi_s|\phi^b\theta^{-b}$$

and

$$K_h(\theta) = K_{hsat}\phi^{-c}\theta^c$$

Clapp and Hornberger showed with the first equation that at saturation ($S = 1$), $\Psi = \Psi_s$, and Ψ_s is thus equivalent to the air-entry tension head (Ψ_{ae}). This implies that the curve of S vs. Ψ would be a vertical line from $|\Psi| = 0$ to $|\Psi| = |\Psi_s|$ (Dingman 1994), however, this is only an approximation of what happens in real soils.

The parameters b and c are empirical (where b is the pore-size distribution index and c is the pore-disconnectedness index), and Clapp and Hornberger showed that $c \cong 2b + 3$ (Dingman 1994). Values of b and c depend mainly on soil texture, and typical values for common types can be found in Dingman (1994) and other similar references.

Two key values of soil moisture exist in natural soils, and are useful when describing the conditions of the hydrologic soil profile. They are known as the field capacity (θ_{fc}) and the permanent wilting point (θ_{pwp}) and are shown on Figures 2.5 and 2.6.

Field capacity is the amount of water in a soil column that can be held against the force of gravity (Dingman 1994). Water can only be removed from a soil at field capacity through evapotranspiration; that is, by direct evaporation or by plant uptake as part of transpiration. Although the value of θ_{fc} varies for different soil types (as low as 0.1 for sand and as high as 0.3 for clays), the soil pressure head at field capacity (Ψ_{fc}) is close to –340 cm for all soils (Dingman 1994). Figure 2.5 shows the field capacity pressure head and its relation to saturation, soil water which can be drained by gravity, and that available only to plants (and direct evaporation).

Permanent wilting point corresponds to the soil moisture value at which transpiration ceases and plants wilt. Similar to field capacity, θ_{pwp} ranges from 0.05 for sands up to 0.25 for clays, but Ψ_{pwp} is approximately –15 000 cm for all soils, as plants cannot generate suctions greater than this value (Dingman 1994). Figure 2.5 shows the permanent wilting point, and the amount of soil moisture between this value and field capacity is called the available water content (θ_a):

$$\theta_a = \theta_{fc} - \theta_{pwp}$$

where θ_{fc} is the soil moisture at field capacity and θ_{pwp} is the soil moisture at permanent wilting point. Because these values depend on soil type, θ_a will be different for various soils.

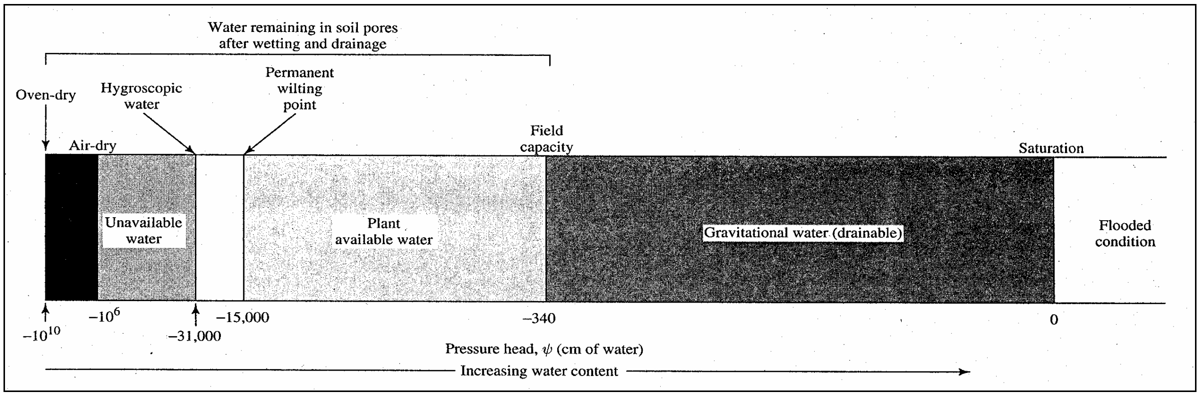

Figure 2.5: Hydrologic soil-profile horizons (after Dingman 1994)

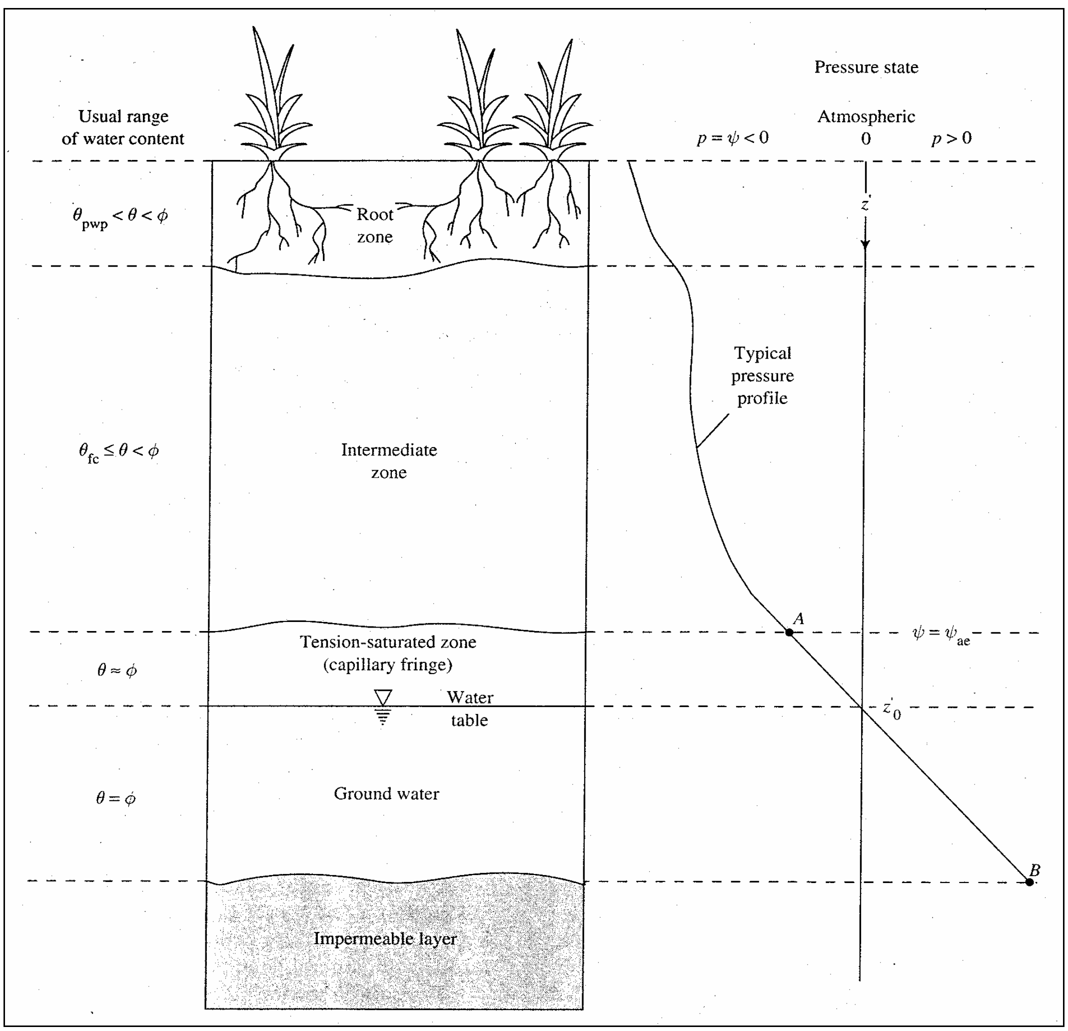

Figure 2.6: Soil water status as a function of pressure head (tension) (after Dingman 1994)

Figure 2.6 summarizes the soil moisture values in the different hydrologic soil horizons. The root zone ranges from permanent wilting point in dry seasons to saturation during heavy or prolonged rain events. The intermediate zone, which lies between the root zone and the saturated zone, ranges from field capacity to saturation. The value does not decrease below field capacity as plant roots do not extend into this area and it is also not subject to direct evaporation, thus the soil moisture will not decrease below that which can be drained by gravity. There is a tension-saturated zone, also called the capillary fringe, above the saturated (or groundwater) zone where the soil moisture values are approximately at saturation as a result of capillary rise. The pressure at the top of this zone is the air-entry tension (see also Figure 2.1), and the height of this zone can range from almost 0 in coarse sands up to several meters in clays (Dingman 1994). The top of the saturated zone represents the water table, and also the point at which pressures shift from negative to positive. The pressure at the top of the saturated zone is 0 (or atmospheric) and increases with increasing depth downward.

Infiltration rates vary with time for any precipitation event, and depend on a number of factors including precipitation rate, saturated hydraulic conductivity of the soil, initial soil moisture, surface roughness, and physical and chemical properties of the soil and the water (Dingman 1994). In general, rates are highest at the beginning of a precipitation event and decrease exponentially once surface ponding has begun, due to the steadily decreasing capillary gradient as the wetting front descends through the soil column (Dingman 1994).

Various models have been developed to approximate infiltration over time, including the Richards Equation, the Phillip Formula, the Horton Model, and the Green-Ampt Model. These can be incorporated into larger-scale hydrologic models, however, the choice of infiltration model depends largely on the purpose and objectives of the hydrologic model.

For physically-based hydrologic models such as WATFLOOD (see Section 2.4), the Richards Equation is unsuitable. It requires detailed soil data that are not readily available, and its numerical solution is complex and computationally laborious (Dingman 1994). The Green-Ampt Model or the Phillip Formula are better choices as they still use Darcy's Law and the conservation of mass principles, but use finite difference formulas that make them more computationally efficient. The only difference between the Phillip Formula and the

Green-Ampt Model is that the Phillip Formula includes the head due to surface ponding, whereas the Green-Ampt Model neglects it. Both capture the essential aspects of infiltration, including complete infiltration of precipitation until time of ponding and exponential decline of the infiltration rate afterward. The results obtained using these methods compare very well to those obtained with the Richards Equation.

2.1.2 Soil Moisture and Evapotranspiration

Evapotranspiration encompasses all processes by which liquid or solid water becomes atmospheric water vapour. These processes include direct evaporation from lakes, rivers, streams, oceans, bare soils, and vegetation, transpiration of plant water through their leaves, and sublimation from ice and snow covers (Dingman 1994). For a comprehensive review of the physics of evapotranspiration, see Dingman (1994), Viessman and Lewis (1996), or other similar hydrology textbooks.

For hydrologic modeling, it is important to be able to accurately estimate evapotranspiration so that simulated streamflows will also be accurate. Various methods exist, two of which involve soil moisture measurements.

The Soil-Moisture Balance method estimates the total actual evapotranspiration (ET) in a time period by monitoring rainfall and soil-water content throughout the root zone (Figure 2.6) and solving the water balance equation in the form

$$ET = W - Q_d + \int_0^{z_{rz}} \theta_1(z)dz - \int_0^{z_{rz}} \theta_2(z)dz$$

where W is total water input, Q_d is downward drainage, z is depth, z_{rz} is depth of the root zone, and $\theta_1(z)$ and $\theta_2(z)$ are the water content profiles at the beginning and the end of the time period (Dingman 1994). This equation assumes that all water input infiltrates and that there is no lateral inflow or outflow. Darcy's Law can be used to estimate Q_d if the relationship between K_h and θ is known (see previous section). This method has proven to be especially useful in forests, however it does have areal problems. Because of the spatial and temporal variation in θ(z), representative values are not easily obtained. As well, the equation will not give good results if any of the assumptions are violated, if Q_d is large, if the water table is near the surface, or if soil properties are highly variable (Dingman 1994).

The Soil Moisture Functions method is a widely-used approach that relates potential evapotranspiration (PET) to actual evapotranspiration (ET). PET is estimated using various relationships that involve temperature and radiation data (see Dingman 1994), and then related to ET by:

$$ET = f(\theta)\, PET$$

where θ is the water content of the root zone soil and $f(\theta)$ is based on the relative water content (Dingman 1994). Relative water content (θ_{rel}) is defined as:

$$(\theta_{rel}) = (\theta - \theta_{pwp}) / (\theta_{fc} - \theta_{pwp})$$

Figure 2.7 shows a typical relationship between $f(\theta)$ and θ_{rel}. The area to the left of the vertical dashed line is the zone where ET is less than PET, and the plants are considered under water stress (Dingman 1994).

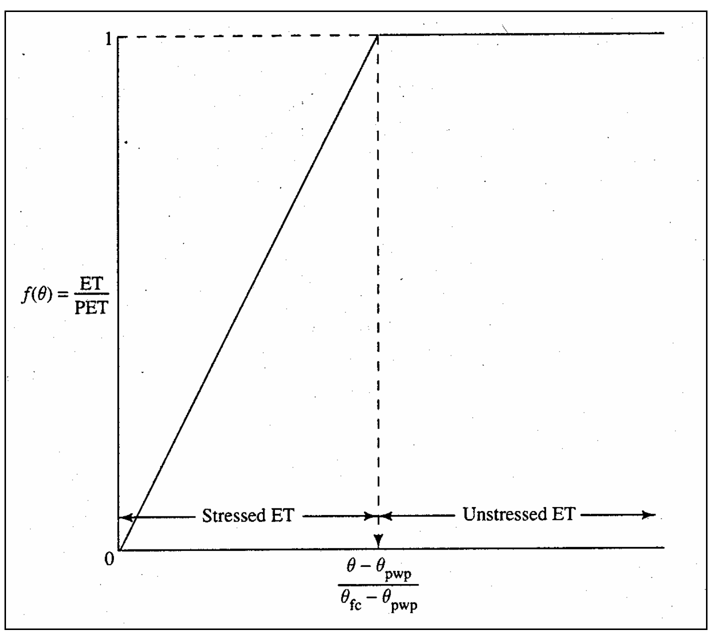

Figure 2.7: Relationship between $f(\theta)$ and soil water content θ (after Dingman 1994)

2.2 Soil Moisture Measurement Techniques

2.2.1 Gravimetric (Lab) Method

The Gravimetric Method is the standard method for calculating soil moisture to which all other methods are compared (Maidment 1993). Samples of 100 g to 200 g of soil are taken from the field and placed in a container of a known weight. The samples and containers are weighed, placed in a drying oven, and dried at 105 ºC to 110 ºC until all water has evaporated. A drying period of 24 h is normally adequate for most soils (Craig 1992). After drying, the samples are weighed again and the moisture content (θ) is determined by:

$$\theta = (M_{swet} - M_{sdry}) / \rho_w V_s$$

where M_{swet} and M_{sdry} are the weights before and after drying, ρ_w is the density of water, and V_s is the volume of the soil. Note that the denominator $\rho_w V_s$ is equivalent to M_{sdry} (Maidment 1993, Craig 1992).

The Gravimetric Method uses simple equipment and is indispensable for calibration of instruments (Roth et al. 1990). However, it is a time-consuming and destructive procedure, and not suitable for monitoring field conditions (Maidment 1993, Dingman 1994).

2.2.2 Time Domain Reflectometry

The Time Domain Reflectometry (TDR) technique estimates volumetric soil moisture (θ) by measuring the velocity of an electromagnetic wave pulse transmitted through two or three parallel probes ("waveguides") embedded in the soil. The velocity of the pulse (V) is related to the dielectric constant (ε_r) of the material surrounding the waveguides by

$$V = C_0 / (\varepsilon_r * \mu_r)^{1/2}$$

where C_0 is the speed of light in a vacuum ($3*10^8$ m/s) and μ_r is the magnetic permeability, which is equal to 1 in non-magnetic materials (DMP Ltd. 1999). Because C_0 and μ_r are constant for soil applications, V is inversely dependent only on ε_r; thus, the higher the dielectric constant of the soil, the slower the velocity of the pulse.

The length of the waveguides (L) is known and constant, so V can also be expressed as a distance travelled over the time required to propagate the pulse through the waveguides and back to the transmitter (t):

$$V = 2*L / t$$

By rearranging the previous two equations, it can be shown that

$$\varepsilon_r = (C_0*t / 2*L)^2$$

Soil is composed of air, water, and mineral particles, each of which has a different dielectric constant. The accepted values measured at 1 GHz and 20°C are 1 for air, 80.36 for water, and 3 to 5 for major soil minerals (Roth et al. 1990). Because of the large difference between the value for water and those for soil and air, the velocity of the pulse in a soil sample is largely dependent on its water content.

Topp et al. (1980) determined an empirical relation between θ and the apparent dielectric constant K_a by fitting a third order polynomial equation to data collected for 4 different inorganic soil types for the range of θ from 0 to approximately 0.55 and frequencies between 1 MHz and 1 GHz:

$$K_a = 3.03 + 9.3\theta + 146.0\theta^2 – 76.7\theta^3$$

In practice, K_a is measured and θ is calculated, so the previous equation can be rearranged for θ (Topp et al. 1980):

$$\theta = -5.3*10^{-2} + 2.92*10^{-2}K_a – 5.5*10^{-4}K_a^2 + 4.3*10^{-6}K_a^3$$

K_a is an approximation of the complex dielectric constant (K*), which consists of both a real (K') and an imaginary (K'') part and represents the electrical properties of a soil. The imaginary part encompasses the effects of electrical losses and frequency dependence in the soil, which although measurable, were determined to be insignificant (Topp et al. 1980). Thus, the measured dielectric constant was termed the apparent dielectric constant K_a, and is effectively equivalent to ε_r as defined previously.

Roth et al. (1990) developed a calibration curve for the TDR method that is not restricted to specific soil types, and that is valid over a large range of porosity and soil moisture values. The curve is based on the dielectric mixing model by Dobson et al. (1985):

$$\varepsilon_c = (\theta^*\varepsilon_w^{\alpha} + (1\text{-}\eta)\varepsilon_s^{\alpha} + (\eta\text{-}\theta)\varepsilon_a^{\alpha})^{1/\alpha}$$

where η is the soil porosity, $1\text{-}\eta$, θ, and $\eta\text{-}\theta$ are volume fractions, ε_c is the composite dielectric number, and ε_s, ε_w, and ε_a are the dielectric numbers of the solid, aqueous, and gaseous phase respectively. The parameter α summarizes the geometry of the medium (including soil stratification) with relation to the applied electric field with limiting values of +1 and –1 (Roth et al. 1990). It is important to note that ε_r, K_a, and ε_c all refer to the same measured soil property and thus are equivalent to one another.

Each of the dielectric numbers was normalized to relate them to pure water at 20°C rather than to vacuum conditions. Thus, the previous equation becomes

$$\zeta_c = (\theta\zeta_w^{\alpha} + (1\text{-}\eta)\zeta_s^{\alpha} + (\eta\text{-}\theta)\zeta_a^{\alpha})^{1/\alpha}$$

where $\zeta_c = \varepsilon_c/\varepsilon_w(20°C)$, $\zeta_w = \varepsilon_w/\varepsilon_w(20°C)$, $\zeta_s = \varepsilon_s/\varepsilon_w(20°C)$, and $\zeta_a = \varepsilon_a/\varepsilon_w(20°C)$. Values of the dielectric numbers were taken as 80.36 for water, 3.9 for mineral soils, 5.0 for organic soils, and 1.0 for air (Roth et al. 1990). The normalized ratios were calculated using these values, and resulted in $\zeta_w = 1.0$, $\zeta_a = 0.0012$, $\zeta_s = 0.048$ for mineral soils, and $\zeta_s = 0.060$ for organic soils.

Roth et al. included temperature dependence of ε_w through the following equation (Handbook of Physics and Chemistry 1986):

$$\varepsilon_w(T) = 78.54[1 - 4.579*10^{-3}(T - 25) + 1.19*10^{-5}(T - 25)^2 - 2.8*10^{-8}(T - 25)^3]$$

and also the relationship between η and θ by fitting a third-order polynomial to measured data:

$$\eta(\theta) = 0.710 - 1.868\theta + 3.954\theta^2 - 1.796\theta^3$$

Plots of ζ_c against θ showed a distinct non-linear trend. The equation of Topp et al. (1980) represented the measured data well up to $\theta = 0.55$, but showed considerable deviations above this value, suggesting the extrapolation of this function to higher water contents leads to results which are physically questionable (Roth et al. 1990). Curves for the mixing model were calculated using T = 15°C and a range of α values from –1 to +1, and the optimum value of $\alpha = 0.46$ was determined by a weighted nonlinear regression of the collected data.

Upon comparing measured to calculated θ using $\alpha = 0.46$, the data lie almost entirely along the 1:1 correlation line.

Roth et al. (1990) did find that the relationship between the dielectric number for soil and water content was stronger if temperature dependence of the liquid phase dielectric number was included, but that this influence decreases with lower water content. Topp et al. (1980) did not observe a temperature effect as their research was conducted at comparatively lower water contents.

To use the dielectric mixing model, T, η, and ε_s must be known. Temperature can be easily measured, however, measuring η and ε_s is time-consuming, expensive, and destructive. Roth et al. (1990) performed uncertainty studies for these parameters, and found that the uncertainty of the calculated water content due to the estimation of η and ε_s was of the same order as the uncertainty due to the TDR measurement equipment. Thus, estimation rather than measurement of η and ε_s is justifiable (Roth et al. 1990).

TDR is likely the most popular method for collecting soil moisture data, and can accurately measure θ_v to within +/- 2.5 % (Cuenca 1998). Countless research projects have successfully used TDR technology under a wide variety of field conditions (see Western et al. 1999, Mastrorilli et al. 1998, Cuenca et al. 1997, and Zappa et al. 2000). TDR techniques are now being used in less traditional applications such as solute concentration determination (Ferre et al. 2000), actual daily ET measurements (Mastrorilli et al. 1998), and in the development of methodology for determining sampling regimes that provide reliable estimates of areal mean soil moisture in complex terrain from a limited number of sample locations (Grayson and Western 1998, Western et al. 1998).

Advantages of TDR systems include their adaptability from point measurements with hand-installed waveguides to more permanent installations with buried probes at multiple levels connected to dataloggers and modems for data transfer. Unlike neutron probes (see Section 2.2.3), there is no radiation hazard with TDR systems. TDR technology is also suitably advanced to allow for accurate soil moisture measurement in a wide range of field conditions.

TDR systems do have disadvantages. They are expensive and the analysis to determine travel time in the waveguides is complex (Campbell and Anderson 1998). Furthermore, Rothe et al. (1997) found that TDR systems are highly sensitive to installation effects because the sampling volume is more heavily weighted close to the transmission line elements. Research into the methods of installation showed that merely pushing the waveguides into the ground could reduce the measured soil moisture by up to 0.10 cm^3/cm^3, but that using both smaller probes and a drill to create the holes for the probes mitigated installation effects (Rothe et al. 1997).

2.2.3 Neutron Probes

Neutron probes are another common method of measuring volumetric soil moisture. A probe containing a high-energy neutron source with a slow neutron detector is lowered into a 1.5 inch (3.8 cm) cased aluminum access hole. At depths selected by the operator, the probe emits "fast" neutrons into the surrounding soil which collide with similar-sized hydrogen atoms found in water molecules. The collisions result in "slow" neutrons being reflected, which are counted by the detector installed on the probe. The number counted by the detector is proportional to the number of water molecules present in the effective sphere of influence of the probe, approximately 7 to 15 cm in diameter (Maidment 1993). The detector count is converted to volumetric soil moisture by using a linear regression equation similar to the form:

$$\theta_v = A*(NMR/STD) + B$$

where θ_v is the volumetric soil moisture, NMR is the neutron detector count, STD is the standard neutron probe count (instrument-specific), and A and B are soil-specific coefficients (Cuenca 1998). Because all neutron probe instruments are manufactured differently, some probes allow for the user to input soil data and obtain θ_v directly on the instrument display.

Neutron probes are another very common method for measuring θ_v and have been widely used in field studies. They are advantageous as the equipment required is portable and relatively easy to use. Observation sites are permanent, so data is always taken from the same location and reliable time series can be developed. Similar to TDR, neutron probes are also nondestructive and measure θ_v to within +/- 2.5 % (Western et al. 1999).

Disadvantages of neutron probes include the inherent radiation hazard and the need for site-specific soil calibration (Topp et al. 1980, Roth el al. 1990). As well, the sampling volume of the neutron probe strongly depends on the water content itself (Roth et al. 1990). Unlike TDR systems, neutron probes are not adaptable to permanent-style installations that involve dataloggers and modem transmission lines.

2.2.4 Active Microwave Remote Sensing (Radar)

Remote sensing methods have a distinct advantage over traditional point measurement methods in that they allow for wide ranges of spatial and temporal coverage over even the most remote regions of the world. Soil moisture is inherently variable in space and time, so much research has been performed in anticipation that suitable systems can be developed for the remote sensing of soil moisture.

High-resolution radar systems are used for many environmental applications, including precipitation estimation and land cover depiction, however, they also show promise as being a useful tool for estimating soil moisture. Radar systems are termed active microwave remote sensing systems, meaning that they transmit a signal in the microwave frequency range which is reflected by the earth back to the antenna where variations in the signal's attributes are measured. These signal variations can be related to various characteristics of the earth, including vegetation, surface roughness, and soil moisture. Conversely, passive microwave systems (Section 2.2.5) do not transmit signals; they simply measure emitted thermal microwave radiation from the earth's surface.

The most common type of imaging radar used today is the synthetic aperture radar (SAR), which transmits electromagnetic pulses as the radar antenna flies across the image scene (Ulaby et al. 1996). The pulses are reflected ("backscattered") by the earth, and the quantity (amplitude) and polarization (phase, or direction of the electric field) of the reflected pulses depend on various features including surface roughness, vegetation, and the dielectric properties of the soil, which are directly related to water content (see Section 2.2.2). A set of backscatter coefficients (σ°) can be calculated for each pixel of the radar image by comparing the phase and amplitude of both the transmitted and reflected pulses (horizontal-vertical / vertical-horizontal, horizontal-horizontal, and vertical-vertical), and it is these coefficients that are used in determining soil water content.

Rather than taking only one image of a given area at a certain time, the SAR processor averages reflected pulses from a number of images and creates a composite "multi-look" image with a square pixel size in the range of 30 m x 30 m. This processor averaging helps reduce image noise ("speckle") and create a more meaningful image (Ulaby et al. 1996). Typically, "single-look" images are used only for special purposes such as system performance evaluation and calibration experiments (Ulaby et al. 1996).

Radar antennas can be airborne for specific project applications, or more commonly, spaceborn. The most prominent environmental radar systems are the European Remote Sensing (ERS) 1 and 2 satellites, which travel in a sun-synchronous orbit at a nominal altitude of 785 km above the earth's surface (Verhoest et al. 1998). ERS-1 was launched in 1991 and ERS-2 in 1995, and both operate at a fixed wavelength of 5.6 cm (C-band), a fixed mean incidence angle (23°), and VV (vertical transmit, vertical receive) polarization (Tansey et al. 1999). Another common system is the Shuttle Imaging Radar-C (SIR-C), which flew on the Space Shuttle in April and October 1994. The SIR-C is a joint US-European design consisting of two polarimetric SARs operating at L-band (23.5 cm wavelength) and C-band (5.8 cm wavelength), and a single polarization SAR operating at X-band (3.1 cm wavelength) (Ulaby et al. 1996). Various operational frequency bands and wavelengths exist for SAR systems (Table 2.1), however, research has shown the optimal specification of an SAR system for maximum soil moisture sensitivity is a C-band system operating at an incidence angle of 10° to 20° (Ulaby et al. 1996, Tansey et al. 1999).

Table 2.1: SAR frequency bands in the 0.2-15 GHz range (after Ulaby et al. 1996)

Letter designation	Frequency (GHz)	Wavelength (cm)	Space SARs
P-Band	0.44	68	
L-Band	1.28	23	SIR-A, SIR-B, SIR-C, ERS-1
S-Band	3.0	20	Almaz-1
C-Band	5.3	5.7	ERS-1, SIR-C, Radarsat
X-Band	9.6	3.1	SIR-C

The backscatter measured by a SAR system is a combination of surface scattering (caused by topography, vegetation, and surface roughness) and volume scattering (caused by variations in soil moisture). Western et al. (1999) and Rotunno Filho (1995) made pixel by pixel comparisons between TDR measurements and ERS-SAR images with very poor results, and concluded that the combined influences of terrain, surface roughness, and vegetation confounded the SAR image such that it is not useful for estimating soil moisture directly. However, Western et al. (1999) acknowledged that other research suggests that multitemporal analysis (comparison of images taken at different times) or multifrequency analysis (comparison of images taken at different frequencies) may be beneficial as the influence of vegetation and surface roughness can potentially be computed out of the image.

Wang et al. (1997) made extensive measurements over the Little Washita River watershed in Oklahoma in 1992 using AIRSAR (L-band) and in 1994 using SIR-C (L-band) to test the usefulness of radar for measuring soil moisture. In processing the images, they used the algorithm developed by Dubois et al. (1995) which estimates the soil moisture and surface roughness heights by using two polarizations of the backscattering coefficient ($\sigma°_{HH}$ and $\sigma°_{VV}$), but only a single frequency and single time period image. This algorithm was developed specifically for bare soil, and no attempt was made to correct or account for vegetation cover in applying it to the Little Washita data set. These results were found to agree fairly well with those measured by ground sampling in bare areas. However, the algorithm tended to underestimate soil moisture in vegetated fields and wooded areas (Wang et al. 1997). These results, based on only L-band observations, are strong testimony to radar's potential as a soil moisture mapper (Ulaby et al. 1996).

Verhoest et al. (1998) used 8 ERS-1 and ERS-2 images of the Zwalm catchment in Belgium taken between October 1995 and March 1996 to determine if multitemporal analysis would be capable of separating soil moisture from other physical factors such as topography and land cover. They used Principle Component Analysis (PCA), which is a technique that is widely used in optical remote sensing but less so in SAR image processing. PCA linearly transforms multispectral or multidimensional data into a new coordinate system in which the data can be represented without correlation. The new coordinate axes are orthogonal to each other and point in the direction of decreasing order of the variances, so that the first principal component contains the largest percentage of the total variance (hence the maximum or dominant information), the second component contains the second largest percentage, and so on (Verhoest et al. 1998). The benefit of PCA is that transformed images may show evident features that are not discernable in the original data (Verhoest et al. 1998). For further details on PCA, the reader is referred to Verhoest et al. (1998) and related references. In applying PCA, they found that the first principal component was related to the topography of the basin. The second principal component appeared to reflect the soil moisture response from rainfall and drainage episodes, and it corresponded well with the seasonal drainage conditions of the soil. This research suggests that current SAR instruments can effectively provide soil moisture information when used within a multitemporal framework together with analysis techniques that are capable of separating dominant effects from less predominant ones (Verhoest et al. 1998). However, these results are preliminary and require further testing on other basins in various seasonal conditions.

Mancini et al. (1999) performed a laboratory experiment using a 2 m diameter cylindrical container filled with a sandy loam soil, subjected to successive wetting and drying cycles and two different surface profiles (rough and smooth). TDR probes were used to measure soil moisture profiles, and for each profile, polarimetric radar measurements were collected at three different incident angles (11°, 23°, and 35°) and between 1 and 10 GHz using an 11.25 MHz frequency step (Mancini et al. 1999). The radar data were analyzed using the Integral Equation Model (IEM) designed to simulate backscattering from randomly rough surfaces. The principle of the IEM is that the backscattering coefficient is expressed as a function of the radar configuration (frequency, polarization, and incidence angle), the soil dielectric constant, and the roughness parameters (Mancini et al. 1999). Further description of the use of the IEM for soil moisture measurement can be found in Altese et al. (1996). Results from this experiment showed that for low incidence angles and low frequencies, the radar-derived soil moisture estimates are of the same accuracy as the in-situ measurements made by the TDR probes. Significant differences occurred only when the TDR measurements at 2.5 cm or 4 cm were not representative of the surface moisture conditions, which the radar measures. As well, the IEM estimates made for higher incidence angles and higher frequencies are unreliable for the smooth surface, but improve for the rough surface. As well, a system operating at low incidence angles (11°-23°) and low frequencies (1-3 GHz) was recommended for maximum quality of soil moisture information on a basin scale (Mancini et al. 1999).

Radar systems show much promise for being an operational tool for basin-scale measurements of soil moisture as their all-weather spatial and temporal coverage would be very useful to scientists. However, image processing to retrieve reliable quantitative soil moisture data is unproven as well as time-consuming and computationally intense, and no consensus has been reached on a single suitable method or radar configuration. As research in this area continues, it is hoped that these questions will be answered and some conclusions reached, but basin-scale radar measurements for soil moisture remain only experimental at this time.

2.2.5 Passive Microwave Remote Sensing (Microwave)

Similar to the radar systems described in Section 2.2.4, microwave systems have the advantage of covering a much larger spatial and temporal range than traditional point measurements.

Microwave systems are termed 'passive systems' because they do not transmit signals in the manner that radar systems do. Instead, the microwave antenna, called a radiometer, measures the thermal emission from the surface of the earth in the microwave region (wavelengths from about 1 to 30 cm, and frequency ranges from 0.3 to 300 GHz) (Schmugge 1998, Wigneron et al. 1998). In this region of the electromagnetic spectrum, soil reflectivity (or surface emissivity) is mainly driven by the soil moisture content (Wigneron et al. 1998) as the reflectivity contrast is caused by the large difference in the dielectric constants for soil and water (see Sections 2.2.2 and 2.2.4).

The product of this reflectivity and the thermodynamic temperature of the soil is called the brightness temperature (T_B), and is directly proportional to the thermal emissions of the land surface measured by the radiometer (Schmugge 1998). T_B is calculated by

$$T_B = \tau\ (R^*T_{sky} + (1\text{-}R)T_{soil}) + T_{atm}$$

where R is the surface reflectivity measured by the radiometer, τ is the atmospheric transmission, and T_{soil} is the surface temperature. The first term is the reflected sky brightness, which depends on atmospheric conditions and frequency. Typical values of T_{sky} are 5 to 10 K for the normal range of atmospheric conditions with 3 K of that value being the constant cosmic background radiation. The third term is the direct atmospheric contribution, T_{atm}, and as noted for T_{sky} will be approximately 5 K. Because the value of τ is approximately 99% at longer microwave wavelengths (> 10 cm) and a typical value of R for wet smooth soil is about 0.4, the second term is the main contributor to the value of T_B (Schmugge 1998). For more detailed background information on microwave emission physics, the reader is referred to Njoku and Entekhabi (1996).

Microwave systems are traditionally spaceborn, and it is well known that instruments operating at low frequencies (less than 1.4 GHz L band) can provide the most useful observations for surface soil moisture (Jackson 1997). The majority of microwave systems research has focused on the development of single frequency systems operating at 1.4 GHz, horizontal polarization, 10 km spatial resolution, and global mapping capabilities of every 3 days (Njoku and Entekhabi 1996). The best-known example of this system configuration is the Electronically Scanned Thinned Array Radiometer (ESTAR) operated by NASA. The ESTAR satellite operates at approximately 350 km above the earth with a swath width of 40° and a ground spatial resolution of 10 km (Njoku and Entekhabi 1996). ESTAR uses synthetic aperture radiometry technology that consists of using an array of small antennas to mimic a larger one. This is very beneficial in that these antenna setups can achieve the same ground resolution of the larger antennas without the associated mass (Wigneron et al. 1998).

Similar single frequency, horizontally polarized instruments have been mounted on aircraft for more localized studies, such as the NASA Pushbroom Microwave Radiometer (PBMR) which also operates at 1.42 GHz (L-band). The PBMR has 4 beams, angled at +\- 8° and +\- 24°, and has a total swath width of 1.2 times the flight altitude of the aircraft (Schmugge et al. 1994). The benefit of the PBMR is that by using the 4-beam configuration, it allows for more efficient mapping than its single-beam predecessors (Jackson et al. 1995). The PBMR is best suited for aircraft applications, as it would not provide suitable ground resolution as a satellite system. ESTAR systems have also been tested on aircraft, and have been touted as highly suited for the task as they can provide at least twice as many footprints as the PBMR with the same resolution (Jackson and Le Vine 1996).

Some research has been done using multi-channel, multi-frequency instruments such as the Special Sensor Microwave/Imager (SSM/I). The SSM/I has four channels operating between 19 and 85 GHz with dual polarization and spatial resolutions ranging from 14 to 56 km (Jackson 1997). Although the SSM/I was not designed for soil moisture sensing, it is theoretically possible to extract soil moisture information using it under some conditions (Jackson 1997). The benefits of the SSM/I include frequent measurements and wide global coverage via two operating satellite systems, so that almost daily coverage including A.M. and P.M measurements are available for most of the Earth. However, because the channel frequencies are much higher than L-band, its usefulness will be limited and the measurements will be significantly affected by vegetation (Jackson 1997). Preliminary research has shown that the data can be used for certain vegetative conditions, however, no quantitative studies have been done to date, and a different approach is needed to adapt the system for other vegetation regimes (Jackson 1997).

Like radar systems, microwave radiometer readings are directly linked to soil moisture, but can be affected by land cover, soil texture, surface roughness, soil and vegetation temperature, and vegetation type and water content (Njoku and Entekhabi 1996, Jackson and Le Vine 1996). These factors can be substantial, and corrections need to be made when they introduce significant errors.

For a single frequency, horizontally polarized system, making observations at low frequencies (1 to 3 GHz) can initially reduce the magnitudes of the vegetation and roughness corrections. Because the system only has a single channel, information from other sources will be required to further correct measurements (Njoku and Entekhabi 1996). Land cover and soil type databases can be used to determine the general classification of surface type in the measurement area, such as forest, grassland, or crops. A land use map or remotely sensed vegetative index can be used to correct for vegetation opacity and water content of each class of surface type. Surface temperature can be obtained either from simultaneous thermal infrared radiometer measurements, or by extrapolating from local air temperatures and assuming that the soil temperature is equal to the canopy temperature (Njoku and Entekhabi 1996). Soil texture and roughness data can be obtained from direct field measurements or land management practice information (Njoku and Entekhabi 1996), but dependent on field conditions, a constant value for roughness may be suitable (Jackson and Le Vine 1996).

Jackson and Le Vine (1996) present a case study using this approach, and a useful flowchart for making corrections to measurements from single frequency, horizontally polarized systems.

Each step of the correction process and the possible errors depend entirely on the observed scene, and under certain conditions such as dense vegetation, corrections may not be feasible. As well, if the actual soil moisture is known with good accuracy at a number of ground truth 'calibration' sites, it may be possible to develop empirical relations to infer moisture over the entire scene directly from the brightness temperature observations (Njoku and Entekhabi 1996). This approach is valid only if the ground truth sites represent the full range of conditions over the entire scene.

Microwave systems have much potential for soil moisture measurement and preliminary research on such projects as Washita 92 (Jackson et al. 1995, Jackson and Le Vine 1996), FIFE (Peck and Hope 1995, Wang 1995, Schmugge 1998), Monsoon 90 (Schmugge et al. 1994, Schmugge 1998), and HAPEX-Sahel (Schmugge 1998) shows a good correlation between soil moisture and microwave response. However, more research is required before these types of systems will be operational as satellite platforms doing mapping on a global basis.

2.3 Soil Moisture Modelling

Various researchers have modelled the spatial and temporal distributions of soil moisture using both physically based and statistical hydrological models. Although the research performed in this area is not limited to the three models described in this section, these projects give a good overview of the various undertakings in research at the present time.

2.3.1 THALES Model

Western et al. (1999) used the process-based THALES model to simulate spatial and temporal patterns of soil moisture on the 10.5 hectare Tarrawarra catchment in southern Victoria, Australia. The THALES model is a process-based distributed parameter hydrological model that uses the water balance approach. Inputs of water to an element in the model grid are rainfall, subsurface flow from upslope, and surface flow (with runon infiltration) from upslope. Outputs of water are evapotranspiration, subsurface flow to downslope, and surface flow to downslope (Western et al. 1999).

The results obtained using the model were compared to measured soil moisture patterns obtained with neutron probes and TDRs. The model simulated the general seasonal changes in soil moisture very well, however, the differences between the observed and modelled patterns indicated some problems with the soil moisture component in the model. The simulated patterns are much smoother than the observed patterns due to spatially uniform soils in the model, which is not a reflection of actual field conditions. As well, the TDR measurements are made at a point whereas the element size in the THALES model is 140 m^2, thus spatial averaging must be taken into consideration (Western et al. 1999). The model consistently overestimated soil moisture on north-facing slopes in the catchment, which indicated that the potential evapotranspiration is also spatially variable. The model also consistently underestimated soil moisture in areas of high topographic convergence, suggesting that more redistribution had occurred than was predicted by the model.

These results indicated some problems within the internal structure of the model that may not have been found simply by examining the hydrographs. These types of internal comparisons are crucial in distributed hydrological model testing as different process descriptions often lead to very similar outflow hydrographs without identifying specific problem sources in the simulations (Western et al. 1999).

2.3.2 VIC Model

Western et al. (1999) also used the VIC model in the Tarrawarra catchment to simulate the spatial average of soil water storage and the fraction of catchment area that is saturated. The VIC (variable infiltration capacity) model is statistically based and assumes that scaled infiltration (or storage) capacity is a random variable with its cumulative distribution function given by the Xinanjiang distribution (Western et al. 1999). The model uses the distributions of saturation deficit to determine the runoff from the catchment. A daily time step is used, and the spatial variability in soil moisture is treated in a statistical manner without any allowance for deep drainage or other subsurface water to exit the catchment, except by baseflow (Western et al. 1999).

The results showed that the agreement between the temporal patterns in the simulated and observed total storage is very good, however, the cumulative distribution of spatial storage and the values of saturated area predicted by VIC are different from what was measured in the field. A possible cause of these errors is the assumption of a 50% uniform porosity in the upper 30 cm of the soil profile. The hydrograph comparison was significantly better, so this gives some confidence in the statistical distribution approach for simulating runoff generation (Western et al. 1999).

2.3.3 TOPOG_IRM Model

The TOPOG_IRM Model is a biophysically based distributed parameter ecohydrological model which predicts the dynamic interactions and fluxes of mass and energy within the soil-vegetation-atmosphere system over a range of scales from plot size to catchments up to 10 km^2 (Zhang et al. 1999). Part of the model accounts explicitly for the spatial distribution of soil properties, including soil moisture. In TOPOG_IRM, soil hydrology is modelled according to the Richard's equation. The inputs into the model include temperature, precipitation, vapour pressure deficit, solar radiation, and topographical information from a DEM.

The TOPOG_IRM model was applied to a 161 ha catchment in Wagga Wagga, New South Wales. Model output was compared to bi-weekly TDR soil moisture measurements made during 1992 to 1994 at 9 sites across the catchment from surface to a depth of 1 m (Zhang et al. 1999). The modelled and measured results compared quite well at shallow depths. This may suggest that the surface infiltration and evaporation are represented accurately by the model, and the offsets in the deeper soil may be caused by variations in root water uptake patterns (Zhang et al. 1999). The only significant problem was that the model appears to dry out too slowly in the springtime, however, given that the majority of the results were a good fit, this is not a significant concern. These results show that it is possible for the model to capture the key processes relating to soil moisture dynamics and evapotranspiration.

2.4 The WATFLOOD Hydrologic Model

2.4.1 Outline

The WATFLOOD hydrologic model is a fully distributed, physically based model of the hydrologic budget of a watershed. Its main purposes are flood forecasting and long term hydrologic simulations using gridded precipitation from rain gauges, radar, or numerical weather models (Kouwen 2000b). 'Fully distributed' implies that the model operates using a square grid system for all input and output information in a given watershed, and that water balance calculations are made separately for each hydrologically significant land cover class. 'Physically based' implies that WATFLOOD models those physical processes that have a prominent effect on runoff and resulting streamflows, including:

- interception;
- infiltration;
- evaporation and transpiration;
- snow accumulation and ablation;
- interflow;
- recharge;
- baseflow; and
- overland, wetland, and channel routing.

The WATFLOOD grid size is selected based on the watershed size, the available input data, and the required output. For very large watersheds where the meteorological data may be provided by a numeric weather model, a grid of 25 km by 25 km would be appropriate, whereas for a small watershed of 100 km^2, a grid of 1 km by 1 km would be more suitable (Kouwen 2000b). Using the appropriate grid size is very important to preserve the distribution of the meteorological inputs, hydrologic properties, and response of the watershed.

The WATFLOOD model uses remotely-sensed land cover images for the watershed, and classifies each pixel of the image into one of 11 different land classes (called Grouped

Response Units, or GRUs), in addition to the impervious class. Each GRU has its own set of parameter values that represent its hydrologic response characteristics. The model then routes the hydrologic response of each GRU to the channel based on the percentages and user-defined parameter values. This approach is advantageous as there is no need for a given model grid square to be homogeneous, and the pixels of each GRU need not be contiguous as the routing is not significantly affected by their position in the grid square (Kouwen et al. 1993). This approach also allows the user to use similar parameter values for similar GRUs, and should the land use change over time, the user only needs to adjust the percentages of each GRU in each grid rather than redo the entire model grid to create homogeneous land classes.

2.4.2 Model Processes requiring Soil Moisture

2.4.2.1 Infiltration

To model infiltration in WATFLOOD, the Philip Formula is selected as it represents the important physical aspects of the infiltration process (Kouwen 2000b). Also, it includes the head due to surface ponding as well as capillary potential, which the Green-Ampt equation does not.

The Philip Formula is as follows:

$$\frac{dF}{dt} = K\left[1 + \frac{(m - m_0)(Pot + D1)}{F}\right]$$

where F is the total depth of infiltrated water (mm), t is time (s), K is hydraulic conductivity (mm/hr), m is the average moisture content of the soil to the depth of the wetting front (%), m_0 is the initial soil moisture content based on the antecedent precipitation index (API) calculation or input value (%), Pot is the capillary potential at the wetting front (mm), and D1 is the depth of water on the soil surface (mm). WATFLOOD uses the following relationship to calculate capillary potential from hydraulic conductivity (K) (Kouwen 2000b):

$$Pot = 250*\log(K) + 100$$

The infiltration at the beginning of a precipitation event is very high because of the shallow depth of the wetting front and the resulting high-pressure gradient (Kouwen 2000b). As the wetting front descends and the pressure gradient is reduced, the rate of potential infiltration decreases. Figure 2.8 shows the WATFLOOD calculation of the infiltration rate (dF/dt) for a typical precipitation event.

WATFLOOD stores water in 3 soil layers: the saturated Upper Zone (UZ), the unsaturated Intermediate Zone (IZ), and the saturated Lower Zone (LZ). The parameter m_0 in the Philip formula refers to the initial soil moisture content of the IZ and affects the infiltration rate of rain and melt water (Kouwen 2000b). It is related to the API by:

$$m_0 = API / 100$$

where the maximum allowed value of m_0 is the porosity of the soil in the IZ. The API changes on an hourly basis, thus the API for a given hour 'i' is:

$$API_i = k^*(API_{i-1}) + P_i$$

where k is an optimized recession constant represented by A5 in the parameter file (ranging from 0.985 to 0.998) and P_i is the precipitation in hour i (mm). In terms of soil moisture, the API is modified hourly using:

$$m_{0\,(t + \Delta t)} = A5^*(m_{0\,(t)} + P_i / 100)$$

The previous two equations are for temperatures above 0°C. If the temperature is less than 0°C, the soil moisture is not changed (Kouwen 2000b).

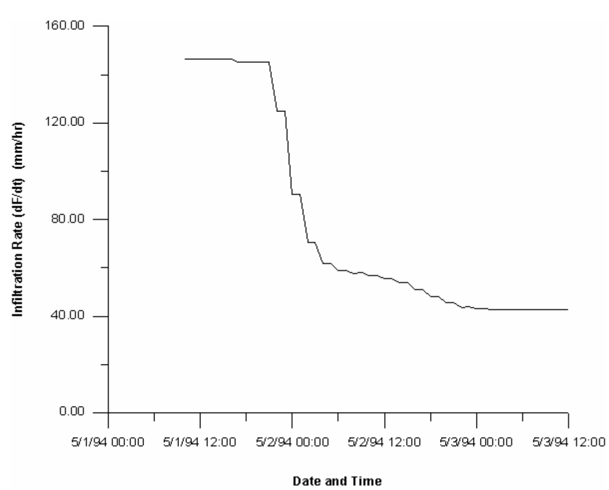

Figure 2.8: Infiltration Rate curve produced by WATFLOOD for a precipitation event

2.4.2.2 Evapotranspiration

WATFLOOD allows the user to choose one of three methods to calculate potential evapotranspiration (PET). If radiation data are available, the Priestley-Taylor equation can be used; if only temperature data are available, the Hargreaves equation can be used. If neither radiation nor temperature data are available, PET should be estimated from published values (Kouwen 2000).

To calculate the actual evapotranspiration (AET), the PET is reduced using up to three coefficients, one of which is the soil moisture coefficient (UZSI). If the soil moisture in the upper zone is at saturation (SAT), then the AET is assumed to be equal to the calculated PET. The USZI ranges from a value of 1 for soil moistures equal to SAT down to a value of 0 at the permanent wilting point. Thus, the USZI is calculated using:

$$\mathrm{UZSI} = \sqrt{\frac{\mathrm{UZS}}{\mathrm{SAT}}}$$

where the root of the fraction is used to simulate the increased difficulty for vegetation to extract moisture from the soil as it dries (Kouwen 2000). In WATFLOOD, soil moisture in the upper (unsaturated) zone is expressed as a depth of water (mm) called the Upper Zone Storage (UZS) rather than as Volume % as it would be measured in the field.

Drainage of water from the UZS is controlled by the retention factor (RETN), which is the specific retention of the soil in the UZ and also an optimized parameter. Water cannot be drained from the UZS by gravitational force, which is the driving force in the interflow and drainage to the LZ, if the UZS is less than the RETN. Amounts of water in the UZS that are less than the RETN can only be drained by evapotranspiration, thus RETN is related to the field capacity of a soil by:

$$\mathrm{RETN} = (\text{soil depth})*(\text{field capacity})$$

as discussed in Section 2.1.1.

2.4.2.3 Interflow and Groundwater Recharge

Water that percolates through the UZ and is exfiltrated to nearby water courses is called interflow, and is represented in WATFLOOD by:

$$D_{uz} = REC*(UZS\text{-}RETN)*S_i$$

where D_{uz} is the amount of water drained from the upper zone to the intermediate zone (mm/hr), REC is the depletion fraction of UZS (1/hr) and is an optimized coefficient (range of 0.001 to 0.005), and S_i is the maximum land surface slope (m/m) calculated for each grid square from the digital elevation maps.

After calculating interflow, remaining water can also drain from the UZ to the LZ by:

$$DRNG = AK2*(UZS - RETN)$$

where DRNG is the amount of water that drains to the LZ (mm/hr), and AK2 is an intermediate zone (IZ) resistance parameter (1/hr), which is also optimized (range of 0.001 to 1.00). The state of the IZ is not considered to affect this process, although it does affect the value of m_0 and, as a result, the infiltration rates. D_{uz} and DRNG are applied simultaneously, and if there is not enough water to supply both demands, the water is prorated according to the relative values of D_{uz} and DRNG (Kouwen 2000).

3.0 STUDY REGIONS

This thesis uses soil moisture data collected during two major scientific projects (Sections 3.1 and 3.2). Although these projects had much larger scopes than simply matching soil moisture budgets in hydrologic modelling, the data sets collected during these projects are very comprehensive, making them ideal for this purpose. Descriptions of these projects will be limited to a general overview with a more in-depth description of each of the soil moisture measurement sites.

3.1 Mesoscale Alpine Programme (MAP)

3.1.1 Overview

MAP is a multi-disciplinary project involving hydrologists and atmospheric scientists from Europe, Canada, and the USA. The project's overall aims are to further the basic understanding and forecasting capabilities of the physical and dynamical processes that govern precipitation over major complex topography, including hydrological aspects, and determine three-dimensional circulation patterns in the vicinity of large mountain ranges. The strategy is to focus on key orographic-related mesoscale effects that are exemplified in the alpine region (MAP Design Proposal 96/12).

Because flooding is a significant problem in the MAP alpine regions, one portion of MAP focussed on developing reliable real-time flood forecasts using hydrological models coupled with advanced mesoscale atmospheric prediction models. Dr. Nicholas Kouwen of the University of Waterloo participated in the hydrological portion of MAP using WATFLOOD to generate real-time flood forecasts. The Toce-Ticino watershed (6599 km^2) in southern Switzerland and northern Italy (Figures 3.1 and 3.2) was selected as the test site for hydrologic modelling. The forecasts were made daily during the Special Operating Period (SOP) from 15 August to 15 November 1999, using output from the Mesoscale Compressible Community (MC2) regional atmospheric model, operated by Environment Canada.

Forecasts were also made using conventional weather radar to compare the results to those obtained using MC2.

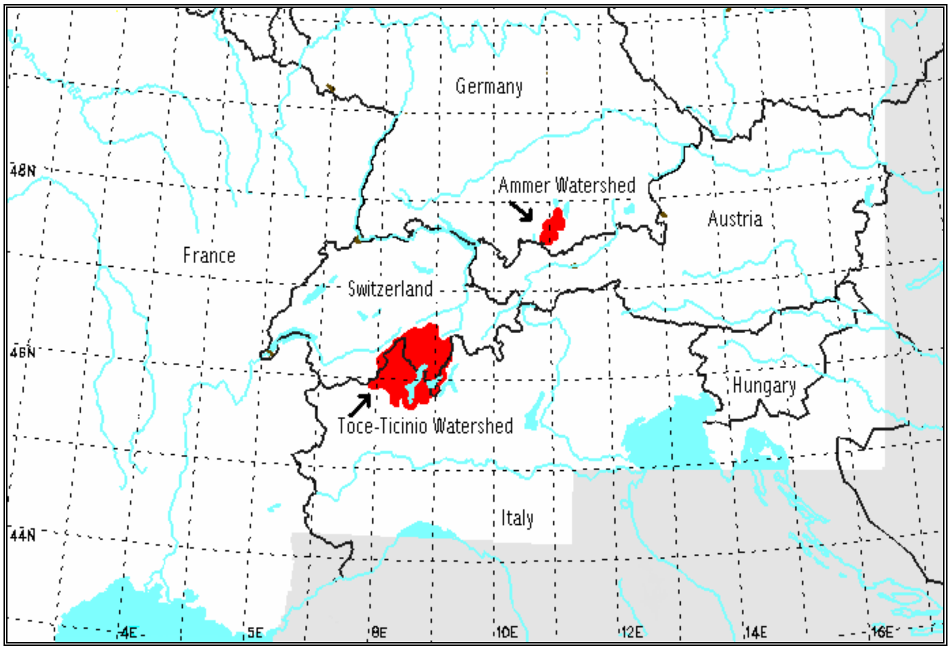

Figure 3.1: Toce-Ticino Watershed (from Kouwen and Innes 2000)

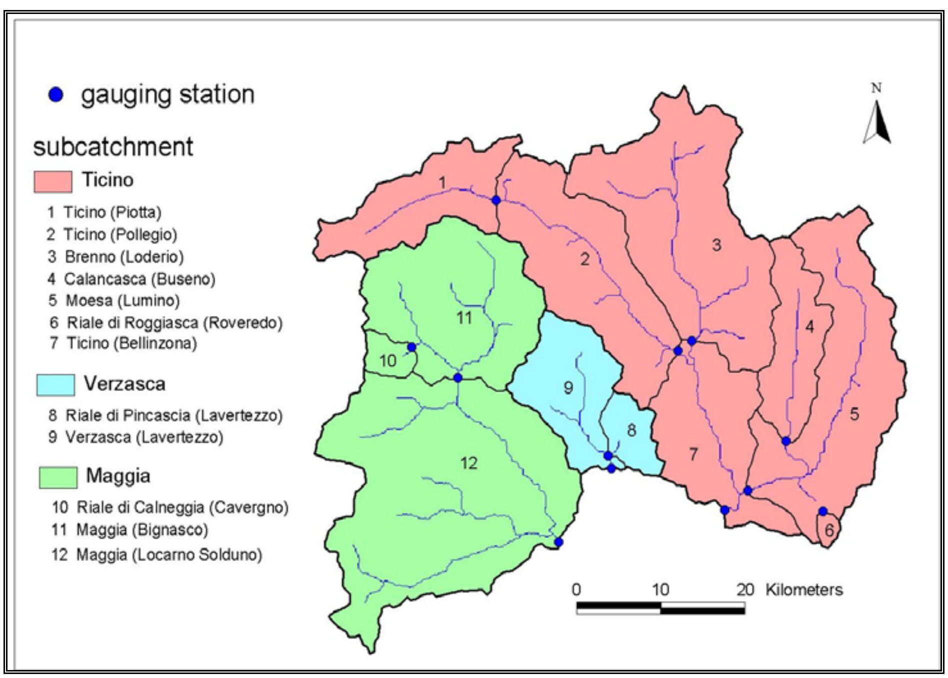

Figure 3.2: Toce-Ticino Watershed, showing basin divisions (from Bacchi and Ranzi 2000)

3.1.2 Soil Moisture Measurement Sites

The Lago Maggiore - Toce-Ticino area was selected as the test area for hydrologic modelling. The soil moisture data collection sites were located within the Riviera Valley in the test area, in the Ticino, Verzasca, and Maggia basins (Figures 3.2 and 3.3). The Riviera Valley is located in the Ticino basin, approximately halfway between Lago Maggiore and the crest of the Swiss Alps. This area is typical of mountain range topography, with elevations ranging from approximately 4600 mASL to 135 mASL, with an average elevation of 1360 mASL (Bacchi and Buzzi 1999). Average percentages of the primary land covers are coniferous forest (6%), deciduous forest (25%), mixed forest (5%), agriculture (0.3%), alpine meadows (10%), grasslands (7%), bare rock (10%), snow (23% in May, 1.5% in October), water (1.3%), and urban settlements (2%) (Bacchi and Buzzi 1999).

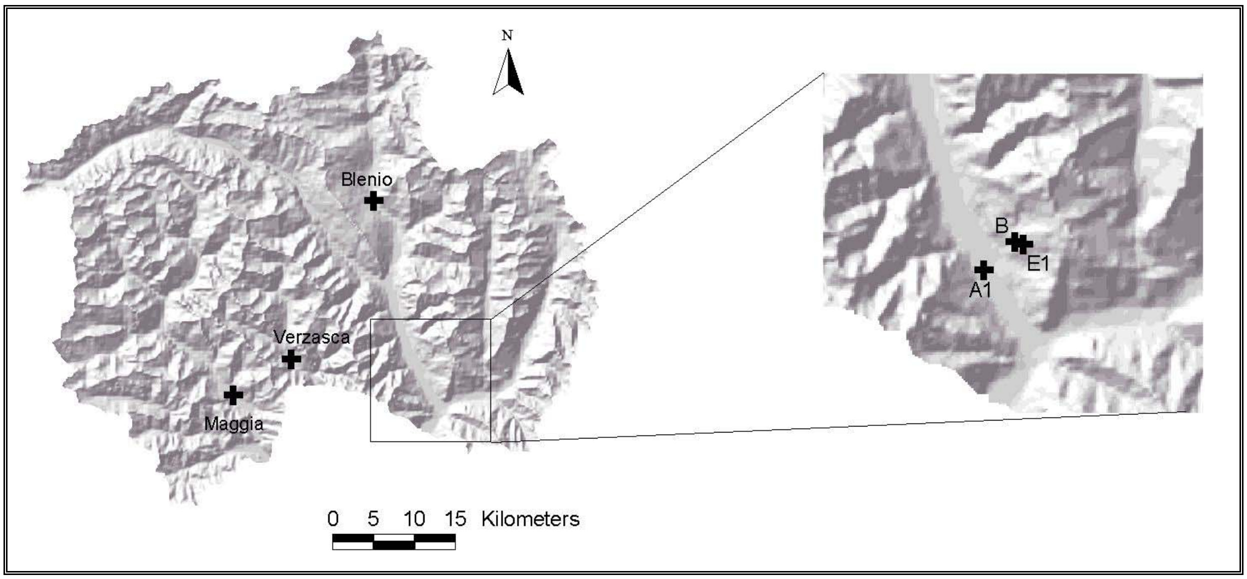

Figure 3.3: MAP Soil Moisture Measurement Sites (from Zappa et al. 2000)

The sites in Figure 3.3 were selected as they represent a range of climate, topographic, land use, and soil conditions (Table 3.1). Data were collected at these sites during the Special Operating Period from 13 September 1999 to 15 November 1999, which is the same period chosen for the hydrologic modelling.

Table 3.1: MAP Soil Moisture Measurement Sites

Site Name	Latitude	Longitude	Altitude (mASL)	Location in basin	Porosity	Land use
Claro (A1)	46° 16’ N	9° 1.3’ E	250	Valley bottom	0.52	Corn field
Telescope Tower (B)	46° 16’ N	9° 1.5’ E	800	Hillside	0.45	Forest
Maruso (E1)	46° 16’ N	9° 1.6’ E	1050	Hillside	0.45	Meadow
Verzasca	46° 27’ N	8° 57.1’ E	650	Valley bottom	0.52	Meadow
Blenio	46° 16’ N	8° 51.0’ E	500	Valley bottom	0.50	Meadow
Maggia	46° 15’ N	8° 35.1’ E	320	Valley bottom	0.55	Meadow

The Claro (A1) site was located at the edge of a corn field in the valley bottom. Volumetric soil moisture measurements were made hourly from 24 July 1999 to 11 November 1999 using buried Textronix TDR probes attached to a Campbell Scientific 21X datalogger, and recorded measurement depths were 50 mm, 150 mm, 350 mm, and 500 mm.

The Telescope Tower (B) site was located on a forested hillslope on the eastern side of the Ticino valley with heavy canopy cover. Volumetric soil moisture measurements were made hourly from 15 August 1999 to 27 October 1999 using buried TRIME-EZ TDR probes attached to a Campbell Scientific 21X datalogger, and recorded measurement depths were 150 mm, 300 mm, and 500 mm.

The Maruso (E1) site was located in a meadow on a hillslope on the eastern side of the Ticino valley. Volumetric soil moisture measurements were made weekly from 02 September 1999 to 28 October 1999 using the handheld TRIME-FM3 TDR system. The recorded measurement depth was 150 mm.

The Blenio, Verzasca, and Maggia sites were all located in meadows in the valley bottoms as shown in Figure 3.3. Weekly measurements were made from the end of August 1999 to the end of October 1999 using the handheld TRIME-FM3 TDR system with recorded measurement depths of 100 mm, 200 mm, 300 mm, 400 mm, and 500 mm.

3.2 Boreal Ecosystem Atmosphere Study (BOREAS)

3.2.1 Overview

The Boreal Ecosystem-Atmosphere Study (BOREAS) was initiated in 1990 to investigate the interactions between the boreal forest biome and the atmosphere. Surface, airborne, and satellite-based observations were collected and used for developing techniques to measure biological and physical processes and conditions that govern the exchanges of energy, water, heat, carbon, and trace gases between boreal forest ecosystems and the atmosphere, particularly those processes that may be sensitive to global change. Remote-sensing techniques, along with field measurements, were used for developing and testing models and algorithms to transfer the understanding of processes from the local scale to the regional scale (BOREAS 2000). BOREAS was set up in the northern and southern edges of the Canadian boreal forest in a 1000 km by 1000 km region covering parts of Manitoba and Saskatchewan (Figure 3.4).

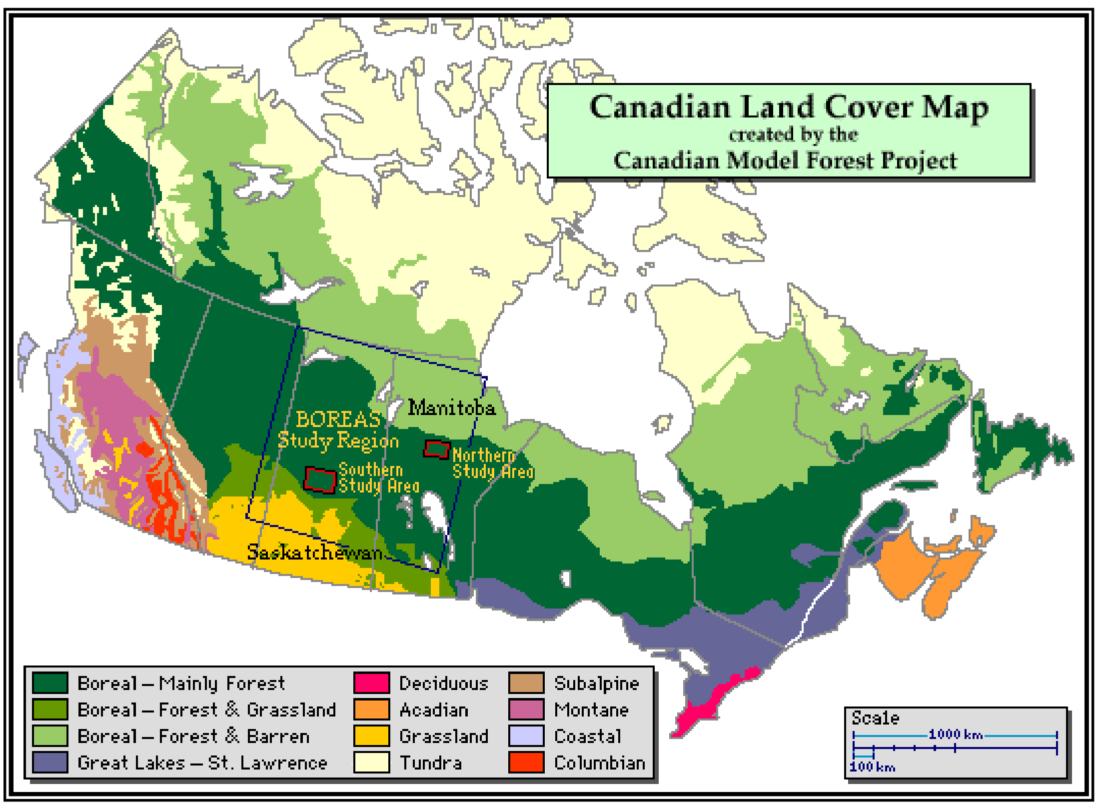

Figure 3.4: BOREAS Northern and Southern Study Areas (from BOREAS 2000)

Two different study areas were selected for data collection: the Northern Study Area (NSA) and the Southern Study Area (SSA). The NSA is an area of 8000 km^2, located between Thompson, Manitoba and Nelson House, Manitoba (Figure 3.4), and has 5 flux tower (TF) sites. The SSA covers a total area of 11 170 km^2 over the area of Prince Albert National Park through to Candle Lake, Saskatchewan (Figure 3.4). Researchers found it was difficult to find extensive stands of the required cover types grouped together, thus the 6 TF sites are widely distributed throughout the study region (BOREAS 2000).

3.2.2 Soil Moisture Measurement Sites

3.2.2.1 NSA

The NSA is an 80 km by 100 km site located 780 km northeast of the SSA, within the Canadian Shield Province (Figure 3.5). Conditions in the NSA are typical of the extreme northern boreal forest. The terrain is very low relief (less than 15 m), with numerous small lakes. In low-lying areas, up to 17 m of poorly-drained glacial lake sediments exist, typically as varved clays. In higher areas, no sediments exist and the Precambrian granitic gneiss bedrock outcrops. Permafrost exists a few feet below the surface in bogs, and slightly deeper in wooded areas. The vegetation is mostly Black Spruce with some Jack Pine in the southern and western areas. The stands are mature with some trees up to 80 years old, and heights range from stunted trees in bog areas up to 15 m. In addition, some White Birch and Trembling Aspen exist, however, these occur only in small patches (BOREAS 2000).

At the OBS site (Figure 3.5, Table 3.2), manual TDR measurements were made from 04 August 1994 to 18 September 1994 along a N 37° E transect. Measurements were made at depths of 150 mm, 300 mm, 600 mm, and 900 mm at 4 sites along the transect, starting 25 m from the flux tower and spaced 5 m apart. In 1995, automated TDR equipment was installed along a N 47° E transect. Measurements were made every hour at 150 mm, 300 mm, 600 mm, 900 mm, and 1200 mm from 13 July 1995 to 26 June 1997 at 8 sites, starting 25 m from the flux tower and spaced 5 m apart (Cuenca 1998). It should be noted that measurements were recorded during frozen winter conditions even though the soil moisture did not change.

At the OJP site (Figure 3.5, Table 3.2), manual neutron probe measurements were made from 30 May 1994 to 17 September 1994 along a N 37° E transect. Measurements were made every 100 mm from the surface to a depth of 1600 mm (1400 mm at location 2) for 5 sites, numbered 2 through 6. Site 2 was 100 m from the flux tower, site 3 was 104.8 m, site 4 was 109.8 m, site 5 was 114.2 m, and site 6 was 96.2 m. In 1996, 5 new sites were installed along a N 70° W transect. Manual measurements were made at 150 mm, 300 mm, 600 mm, 900 mm, and 1200 mm at the 5 sites, starting 35 m from the tower and spaced 5 m apart. As well, two additional automated TDR systems were installed on the transect (sites 6 and 7) and measurements were made every hour at 150 mm, 300 mm, 600 mm, and 900 mm (Cuenca 1998).

At the YJP site (Figure 3.5, Table 3.2), manual TDR measurements were made in 1996 at 5 sites installed along a N 110° S transect. Measurements were made at 150 mm, 300 mm, 600 mm, 900 mm, and 1200 mm at the 5 sites, starting 25 m from the flux tower and spaced 5 m apart. One additional automated site was installed, and measurements were made at 150 mm, 300 mm, 600 mm, and 900 mm (Cuenca 1998).

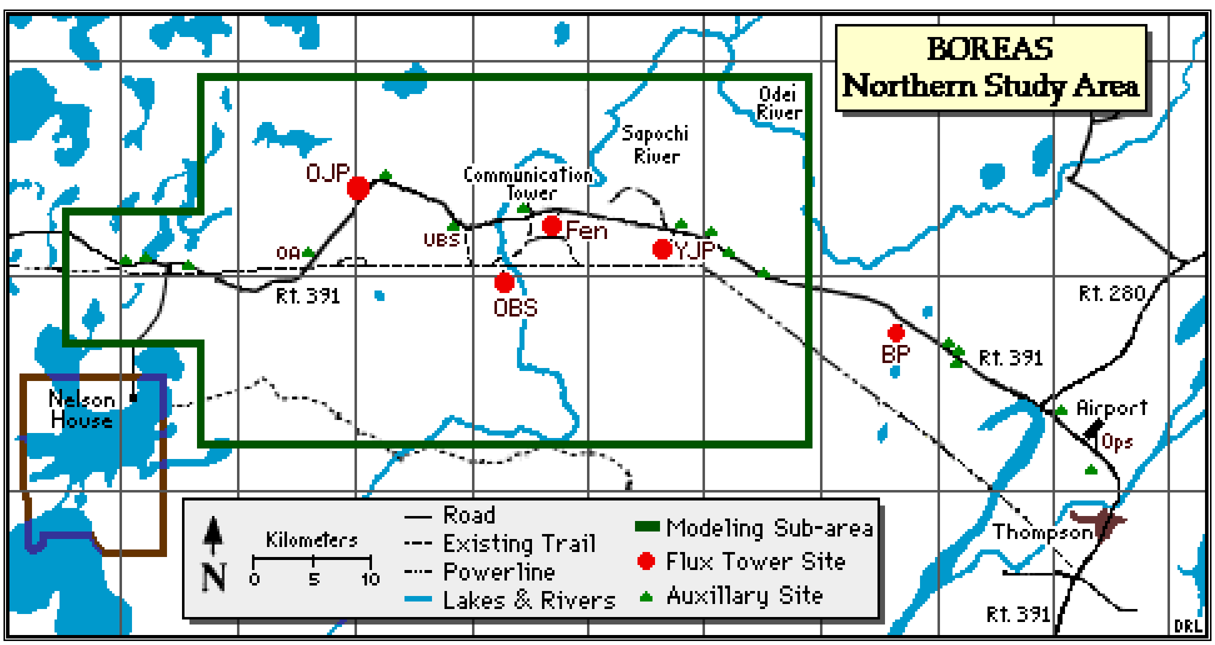

Figure 3.5: Northern Study Area (from BOREAS 2000)

Table 3.2: NSA Soil Moisture Measurement Sites

Site Name	Latitude	Longitude	Altitude (mASL)	Characteristics
OBS	55.88007 °N	98.48139 °W	259	Old growth Black Spruce (wet)
OJP	55.92842 °N	98.62396 °W	255.1	Old growth Jack Pine (dry)
YJP	55.89575 °N	98.28706 °W	249.29	Young growth Jack Pine (dry)

3.2.2.2 SSA

The SSA is a 130 km by 90 km area located in the Saskatchewan Plains (Figure 3.6). The topography ranges from gently undulating to moderately rolling, with elevations ranging from 400 to 700 mASL. The SSA represents the southern limit of the boreal forest as the transition to prairie grasslands is approximately 15 km southeast of the study area. The surficial deposits are Pleistocene age and consist of glacial tills, glaciolacustrine, and glaciofluvial sediments ranging from 100 m to 400 m deep. Gently undulating Cretaceous bedrock lies below the sediments.

The forest types are linked to the relief and drainage of the SSA:

- Aspen and White Spruce are typically found in well-drained upland areas;
- Jack Pine and Black Spruce mixed forests are found around river plains;
- Pure Jack Pine are found on well-drained, dry sites with coarse soil; and
- Black Spruce and Tamarack are found in the lower, more poorly drained bogs.

The ages of the stands range between 50 and 100 years with typical heights of 15 m to 22 m. Some stunted Black Spruce can be found in bogs.

At the OBS site (Figure 3.6, Table 3.3), manual TDR measurements were made from 04 June 1994 to 17 September 1994 along a N 60° E transect. Measurements were made at depths of 150 mm, 300 mm, 600 mm, 900 mm, and 1200 mm at 3 sites along the transect, starting 45 m from the flux tower and spaced 5 m apart. In 1995, manual TDR measurements were continued at the previous 3 sites as well as two new installations along the original N 60° E transect. Five additional sites were installed along a parallel transect located 5 m northwest of the original one.   Measurements were made from 10 May 1996 to 06 October 1996 at all sites at the original established depths (Cuenca 1998).

At the OJP site (Figure 3.6, Table 3.3), manual neutron probe measurements were made at 5 sites from 25 May 1994 to 18 September 1994 along a N 60° E transect. Measurements were made every 100 mm from the surface to a depth of 1700 mm. The first site was located 55 m from the flux tower, site 2 was 65 m, site 3 was 75 m, site 4 was 85 m, and site 5 was 105 m (Cuenca 1998).

At the YJP site (Figure 3.6, Table 3.3), manual neutron probe measurements were made in 1994 at 6 sites installed along a N 60° E transect. Measurements were made every 100 mm from the surface to a depth of 1000 mm. The 6 sites were spaced at 50 m, 70 m, 75 m, 80 m, 85 m, and 90 m respectively from the flux tower (Cuenca 1998).

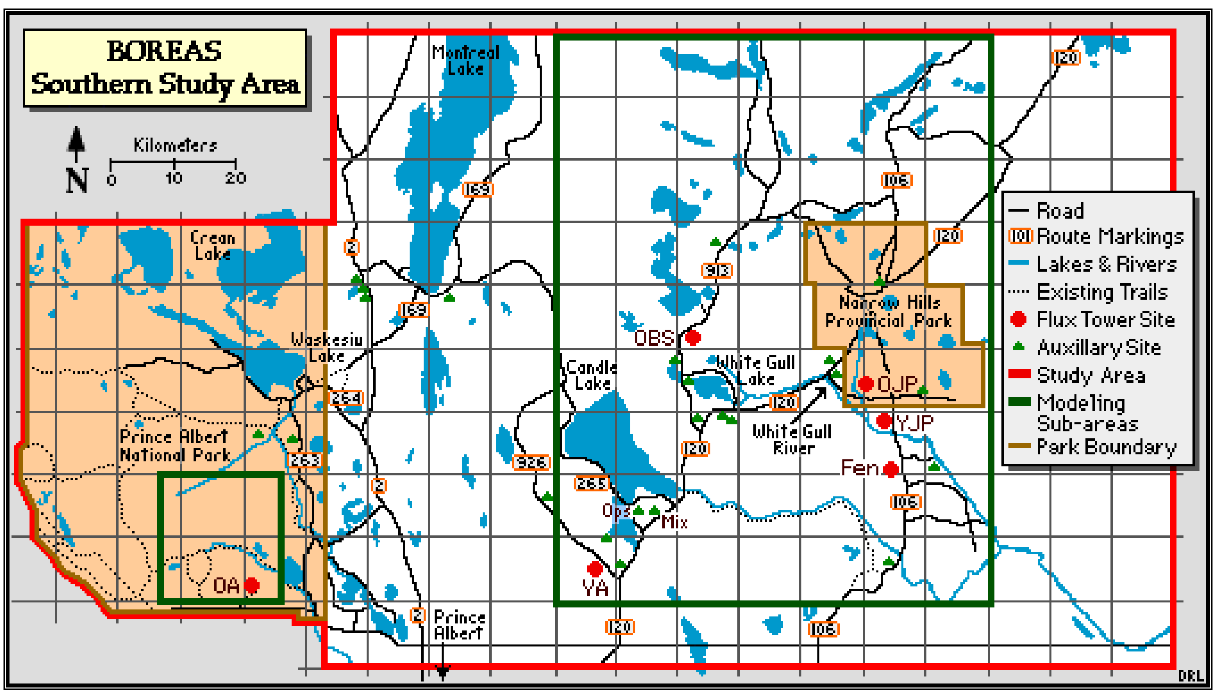

Figure 3.6: Southern Study Area (from BOREAS 2000)

Table 3.3: SSA Soil Moisture Measurement Sites

Site Name	Latitude	Longitude	Altitude (mASL)	Characteristics
OBS	53.98717 °N	105.11779 °W	628.94	Old growth Black Spruce (wet)
OJP	53.91634 °N	104.69203 °W	579.27	Old growth Jack Pine (dry)
YJP	53.87581 °N	104.64529 °W	533.54	Young growth Jack Pine (dry)

3.3 First ISLSCP Field Experiment (FIFE)

3.3.1 Overview

FIFE (First International Satellite Land Surface Climatology Project Field Experiment) was conducted in 1987 to 1989, with a "follow-on" campaign from 1989 to 1993. FIFE was designed to improve the understanding of the carbon and water cycles, coordinate data collection by satellites, aircraft, and ground measurements, and use satellite remote sensing systems to measure these cycles. It is an important part of NASA's plan to develop physically based approaches to using satellite remote sensing systems (FIFE 2000).

FIFE was conducted on the Konza Prairie in central Kansas, about 10 km from Manhattan, Kansas. The Konza Prairie is a typical native tallgrass prairie with relatively steep topography and rocky soils. The northeast section of the area is managed as a Long Term Ecological Reserve for studying grassland ecosystem dynamics, while the remainder of the area is under private management for grazing. A 15 km by 15 km area was outlined and divided into 1 km by 1 km grid squares, with the northwest corner of the grid defined by the UTM (Zone 14) coordinates of 4334000 N and 705000 E.

3.3.2 Soil Moisture Measurement Sites

Figure 3.7 shows an elevation map of the Konza Prairie site with a 20 km by 20 km grid overlain. Each square on this grid represents 2 km by 2 km, so there are 4 FIFE model grid squares in each large square shown on Figure 3.7.

Approximately biweekly neutron probe soil moisture measurements were taken at 37 sites at depths of 200, 250, 300, 400, 500, 600, 750, 800, 1000, 1200, 1400, 1600, 1800, and 2000 mm below surface. Measurements were not taken above 200 mm as the neutron probe is deemed unreliable above this level (FIFE 2000). Eight sites were selected from the list of 37 to compare to WATFLOOD's modelled UZS as these sites had measurements available for both 1987 and 1988, with some having measurements in 1989 also. The numbers 1 through 8 on Figure 3.7 correspond to the selected locations, and Table 3.4 shows the UTM coordinates of the sites and their altitudes, as well as the soil types found at each of the sites.

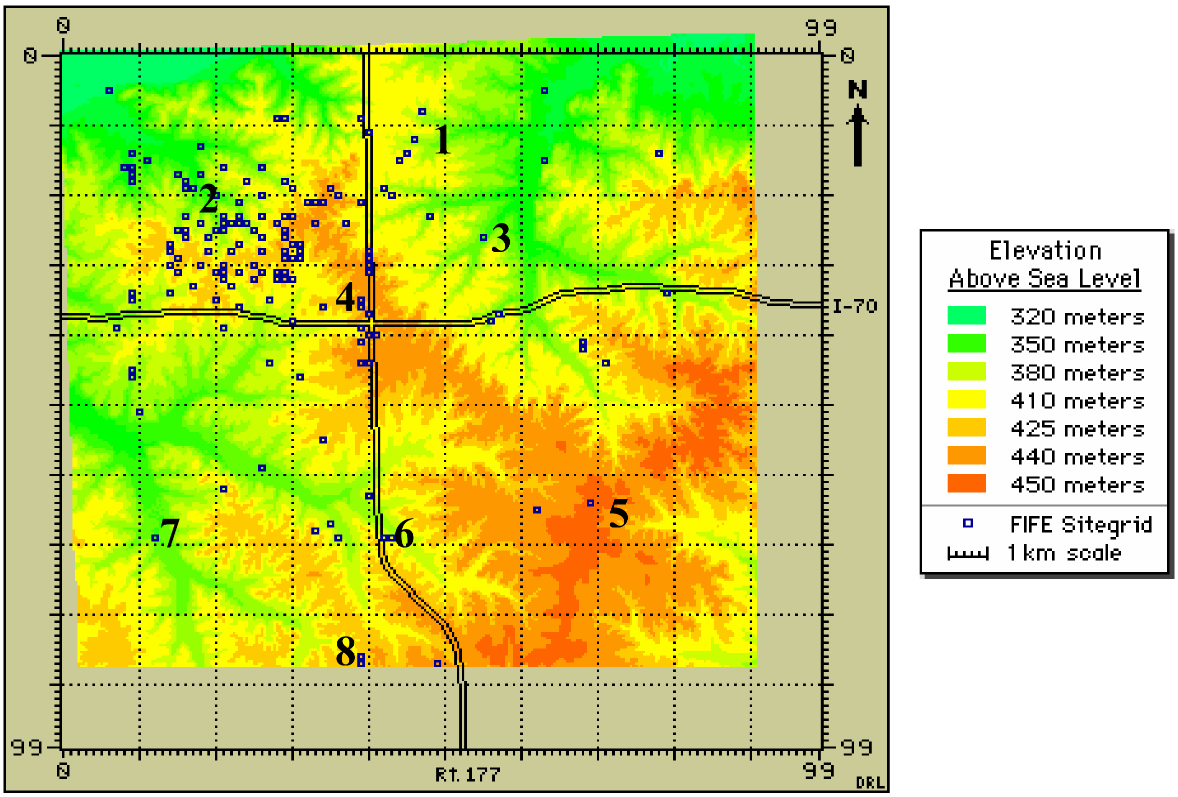

Figure 3.7: FIFE Experimental Site (after FIFE 2000)

Table 3.4: FIFE Soil Moisture Measurement Sites

No.	Site ID	Northing	Easting	Altitude (mASL)	Soil Type
1	0847	4332344	714439	418	Clime silty clay loam
2	2123	4329866	709506	405	Florence silty clay loam
3	2655	4328787	716070	367	Tully silty clay loam
4	4439	4325219	712795	445	Dwight silty loam
5	6469	4321189	718752	440	Benfield silty loam
6	6735	4320652	712073	385	Dwight silty loam
7	6912	4320178	707307	385	Tully silty clay loam
8	8639	4316771	712827	440	Dwight silty loam

4.0 WATFLOOD MODELLING

The purpose of the WATFLOOD model is to provide an accurate streamflow forecast for a given watershed based on various inputs including precipitation, temperature, watershed slope, channel characteristics, and land cover type. Because of the direct relationship between the volume of runoff and the soil moisture for a given precipitation event, proper accounting of both parameters is required.

WATFLOOD does not calculate soil moisture. Instead, it calculates the moisture in the upper layer of soil as a depth of water, called the Upper Zone Storage (UZS), by multiplying soil moisture contents by the porosity of the soil layer. During model calibration, the retention factor (RETN) is optimized. Values of UZS below the RETN cannot be drained by gravitational force, which is the driving force in interflow and drainage to the intermediate and lower zones. Volumes of water in the UZS that are less than the RETN can only be removed by evapotranspiration (Kouwen 2000). Thus, the RETN factor represents the amount of water in the UZ at field capacity (see Section 2.1.1).

The purpose of this thesis is to compare the UZS computed by WATFLOOD with the water contents measured at the selected locations within the MAP and BOREAS study areas. This section outlines the WATFLOOD setup for MAP and BOREAS and discusses initial model parameter selection.

4.1 MAP

4.1.1 Watershed Delineation and WATFLOOD Grid

Figures 3.1 and 3.2 show the outline of the Toce-Ticino watershed. The watershed was defined using Swiss and Italian digital elevation models (DEMs) with resolutions ranging from 50 m to 250 m per pixel. The Toce-Ticino spans 45° 40’ N to 46° 40’ N, and 7° 30’ E to 9° 18’ E, and is defined in latitude-longitude coordinates for reference. The WATFLOOD grid size is 1° (north-south) by 1.5° (east-west) to enable the model to use the output from the

MC2 numerical weather prediction (NWP) model without adjustments. This grid size corresponds to approximately 1.898 km by 1.898 km.

Topographical maps were used to delineate the watershed boundaries as also shown in Figure 3.2. Because the watershed lies within a mountainous region, the topographical divides between basins were more easily discernable than those in the BOREAS watersheds.

4.1.2 Data Inputs

The WATFLOOD model requires several data input sources in order to generate streamflows. These include meteorological data (temperature and precipitation), streamflow data, channel classifications, and land cover data (including topography and cover type). Only the initial streamflow measurements are used as input into the model; the remaining data are required only for comparison with the model output.

As MAP was a real-time experiment to test the forecasting capabilities of hydrological and atmospheric models, the data available for modelling were those which could be obtained on a daily basis, rather than a large comprehensive set such as that collected for BOREAS.

Real-time daily streamflow data were available from the Swiss National Hydrological and Geological Survey for two permanent gauging stations (Figure 3.2): Bellinzona on the Ticino River, and Candoglia (also called Locarno Solduno) on the Toce River. Hourly data would have been preferred, however, this was the only gauging data available for the watershed.

Precipitation data were available from three sources. First, real-time hourly composite Alpine Radar GIF images were compiled based on weather radar in Germany, Switzerland, Austria, the Czech Republic, and France. Because WATFLOOD requires digital images, these GIF files were converted to digital data using PCI Geomatics EASI/PACE image analysis software. The six available pixel colours were converted into six precipitation rates, and then converted to latitude-longitude coordinates to match with the WATFLOOD grid (Kouwen and Innes 2000).

The second precipitation source was output from the MC2 NWP model. Because one phase of MAP involved testing the ability of NWP models to predict conditions in alpine regions and their ability to ‘couple’ with hydrological models for flow forecasts, hourly output was provided for each day of the Special Operating Period (SOP). This output was available in 1° by 1.5° latitude-longitude coordinates, so it transferred easily into WATFLOOD format.

The third precipitation source was daily measurements from 4 rain gauges located in the Riviera Valley. Because of their extremely limited coverage, these gauges were used mainly as ground 'checks' for the radar and MC2 data rather than for actual hydrological modelling. But also, these gauges were within close proximity to the TDR sites, so they should theoretically give the best precipitation measurements for soil moisture modelling.

The MC2 model provided hourly forecasted temperature data as its predictive capabilities were deemed suitably accurate as an input source for WATFLOOD.

4.1.3 Land Cover and Channel Classifications

Information from the Swiss land use database ("Arealstatistik") and LANDSAT imagery taken on May 30, 1996 and October 16, 1994 were used to classify the land cover in the Toce-Ticino watershed (Bacchi and Ranzi 2000). The image contained 14 classes: snow, gravel, rock, alpine meadows, alder, larches, settlements, agriculture, grassland, deciduous forest, mixed forest, coniferous forest, water, and unclassified areas. These classes were condensed into 9 classes for modelling in WATFLOOD, including barren, crops, needle forest, broadleaf forest, mixed forest, wetland, glacier, water, and impervious. The LANDSAT image was also referenced in latitude-longitude coordinates corresponding to the WATFLOOD grid.

Two different types of river channels were identified in the Toce-Ticino watershed. These different classifications are used to represent varying hydraulic conditions throughout the watershed, enabling the model to correctly route the streamflow. The classes selected for the Toce-Ticino were flat bottom-land valley streams and steep rocky V-shaped mountain gullies.

4.1.4 Model Parameters

The parameter file specifies the characteristics of each river type and land class, and controls how they will respond to the various model inputs. By adjusting these parameters within scientifically feasible ranges, a more accurate match can be obtained between modelled and measured streamflows. The final version of the parameter file used for the Toce-Ticino watershed is found in Appendix A.

Values for the parameter file were taken from the Columbia watershed in the Rocky Mountains in Canada. This area has topographically and climatologically similar conditions as those found in the Toce-Ticino, and extensive modelling with WATFLOOD by Dr. Nick Kouwen in the Columbia watershed has provided an excellent basis for the parameter file used in the Toce-Ticino. Only the stream roughness and groundwater depletion characteristics were adjusted for this watershed (Bacchi and Ranzi 2000).

4.2 BOREAS

The WATFLOOD model for the BOREAS NSA and SSA was originally set up and calibrated by Neff (1996), and the modelling for this thesis builds directly on that work.

4.2.1 NSA

4.2.1.1 Watershed Delineation and WATFLOOD Grid

Figure 4.1 shows the outline of the NSA watershed with the WATFLOOD model grid superimposed over top. Both the study area and the grid have been defined using 1:50000 topographical base maps from 1979 and Universal Transverse Mercator (UTM) coordinates for reference. The NSA spans UTM 6170000 N to 6202000 N, and 514000 W to 548000 W (Whidden 1999).

The topographical maps were used to estimate the watershed limits, however, lack of pronounced topography in some areas made it difficult to identify the boundaries. Small-scale aerial photographs (1:15840) and investigative field trips by Neff and other researchers from the University of Waterloo helped to verify the boundaries as well as channel routes and wetland extents. Some uncertainties still exist in inaccessible lowlands and the western section of the area gauged by NW2, however, these areas are small and far enough away from the outlet that their impact on short-term hydrologic events will be negligible (Neff 1996).

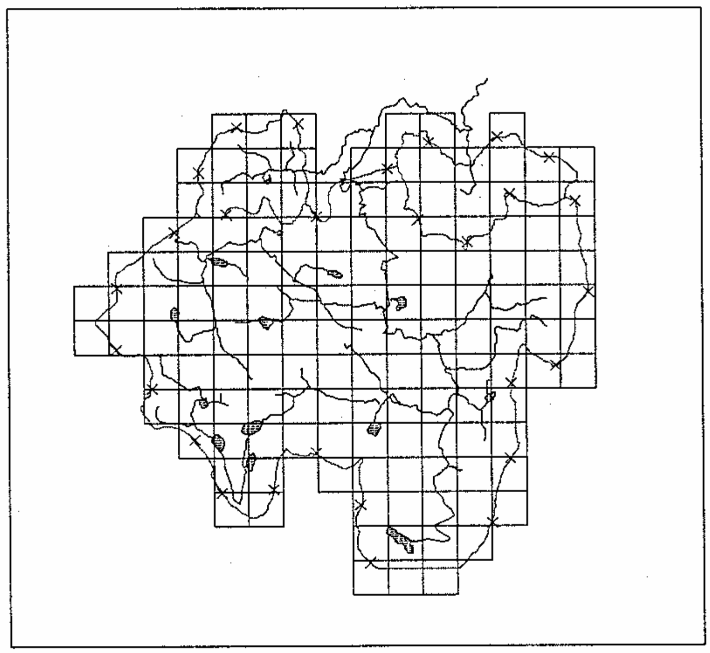

Figure 4.1: NSA Watershed and WATFLOOD Grid (from Neff 1996)

4.2.1.2 Data Inputs

The WATFLOOD model requires several data input types to produce streamflow. These include meteorological data (temperature and precipitation), streamflow data, channel classifications, and land cover data (including topography and cover type). Only the initial streamflow measurements are used as input into the model to initialize channel and lower zone storage; the remaining streamflow data are useful as a comparison for the model output.

Streamflow data were collected at 3 locations every 15 minutes from gauging locations in the NSA that were installed during BOREAS. Two installations (NW2 and NW3) used floats to measure the water level and stage-discharge (rating) curves to calculate streamflow based on the water level. These two stations operated only during ice-free periods. Station NW1 was operated year-round by Environment Canada, and used a bubbler system to measure flow. The 15-minute flows were integrated into hourly intervals to match with the time step used in WATFLOOD (Neff 1996).

Precipitation data were measured using 10 rain gauges distributed throughout the basin. WATFLOOD has a utility program that creates distributed rainfall files from these point measurements. Other scientific groups involved in BOREAS measured temperature data at the flux tower sites. These point measurements were then distributed into WATFLOOD format to represent conditions in each grid square.

4.2.1.3 Land and Channel Classifications

LANDSAT 5 imagery taken on August 20, 1990 was used to classify the land cover in the NSA. The LANDSAT image contained 11 classes: wet conifer, dry conifer, deciduous, mixed (including deciduous and conifer where the dominant class had less than 80% coverage), fen (including fens and bogs), regeneration (young, medium, and old), disturbed (bare soil, rocks, and roads), burn, and water. Six classes were selected for modelling in WATFLOOD including barren (including disturbed and burn), dry conifer (including deciduous, mixed, and regeneration), wet conifer, fen, water, and impervious. These groupings maintained the best similarity of land covers per class while keeping a reasonably uniform arrangement of land cover percentages in each class (Neff 1996). The NSA MAP file is included in Appendix A and lists the percentages of each land class for each model grid square.

The LANDSAT image was referenced to the UTM coordinates to correspond with the WATFLOOD grid. The model grid and the image were not exactly compatible though as the grid measured 4.0 km^2 and the closest grouping of image pixels (67 by 67) measured 4.04 km^2. This size of error is negligible and becomes even less significant if it is assumed that the distribution of land cover types along the edges of the elements is the same as the distribution within the elements (Neff 1996).

Five different types of river channels were identified in the NSA watershed. These different classifications are used to represent varying hydraulic conditions throughout the watershed, enabling the model to correctly route the streamflow. The classes used in the NSA were meandering channels, wetlands, rolling terrain, straight channels, and lakes/ponds.

4.2.1.4 Model Parameters

The parameter file specifies the characteristics of each river type and land class, and controls how they will respond to the model input. By adjusting these parameters within scientifically feasible ranges, one can obtain a more accurate match between modelled and measured streamflows. The final version of the parameter file used for the NSA modelling can be found in Appendix A.

Initial values for this file were taken from the work of Neff (1996) and Kouwen (2000a), and certain parameters were optimized to help match the UZS output with the measured values while still maintaining reasonable modelled hydrographs. These specific optimized parameters will be discussed in Section 5.0.

4.2.2 SSA

4.2.2.1 Watershed Delineation and WATFLOOD Grid

Figure 4.3 shows the outline of the SSA watershed superimposed on the WATFLOOD model grid. Both the study area and the grid have been defined using 1:50000 topographical base maps from 1977 and 1987, and Universal Transverse Mercator (UTM) coordinates for reference. The SSA spans UTM 5964000 N to 6000000 N, and 488000 W to 528000 W (Whidden 1999).

The topographical maps were used to estimate the watershed limits. Relief in the western part of the basin made it easy to distinguish the boundaries, however, extensive wetlands in the northern section made it difficult to determine the limits. Small-scale aerial photographs (1:15840) and investigative field trips by Neff and other researchers from the University of Waterloo helped to verify the boundaries as well as channel routes and wetland extents.

Some uncertainties still exist in the area gauged by SW3, however, the area is far enough away from the outlet that its impact on short-term hydrologic events will be negligible.

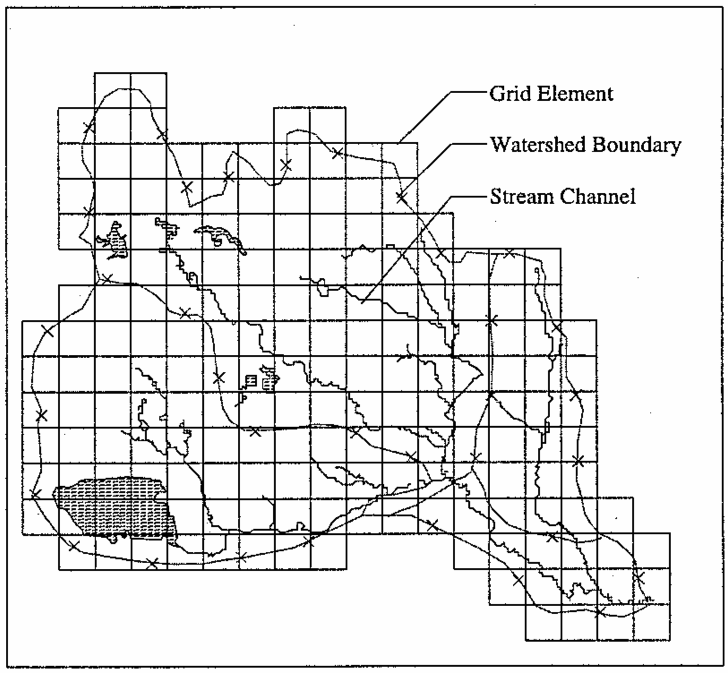

Figure 4.2: SSA Watershed and WATFLOOD Grid (from Neff 1996)

4.2.2.2 Data Inputs

Streamflow data were collected at 4 locations every 15 minutes from April to October in 1994, 1995, and 1996. These locations used floats to measure the water level and stage-discharge (rating) curves to calculate streamflow based on the water level. The 15-minute flows were integrated into hourly intervals to match with the time step used in WATFLOOD (Neff 1996).

Precipitation data were measured using 12 rain gauges distributed throughout the basin. WATFLOOD has a utility program that creates distributed rainfall files from these point measurements. Other scientific groups involved in BOREAS measured temperature data at the flux tower sites. These point measurements were then distributed into WATFLOOD format to represent conditions in each grid square.

4.2.2.3 Land and Channel Classifications

LANDSAT 5 imagery taken on August 6, 1990 was used to classify the land cover in the SSA, and the image contained the same 11 classes as the NSA. Eight classes were selected for modelling the SSA in WATFLOOD including wet conifer, dry conifer, mixed and deciduous, regeneration, burn (including disturbed and barren), wetland (including fen), water, and impervious. Neff (1996) determined that the 6-class parameter set gave better modelled hydrographs, however, the 8-class set was used here to test if better UZS results would be obtained with more choices for land classes. The SSA MAP file is included in Appendix A and lists the percentages of each land class for each model grid square.

Similar to the NSA, the LANDSAT image was referenced to the UTM coordinates to correspond with the WATFLOOD grid. Although the model grid (4.0 km^2) and the image pixel groupings (4.04 km^2) were not exactly compatible, the error is negligible (Neff 1996).

The same five types of river channels were identified for the SSA watershed as for the NSA watershed. The classes used were meandering channels, wetlands, rolling terrain, straight channels, and lakes/ponds.

4.2.2.4 Model Parameters

The final version of the parameter file used for the SSA modelling is in Appendix A. Initial values for this file were taken from the work of Neff (1996) and Kouwen (2000a), and certain parameters were optimized to help match the UZS output with the measured values while still maintaining reasonable modelled hydrographs. These specific optimized parameters will be discussed in Section 5.0.

4.3 FIFE

4.3.1 Watershed Delineation and WATFLOOD Grid

Figure 3.7 outlines the 20 km by 20 km grid selected for WATFLOOD modelling. The boundaries for modelling were defined using a digital elevation model (DEM) of the Konza Prairie, and the large grid was split up into smaller 1 km by 1 km squares for WATFLOOD. The FIFE watershed spans UTM 4314000 N to 4334000 N, and 705000 E to 725000 E. The WATFLOOD MAP file is included in Appendix A, and shows an outline of the watershed grid squares with their elevations, areas, drainage directions, and land covers.

4.3.2 Data Inputs

Precipitation and temperature data were collected every 5 minutes at automated micrometeorological stations within the Konza Prairie region from May 1, 1987 to November 10, 1989 (FIFE 2000). The 5 minute measurements were averaged to produce 30 minute averages, and data from 17 stations located throughout the basin were averaged into hourly intervals to drive the WATFLOOD model.

Streamflow data were measured at the Kings Creek USGS gauging station, located at UTM 4330650 N and 707973 E. Measurements were made every 15 minutes using a water level recorder and stage-discharge curve when the flowrate was greater than 0.0002837 m^3/s. These measurements were averaged into hourly flows for comparison to the WATFLOOD output.

4.3.3 Land Cover and Channel Classifications

LANDSAT imagery was used to classify the Konza Prairie into two major classes: agriculture and rangeland. The large majority of this area is rangeland with only very small portions attributed to agriculture. The FIFE MAP file is included in Appendix A and lists the percentages of each land class for each model grid square.

Two channel classifications were used for modelling: main channels and upland tributaries. The only difference between these two types is their channel roughness coefficient, R2 in the parameter file.

4.3.4 Model Parameters

The final version of the parameter file used for modelling the FIFE region is found in Appendix A. Initial values for this file were based on similar areas in other study regions (Kouwen 2000a), and certain parameters were optimized to help match the UZS output with the measured data while maintaining reasonable modelled hydrographs. Specific parameters and modelling results are discussed in Section 5.0.

5.0 RESULTS

5.1 Assessment Methodology

Because WATFLOOD only writes runoff values to a file for one grid square during each model run, the model had to be run for each grid square that contained a soil moisture measurement site. The different grid square numbers for each soil moisture measurement site were identified, and then entered for each successive run to obtain the output files for each site. Table 5.1 shows the grid square values for each soil moisture measurement site for MAP, BOREAS, and FIFE, and the geographic locations of each site are found in Section 3.0. Note that the origin value (0,0) in the WATFLOOD grids for each data set (shown in the MAP files in Appendix A) is the lower left corner. When counting squares, the rows (y) are counted first and then the columns (x), thus a grid value of (14,5) would indicate the 14th row and the 5th column.

Table 5.1: WATFLOOD Grid Numbers for Soil Moisture Measurement Sites

Project	Soil Moisture Measurement Site	WATFLOOD Grid number (y,x)
MAP	Claro	37, 62
	Telescope Tower	37, 62
	Maruso	37, 62
	Blenio	48, 59
	Verzasca	37, 55
	Maggia	36, 44
BOREAS	NSA Old Black Spruce (OBS)	12, 10
	NSA Old Jack Pine (OJP)	14, 5
	NSA Young Jack Pine (YJP)	13, 16
	SSA Old Black Spruce (OBS)	10, 3
	SSA Old Jack Pine (OJP)	6, 17
	SSA Young Jack Pine (YJP)	3, 18
FIFE	0837	20, 11
	2123	17, 6
	2655	16, 13
	4439	13, 9
	6469	9, 15
	6735	8, 9
	6912	8, 4
	8639	4, 9

The measured soil moisture values were translated to water contents for comparison. The TDR and neutron probe volume % soil moisture measurements were made at various depths below the surface (Figure 5.1), and the water content values used for plotting were calculated by multiplying the volume % soil moisture by the depth of measurement to get a water content in mm to a given depth. Both the TDR and neutron probe devices report % soil moisture over the entire volume of soil sampled, rather than % soil moisture in the void space of the sample. Cumulative values were calculated by adding the water content at a given depth to the sum of the water contents at the shallower depths. These values represent the total amount of water in the soil column from the surface to the stated depth, and will allow for a direct comparison with the UZS model output.

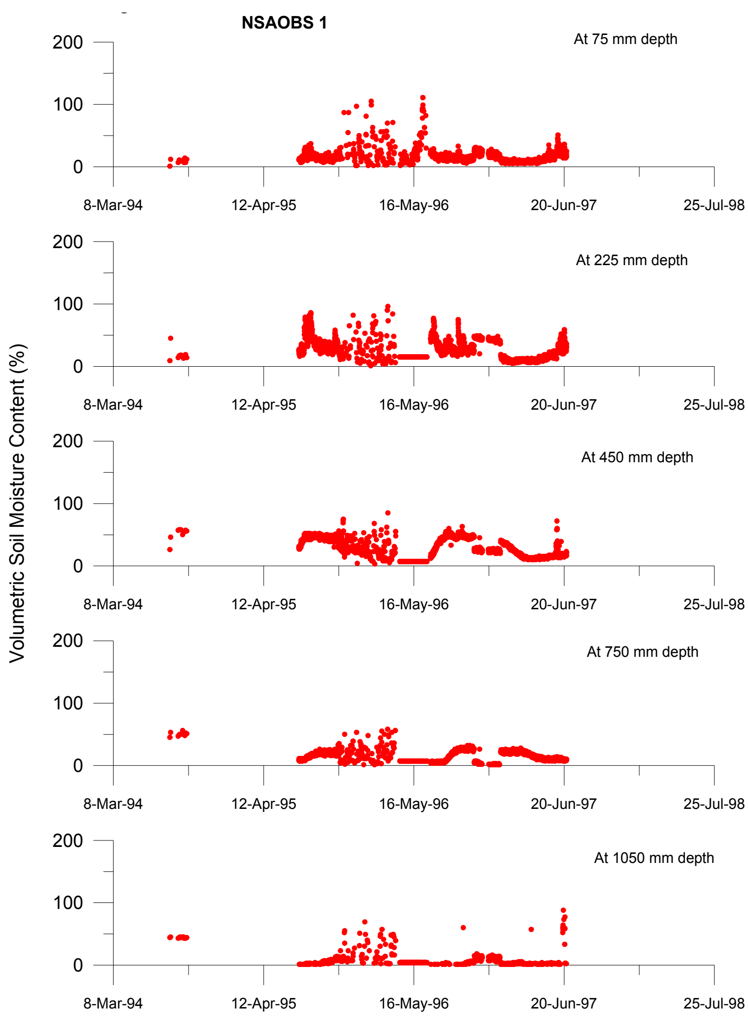

Figure 5.1: Measured Volumetric Soil Moistures at depth

Comparison plots were created in Grapher™ showing the UZS calculated by WATFLOOD and the cumulative water contents calculated from the measured TDR and neutron probe data. For each model run, the UZS for each land class is reported in a file named RFF*.txt, where the * corresponds to the land class number from the parameter file (Appendix A). The correct land class file was selected by examining the land cover and climate conditions at the site, and then choosing the file that most closely matched the characteristics of the observed conditions. Plots were also made for the measured and modelled hydrographs for each project.

Initial model runs were plotted, and output was improved by adjusting certain parameters to better fit with observed soil moistures and streamflows. The parameters used to fit the UZS and modelled streamflows were LZF, PWR, R2, RETN, REC, AK, AK2, FPET, and FTAL.

The hydrographs were used as a first check to determine the success of the model run, and the channel parameters R2, PWR, and LZF were adjusted first. R2 represents channel roughness (equivalent to Manning's n) and was used to control the peaks of the hydrographs; if the peaks were too high, R2 was increased to make the channel rougher and decrease their magnitude. PWR and LZF were adjusted at the same time to control the base flow. LZF stands for lower zone function and controls the gradual depletion of base flow between precipitation events, and PWR is the exponent placed on the value of the lower zone storage (LZS) and controls the curvature of the recession limbs of the hydrographs (Kouwen 2000a). Because the base flow does not change significantly during short term simulations, PWR and LZF have little effect on the hydrographs. However, during long term simulations with both wet and dry periods, these two parameters become more important and must be calibrated (Kouwen 2000b).

The evapotranspiration (ET) parameters FPET and FTAL were adjusted next. Based on the precipitation, the resulting modelled runoff, and the type of vegetation, ET was increased or decreased to match with observed results. FPET is a multiplier for interception ET that adjusts the amount of water lost through interception ET (IET):

$$IET = FPET*PET$$

where PET is potential evapotranspiration. During a rainfall event, FPET is set to a value of 1.0 and thus makes IET equal to PET because the interception surface is open to the atmosphere and is covered with water (Neff 1996). However, after the rain ceases, research has shown that the ET rate of intercepted water can be well in excess of the potential rate, thus the value of FPET increases. FPET was adjusted for the land classes in each parameter file based on the type of vegetation each represents, where higher numbers indicate higher vegetation-covered areas.

FTAL is a soil ET multiplier that is used to reduce the actual ET (AET) from the ground surface based on the amount of vegetation covering the soil. For dense vegetation covers, FTAL is approximately 0.7, and for less dense or sparse covers, FTAL is approximately 1.00 (Neff 1996).

The final parameters to be adjusted were REC, AK2, RETN, and AK, which control the movement of water between the upper (UZ), intermediate (IZ), and lower (LZ) zones. REC is the upper zone depletion factor expressing how fast water drains out of the UZ to the IZ and LZ. AK2 is the IZ resistance factor that controls the drainage from the IZ to the LZ. RETN represents the specific water retention of the soil in the UZ, and AK is the saturated hydraulic conductivity of the UZ soils. These parameters were adjusted by examining the hydrographs and soil moisture plots to determine if the amounts of water within the three zones were correct. The particular sections examined included the slopes of the recession limbs of the hydrographs and the upper zone storage plots, the baseflow amounts, and the timing of the rising limbs of the hydrographs.

It should be noted that previous modelling done by Neff (1996) and Kouwen (2000a) greatly assisted in forming 'baseline' parameter sets for all three projects. As well, the modelling assistance of Kouwen (2000a) was invaluable as the adjustments of parameters is not an explicit process, and requires in-depth knowledge of both the WATFLOOD model and previous values used for other watersheds, as well as knowledge of scientific limits on the processes involved.

5.2 Performance Criteria

The criteria for assessing goodness-of-fit between the measured and modelled UZS curves are qualitative rather than quantitative. Because the actual measured UZS data are not incorporated into the model as a performance criteria the way that measured streamflows are, regression statistics such as R^2 are not calculated. As well, a 'good' result can be obtained without having the UZS values calculated by WATFLOOD exactly the same as those measured in the field.

The primary criterion for fit assessment was matching the shapes of the UZS to those of the measured soil water contents. Although the actual magnitudes may be different, the timing of peaks and rising limbs, the slopes of the recession curves, and the trend of the whole time series should be parallel to, or 'mirror' one of the measured traces (Figure 5.1). One objective of this thesis is to determine the approximate depth of the 'active' upper zone modelled by WATFLOOD, so finding the trace that matches the modelled UZS will help identify that depth. The active upper zone is defined as the shallow part of the soil column in which water can be added by infiltration and removed by evaporation and transpiration, and this depth has previously been assumed to be between 50 and 100 mm (Kouwen 2000a).

To further assist in determining the depth of the active upper zone, plots of the ranges of volumetric soil moisture with depth were created for each measurement location. The plots were created by calculating the average volumetric soil moisture, the average plus one standard deviation, the average minus one standard deviation, and the maximum and minimum values at each measurement depth. Theoretically, each plot will show a wide range of soil moisture values in the active upper zone which converges to a significantly narrower range at deeper depths. The depth of the active upper zone will be determined by estimating the transition point between the wide and narrower range zones.

When assessing the fit of the modelled curves, the definition of UZS within WATFLOOD must be considered. The UZS modelled in WATFLOOD expresses the amount of 'mobile' water in the active upper zone available for gravity drainage and evapotranspiration. UZS values between saturation and the specified RETN can be drained by both gravity and evapotranspiration, but those between RETN and the permanent wilting point (PWP) can only be removed by evapotranspiration. UZS values that are equal to or less than the PWP are not available to evaporate or transpire, so the UZS calculated would be equal to zero as this water is not available for removal. However, when measuring this situation in nature, measurement devices (i.e. TDRs and neutron probes) would still indicate a small value for the % soil moisture. When assessing the comparison plots, this situation must be kept in mind.

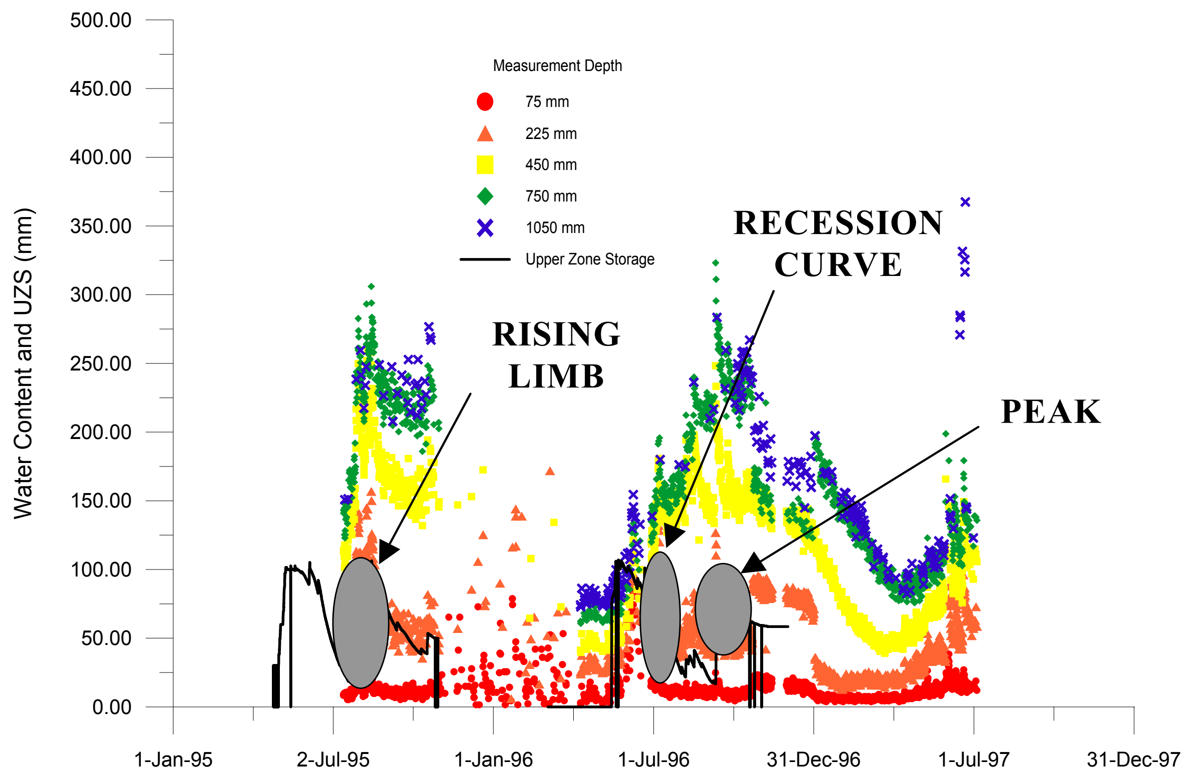

Figure 5.1: Comparison Plot Performance Criteria

A secondary criterion for assessing the goodness-of-fit of the comparison plots is the match between the measured and modelled hydrographs. While this thesis is mainly concerned with the accuracy of the UZS comparison plots, it is inherent that suitable UZS output should not result in poor modelled hydrographs, nor should suitable modelled hydrographs result in poor UZS output. Although adjusting various parameters in the model to improve the UZS will have an effect on the hydrographs, that effect should not be detrimental; an improvement in the UZS accounting should also be an improvement in the calculated hydrographs. If some other relationship were detected, i.e. an acceptable UZS plot is only obtained by sacrificing the modelled hydrograph, this would indicate a serious fundamental problem within the model that would need to be addressed.

5.3 MAP

Modelled WATFLOOD UZS was compared with water contents measured at six soil moisture sites (Figure 3.3). The soil moisture data were measured from September through to November of 1999, and WATFLOOD UZS results are available from September 13 to November 15 of 1999, the limits of both the Special Operating Period (SOP) for MAP and data available for running the model. Unfortunately, some model input data were unavailable in late October and as a result, the model did not calculate the UZS. This period is shown by a flat line and was not considered during the assessment of the plots. The model was run 3 times using 3 different precipitation input sources: rain gauges, radar, and predicted precipitation from the MC2 atmospheric model. The reason for using these three sources is because they reflect 3 operational approaches to flood forecasting and it is useful to see how they compare with respect to measured soil moistures. The MAP project is considered to be 'short term' as only 3 months of data were collected.

5.3.1 Rain Gauge Precipitation Input

The rain gauge precipitation comparison plots for the 6 MAP sites are in Appendix B (Figures B.1 to B.6). All 6 sites used the 'grassland' land class as conditions at each one were very similar. For the Telescope Tower site, a plot was made using the 'broad leaf forest' class as both covers existed equally at the site. The results were marginally better using the grassland class, so it was selected for the final plot.

Overall, the comparison results at all sites were very good. Claro provided the most comprehensive water content data set as measurements were made hourly at 4 different depths. The modelled UZS is virtually parallel with all 4 traces, however, the magnitudes of the peaks match best with the 150 mm trace. The slopes of the recession curves match best with the 350 mm trace, especially during October. The timing of the events is very good, but the large peak in late September is slightly early. Each of the 4 water content traces show larger fluctuations in water content than the modelled data, and became increasingly pronounced at depth, suggesting water is still active in excess of 350 mm below the surface.

The results from the Telescope Tower showed almost identical results to Claro. The best match for the slopes of the recession curves was the 300 mm trace, and the peak in mid-September was slightly early. The magnitudes of the UZS fluctuations were considerably less than what was observed. The overall range of UZS was approximately 40 mm, which is comparable to the range in each of the measured traces.

The installation at Maruso only reported weekly measurements at the 150 mm level. Although a detailed analysis is not possible regarding the timing of the peaks, the overall trend of the observed water content is very similar to the modelled UZS. The general slopes of the recession curves are similar, and it appears that the model reflects measured increases in water content quite well.

Blenio, Verzasca, and Maggia all reported weekly measurements at 5 depths. As discussed for the previous 3 sites, the general trend of the modelled UZS is very similar to that of the measured water contents. The magnitudes of the UZS appear to match best with the 100 mm trace, but the slopes of the recession curves match better with the 200 mm (Verzasca) and 300 mm (Blenio and Maggia) traces. The ranges are similar to those at the previous 3 sites, but no comment can be made on the range of individual peaks as the data are not available for comparison.

5.3.2 Radar Precipitation Input

The radar precipitation comparison plots for the 6 MAP sites are in Appendix B (Figures B.7 to B.12). All 6 sites were very similar and used the ‘grassland’ land class, which best reflected the conditions observed.

Using radar as precipitation input also resulted in very good comparison plots. For this model run, the water content in the model was initialized at a value of approximately 40 mm, the same value that was measured at the 150 mm depth. This was done to see if the modelled UZS would improve by providing the model with some ‘initial’ water.

The results at Claro were excellent. The model parallels the 150 mm trace almost exactly, and the first part of the plot compares better with the measured results than it did on the rain gauge plots. The timing of the events is excellent, and only the ‘extra’ event seen at the beginning of November is overestimated. Although the magnitudes of the UZS match best with the 150 mm trace, the slopes of the recession curves match best with the 350 mm trace. The range of UZS values and measured water contents was approximately 30 mm.

The Telescope Tower results were similar to those of the Claro site. The timing of all events is excellent, and the recession curve slopes match best with the 300 mm trace. The magnitudes of UZS variation, however, are much less than those measured at the 150 mm level.

The Maruso modelled UZS parallels the measured water contents well. Because of the lack of points, it is difficult to say if all the events that the model predicted actually happened, however, the general trend of the two curves is the same. The recession curve slopes match very well, and the model nicely depicts the increase in late October.

Similar to the rain gauge results, the modelled UZS at Blenio, Verzasca, and Maggia match well in magnitude with the 100 mm traces at each site. However, the slopes of the recession curves match better with the 200 mm (Verzasca) and 300 mm (Blenio and Maggia) traces. The overall trend of the UZS matches the measured points well, and the range of UZS values and measured water contents was approximately 30 mm.

5.3.3 MC2 Precipitation Input

The MC2 precipitation comparison plots for the 6 MAP sites are in Appendix B (Figures B.13 to B.18). All 6 sites were very similar and used the ‘grassland’ land class, which best reflected the conditions observed.

The UZS results at Claro showed a good fit with the measured water contents. The magnitudes fit well with the 50 mm trace, but the slopes of the recession curves matched better with the 150 mm trace. The initialization of the water content in WATFLOOD did not have a pronounced effect on increasing the range of the modelled results. The range of the modelled UZS values is slightly less than the observed water contents, even for the 50 mm trace. Although the fit here is good and the timing of the events is correct, the fit using the radar inputs is better as the radar data is observed, while the MC2 data is forecasted.

The results for the Telescope Tower show the same trends as those at the Claro site. The peaks in the modelled UZS are smaller than the measured values, and although the timing is correct, the UZS trace is too ‘flat’. The slopes of the recession curves match well with the 300 mm trace, suggesting the model is draining the water out of the active zone correctly. Again, the initial water content value had no pronounced effect on increasing the range of the modelled results.

The results from the Maruso site are also good, however, the model underestimates a rise that occurred early October which is indicated by the water content plot. The slopes of the recession curves match well, and it appears that timing of events depicted by the model fit with those that can be distinguished from the limited number of points on the plot.

Similar to the rain gauge and radar results, the modelled UZS at Blenio, Verzasca, and Maggia match well in magnitude with the 100 mm traces at each site. However, the slopes of the recession curves match better with the 200 mm traces. The range of measured water contents is larger than the modelled UZS, further confirming that the model is slightly underestimating the amount of water infiltrating into the upper zone.

5.3.4 MAP Hydrographs

The three hydrograph plots obtained from the three different MAP model runs are shown in Appendix B (Figures B.19 to B.21).

The hydrographs obtained using the rain gauge inputs (Figure B.19) are consistently overestimated. Because of a large isolated storm that occurred in late September near Claro, WATFLOOD calculated a large flow for both gauging stations that did not occur. As part of the model processes, WATFLOOD averages rain gauge data and then distributes it over the entire watershed. Because this storm was so localized, this model-induced average caused an extremely large peak to be predicted. The model predicted other peak flows at the same time as they were measured, but the values estimated by the model were larger than those recorded. These hydrographs serve to show the problem with using point rainfall measurements for flood forecasting.

The hydrographs using the radar inputs (Figure B.20) showed the best fit with measured flows. Although some peaks were slightly underestimated, the general fit at both stations is quite good. This is to be expected as the radar precipitation data provides distributed precipitation data, thus avoiding the averaging problem discussed in the paragraph above.

The MC2 hydrographs (Figure B.21) show mixed results. Although the timing of the peak flows is accurate at both stations, the match between observed and modelled values at the Candoglia station is much better than at the Bellinzona station. The MC2 model did not predict the isolated storm in late September at all, thus the large flow recorded at Bellinzona was not predicted by the model. Had the MC2 data reflected that isolated storm cell, the results likely would have been better as the recession of that flow and the resulting higher peaks carried on into early October, affecting the comparison results for the next event as well. These hydrograph inaccuracies simply reflect the uncertainties associated with using forecasted data, such as that from a model like MC2.

5.3.5 MAP Active Zone Estimation

The soil moisture content range plots for the MAP measurement sites are found in Appendix E (Figures E.1 to E.5). The plot for Maruso was not included as data were only available for one measurement depth below surface.

The plots for the Tower, Blenio, and Verzasca all show an active zone depth of approximately 300 mm, with Claro being slightly deeper at approximately 350 mm and Maggia slightly shallower at approximately 200 mm. These minor differences can be attributed to the varying geologic profiles and the number of data points collected at the sites. These results compare well with the findings of the cumulative comparison plots found in Appendix B.

5.4 BOREAS

5.4.1 NSA OBS

The comparison plots for the NSA OBS sites are in Appendix C (Figures C.1 to C.8). Soil moisture data were measured from July 1995 through to June 1997, and WATFLOOD UZS results are available from January 1994 to December 1996, the limits of the data available for running the model. However, only the modelled UZS data for the time periods matching the soil moisture measurements were shown on the plots. Although WATFLOOD calculates UZS during frozen winter periods, these times are not considered in assessing the results because no evaporation, infiltration, transpiration, or soil water movement is occurring, thus these processes are not affecting streamflow. For periods in the early spring and late fall where some snow still existed, the UZS shows a vertical line as it is automatically set to zero for those conditions. A few of these lines are visible on the plots, however, they are not considered in assessing the results.

The NSA OBS flux tower site had 8 automated TDR installations, so the measured data provided an excellent comparison set for the UZS results. The 'wet forest' land class was selected for comparison as it best matched with the conditions of the site. The OBS is a wetter site than the OJP or YJP but not as wet as the OBS site in the SSA, which was considered as a 'wetland' land class (Section 5.4.5).

The modelled UZS matched very well with the top 225 mm water content measurements. The timing of peaks and the slopes of the recession curves were accurately predicted, although the modelled UZS did go to zero while the measured water contents did not. Because of the way WATFLOOD calculates UZS, this was expected and is not considered to be a problem (see Section 4.0). Frozen conditions are indicated in the measurements by the irregular traces in the winter of 1995 and the almost-flat lines during the winter of 1996. As stated above, these sections were not considered during the plot assessments as the soil moisture is not a significant concern during frozen periods. The total range of soil water content in both the measured and modelled traces is approximately 100 mm.

The model does not follow the 75 mm trace as was initially expected, based on the theory that the active zone is between 50 and 100 mm. In all the plots, the 75 mm trace was much flatter than both the modelled UZS and the other measured traces, indicating that the active upper zone is deeper than that. This also shows that the soil moisture at shallower depths does not experience as much fluctuation as that in deeper profiles. This is to be expected as the magnitudes of soil moisture variations are limited by the void space (porosity), and there is less void space available over shallow depths than there is over deeper depths. Also, as a result of the good correlation of the modelled UZS with the 225 mm water content trace, the active upper zone is in the range of 200 to 300 mm, rather than 75 mm.

In all plots, the top three traces (450 mm, 750 mm, and 1050 mm) are very similar in pattern. This suggests that a similar amount of water was added to each previous trace to create the next one. Upon examining the individual water contents at the larger depths (i.e. not cumulative values), they showed a much smaller range of soil moisture variation than those traces closer to surface, in particular, the 225 mm and 450 mm depths. This further confirms an active upper zone depth in the range of 200 mm to 300 mm.

Only the plot for NSA OBS 4 (Figure C.4) showed a modelled peak that did not match the measured results. The peak in April 1996 does not match with the measured conditions, however, all measurement sites were in close proximity and only this site does not show that peak. The rise in the measured soil moisture in April occurs as the ground thaws out, however, that occurs earlier in each of the other 5 plots. Because of the good match between the measured data and the plots at those sites, the data measured at site 4 is suspect. Furthermore, the plot indicates inconsistent measurements after the end of June 1996 at this site, so little weight is given to the results observed here.

Overall, the modelled UZS matched very well with the measured water contents. This site is especially good for assessing modelled results, as there is an abundance of measured data for comparison.

5.4.2 NSA OJP

The comparison plots for the NSA OJP sites are in Appendix C (Figures C.9 to C.15). Soil moisture data were measured from May through to September of 1994, and again from July to October of 1996. WATFLOOD UZS results are available from January 1994 to December

1996, the limits of the data available for running the model. However, only the modelled UZS data for the time periods matching the soil moisture measurements were shown on the plots. Although WATFLOOD calculates UZS during frozen winter periods, these times are not considered in assessing the results because no evaporation, infiltration, transpiration, or soil water movement is occurring, thus these processes are not affecting streamflow. For periods in the early spring and late fall where some snow still existed, the UZS shows a vertical line as it is automatically set to zero for those conditions. A few of these lines are visible on the plots, however, they are not considered in assessing the results.

The NSA OJP flux tower site (Figure 3.5) had 7 installations: 3 were measured in 1994 and 4 were measured in 1996. While other measurements were also available for these sites for different time periods, the selected sets provided the most comprehensive sets for comparison with the UZS results. The ‘dry forest’ land class was selected for the OJP measurements as it best matched with the conditions of the site. The OJP is a drier site than the YJP, and neither are as wet as the OBS site.

Sites 2, 4, and 5 were monitored in 1994 (Figures C.10, C.12, and C.13). Unfortunately, there are less data available here than at the OBS sites, but there are still enough points to make a valid assessment. The UZS matches reasonably well with the 225 mm measured data, especially from late July through to September. The peaks and recession curves are predicted well by the model, and the timing is very good. The UZS recession curve in early June is slightly steeper than the measured data, but the large peak in the middle of June (shown by only one measured point) is well matched. The measured data show water content ranges of approximately 10 mm, while the UZS range is approximately 20 mm. In general, the modelled UZS appears to drain out of the upper zone slightly more quickly than the measured data indicate, however, the results are still very good. Similar to the OBS site, the match between the 225 mm trace and the UZS indicates that the active upper zone is between 200 mm and 300 mm.

Sites 1, 3, 6, and 7 were monitored in 1996 (Figures C.9, C.11, C.14, and C.15). The lack of data at sites 1 and 3 do not allow for a very detailed assessment. There is a reasonable match in both cases to the 225 mm trace, however, the UZS values are larger than those measured. The second recession curve in early August appears later than measured, and upon examining sites 6 and 7, the same problem is seen. Sites 6 and 7 were automated, thus they provide a better time series for comparison. The peaks in July and August appear approximately 1 week earlier than modelled, however, the shape of the UZS and the slopes of the recession curves match the earlier data of the 300 mm trace well. The hydrographs for 1996 (Section 5.4.4) confirmed that the model predicted that flow event later than it should have been, thus the reason for the mismatch in the comparison plots. The range of measured water contents is approximately 25 mm, higher than the 3 sites from 1994, while the modelled UZS range is approximately 30 mm.

5.4.3 NSA YJP

The comparison plots for the NSA YJP sites are in Appendix C (Figures C.16 to C.21). Soil moisture data were measured from May through to October 1996, and WATFLOOD UZS results are available from January 1994 to December 1996, the limits of the data available for running the model. However, only the modelled UZS data for the time periods matching the soil moisture measurements were shown on the plots. Although WATFLOOD calculates UZS during frozen winter periods, these times are not considered in assessing the results because no evaporation, infiltration, transpiration, or soil water movement is occurring, thus these processes are not affecting streamflow. For periods in the early spring and late fall where some snow still existed, the UZS shows a vertical line as it is automatically set to zero for those conditions. A few of these lines are visible on the plots, however, they are not considered in assessing the results.

The NSA YJP flux tower site had 6 installations (Figure 3.5), all of which were monitored in 1996. While other measurements were also available for these sites for different time periods, the selected sets provided the most comprehensive sets for comparison with the UZS results. The 'dry forest' land class was selected for the YJP measurements as it best matched with the conditions of the site. The YJP is a slightly wetter site than the OJP, and neither is as wet as the OBS site.

Sites 1 through 4 show a reasonably good match between the modelled UZS and the measured water content at 225 mm. Because of the 'late' arrival of the flow event in June 1996, the modelled UZS event appears slightly after the measured event it matches. The slopes of the modelled recession curves fit well with the measured plots, and the timing of the peaks matches well if the time lag is considered. Only weekly measurements were made at these sites, and while they do not depict all the events shown in the modelled UZS, there are enough points to show a good match. The measured data at site 5 for the 225 mm trace begins at the end of the modelled time series, so unfortunately no assessment can be made for that site.

Site 6 was an automated installation with measured data starting at the end of June and finishing at the end of October. While there is obvious dispersion in some of the measured data, the UZS matches the observed trace at 300 mm reasonably well if the time lag is taken into consideration. The measured data in August shows 3 distinct peaks that are not reflected by the model, however, those are not as obvious in the first 4 measurement sites. The measured data show water content ranges of approximately 15 mm for the first 4 sites and approximately 30 mm for site 6, while the UZS range is approximately 35 mm.

5.4.4 NSA Hydrographs

The NSA Hydrographs are shown on Figures C.22 and C.23 (Appendix C). The first plot shows the model results using the calibrated NSA parameter file, and the second plot shows the results using the calibrated SSA parameter file for the NSA data. The hydrographs were calibrated over 1 year (1994) and then the model was run to obtain results for 1994 to the end of 1996. The purpose of these plots was to check that acceptable modelled UZS did not result in unacceptable modelled hydrographs.

NW1 is the Environment Canada gauging station operated year-round. Although the match between the measured and modelled hydrographs is not exact, it is still acceptable. The timing of the flow event in June 1994 is slightly late, the peak in early June 1995 is overestimated, and the peak in early June 1996 is both late and overestimated. Because of the wide range of parameters available for adjustment in the model, these problems may be a result of another process that has no bearing on the modelled UZS.

NW2 and NW3 are temporary installations where data were collected only during the summer months. The results at both gauges were acceptable, with only a few peaks being overestimated in early June of 1995. At NW3, the peak for June 1996 was also overestimated, but matched well at NW2 for the same event. The timing of the events is quite good.

A second set of hydrographs was generated using the SSA parameter values and the NSA data (Figure C.23). A new 5 land class parameter file was created for the NSA to see if the results would be similar to those obtained using the calibrated NSA parameter values. Although the results were acceptable and the hydrographs were somewhat smoother, the timing was later and the peaks were lower for each major event at all three gauging stations.

5.4.5 NSA Active Zone Estimation

The soil moisture content range plots for the NSA measurement sites are found in Appendix E (Figures E.6 to E.27).

All plots for the NSA OBS sites (Figures E.6 to E.13) consistently show an active upper zone of approximately 450 mm. The maximum and minimum lines for sites 4, 5, and 8 are virtually straight as erroneous points were filtered out of the data set, and the resulting values shown on the plots are the limits of the data filters that were applied. Because of the large volume of data available for the OBS sites, these results are considered to be fairly reliable and agree well with the results obtained from the cumulative plots in Appendix C.

The NSA OJP plots (Figures E.14 to E.20) show a range of active upper zone depths: approximately 450 mm at sites 1, 3, and 5; approximately 750 mm at sites 2 and 4; and approximately 900 mm at sites 6 and 7. Because of the dry, high permeability soils found at the OJP sites, it is expected that the active upper zone will be deeper than that found at the OBS or the YJP sites. Although sites 6 and 7 indicate an active depth of 900 mm, this is most likely a result of only 1996 data being available, whereas data from both 1994 and 1996 were available for sites 1 through 5.

The NSA YJP plots (Figures E.21 to E.27) also show a range of active upper zone depths: approximately 225 mm at sites 4 and 5; approximately 450 mm at sites 1, 2, and 3; and approximately 600 mm at sites 6 and 7. The 225 and 450 mm depths at sites 1 through 5 are well within the range predicted by Western et al. (1999) and match with the results of the cumulative plots. The slight depth differences between the sites could be a result of varying geologic conditions. Similar to the OJP, there is only 1996 data available at sites 6 and 7, thus the estimated 600 mm upper zone could be slightly deeper than the actual value.

5.4.6 SSA OBS

The comparison plots for the SSA OBS sites are in Appendix C (Figures C.24 to C.33). Soil moisture data were measured from June 1994 to October 1994 at sites 1-1 and 1-3, and from May 1996 to October 1996 at the remaining sites. WATFLOOD UZS results are available from January 1994 to December 1996, the limits of the data available for running the model. However, only the modelled UZS data for the time periods matching the soil moisture measurements were shown on the plots. Although WATFLOOD calculates UZS during frozen winter periods, these times are not considered in assessing the results because no evaporation, infiltration, transpiration, or soil water movement is occurring, thus these processes are not affecting streamflow. For periods in the early spring and late fall where some snow still existed, the UZS shows a vertical line as it is automatically set to zero for those conditions. A few of these lines are visible on the plots, however, they are not considered in assessing the results.

The SSA OBS flux tower site had two separate transects for soil moisture measurements, so the first digit of the site number indicates which transect the measurements were taken on. The ‘wetland’ land class was selected for comparison with the measured results as this site was very marshy, often with visible water near the surface.

The 1994 results from site 1-3 matched very well with the 225 mm water content, although the UZS in early July drops lower than the measured results showed. There was an excellent correlation between the recession curves and timing of events, even in the late fall when the UZS began to decrease significantly. The results from site 1-1 are not as favourable. This site exhibited far less variation in water content; approximately 50 mm as compared to approximately 100 mm at site 1-3. Although the timing of the peaks matches well with the 225 mm water content, the slopes of the measured recession curves are much less than the modelled UZS. A ‘flat’ line in these plots indicates either frozen conditions or saturated conditions; in this case, the flat section measured at site 1-1 during the late summer was likely caused by saturated conditions.

The 1996 results at all sites show a very similar response as site 1-1 during 1994. Although the modelled UZS predicts peaks at the same time as the measured results, the slope of the recession curve from June to the end of August is much steeper than the measured one. Given that this site is known to be very marshy and wet even in the summer (Kouwen 2000a), it is likely that these measured flatter sections are caused by near-saturated conditions at the measurement sites. The range of measured water contents shown on the 1996 plots is approximately 50 mm, compared with 100 mm at site 1-3 in 1994 and 150 mm for the modelled UZS.

5.4.7 SSA OJP

The comparison plots for the SSA OJP sites are in Appendix C (Figures C.34 to C.38). Soil moisture data were measured from May through to September of 1994, and WATFLOOD UZS results are available from January 1994 to December 1996, the limits of the data available for running the model. However, only the modelled UZS data for the time periods matching the soil moisture measurements were shown on the plots. Although WATFLOOD calculates UZS during frozen winter periods, these times are not considered in assessing the results because no evaporation, infiltration, transpiration, or soil water movement is occurring, thus these processes are not affecting streamflow. For periods in the early spring and late fall where some snow still existed, the UZS shows a vertical line as it is automatically set to zero for those conditions. A few of these lines are visible on the plots, however, they are not considered in assessing the results.

The SSA OJP flux tower site had 5 soil moisture installations, all of which were monitored in 1994 at depth increments of 100 mm. The ‘dry conifer land class was selected for the OJP measurements as it best matched with the conditions of the site. The OJP is a slightly drier site than the YJP, and neither is as wet as the OBS site.

The comparison plots for the SSA OJP sites are very similar to those for the NSA OJP sites. The best matches to the modelled data are the 350 mm traces, and the timing of the peaks is excellent. The model predicted all the rises in water content shown in the measured traces, however, missing data from mid-June to mid-July prevent further assessment of the UZS during that time. The recession curves in early June and early August are slightly steeper than measured, showing that the model is draining water out of the upper zone too quickly. The range of measured water contents at these sites is approximately 20 mm, compared to approximately 30 mm as predicted by WATFLOOD.

5.4.8 SSA YJP

The comparison plots for the SSA YJP sites are in Appendix C (Figures C.39 to C.44). Soil moisture data were measured from May to September 1994, and WATFLOOD UZS results are available from January 1994 to December 1996, the limits of the data available for running the model. However, only the modelled UZS data for the time periods matching the soil moisture measurements were shown on the plots. Although WATFLOOD calculates UZS during frozen winter periods, these times are not considered in assessing the results because no evaporation, infiltration, transpiration, or soil water movement is occurring, thus these processes are not affecting streamflow. For periods in the early spring and late fall where some snow still existed, the UZS shows a vertical line as it is automatically set to zero for those conditions. A few of these lines are visible on the plots, however, they are not considered in assessing the results.

The SSA YJP flux tower site had 5 installations, all of which were monitored in 1994. The ‘dry conifer’ land class was selected for the YJP measurements as it best matched with the conditions of the site. The YJP is a slightly wetter site than the OJP, but neither is as wet as the OBS site.

The modelled UZS matches well with the 350 mm traces on all 5 comparison plots. The timing of the peaks fits well with measured water contents, although the UZS is not as smooth as the measured data. The slopes of the recession curves match well for the most part, but the UZS peak at the end of July recesses more quickly than the actual water contents. The range of UZS is approximately 35 mm compared to 20 mm for the measured data. Despite the larger range, the match between the measured water contents and modelled UZS is very good.

5.4.9 SSA Hydrographs

The SSA Hydrographs are shown on Figure C.45 (Appendix C). The hydrographs were calibrated over 1 year (late 1993 to 1994) and then the model was run to obtain results for November 1993 to the end of October 1996. The purpose of these plots was to check that acceptable modelled UZS did not result in unacceptable modelled hydrographs.

The SSA hydrographs matched better with observed flows than those in the NSA. For SW1, the timing of events was well matched, except for one late peak in May 1995 and 3 very small peaks in March 1994 and March 1996. The large peak in July 1994 is well matched, however, the recession curve did not drop off quickly enough.

At SW2, most peaks were well matched and the timing was very good. The peaks in early May 1995 and May 1996 were slightly late and the flows in the late fall of 1996 were higher than measured, but the overall fit was still excellent.

At SW3, the peaks were overestimated at the start of May 1995. The flow recession curves in late August and early September of 1994 and 1995 were slower to decrease than the measured flow. Two small peaks in September and October of 1996 were slightly overestimated, and the peak of May 1996 was predicted earlier than it occurred. Of all the stations, this one had the least accurate fit, however, it is still a suitable modelled hydrograph.

At SW4, the results were very similar to those from SW2. The modelled and measured traces are very close, except for a few minor discrepancies.

5.4.10 SSA Active Zone Estimation

The soil moisture content range plots for the SSA measurement sites are found in Appendix E (Figures E.28 to E.47).

All plots for the SSA OBS sites (Figures E.28 to E.36) consistently show an active upper zone of approximately 450 mm. Because of the large volume of data available for the OBS sites, these results are considered to be fairly reliable. They agree well with both the results obtained from the cumulative plots in Appendix C, and the results obtained from the NSA soil moisture content range plots (Figures E.6 to E.13).

The SSA OJP plots (Figures E.37 to E.41) show a range of active upper zone depths from approximately 450 mm at sites 2, 3, and 4 to approximately 525 mm at sites 1 and 5. Because of the dry, high permeability soils found at the OJP sites, it is expected that the active upper zone will be deeper than that found at the OBS or the YJP sites. These results are similar to those found at the NSA OJP sites and agree well with the cumulative plots.

The SSA YJP plots (Figures E.42 to E.47) show active upper zone depths from approximately 350 mm at sites 1, 2, and 5, and approximately 450 mm at sites 3, 4, and 6. Both depths are well within the range predicted by Western et al. (1999) and match with the results of the cumulative plots.

5.5 FIFE

The WATFLOOD model was run for the FIFE watershed (Figure 3.7) and the UZS results were compared to the measured water contents at 8 different sites. Unlike the results for both the MAP and BOREAS projects, the modelled UZS for the FIFE sites was not even close to the measured values. Much investigation was done into the cause of these discrepancies, however, no fundamental problems were discovered within the WATFLOOD model files or parameter sets. There was a limited amount of streamflow, precipitation, and temperature data available as inputs for WATFLOOD, however, this limited data does not explain the major discrepancies seen in the UZS plot (Figure D.1) and the hydrograph at the Kings Creek gauging station.

On Figure D.1, the recorded precipitation was plotted with the measured water content and UZS calculated by the model for Site 2123. Although some precipitation events result in increased measured water contents, some do not – especially the event in early June 1997 and the large event at the beginning of October 1997. Upon further examination of the actual values of the water contents, there is some suspicion that these values may be inaccurate. During mid-August of 1997, water contents in excess of 50 mm were measured at the 200 mm depth. Given that the Konza Prairie is a rocky grassland region in arid Central Kansas, these values do not make sense scientifically. The increments in cumulative water content between the measured depths are probable, however, it is suspected that the values recorded at the 200 mm depth level are not representative of the actual water content at that depth. As well, the hydrograph plot does not necessarily show a rise in flow when a recorded precipitation event occurred. This also leads to suspicion of errors in the data, thus no further modelling was done.

6.0 CONCULSIONS AND RECOMMENDATIONS

6.1 Conclusions

6.1.1 MAP

The modelled UZS calculated using the rain gauge precipitation input best matched the measured water contents at all 6 measurement sites. The only discrepancy was the larger range of fluctuations of the measured water contents than what WATFLOOD predicted. This increased range could be a result of higher infiltration and retention amounts in the actual soils than what the model calculated. As well, these lower modelled results could be due to an underestimation of the precipitation that actually occurred at the measurement sites. Because of the extreme range in precipitation amounts in alpine regions and the measurement errors that can result when using rain gauges, this explanation is more likely. The depth of the active upper zone as calculated by the model is approximately 150 mm.

The results obtained using radar precipitation inputs were also well matched to the measured water contents. Similar to the results using the rain gauge inputs, WATFLOOD predicted smaller UZS values than expected, thus indicating an active upper zone of only 50 to 100 mm. Measured water contents show that the active zone is in the range of 350 mm, based on the increased fluctuations seen at increasing depths. Kouwen and Innes (2000) found that the radar data used were consistently underestimating precipitation in the Toce-Ticino area, which explains the lower modelled UZS values.

The UZS calculated using the MC2 precipitation inputs was the least accurate of all 3 cases, however, the results were still acceptable. These inaccuracies are to be expected as the precipitation inputs produced using MC2 were predicted values rather than actual measured values, like those from radar and rain gauges. It is hoped that continued research on the linking of atmospheric and hydrologic models will assist in improving the output of both models, creating an accurate and reliable real-time forecasting tool for both weather and streamflow systems. Of course, in real-time forecasting, the UZS can be based on radar measurements up to the initiation of a forecast and use the predicted measurements for the forecast period.

For the hydrographs produced using the rain gauge inputs, the underestimations of modelled UZS coupled with the overestimations of peak flows suggests that the model infiltration rates may be too low. As well, the large overestimations were partly caused by averaging of the rain gauge values by WATFLOOD, including a large isolated storm that occurred in late September near Claro but not at the other 5 sites. This averaging by the model resulted in a much larger estimated flow than what was observed, which further reinforces the fact that rain gauges do not accurately predict the areal distribution of rainfall. They are best used as a ground truth check and calibration tool for radar precipitation measurements.

The hydrographs produced using radar input were the best overall of the three hydrograph plots, however, the peak flows were slightly underestimated in all cases, which is directly linked to the consistent underestimation of precipitation by the radar.

The hydrographs produced with MC2 data were the best for the Candoglia station, however, MC2 did not predict the isolated storm in late September causing the large flow at the Bellinzona gauge. This 'missed' event affected the flows for the following weeks, thus the model results are not as good as they otherwise would have been.

6.1.2 BOREAS

The NSA OBS measured data set provided an excellent assessment opportunity for the modelled UZS as an abundance of measured data were available for comparison. The model consistently matched the 225 mm water content trace at all 8 OBS sites. The only periods that did not match well were those during frozen and/or snow-covered conditions, however, these are not critical periods for flow forecasting as the soil moisture does not change under these circumstances. These times are also not critical periods for flood forecasting.

The NSA OJP and YJP results also match well with the 225 mm water contents, however, the recession curves calculated by the model for the OJP sites are very slightly steeper. This might be improved with minor calibration of the model, however, the overall match was good enough that this is not really necessary.

Overall, the calibrated NSA parameter set provided better results for the modelled hydrographs than using the SSA values for the NSA. Increasing the channel roughness and using a 7-land class parameter file might possibly reduce the overestimations of the peaks.

The results for the SSA OBS indicate the model is predicting the UZS quite well based on wetland 'type' parameters, however, the model has difficulty when saturated conditions occur at the surface. This is caused by the lack of a wetland routing model within WATFLOOD for dealing with evapotranspiration, infiltration, and flow through wetlands.

The SSA OJP results show flatter modelled recession curves that are not caused by saturated conditions. The site characteristics state that OJP stands exist on well-drained, coarse soils. Because of the porosities and retentions that would be associated with such soils, it is logical that the water content range would be lower.

The SSA YJP results show better agreement with the measured data than the SSA OJP for the same time period. Both sites used the dry conifer land class and the parameters were not adjusted to reflect the slight differences in the sites. These results show that the parameters were better suited to the wetter conditions at the YJP, thus explaining the larger differences between the measured and modelled values at the OJP sites.

The use of more land classes in the SSA seemed to improve modelled hydrographs, however, the use of a larger variety of land classes for the UZS comparison plots did not result in noticeably better matches between measured and modelled data than what was achieved in the NSA.

Results from comparison plots for both the NSA and the SSA suggest that the active upper zone modelled by WATFLOOD and seen in soil moisture measurements is between 200 and 400 mm, deeper than the 75 mm that was expected. This matches with depths in the 300 mm range observed by Western et al. (1999).

6.1.3 FIFE

The results obtained for both the UZS plot and hydrographs bear little resemblance to any measured data for the FIFE watershed. After investigating the relationships between recorded precipitation, soil water contents, and streamflows, it was evident that some fundamental problems exist in the data set and that further model calibration would not improve results. Because of these evident problems and the sound performance record of WATFLOOD, an internal model error was ruled out. This further shows that modelling is a useful tool to check data sets and possibly identify erroneous points.

6.2 Recommendations

The UZS calculated by WATFLOOD is accurate, and acts as a reliable check for data used within the model. It is recommended that when modelling other watersheds with WATFLOOD, the modelled UZS be compared to soil moisture data sets (if available) to ensure that the modelled and measured data agree in the top 300 mm of the soil column. By matching the modelled UZS to the measured water contents, the hydrographs should be improved for both short and long term simulations. As well, if an initial soil moisture value is available, it should be included in the model.

To allow WATFLOOD to properly model wetlands, a wetland utility program should be included in the code. Work is currently underway to incorporate the work of McKillop et al. (1999), which describes the important physical wetland processes for hydrological modelling.

Future efforts should focus on improving the modelled UZS in wetland areas, and further investigating the usefulness of remotely sensed data as a source of measured soil moisture values. This is subject to the availability of the data and the level of processing required to obtain reasonably accurate soil moistures from the raw files.

REFERENCES

Altese, E., O. Bolognani, M. Mancini, and P.A. Troch. 1996. Retrieving soil moisture over bare soil from ERS 1 synthetic aperture radar data: Sensitivity analysis based on a theoretical surface scattering model and field data. Water Resources Research, V.32, N.3, 653-661.

Bacchi, B. and A. Buzzi, Editors. 1999. RAPHAEL (Runoff and Atmospheric Processes for Flood Hazard Forecasting and Control) First Year Progress Report. Coordinated by Prof. B. Bacchi, University of Brescia, Brescia, Italy.

Bacchi, B. and R. Ranzi, Editors. 2000. RAPHAEL (Runoff and Atmospheric Processes for Flood Hazard Forecasting and Control) Final Report. Coordinated by Prof. B. Bacchi, University of Brescia, Brescia, Italy.

BOREAS. 2000. The Boreal Ecosystem Atmosphere Study Information System. Managed by Oak Ridge National Laboratory Distributed Data Archive Centre. http://www-eosdis.ornl.gov/BOREAS/boreas_home_page.html

Campbell, G.S. and R.Y. Anderson. 1998. Evaluation of simple transmission line oscillators for soil moisture measurement. Computers and Electronics in Agriculture, V.20, 31-44.

Clapp, R.B. and G.M. Hornberger. 1978. Empirical equations for some soil hydraulic properties. Water Resources Research, V.14, pp. 601-604.

Craig, R.F.. 1992. Soil Mechanics, 5th Edition. © by Chapman & Hall USA, New York, New York, USA. 427 pp.

Cuenca, R.H., D.E. Stangel, and S.F. Kelly. 1997. Soil water balance in a boreal forest. Journal of Geophysical Research, V.102, N. D24, 29355-29365.

Cuenca, R.H. 1998. BOREAS HYD-01 Volumetric Soil Moisture Data Text Document. http://www-eosdis.ornl.gov/BOREAS/boreas_home_page.html

Dingman, S. Lawrence. 1994. Physical Hydrology. © by Prentice-Hall, Inc., Englewood Cliffs, New Jersey, USA. 575 pp.

DMP Limited. 1999. TRIME® Measuring Moisture Theory. © by DMP Ltd., CH-8320 Fehraltorf, Switzerland. 21 pp.

Dobson, M.C., F.T. Ulaby, M.T. Hallikainen, and M.A. El-Rayes. 1985. Microwave dielectric behavior of wet soil, II, Dielectric Mixing Models. IEEE Trans. Geosci. Remote Sens., GE-23(1), 35-46.

Ferre, P.A., D.L. Rudolph, and R.G. Kachanoski. 2000. Identifying the conditions amenable to the determination of solute concentrations with time domain reflectometry. Water Resources Research, V.36, N.2, 633-636.

FIFE. 2000. The FIFE Information System. Managed by Oak Ridge National Laboratory Distributed Data Archive Centre. http://www-eosdis.ornl.gov/FIFE/FIFE_home.html

Grayson, R.B. and A.W. Western. 1998. Towards areal estimation of soil water content from point measurements: time and space stability of mean response. Journal of Hydrology, V.207, 68-82.

Handbook of Physics and Chemistry, 67th Edition. 1986. © by CRC Press, Boca Raton, Florida, USA.

Jackson, T.J. 1997. Soil moisture estimation using special satellite microwave/imager satellite data over a grassland region. Water Resources Research, V.33, N.6, 1475-1484.

Jackson, T.J. and D.M. Le Vine. 1996. Mapping surface soil moisture using an aircraft-based passive microwave instrument: algorithm and example. Journal of Hydrology, V.184, 85-99.

Jackson, T.J., D.M. Le Vine, C.T. Swift, T.J. Schmugge, and F.R. Schiebe. 1995. Large area mapping of Soil Moisture Using the ESTAR Passive Microwave Radiometer in Washita '92. Remote Sensing in the Environment, V.53, 27-37.

Kouwen, N. 2000a. Personal communication.

Kouwen, N. 2000b. WATFLOOD/SPL9 Hydrological Model and Flood Forecasting System User's Manual. © by N. Kouwen, Waterloo, ON, Canada.

Kouwen, N. and J. Innes. 2000. Coupled MC2-WATFLOOD Flood Forecasting. In press.

Kouwen, N., E.D. Soulis, A. Pietroniro, J. Donald, and R.A. Harrington. 1993. Grouped Response Units for Distributed Hydrologic Modeling. Journal of Water Resources Planning and Management, V.119, N.3, 289-305.

Maidment, David R., Editor in Chief. 1993. Handbook of Hydrology. © by McGraw-Hill Inc., USA.

Mancini, M., R. Hoeben, and P.A. Troch. 1999. Multifrequency radar observations of bare surface soil moisture content: A laboratory experiment. Water Resources Research, V.35, N.6, 1827-1838.

Mastrorilli, M., N. Katerji, G. Rana, and B. Ben Nouna. 1998. Daily actual evapotranspiration measured with TDR technique in Mediterranean conditions. Agricultural and Forest Meteorology, V.90, 81-89.

McKillop, R., N. Kouwen, and E.D. Soulis. 1999. Modeling the rainfall-runoff response of a headwater wetland. Water Resources Research, V.35, N.4, 1165-1177.

Neff, T.A.M. 1996. Mesoscale Water Balance of the Boreal Forest using Operational Evapotranspiration Approaches in a Distributed Hydrologic Model. MASc Thesis, University of Waterloo, Waterloo, ON, Canada. © by T.A.M. Neff, Waterloo, ON, Canada. 235 pp.

Njoku, E.G. and D. Entekhabi. 1996. Passive microwave remote sensing of soil moisture. Journal of Hydrology, V.184, 101-129.

Peck, E.L. and A.S. Hope. Spatial patterns of soil moisture for the FIFE study area derived from remotely sensed and ground data. Journal of Geophysical Research, V.100, N.D12, 25463-25468.

Roth, K., R. Schulin, H. Fluhler, and W. Attinger. 1990. Calibration of Time Domain Reflectometry for Water Content Measurement Using a Composite Dielectric Approach. Water Resources Research, V.26, N.10, 2267-2273.

Rothe, A., W. Weis, K. Kreutzer, D. Matthies, U. Hess, and B. Ansorge. 1997. Changes in soil structure caused by the installation of time domain reflectometry probes and their influence on the measurement of soil moisture. Water Resources Research, V.33, N.7, 1585-1593.

Rotunno Filho, O.C.. 1995. Soil Moisture Mapping using Remote Sensing and Geostatistics applied to Rainfall-Runoff Models. Ph.D. Thesis, University of Waterloo, Waterloo, ON, Canada. © by O.C. Rotunno Filho, Waterloo, ON, Canada. 396 pp.

Schmugge, T. 1998. Applications of passive microwave observations of surface soil moisture. Journal of Hydrology, V.212-213, 88-197.

Schmugge, T., T.J. Jackson, W.P. Kustas, R. Roberts, R. Parry, D.C. Goodrich, S.A. Amer, and M.A. Weltz. 1994. Push broom microwave radiometer observations of surface soil moisture in Monsoon '90. Water Resources Research, V.30, N.5, 1321-1327.

Tansey, K.J., A.C. Millington, A.M. Battikhi, and K.H. White. 1999. Monitoring soil moisture dynamics using satellite imaging radar in northeastern Jordan. Applied Geography, V.19, 325-344.

Topp, G.C., J.L. Davis and A.P. Annan. 1980. Electromagnetic Determination of Soil Water Content: Measurements in Coaxial Transmission Lines. Water Resources Research, V.16, N.3, 574-582.

Ulaby, F.T., P.C. Dubois, and J. van Zyl. 1996. Radar mapping of surface soil moisture. Journal of Hydrology, V.184, 57-84.

Verhoest, N.E.C., P.A. Troch, C.Paniconi, and F.P. De Troch. 1998. Mapping basin scale variable source areas from multitemporal remotely sensed observations of soil moisture behavior. Water Resources Research, V.34, N.12, 3235-3244.

Viessman, Warren Jr. and Gary L. Lewis. 1996. Introduction to Hydrology, 4th Edition. © by HarperCollins College Publishers, New York, NY, USA. 760 pp.

Wang, J.R. 1995. Some features observed by the L-band push broom microwave radiometer over the Konza Prarie during 1985-1989. Journal of Geophysical Research, V.100, N.D12, 25469-25479.

Wang, J.R., A. Hsu, J.C. Shi, P.E. O'Neill, and E.T. Engman. 1997. A Comparison of Soil Moisture Retrieval Models Using SIR-C Measurements over the Little Washita River Watershed. Remote Sensing of Environment, V.59, 308-320.

Western, A.W., G. Bloschl, and R.B. Grayson. 1998. Geostatistical characterisation of soil moisture patterns in the Tarrawarra catchment. Journal of Hydrology, N.205, 20-37.

Western, A.W., R.B. Grayson, and T.R. Green. 1999. The Tarrawarra project: high resolution spatial measurement, modelling and analysis of soil moisture and hydrological response. Hydrological Processes, V.13, 633-652.

Whidden, E.A.. 1999. Distributed Hydrological Modelling in the Canadian Boreal Forests: Subsurface Model Development, Land Surface Model Improvement, and Modelling Results. MASc Thesis, University of Waterloo, Waterloo, ON, Canada. © by E.A. Whidden, Waterloo, ON, Canada. 266 pp.

Wigneron, J-P., T. Schmugge, A. Chanzy, J-C. Calvet, and Y. Kerr. 1998. Use of passive microwave remote sensing to monitor soil moisture. Agronomie, V.18, 27-43.

Zappa, M., N. Matzinger, and J. Gurtz. 2000. Mesoscale Alpine Programme (MAP) Hydrological and Meteorological Measurements at Claro (CH) – Lago Maggiore Target Area. DRAFT Report. Universita' Degli Studi Di Brescia, Departimento Di Ingegneria Civile, Brescia, Italy. 34 pp.

Zhang, L., W.R. Dawes, T.J. Hatton, P.H. Reece, G.T.H. Beale, and I. Packer. 1999. Estimation of soil moisture and groundwater recharge using the TOPOG_IRM model. Water Resources Research, V.35, N.1, 149-161.

APPENDIX A

Selected WATFLOOD Data Files

WATFLOOD TOCE-TICINO PARAMETER FILE

```
# mod. 23/05/00 changes ak2 to be same as colum
# modified Jan 13/2000 nk
# changed forest ds to 20 mm, crop ak to 3.0, spore to 0.3
d1      01    0   00    1    5 2001                          8.99
d2    0.500        1    4
d3       6    3
a1    0.100E+01 0.110E+02 0.430E+00 0.100E+01 0.984E+00
a6    0.900E+03 0.200E-01 0.000E+00 0.000E+00 0.000E+00
      valley    mountain  mountain
lzf   0.113E-05 0.113E-05 0.113E-05
pwr   0.214E+01 0.214E+01 0.214E+01
r1    0.200E+01 0.200E+01 0.200E+01
R2    0.218E+00 0.650E+00 0.650E+00
      barren    crops     needle    broadleaf mixed     wetland   glacier   water     impervious
ds    0.100E+01 0.200E+01 0.200E+02 0.200E+02 0.200E+02 0.100E+10 0.000E+00 0.000E+00
dsfs  0.100E+01 0.200E+01 0.200E+02 0.200E+02 0.200E+02 0.100E+10 0.000E+00 0.000E+00
Re    0.030E+00 0.050E+00 0.080E+00 0.080E+00 0.080E+00 0.100E+00 0.600E+00 0.100E+00
AK    0.030E+02 0.030E+02 0.120E+02 0.120E+02 0.120E+02 0.999E+02 0.100E-09-0.100E+00
AKfs  0.030E+02 0.030E+02 0.120E+02 0.120E+02 0.120E+02 0.999E+02 0.100E-09-0.100E+00
retn  0.150E+02 0.250E+02 0.250E+02 0.250E+02 0.250E+02 0.250E+00 0.000E+00 0.100E+00
ak2   0.201E+00 0.202E+00 0.202E+00 0.202E+00 0.202E+00 0.240E-03 0.240E-09 0.200E-01
ak2fs 0.201E+00 0.202E+00 0.202E+00 0.202E+00 0.202E+00 0.240E-03 0.240E-09 0.200E-01
R3    0.368E+02 0.271E+02 0.394E+02 0.381E+02 0.381E+02 0.898E+01 0.902E+01 0.400E+01
R3fs  0.368E+02 0.271E+02 0.394E+02 0.381E+02 0.381E+02 0.898E+01 0.902E+01 0.400E+01
r4    0.100E+02 0.100E+02 0.100E+02 0.100E+02 0.100E+02 0.100E+02 0.100E+02 0.100E+02
ch    0.100E+01 0.700E+00 0.900E+00 0.900E+00 0.900E+00 0.700E+00 0.700E+00 0.600E+00
MF    0.165E+00 0.122E+00 0.122E+00 0.122E+00 0.122E+00 0.121E+00 0.166E+00 0.120E+00 0.100E+00
BASE  0.300E+01 0.100E+01 0.100E+01 0.200E+01-0.200E+01-2.000E-01 0.300E+01 0.000E+00 0.000E+00
nmf   0.000E+00 0.000E+00 0.000E+00 0.000E+00 0.000E+00 0.100E+00 0.000E+00 0.000E+00 0.000E+00
UADJ  0.000E+00 0.000E+00 0.000E+00 0.000E+00 0.000E+00 0.000E+00 0.000E+00 0.000E+00 0.000E+00
TIPM  0.200E+00 0.200E+00 0.200E+00 0.200E+00 0.200E+00 0.100E+00 0.200E+00 0.200E+00 0.200E+00
RHO   0.333E+00 0.333E+00 0.333E+00 0.333E+00 0.333E+00 0.333E+00 0.333E+00 0.333E+00 0.333E+00
WHCL  0.350E-01 0.350E-01 0.350E-01 0.350E-01 0.350E-01 0.350E-01 0.350E-01 0.350E-01
fmadj     0.000     0.000     0.000     0.000     0.000     0.000     0.000
flgev      2.00     1.500           pan; 2 = Hargreaves; 3 = Priestley-Taylor
albed      0.11
albii      0.18      0.11      0.11      0.11      0.11      0.15      0.15
fpet       1.50      2.00      3.00      3.00      3.00      1.00      1.00
fveg       1.00      0.90      0.90      0.90      0.90      1.00      1.00
flint        1.        1.        1.        1.        1.        0.        0.
fcap       0.20      0.20      0.20      0.20      0.20      0.20      0.20
pwp        00.0      00.0      00.0      00.0      00.0      00.0      00.0
spore      0.30      0.30      0.30      0.30      0.30      0.30      0.30      0.55
temp1        0.
temp2        0.
temp3      500.
tton         0.
lat.        50.
mxmn  10.2 12.3 12.1 12.3 14.3 14.2 13.8 14.0 13.1 10.6  8.2  9.3
humid 59.5 60.5 62.5 55.5 50.0 54.5 59.0 58.5 63.5 58.0 64.5 62.5
pres  95.1 95.1 95.1 95.1 95.1 95.1 95.1 95.1 95.1 95.1 95.1 95.1
ti2    jan  feb  mar  apr  may  jun  jul  aug  sep  oct  nov  dec
h1    0.10 0.10 0.10 0.10 0.10 0.10 0.10 0.10 0.10 0.10 0.10 0.10
h2    0.90 0.90 0.90 0.90 0.90 0.90 0.90 0.90 0.90 0.90 0.90 0.90
h3    1.80 1.80 1.80 1.80 1.80 1.80 1.80 1.80 1.80 1.80 1.80 1.80
h4    1.80 1.80 1.80 1.80 1.80 1.80 1.80 1.80 1.80 1.80 1.80 1.80
h5    1.80 1.80 1.80 1.80 1.80 1.80 1.80 1.80 1.80 1.80 1.80 1.80
h6    0.90 0.90 0.90 0.90 0.90 0.90 0.90 0.90 0.90 0.90 0.90 0.90
h7    0.01 0.01 0.01 0.01 0.01 0.01 0.01 0.01 0.01 0.01 0.01 0.01
h8    0.01 0.01 0.01 0.01 0.01 0.01 0.01 0.01 0.01 0.01 0.01 0.01
ti3       delta       low      high parameter
AK    0.200E+00 0.500E+00 0.400E+01 0.127E+01
AK    0.200E+00 0.500E+00 0.400E+01 0.152E+01
AK    0.200E+00 0.500E+00 0.400E+01 0.800E+00
AK    0.200E+00 0.500E+00 0.400E+01 0.200E+01
AK    0.200E+00 0.500E+00 0.400E+01 0.152E+01
AK   -0.200E+00 0.500E+00 0.400E+01 0.100E-09
AKfs  0.200E+00 0.500E+00 0.400E+01 0.200E+01
AKfs  0.200E+00 0.500E+00 0.400E+01 0.200E+01
AKfs  0.200E+00 0.500E+00 0.400E+01 0.200E+01
AKfs  0.200E+00 0.500E+00 0.400E+01 0.200E+01
AKfs  0.200E+00 0.500E+00 0.400E+01 0.200E+01
AKfs -0.200E+00 0.500E+00 0.400E+01 0.100E-09
Re    0.200E-01 0.200E-01 0.200E+00 0.980E-01
Re    0.200E-01 0.200E-01 0.200E+00 0.100E+00
Re    0.200E-01 0.200E-01 0.200E+00 0.980E-01
```

```
Re     0.200E-01 0.200E-01 0.200E+00 0.100E+00
Re     0.200E-01 0.200E-01 0.200E+00 0.100E+00
Re    -0.200E-01 0.200E-01 0.200E+00 0.900E+00
R3    -0.200E-01 0.500E+01 0.500E+02 0.368E+02
R3    -0.200E-01 0.500E+01 0.500E+02 0.394E+02
R3    -0.200E-01 0.500E+01 0.500E+02 0.381E+02
R3    -0.200E-01 0.500E+01 0.500E+02 0.271E+02
R3    -0.200E-01 0.500E+01 0.500E+02 0.305E+02
R3     0.200E-01 0.500E+01 0.500E+02 0.902E+01
fpet -0.500E-01 0.500E-01 0.200E+01 0.700E+00
fpet -0.500E-01 0.500E-01 0.200E+01 0.700E+00
fpet -0.500E-01 0.500E-01 0.200E+01 0.700E+00
fpet -0.500E-01 0.500E-01 0.200E+01 0.700E+00
fpet -0.500E-01 0.500E-01 0.200E+01 0.700E+00
fpet -0.500E-01 0.500E-01 0.200E+01 0.700E+00
ftal  0.500E-01 0.700E+00 0.300E+01 0.150E+01
ftal  0.500E-01 0.700E+00 0.300E+01 0.200E+01
ftal  0.500E-01 0.700E+00 0.300E+01 0.200E+01
ftal  0.500E-01 0.700E+00 0.300E+01 0.150E+01
ftal  0.500E-01 0.700E+00 0.300E+01 0.100E+01
ftal -0.500E-01 0.700E+00 0.300E+01 0.100E+01
MF     0.200E-01 0.900E-01 0.150E+00 0.104E+00
MF     0.200E-01 0.900E-01 0.150E+00 0.106E+00
MF     0.200E-01 0.900E-01 0.150E+00 0.104E+00
MF     0.200E-01 0.900E-01 0.150E+00 0.116E+00
MF     0.200E-01 0.900E-01 0.150E+00 0.118E+00
MF     0.200E-01 0.900E-01 0.150E+00 0.116E+00
BASE -0.100E-03-0.400E+01 0.000E+00-0.100E+01
BASE -0.100E-03-0.400E+01 0.000E+00-0.200E+01
BASE -0.100E-03-0.400E+01 0.000E+00-0.300E+01
BASE -0.100E-03-0.400E+01 0.000E+00-0.200E+01
BASE -0.100E-03-0.400E+01 0.000E+00-0.300E+01
BASE -0.100E-03-0.400E+01 0.000E+00-0.100E+01
nmf  -0.200E-01 0.100E+00 0.200E+00 0.000E+00
nmf  -0.200E-01 0.100E+00 0.200E+00 0.000E+00
nmf  -0.200E-01 0.100E+00 0.200E+00 0.000E+00
nmf  -0.200E-01 0.100E+00 0.200E+00 0.000E+00
nmf  -0.200E-01 0.100E+00 0.200E+00 0.000E+00
nmf  -0.200E-01 0.100E+00 0.200E+00 0.000E+00
retn  0.200E+00 0.100E+01 0.200E+02 0.280E+01
retn  0.200E+00 0.100E+01 0.200E+02 0.918E+01
retn  0.200E+00 0.100E+01 0.200E+02 0.673E+01
retn  0.200E+00 0.100E+01 0.200E+02 0.588E+01
retn  0.200E+00 0.100E+01 0.200E+02 0.492E+01
retn -0.200E+00 0.100E+01 0.200E+02 0.000E+00
ak2   0.200E+00 0.500E-01 0.200E+00 0.131E+00
ak2   0.200E+00 0.500E-01 0.200E+00 0.139E+00
ak2   0.200E+00 0.500E-01 0.200E+00 0.992E-01
ak2   0.200E+00 0.500E-01 0.200E+00 0.151E+00
ak2   0.200E+00 0.500E-01 0.200E+00 0.126E+00
ak2  -0.200E+00 0.500E-01 0.200E+00 0.240E-09
ak2fs 0.200E+00 0.500E-01 0.200E+00 0.131E+00
ak2fs 0.200E+00 0.500E-01 0.200E+00 0.635E-01
ak2fs 0.200E+00 0.500E-01 0.200E+00 0.635E-01
ak2fs 0.200E+00 0.500E-01 0.200E+00 0.576E-01
ak2fs 0.200E+00 0.500E-01 0.200E+00 0.576E-01
ak2fs-0.200E+00 0.500E-01 0.200E+00 0.240E-09
lzf   0.100E+00 0.100E-06 0.100E+04 0.213E-05
pwr   0.100E-01 0.500E+00 0.300E+01 0.194E+01
a5   -0.100E-02 0.983E+00 0.992E+00 0.984E+00
R2    0.500E-01 0.300E+00 0.300E+01 0.153E+01
R2    0.500E-01 0.300E+00 0.300E+01 0.242E+01
R2    0.500E-01 0.300E+00 0.300E+01 0.217E+01
```

WATFLOOD BOREAS NSA MAP FILE

```
    3    1    9  123   -2
     2000. 7.62    5    50.305
 6170 6200  514  546

elevations
   0   0   0   0   0   0   0   0 780   0   0   0 778   0   0   0   0
                     925 925 880 781     880 880 780 890
                 900 825 820 810 782 825 835 830 805 850 9151010
                 880 850 850 860 783 784 825 825 810 825 900 960
             875 855 813 810 820 837 785 788 865 875 845 865 875
         880 820 815 820 808 805 835 875 789 825 825 830 860 875
     890 870 880 820 830 820 803 801 799 791 810 810 815 830 885
     890 880 910 855 840 840 830 820 850 792 794 800 815 830 880
             875 855 862 875 840 870 800 830 795 800 810 850 880
             885 845 848 814 810 806 802 799 796 798 800
                 840 818 820 830 840 825 810 797 805 830
                     830 822         875 830 815 798 800 880
                     823 850             832 825 805 825 850
                                         835 825 820 830
                                         838 830 850
   0   0   0   0   0   0   0   0   0   0   0   0   0   0   0   0   0

element areas
   0   0   0   0   0   0   0   0   0   0   0   0   0   0   0   0   0
                      40  55  45   1      13  10   1  20
                  26 100 100  78   1  18  88  80  55 103  75  20
                  24  65 125  80  50 100  85 100 130  88 125  55
              20  80 135  75  90  90 100  80  60  75  87 100  62
          40  95 100 100 100  95 100  75 125 140 125 100 100  77
       5  85 125 100 100 100 100 140 100 100 100 100 100 100  70
      12  90  75 100 100 100 100  85  50 130 100 100  96  48  40
              90  75 100 100 120  55 200  20 100 100  80  21   5
              85 100 100 100 100 100 100 100 100 100  75
              12  60 100 100  95  98 100 100 100 100  75
                   5  95  85      25  85 100 100 100  35
                      42  50          95  75 100 100  10
                                      85 110 100  75
                                      18  70  60
   0   0   0   0   0   0   0   0   0   0   0   0   0   0   0   0   0

drainage directions
 0 0 0 0 0 0 0 0 8 0 0 0 8 0 0 0 0
           4 4 4 8   3 4 8 4
         3 2 2 2 8 4 2 4 8 5 4 5
         4 8 4 8 8 6 6 2 8 6 5 5
       2 4 2 4 6 8 8 6 8 8 4 5 6
     4 2 1 6 2 4 6 6 7 4 4 5 6 7
   2 1 3 8 8 2 2 2 2 8 4 5 6 6 6
   2 8 4 2 8 2 8 3 7 8 6 5 5 6 6
       3 3 7 7 4 2 3 4 8 6 4 8 7
       3 4 6 2 2 2 2 2 8 7 6
         3 1 6 6 2 8 2 8 8 6
           4 8   8 8 8 8 6 6
           1 8     8 8 8 6 6
                   8 2 8 8
                   8 8 8
 0 0 0 0 0 0 0 0 0 0 0 0 0 0 0 0 0
```

```
 basin number
 0 0 0 0 0 0 0 0 4 0 0 0 4 0 0 0 0
           3 3 2 4   3 3 4 3
         3 4 2 4 4 3 2 2 4 2 3 3
         2 2 2 2 4 1 4 3 2 2 2 3
       3 2 5 2 5 4 1 3 3 3 2 2 3
     2 4 5 5 1 1 5 3 5 3 3 3 3 3
   3 2 5 2 2 3 2 1 1 5 3 4 4 4 3
   2 2 2 4 5 5 5 2 4 2 5 4 4 4 3
       4 5 5 2 5 3 5 3 4 4 4 3 3
       2 5 4 5 1 1 4 5 5 4 3
         5 5 5 2 3 5 3 2 4 3
           5 5   3 3 2 5 3 3
           2 3     2 2 5 2 2
                   2 5 5 2
                   5 2 2
 0 0 0 0 0 0 0 0 0 0 0 0 0 0 0 0 0

contour density
 0 0 0 0 0 0 0 011 0 0 011 0 0 0 0
           4 5 411   9 511 6
         4 9 914 6 611 6 8 8 5 9
         71013 6 910101012 9 5 3
      10 91012 6 911 8 7 9 7 3 2
     816131112 8 81215 9 8 9 8 5
   7121612171321181315 6 7 7 610
  10 9121115141417191311 8 9 9 2
      13 9 7 9112014151010 9 7 1
       7 9 813141411 710 8 9
        10101211 91215 9 610
           912  101112 7 8 3
           7 7     71510 8 7
                  10 715 8
                   8 7 5
 0 0 0 0 0 0 0 0 0 0 0 0 0 0 0 0 0

number of channels
 0 0 0 0 0 0 0 0 1 0 0 0 1 0 0 0 0
           5 5 1 1   5 5 1 5
         5 2 1 1 1 5 1 5 1 5 5 5
         5 1 5 1 1 1 1 5 1 5 5 5
       5 1 1 1 5 1 1 5 5 5 5 5 5
     5 1 1 1 1 1 1 5 1 5 5 5 5 5
   5 5 1 1 1 1 2 1 1 1 5 1 1 1 5
   5 5 5 1 1 1 1 1 1 1 1 1 1 1 5
       1 1 1 5 1 5 1 5 1 1 1 5 5
       1 1 1 1 1 1 2 1 1 1 5
         1 1 2 5 5 5 5 1 1 5
           1 2   5 5 5 1 1 5
           1 5     5 5 1 5 5
                   5 1 1 5
                   5 5 5
 0 0 0 0 0 0 0 0 0 0 0 0 0 0 0 0 0

 routing reach number
 0 0 0 0 0 0 0 0 0 0 0 0 0 0 0 0 0
           0 0 0       0   0
         0 0 0 0   0 0 0 0 0
         0 0 0 0 0 0 0 0 0 0
       0 0 0 0 0 0 0 0 0 0 0
     0 0 0 0 0 0 0 0 0 0 0 0 0
   0 0 0 0 0 0 0 0 0 0 0 0 0 0
   0 0 0 0 0 0 0 0 0 0 0 0 0 0
       0 0 0 0 0 0 0 0 0 0 0
       0 0 0 0 0 0 0 0 0 0 0
         0 0 0 0 0 0 0 0 0 0
           0 0   0 0 0 0 0 0
           0 0     0 0 0 0 0
                   0 0 0 0
                   0 0 0
 0 0 0 0 0 0 0 0 0 0 0 0 0 0 0 0 0
```

bare area (barren)

0	0	0	0	0	0	0	0	0	0	0	0	0	0	0	0	0
					9	5	1				0		0			
				7	1	3	5		4	5	6	4	4			
				1	2	2	1	3	0	2	1	0	0			
			7	3	4	1	0	1	0	1	2	0	0			
		2	2	5	2	0	0	1	0	0	0	1	1	0		
	12	18	18	10	22	10	7	0	0	0	0	0	0	0		
	2	15	17	9	16	23	14	9	2	0	0	0	1	3		
			17	1	3	8	13	22	3	0	1	0	0			
			5	1	3	7	1	2	0	1	1	1	2			
				1	1	1	2	2	1	2	1	0	1			
					0	1		6	10	3	1	1	6			
					1	0			2	5	1	1	2			
									1	3	2	1				
									1	1	2					
0	0	0	0	0	0	0	0	0	0	0	0	0	0	0	0	0

forested area (dry forest)

0	0	0	0	0	0	0	0	0	0	0	0	0	0	0	0	0
					86	87	94				92		86			
				88	96	92	92		92	87	76	80	77			
				93	94	92	95	92	95	94	87	85	75			
			87	82	90	94	93	92	98	96	94	89	69			
		94	80	52	70	95	84	75	87	81	75	74	85	92		
	62	64	52	51	29	56	67	65	68	49	39	31	51	70		
	66	45	51	54	46	42	62	78	82	47	57	61	63	65		
			50	64	66	49	42	49	57	49	72	65	84			
			60	52	56	56	65	59	78	71	71	85	85			
				91	76	59	61	65	55	68	77	92	91			
					98	85		73	57	74	82	93	90			
					96	98			62	72	94	96	89			
									85	64	92	92				
									92	93	93					
0	0	0	0	0	0	0	0	0	0	0	0	0	0	0	0	0

low vegetation (wet forest)

0	0	0	0	0	0	0	0	0	0	0	0	0	0	0	0	0
					1	1	1				1		0			
				1	0	1	1		0	0	3	2	2			
				0	0	1	1	0	0	0	1	1	1			
			2	10	3	1	1	0	0	0	0	2	4			
		1	15	41	16	1	12	14	7	12	20	20	2	0		
	24	15	23	36	47	29	22	29	26	35	59	68	45	22		
	31	39	27	33	33	27	21	8	12	45	38	35	31	25		
			32	32	25	38	42	25	34	47	21	24	6			
			30	42	39	30	29	34	14	17	20	2	2			
				7	5	24	30	28	31	14	8	0	0			
					0	4		15	30	11	9	1	0			
					1	0			35	16	0	0	0			
									2	5	2	0				
									0	1	1					
0	0	0	0	0	0	0	0	0	0	0	0	0	0	0	0	0

wetland

0	0	0	0	0	0	0	0	0	0	0	0	0	0	0	0	0
					4	3	4				7		14			
				2	3	4	2		4	8	15	14	17			
				5	4	4	3	5	5	4	11	14	24			
			4	5	3	4	6	7	2	3	4	9	27			
		3	3	2	4	4	4	6	6	7	5	5	12	8		
	2	3	3	2	2	5	4	6	6	9	2	1	4	8		
	1	1	4	3	5	2	3	5	4	8	5	4	5	7		
			1	3	6	5	3	4	5	4	6	11	10			
			4	1	2	6	5	5	8	9	7	9	9			
				1	1	3	7	5	3	16	11	8	8			
					2	2		6	3	12	8	5	4			
					2	2			1	4	5	3	5			
									5	5	4	7				
									2	3	4					
0	0	0	0	0	0	0	0	0	0	0	0	0	0	0	0	0

water covered area

0	0	0	0	0	0	0	0	0	0	0	0	0	0	0	0	0
					0	4	0				0		0			
				2	0	0	0		0	0	0	0	0			
				1	0	1	0	0	0	0	0	0	0			
			0	0	0	0	0	0	0	0	0	0	0			
		0	0	0	8	0	0	4	0	0	0	0	0	0		
	0	0	4	1	0	0	0	0	0	7	0	0	0	0		
	0	0	1	1	0	6	0	0	0	0	0	0	0	0		
			0	0	0	0	0	0	1	0	0	0	0			
			1	4	0	1	0	0	0	2	1	3	2			
				0	17	13	0	0	10	0	3	0	0			
					0	8		0	0	0	0	0	0			
					0	0			0	3	0	0	4			
									7	23	0	0				
									5	2	0					
0	0	0	0	0	0	0	0	0	0	0	0	0	0	0	0	0

WATFLOOD BOREAS NSA PARAMETER FILE

```
# start runtime  14:56: 7
#       rundate  2000- 5-15
# after optimization on r2, lzf & pwr
# now optimizing ak2, ak2fs, re  date 2000-05-17
d1      01    0   00    1    5 5000                          8.99
d2    0.500        1    4
d3      4    5          parameter set for 5 classes May 12/99
a1    0.100E+01 0.110E+02 0.430E+00 0.100E+01 0.985E+00
a6    0.900E+03 0.200E-01 0.000E+00 0.000E+00 0.000E+00
      meander   wetlands  rolling   straight  lakes
lzf   0.100E-04 0.100E-04 0.100E-04 0.100E-04 0.100E-04
pwr   0.220E+01 0.220E+01 0.210E+01 0.220E+01 0.220E+01
r1    0.200E+01 0.200E+01 0.200E+01 0.200E+01 0.200E+01
R2    0.131E+01 0.149E+01 0.149E+01 0.120E+01 0.149E+01
      barren    dryforest wetforest wetland   water     impervious
ds    0.100E+01 0.200E+01 0.300E+01 0.100E+10 0.000E+00
dsfs  0.100E+01 0.200E+01 0.300E+01 0.100E+10 0.000E+00
Re    0.800E-01 0.800E-01 0.800e-01 0.600E-03 0.100E+00
AK    0.130E+01 0.147E+02 0.300E+01 0.400E+03-0.100E+00
AKfs  0.130E+01 0.200E+01 0.320E+01 0.202E+03-0.100E+00
retn  0.313E+02 0.200E+02 0.100E+03 0.229E+00 0.100E+00
ak2   0.600E-01 0.760E-01 0.920E-01 0.796E-09 0.100E-02
ak2fs 0.300E-01 0.380E-01 0.460E-01 0.100E-09 0.100E-02
R3    0.197E+02 0.848E+01 0.197E+02 0.898E+01 0.400E+01
R3fs  0.100E+02 0.100E+02 0.200E+02 0.100E+02 0.400E+01
r4    0.100E+01 0.100E+02 0.100E+02 0.100E+02 0.100E+02
ch    0.100E+01 0.900E+00 0.700E+00 0.700E+00 0.600E+00
MF    0.165E+00 0.122E+00 0.122E+00 0.150E+00 0.165E+00 0.150E+00
BASE -0.100E+01-0.100E+01-0.100E+01-0.100E+01-0.100E+01-0.100E+01
NMF   0.100E+00 0.100E+00 0.100E+00 0.100E+00 0.100E+00 0.100E+00
UADJ  0.000E+00 0.000E+00 0.000E+00 0.000E+00 0.000E+00 0.000E+00
TIPM  0.200E+00 0.200E+00 0.200E+00 0.200E+00 0.200E+00 0.200E+00
RHO   0.333E+00 0.333E+00 0.333E+00 0.333E+00 0.333E+00 0.333E+00
WHCL  0.350E-01 0.350E-01 0.350E-01 0.350E-01 0.350E-01 0.350E-01
fmadj     0.000     0.000     0.000     0.000     0.000     0.000
flgev      2.00       1 = pan; 2 = Hargreaves; 3 = Priestley-Taylor
albed      0.11
aw-a       0.18      0.11      0.11      0.11      0.11
fpet       1.00      3.00      2.00      2.00      1.00
ftal       1.00      0.70      0.70      1.00      1.00
flint        1.        1.        1.        1.        1.
fcap       0.15      0.15      0.15      0.15      0.15
ffcap      0.10      0.10      0.10      0.10      0.10
spore      0.30      0.30      0.30      0.30      0.30
tempa       40.
tempa       50.
tempa      500.
tton         0.
lat.        50.
dif-m 10.2 12.3 12.1 12.3 14.3 14.2 13.8 14.0 13.1 10.6  8.2  9.3
humid 69.5 70.5 72.5 65.5 60.0 64.5 69.0 68.5 73.5 68.0 74.5 72.5
meanp 95.1 95.1 95.1 95.1 95.1 95.1 95.1 95.1 95.1 95.1 95.1 95.1
ti2    jan  feb  mar  apr  may  jun  jul  aug  sep  oct  nov  dec
h1    0.01 0.01 0.01 0.01 0.50 0.50 0.50 0.50 0.50 0.25 0.01 0.01
h2    1.10 1.10 1.10 1.10 1.50 1.80 1.80 1.80 1.80 1.10 1.10 1.10
h3    0.55 0.55 0.55 0.55 0.75 0.90 0.90 0.90 0.90 0.55 0.55 0.55
h4    0.55 0.55 0.55 0.55 0.75 0.90 0.90 0.90 0.90 0.55 0.55 0.55
h5    0.01 0.01 0.01 0.01 0.01 0.01 0.01 0.01 0.01 0.01 0.01 0.01
ti3       delta       low      high parameter
AK   -0.200E-01 0.400E-02 0.500E+01 0.130E+01
AK   -0.200E-01 0.400E-01 0.200E+02 0.147E+02
AK   -0.200E-01 0.400E-02 0.500E-01 0.300E+01
AK   -0.200E-01 0.400E-01 0.500E+01 0.400E+00
AKfs -0.200E-01 0.400E-02 0.500E+00 0.130E+01
AKfs -0.200E-01 0.400E-01 0.200E+02 0.200E+01
AKfs -0.200E-01 0.400E-02 0.500E-01 0.320E+01
AKfs -0.200E-01 0.400E-01 0.500E+01 0.202E+03
```

```
Re   -0.200E-01 0.500E-03 0.200E+00 0.776E-01
Re   -0.200E-01 0.500E-03 0.200E+00 0.894E-01
Re   -0.200E-01 0.500E-03 0.200E+00 0.970E-01
Re   -0.200E-01 0.500E-03 0.200E+00 0.100E-01
R3   -0.200E-01 0.100E+01 0.250E+02 0.197E+02
R3   -0.200E-01 0.100E+01 0.100E+02 0.848E+01
R3   -0.200E-01 0.100E+01 0.250E+02 0.197E+02
R3   -0.200E-01 0.100E+01 0.100E+02 0.898E+01
fpet -0.200E-01 0.100E+00 0.100E+01 0.100E+01
fpet -0.200E-01 0.100E+00 0.100E+01 0.300E+01
fpet -0.200E-01 0.100E+00 0.100E+01 0.200E+01
fpet -0.200E-01 0.100E+00 0.100E+01 0.200E+01
ftal -0.200E-01 0.100E+00 0.100E+01 0.100E+01
ftal -0.200E-01 0.100E+00 0.100E+01 0.700E+00
ftal -0.200E-01 0.100E+00 0.100E+01 0.700E+00
ftal -0.200E-01 0.100E+00 0.100E+01 0.100E+01
MF   -0.500E-01 0.500E-01 0.450E+00 0.165E+00
MF   -0.500E-01 0.500E-01 0.500E+00 0.122E+00
MF   -0.500E-01 0.500E-01 0.450E+00 0.122E+00
MF   -0.500E-01 0.500E-01 0.550E+00 0.150E+00
BASE -0.200E-02-0.500E+01 0.500E+01-0.100E+01
BASE -0.200E-02-0.500E+01 0.500E+01-0.100E+01
BASE -0.200E-02-0.500E+01 0.500E+01-0.100E+01
BASE -0.200E-02-0.500E+01 0.500E+01-0.100E+01
NMF  -0.100E-02-0.500E-01 0.500E+00 0.100E+00
NMF  -0.100E-02-0.500E-01 0.500E+00 0.100E+00
NMF  -0.100E-02-0.500E-01 0.500E+00 0.100E+00
NMF  -0.100E-02-0.500E-01 0.500E+00 0.100E+00
retn -0.200E-01 0.100E-01 0.300E+00 0.313E+02
retn -0.200E-01 0.100E-01 0.300E+00 0.200E+02
retn -0.200E-01 0.100E-01 0.300E+00 0.100E+03
retn -0.200E-01 0.100E-01 0.300E+00 0.229E+00
ak2  -0.200E-01 0.100E-02 0.200E+00 0.600E-01
ak2  -0.200E-01 0.100E-02 0.200E+00 0.760E-01
ak2  -0.200E-01 0.100E-02 0.200E+00 0.920E-01
ak2  -0.200E-01 0.100E-02 0.200E+00 0.796E-09
ak2fs-0.200E-01 0.100E-02 0.200E+00 0.300E-01
ak2fs-0.200E-01 0.100E-02 0.200E+00 0.380E-01
ak2fs-0.200E-01 0.100E-02 0.200E+00 0.460E-01
ak2fs-0.200E-01 0.100E-02 0.200E+00 0.100E-09
lzf  -0.200E-01 0.500E-06 0.500E-03 0.130E-05
lzf  -0.200E-01 0.500E-06 0.500E-03 0.121E-04
lzf  -0.200E-01 0.500E-06 0.500E-03 0.885E-05
lzf  -0.200E-01 0.500E-06 0.500E-03 0.131E-05
lzf  -0.200E-01 0.500E-06 0.500E-03 0.142E-05
pwr  -0.200E-01 0.300E+00 0.400E+01 0.376E+00
pwr  -0.200E-01 0.300E+00 0.400E+01 0.211E+01
pwr  -0.200E-01 0.300E+00 0.400E+01 0.210E+01
pwr  -0.200E-01 0.300E+00 0.400E+01 0.720E+00
pwr  -0.200E-01 0.300E+00 0.400E+01 0.449E+00
a5   -0.100E-02 0.980E+00 0.999E+00 0.985E+00
R2   -0.200E-01 0.100E+00 0.150E+01 0.131E+00
R2   -0.200E-01 0.100E+00 0.150E+01 0.149E+01
R2   -0.200E-01 0.100E+00 0.150E+01 0.149E+01
R2   -0.200E-01 0.100E+00 0.150E+01 0.120E+01
R2   -0.200E-01 0.100E+00 0.150E+01 0.149E+01
```

WATFLOOD BOREAS SSA MAP FILE

```
    3    1    9  744   -0
       2000 7.62    0    7 1.00
 5964 5998  488  526

elevations
   0   0   0   0   0   0   0   0   0   0   0   0   0   0   0   0   0   0   0   0   0
   0   0   0 625 614   0   0   0   0   0   0   0   0   0   0   0   0   0   0   0   0
   0   0 677 617 609   0   0   0 609 607   0   0   0   0   0   0   0   0   0   0   0
   0   0 663 617 608 611   0   0 608 604 593 587   0   0   0   0   0   0   0   0   0
   0   0 609 608 607 610 609 616 611 603 590 581   0   0   0   0   0   0   0   0   0
   0   0 617 608 604 605 607 608 607 599 583 575 569   0   0   0   0   0   0   0   0
   0   0   0 617 605 601 604 602 611 594 588 569 564 561 558 532   0   0   0   0   0
   0   0 623 594 602 599 595 593 595 591 582 564 558 556 552 526   0   0   0   0   0
   0 610 591 587 591 588 595 585 582 584 573 547 541 546 539 515 523   0   0   0   0
   0 591 586 583 572 577 587 584 577 568 568 551 533 530 535 509 511   0   0   0   0
   0 595 585 572 568 568 579 585 578 570 557 537 524 525 522 507 514   0   0   0   0
   0 604 602 590 567 565 570 573 565 564 546 533 520 527 514 505 512   0   0   0   0
   0 565 564 564 563 562 567 565 565 558 534 528 518 511 509 503 543   0   0   0   0
   0 566 564 563 562 576 559 557 553 542 537 545 531 508 506 498 494 506   0   0   0
   0   0 564 563 565 561 560 564 561 557   0   0   0 524 504 498 487 498 501   0   0
   0   0   0   0   0   0   0   0   0   0   0   0   0   0 520 493 486 481 477   0   0
   0   0   0   0   0   0   0   0   0   0   0   0   0   0   0 511 499 495 474 469   0
   0   0   0   0   0   0   0   0   0   0   0   0   0   0   0   0   0   0   0   0   0

element areas
   0   0   0   0   0   0   0   0   0   0   0   0   0   0   0   0   0   0   0   0   0
   0   0   0  45  23   0   0   0   0   0   0   0   0   0   0   0   0   0   0   0   0
   0   0  12  96  80   0   0   0  18   4   0   0   0   0   0   0   0   0   0   0   0
   0   0  13  97 100  18   0   0  63  94  61   8   0   0   0   0   0   0   0   0   0
   0   0   3  95 100  59  57  88  99 100 100  63   0   0   0   0   0   0   0   0   0
   0   0  15  98 100 100 100 100 100 100 100 100  27   0   0   0   0   0   0   0   0
   0   0   0  82 100 100 100 100 100 100 100 100  90  86  97 101   0   0   0   0   0
   0   0  43 100 100 100 100 100 100 100 100 100 100 100 100  88   0   0   0   0   0
   0  50 101 100 100 100 100 100 100 100 100 100 100 100 100  99   5   0   0   0   0
   0  77 100 100 100 100 100 100 100 100 100 100 100 100 100 100  36   0   0   0   0
   0  53 100 100 100 100 100 100 100 100 100 100 100 100 100 100  70   0   0   0   0
   0  50 100 100 100 100 100 100 100 100 100 100 100 100 100 100  58   0   0   0   0
   0  78 100 100 100 100 100 100 100 100 100  65  78 148 100 100  64   0   0   0   0
   0  40  98 100 100 100 100 100 100  89  55  70  78 100 100 100  88   5   0   0   0
   0   0  27  49  50  65  47  43  30   2   0   0   0  21  77 100  25  89  10   0   0
   0   0   0   0   0   0   0   0   0   0   0   0   0   0   6  89 175 100  37   0   0
   0   0   0   0   0   0   0   0   0   0   0   0   0   0   0  10  15  27   7   0   0
   0   0   0   0   0   0   0   0   0   0   0   0   0   0   0   0   0   0   0   0   0

drainage direction
 0 0 0 0 0 0 0 0 0 0 0 0 0 0 0 0 0 0 0 0 0
 0 0 0 3 4 0 0 0 0 0 0 0 0 0 0 0 0 0 0 0 0
 0 0 2 2 4 0 0 0 4 4 0 0 0 0 0 0 0 0 0 0 0
 0 0 2 4 4 6 0 0 2 4 4 4 0 0 0 0 0 0 0 0 0
 0 0 2 2 4 6 4 4 4 3 2 4 0 0 0 0 0 0 0 0 0
 0 0 2 3 3 4 4 6 3 4 2 4 4 0 0 0 0 0 0 0 0
 0 0 0 4 8 3 3 3 2 4 8 3 4 4 2 4 0 0 0 0 0
 0 0 3 4 4 2 3 4 4 2 2 2 4 4 4 4 0 0 0 0 0
 0 4 4 3 4 4 4 2 4 4 4 3 3 6 2 4 6 0 0 0 0
 0 3 3 4 4 4 4 2 2 3 4 2 4 4 2 4 6 0 0 0 0
 0 2 2 3 4 4 4 4 2 3 2 4 4 6 3 4 6 0 0 0 0
 0 4 4 4 2 4 4 4 3 4 4 2 4 2 3 4 6 0 0 0 0
 0 2 3 4 4 3 4 4 3 2 2 2 2 4 2 4 5 0 0 0 0
 0 8 2 2 3 4 2 2 2 2 8 2 2 2 4 3 4 5 0 0 0
 0 0 8 8 8 2 8 8 8 8 0 0 0 2 2 4 4 6 4 0 0
 0 0 0 0 0 0 0 0 0 0 0 0 0 0 1 2 2 2 4 0 0
 0 0 0 0 0 0 0 0 0 0 0 0 0 0 0 1 8 8 2 2 0
 0 0 0 0 0 0 0 0 0 0 0 0 0 0 0 0 0 0 0 0 0
```

```
channel class
 0 0 0 0 0 0 0 0 0 0 0 0 0 0 0 0 0 0 0 0 0
 0 0 0 3 3 0 0 0 0 0 0 0 0 0 0 0 0 0 0 0 0
 0 0 3 3 2 0 0 0 2 2 0 0 0 0 0 0 0 0 0 0 0
 0 0 3 3 2 3 0 0 2 2 2 2 0 0 0 0 0 0 0 0 0
 0 0 3 5 5 3 2 2 3 2 2 2 0 0 0 0 0 0 0 0 0
 0 0 3 5 5 2 5 5 2 2 2 2 5 0 0 0 0 0 0 0 0
 0 0 0 3 2 5 2 2 3 5 3 2 4 2 3 2 0 0 0 0 0
 0 0 3 3 3 2 4 2 2 5 4 2 5 2 3 2 0 0 0 0 0
 0 3 3 2 2 2 2 4 5 5 2 4 2 3 2 2 3 0 0 0 0
 0 2 3 2 2 2 2 5 4 4 2 2 4 4 3 2 3 0 0 0 0
 0 3 2 2 5 5 2 2 2 2 4 2 4 4 4 2 2 0 0 0 0
 0 3 3 2 2 1 2 2 2 2 2 2 4 2 2 2 3 0 0 0 0
 0 3 5 5 5 2 2 2 2 2 4 4 4 1 2 2 3 0 0 0 0
 0 3 5 5 5 3 2 2 4 4 4 2 2 1 1 2 1 3 0 0 0
 0 0 3 2 3 2 2 3 3 3 0 0 0 3 1 1 2 4 3 0 0
 0 0 0 0 0 0 0 0 0 0 0 0 0 0 3 1 1 1 1 0 0
 0 0 0 0 0 0 0 0 0 0 0 0 0 0 0 3 3 3 1 1 0
 0 0 0 0 0 0 0 0 0 0 0 0 0 0 0 0 0 0 0 0 0

number of contours
 0 0 0 0 0 0 0 0 0 0 0 0 0 0 0 0 0 0 0 0 0
 0 0 014 9 0 0 0 0 0 0 0 0 0 0 0 0 0 0 0 0
 0 016 8 5 0 0 0 2 1 0 0 0 0 0 0 0 0 0 0 0
 0 010 6 3 1 0 0 1 2 3 3 0 0 0 0 0 0 0 0 0
 0 010 5 3 1 4 6 3 2 2 5 0 0 0 0 0 0 0 0 0
 0 012 6 2 1 2 4 4 3 3 3 3 0 0 0 0 0 0 0 0
 0 0 013 1 3 3 5 6 4 4 1 3 6 610 0 0 0 0 0
 0 0 8 8 2 4 6 3 5 4 3 5 4 4 6 7 0 0 0 0 0
 0 8 7 2 4 4 2 3 3 6 3 5 3 3 4 7 8 0 0 0 0
 0 6 1 3 7 5 2 1 2 9 4 3 5 4 5 711 0 0 0 0
 011 4 5 1 3 5 3 2 2 5 5 3 3 3 3 5 0 0 0 0
 01111 8 3 4 1 1 1 2 5 3 6 2 3 1 4 0 0 0 0
 01011 4 4 5 3 3 1 3 4 5 6 6 4 3 3 0 0 0 0
 0 6 4 1 1 6 3 6 6 8 7 3 5 5 6 3 6 7 0 0 0
 0 2 5 1 3 4 4 3 3 3 0 0 0 3 5 5 7 3 5 0 0
 0 0 0 0 0 0 0 0 0 0 0 0 0 0 3 7 7 4 8 0 0
 0 0 0 0 0 0 0 0 0 0 0 0 0 0 0 3 5 3 3 5 0
 0 0 0 0 0 0 0 0 0 0 0 0 0 0 0 0 0 0 0 0 0

number of channels
 5 5 5 5 5 5 5 5 5 5 5 5 5 5 5 5 5 5 5 5 5
 5 5 5 5 5 5 5 5 5 5 5 5 5 5 5 5 5 5 5 5 5
 5 5 5 5 5 5 5 5 5 5 5 5 5 5 5 5 5 5 5 5 5
 5 5 5 5 5 5 5 5 5 5 5 5 5 5 5 5 5 5 5 5 5
 5 5 5 5 5 5 5 5 5 5 5 5 5 5 5 5 5 5 5 5 5
 5 5 5 5 1 5 5 1 5 5 1 1 1 5 5 5 5 5 5 5 5
 5 5 5 5 5 1 5 1 1 1 1 1 1 5 5 1 5 5 5 5 5
 5 5 5 5 5 5 1 5 1 1 1 1 3 5 5 1 5 5 5 5 5
 5 5 5 5 5 5 5 1 1 5 5 1 2 1 1 2 5 5 5 5 5
 5 5 5 5 1 5 5 1 1 1 5 1 1 1 5 1 5 5 5 5 5
 5 5 5 1 2 1 5 5 5 5 1 1 1 1 1 1 5 5 5 5 5
 5 5 5 1 3 2 5 5 5 1 5 1 2 5 5 2 5 5 5 5 5
 5 5 5 1 5 1 5 1 5 2 2 1 2 1 5 1 5 5 5 5 5
 5 5 5 5 5 5 2 1 1 1 1 5 5 1 1 1 1 5 5 5 5
 5 5 5 5 5 5 1 5 5 5 5 5 5 5 1 1 1 1 5 5 5
 5 5 5 5 5 5 5 5 5 5 5 5 5 5 5 1 2 1 1 5 5
 5 5 5 5 5 5 5 5 5 5 5 5 5 5 5 5 5 5 1 1 5
 5 5 5 5 5 5 5 5 5 5 5 5 5 5 5 5 5 5 5 5 5
```

routing reach number

```
 0 0 0 0 0 0 0 0 0 0 0 0 0 0 0 0 0 0 0 0 0
 0 0 0 0 0 0 0 0 0 0 0 0 0 0 0 0 0 0 0 0 0
 0 0 0 0 0 0 0 0 0 0 0 0 0 0 0 0 0 0 0 0 0
 0 0 0 0 0 0 0 0 0 0 0 0 0 0 0 0 0 0 0 0 0
 0 0 0 0 0 0 0 0 0 0 0 0 0 0 0 0 0 0 0 0 0
 0 0 0 0 0 0 0 0 0 0 0 0 0 0 0 0 0 0 0 0 0
 0 0 0 0 0 0 0 0 0 0 0 0 0 0 0 0 0 0 0 0 0
 0 0 0 0 0 0 0 0 0 0 0 0 0 0 0 0 0 0 0 0 0
 0 0 0 0 0 0 0 0 0 0 0 0 0 0 0 0 0 0 0 0 0
 0 0 0 0 0 0 0 0 0 0 0 0 0 0 0 0 0 0 0 0 0
 0 0 0 0 0 0 0 0 0 0 0 0 0 0 0 0 0 0 0 0 0
 0 0 0 0 0 0 0 0 0 0 0 0 0 0 0 0 0 0 0 0 0
 0 0 0 0 0 0 0 0 0 0 0 0 0 0 0 0 0 0 0 0 0
 0 0 0 0 0 0 0 0 0 0 0 0 0 0 0 0 0 0 0 0 0
 0 0 0 0 0 0 0 0 0 0 0 0 0 0 0 0 0 0 0 0 0
 0 0 0 0 0 0 0 0 0 0 0 0 0 0 0 0 0 0 0 0 0
 0 0 0 0 0 0 0 0 0 0 0 0 0 0 0 0 0 0 0 0 0
 0 0 0 0 0 0 0 0 0 0 0 0 0 0 0 0 0 0 0 0 0
```

impervious

```
   0   0   0   0   0   0   0   0   0   0   0   0   0   0   0   0   0   0   0   0
   0   0   0   0   0   0   0   0   0   0   0   0   0   0   0   0   0   0   0   0
   0   0   0   0   0   0   0   0   0   0   0   0   0   0   0   0   0   0   0   0
   0   0   0   0   0   0   0   0   0   0   0   0   0   0   0   0   0   0   0   0
   0   0   0   0   0   0   0   0   0   0   0   0   0   0   0   0   0   0   0   0
   0   0   0   0   0   0   0   0   0   0   0   0   0   0   0   0   0   0   0   0
   0   0   0   0   0   0   0   0   0   0   0   0   0   0   0   0   0   0   0   0
   0   0   0   0   0   0   0   0   0   0   0   0   0   0   0   0   0   0   0   0
   0   0   0   0   0   0   0   0   0   0   0   0   0   0   0   0   0   0   0   0
   0   0   0   0   0   0   0   0   0   0   0   0   0   0   0   0   0   0   0   0
   0   0   0   0   0   0   0   0   0   0   0   0   0   0   0   0   0   0   0   0
   0   0   0   0   0   0   0   0   0   0   0   0   0   0   0   0   0   0   0   0
   0   0   0   0   0   0   0   0   0   0   0   0   0   0   0   0   0   0   0   0
   0   0   0   0   0   0   0   0   0   0   0   0   0   0   0   0   0   0   0   0
   0   0   0   0   0   0   0   0   0   0   0   0   0   0   0   0   0   0   0   0
   0   0   0   0   0   0   0   0   0   0   0   0   0   0   0   0   0   0   0   0
   0   0   0   0   0   0   0   0   0   0   0   0   0   0   0   0   0   0   0   0
   0   0   0   0   0   0   0   0   0   0   0   0   0   0   0   0   0   0   0   0
```

wet conifer

```
  14  46  50  50  12  23  32  15   9  34  39  11   0   4   2   2   2   3   0   2
   0  33  34  29  11  27  27   9   7  25  43   9   1   3   2   0   2   1   1   0
   9  54  16  17  36  34  38  44  19  33  24  30   6   8   1   0   2   2   0   0
   3  29  11  36  20  33  18  43  28  38  43  35  33  14   2   2   1   0   0   0
   1  23  29  44  15   5  13  34  46  27  32  32  50  31   2   5   3   0   0   0
   4   1  34  22  40  21  22  13  19  39  56  35  45  37   8   2   2   3   4   1
   0   1  45  43   7  15  36  38  45  29  74  33  49  24  19   5   1   1   4   3
  37  50  54  36  30  33  47  33  42  35  66  64  49  41   5  15   2   8   3   0
  29  30  31  44  47  30  43  37  51  35  57  65  37  41  27  33  11   5   3   1
  43  17  35  42  34  26  41  28  48  45  45  38  35  29  22  27  19   1   2   4
  41  23  35  10   9  21  47  52  60  51  38  38  27   1  19  23   3   0   4  10
  29  27  44  50  23  22  39  54  53  41  28  29  22  12  51   6   0   0   9  33
  29  16  14  16  16  14  27  39  41  30  47  57  39  16  33  21   2   0   1  14
  40  31  11   2   3   5  20  25  35  49  59  67  46  64  26  35  18  20   6  15
   6  22  14  21  18   4   8   3  26  40  46  51  42  54  24   9  14  20  29  38
   7  12  13  19  21  15  30  42  57  68  33  24  41  57  46  48  12   6  16  36
   4   1  13  15  14  16  25  47  45  51  28  27  59  45  70  70  16   5  11  55
  11   1   6   5  33  23  14  42  37  31  38  51  33  29  26  63  43  20   3  39
```

dry conifer + O+M reg.

14	6	13	24	11	25	23	28	27	30	51	16	6	10	35	63	61	41	25	53
3	16	17	15	34	25	19	8	12	35	46	46	16	14	29	40	48	53	37	24
5	13	17	21	30	22	30	25	51	38	43	63	28	28	36	26	32	29	34	9
2	11	11	22	31	19	26	19	45	44	39	46	31	31	43	39	35	13	23	10
1	15	22	20	22	23	28	17	35	55	47	24	28	29	37	63	48	6	18	9
3	0	18	11	20	37	19	31	52	50	36	23	26	39	47	44	29	13	33	26
1	1	16	29	15	31	32	40	24	35	21	47	27	50	45	44	25	23	15	39
25	24	31	32	32	28	45	26	33	43	25	24	29	34	57	49	35	49	41	38
27	36	42	30	39	49	49	32	14	32	25	22	31	30	37	37	27	32	51	34
33	38	42	30	37	35	34	19	16	13	22	24	34	47	54	49	49	48	55	53
32	22	21	14	17	33	23	19	10	21	14	26	36	54	46	28	58	64	56	51
20	15	11	29	23	36	21	19	20	22	19	20	40	19	29	28	39	29	46	25
23	22	8	4	10	22	11	11	33	33	20	14	14	27	29	36	76	57	38	27
28	23	13	2	4	3	9	13	21	12	8	13	10	14	44	26	32	30	38	34
54	42	12	19	19	7	5	5	23	30	19	20	24	12	38	5	37	45	25	23
48	51	36	30	29	21	24	31	20	15	28	25	41	23	34	22	34	53	42	33
7	12	44	40	37	20	24	26	21	16	30	40	23	29	20	15	20	66	41	29
11	3	23	15	25	14	16	15	19	19	26	22	39	48	42	24	8	31	40	29

mixed + decid.

21	46	13	17	26	11	16	41	48	21	5	27	71	56	33	5	3	4	61	36
7	43	33	46	25	7	16	61	62	10	6	20	66	65	48	56	22	5	36	70
17	27	53	36	7	6	4	12	16	8	4	1	42	52	37	66	28	42	49	82
22	58	58	21	19	3	6	11	3	3	2	1	14	23	38	23	26	77	65	82
26	32	41	19	19	21	11	16	9	9	3	1	2	7	20	18	15	65	59	81
29	0	17	20	7	5	1	2	6	2	1	4	2	8	17	32	35	17	15	28
7	0	6	10	16	2	2	1	25	12	2	2	4	25	35	20	32	8	4	17
29	17	10	5	5	4	1	3	5	3	1	3	4	9	18	11	21	16	7	19
27	18	6	4	1	1	1	6	1	9	4	8	10	4	1	8	16	25	11	4
11	12	2	1	3	1	4	5	3	27	28	18	4	3	0	5	23	27	19	20
9	21	9	9	8	4	0	4	1	11	37	24	4	0	2	9	7	20	26	25
9	31	15	9	11	3	3	3	4	7	45	22	2	1	7	13	14	8	13	20
13	23	15	6	25	46	19	17	9	22	16	7	3	1	16	18	3	2	2	22
29	37	35	9	8	81	48	49	32	29	21	10	34	13	4	9	2	1	7	18
6	18	44	29	19	65	67	66	35	9	6	3	13	28	28	2	5	8	19	24
3	8	27	30	42	31	15	10	6	2	6	2	5	9	2	11	9	12	12	11
1	3	12	18	2	28	28	11	7	5	19	6	9	12	5	13	37	12	19	7
15	2	28	68	15	11	20	24	8	10	3	6	13	5	6	0	46	38	20	25

disturbed + young reg.

13	0	4	3	20	19	4	2	0	0	0	1	0	1	2	0	3	1	6	3
12	0	0	2	15	6	1	1	8	0	0	0	0	0	0	0	1	3	9	1
16	0	4	13	13	1	0	0	0	0	0	0	0	0	1	1	0	3	7	3
26	1	17	7	9	0	5	11	1	0	0	0	0	3	3	1	1	3	5	1
23	1	3	0	7	25	11	13	1	0	0	0	0	7	4	0	0	16	6	4
2	1	2	8	5	1	0	14	5	0	0	3	1	0	3	6	3	14	8	0
0	1	6	5	13	8	0	0	0	0	0	2	3	0	0	1	8	4	12	4
1	1	1	8	4	1	0	0	0	0	0	0	0	4	6	1	10	1	1	1
0	7	5	0	0	0	0	1	0	0	0	0	0	6	2	7	3	13	0	12
0	3	0	0	1	0	0	0	0	0	0	0	0	7	14	0	1	8	4	4
5	17	0	0	0	0	0	0	0	0	0	0	16	19	3	0	2	5	1	1
0	17	23	0	0	1	0	0	0	0	0	0	8	38	0	0	20	30	13	11
0	11	12	1	3	0	1	0	0	0	0	3	23	19	8	0	3	21	31	26
0	4	9	2	13	0	1	0	0	1	4	0	5	4	8	1	15	27	31	22
0	0	23	18	29	12	4	3	1	0	0	0	0	3	5	65	21	9	12	9
0	0	4	6	1	8	0	0	0	0	0	0	0	0	0	14	33	12	10	2
1	0	6	0	1	6	0	0	0	0	0	0	0	0	0	1	21	10	18	1
3	0	4	2	1	10	2	0	4	4	0	0	1	0	0	0	0	3	20	2

recent burn

16	0	3	1	8	5	2	1	0	0	0	0	1	1	1	0	1	0	1	1
4	1	0	0	4	2	0	1	1	0	0	0	0	0	1	0	0	0	1	0
2	0	0	1	5	2	0	0	0	0	0	0	0	1	1	0	0	0	2	2
1	0	0	2	3	5	2	4	1	0	0	0	0	1	0	0	0	0	1	0
0	0	0	0	5	6	5	4	1	0	0	1	0	0	0	0	1	1	2	1
0	0	1	4	2	1	1	7	1	0	0	1	3	1	1	1	1	1	2	2
0	1	3	2	10	5	0	1	0	0	0	0	0	0	0	1	1	0	0	0
1	2	1	3	12	2	0	0	1	0	1	0	1	0	6	2	5	2	0	2
1	1	1	2	1	1	0	1	0	0	0	0	0	0	0	2	2	5	1	2
0	0	0	1	1	0	0	0	0	1	0	0	0	0	1	1	2	4	3	1
3	2	1	1	1	8	0	0	2	0	1	0	1	0	2	0	3	4	2	1
3	1	2	0	1	2	0	1	0	0	0	0	0	1	0	0	3	4	7	2
0	4	1	0	2	1	0	0	0	0	0	0	1	0	1	2	1	11	6	4
0	0	3	2	2	0	1	1	1	1	0	0	0	0	0	0	1	1	3	2
0	0	0	1	7	1	0	0	0	0	0	0	0	0	0	0	0	0	1	1
12	4	0	1	1	0	0	0	0	0	0	0	0	0	0	0	1	2	1	0
74	40	1	0	1	0	0	0	0	0	0	0	0	0	0	0	1	2	4	0
53	85	3	0	0	1	0	0	0	0	0	0	0	0	0	0	0	2	3	2

wetlands

9	0	6	5	23	17	20	13	2	4	4	21	14	11	17	26	27	40	7	5
5	7	7	8	10	22	28	11	8	30	4	12	13	15	4	4	26	34	15	4
7	5	4	11	9	36	27	19	14	20	28	2	21	9	24	7	21	8	7	4
2	1	4	12	16	40	43	12	22	15	14	15	17	19	13	30	35	7	6	6
2	4	5	10	27	20	32	16	7	5	17	41	16	23	35	11	32	12	13	5
2	0	2	7	14	25	28	30	10	7	5	27	16	13	24	14	24	38	25	43
0	1	5	8	35	28	28	20	3	14	3	12	11	1	1	28	30	33	14	34
2	3	3	9	14	32	6	38	14	7	7	7	16	10	8	21	9	23	48	40
13	8	14	19	11	19	6	23	27	21	14	4	22	16	28	12	5	19	33	28
13	30	21	26	25	38	15	14	31	14	5	21	26	12	5	16	3	11	17	17
10	13	34	66	58	31	25	24	28	16	8	12	14	20	21	40	27	7	10	12
5	6	4	12	41	37	33	24	23	30	7	27	21	28	10	52	24	28	12	7
7	10	5	2	6	17	38	30	17	14	16	17	15	34	12	21	14	9	16	7
2	5	7	3	3	5	16	11	12	8	8	9	3	4	15	20	28	20	13	9
33	18	8	11	8	10	15	21	14	20	28	24	20	2	5	19	20	16	12	4
29	25	20	14	6	24	31	16	18	15	33	48	11	11	16	3	10	16	18	17
13	43	23	27	45	30	23	17	28	28	23	26	7	14	4	1	4	5	6	6
7	8	35	9	25	41	48	19	32	36	32	21	14	18	26	12	2	5	14	3

water

13	2	10	0	0	0	3	0	14	11	1	24	8	17	9	3	3	12	0	0
69	0	9	0	0	11	8	9	4	0	1	13	5	3	16	0	0	3	0	0
43	0	6	0	0	0	0	0	0	0	1	4	2	3	1	0	16	15	1	0
44	0	0	1	2	0	0	0	0	0	1	2	5	10	1	5	1	0	0	0
46	26	0	6	5	0	0	0	1	5	1	2	5	3	2	3	2	0	1	0
59	98	27	29	11	11	28	4	7	2	3	6	7	2	0	0	7	14	14	0
92	96	19	3	3	10	2	0	1	11	1	3	5	0	0	1	4	31	50	3
6	3	1	7	2	0	0	1	4	11	0	1	1	1	0	0	18	1	0	0
2	0	0	1	2	0	0	0	6	3	0	0	0	3	4	2	36	1	0	19
0	0	0	0	1	0	6	33	2	0	0	0	1	2	4	0	4	1	0	2
0	2	1	0	7	3	4	1	0	0	0	0	2	4	8	0	0	0	0	1
33	3	0	0	0	0	4	0	0	0	0	1	6	2	2	0	0	0	0	2
28	13	45	70	39	0	5	2	0	0	0	2	4	4	1	2	1	0	6	1
0	0	22	80	67	5	5	1	0	1	1	0	2	1	3	8	4	1	2	0
0	0	0	0	0	1	1	1	1	0	0	3	1	0	0	1	2	1	1	1
0	0	0	0	0	1	0	0	0	0	0	1	1	0	2	1	0	0	1	1
0	0	0	0	0	0	0	0	0	0	0	1	1	0	0	0	0	0	0	1
0	0	0	0	0	0	0	0	0	0	1	0	1	0	0	0	0	0	0	1

WATFLOOD BOREAS SSA PARAMETER FILE

```
# start runtime  15:26:20
#       rundate  2000-10-17
d1       1    0   00    1    5 2000                          8.99
d2    0.500        1    1
d3       6    5
a1    0.100E+01 0.110E+02 0.430E+00 0.100E+01 0.983E+00
a6    0.900E+03 0.200E-01 0.000E+00 0.000E+00 0.268E+02
      meander   wetland   rolling   straight  lakes
lzf   0.107E-04 0.914E-05 0.947E-05 0.914E-05 0.979E-05
pwr   0.200E+01 0.202E+01 0.213E+01 0.175E+01 0.201E+01
r1    0.200E+01 0.200E+01 0.200E+01 0.200E+01 0.200E+01
R2    0.139E+01 0.170E+01 0.170E+01 0.157E+01 0.170E+01
      wet conif dry conif mixed&dec regener   burn      wetland   water     impervious
ds    0.500E+01 0.500E+01 0.500E+01 0.100E+01 0.200E+01 0.200E+10 0.000E+00
dsfs  0.500E+01 0.500E+01 0.500E+01 0.300E+02 0.300E+02 0.200E+10 0.000E+00
Re    0.314E-01 0.286E-01 0.275E-01 0.275E-01 0.171E-01 0.100E-03 0.100E+00
AK    0.420E+02 0.126E+02 0.270E+02 0.500E+02 0.500E+02 0.200E+03-0.100E+00
AKfs  0.259E+02 0.125E+02 0.270E+02 0.200E+02 0.200E+02 0.200E+03-0.100E+00
retn  0.210E+02 0.220E+02 0.356E+02 0.200E+02 0.220E+02 0.100E+00 0.000E+00
ak2   0.186E+00 0.186E+00 0.173E+00 0.144E+00 0.186E+00 0.349E-09 0.500E-06
ak2fs 0.093E+00 0.093E+00 0.086E+00 0.072E+00 0.093E+00 0.149E-09 0.500E-06
R3    0.300E+02 0.300E+02 0.300E+02 0.920E+03 0.920E+03 0.500E+03 0.300E+02
r3fs  0.300E+02 0.300E+02 0.300E+02 0.500E+03 0.500E+03 0.300E+02 0.300E+02
r4    0.100E+02 0.100E+02 0.100E+02 0.100E+02 0.100E+02 0.100E+02 0.100E+02
ch    0.700E+00 0.900E+00 0.900E+00 0.100E+01 0.100E+01 0.700E+00 0.600E+00
MF    0.112E+00 0.112E+00 0.112E+00 0.112E+00 0.112E+00 0.944E-01 0.110E+00 0.100E+00
BASE -0.548E+00 0.273E+01 0.273E+01 0.273E+01 0.273E+01 0.273E+01 0.000E+00 0.000E+00
NMF   0.660E-01 0.137E+00 0.521E-01 0.102E-01 0.102E-01 0.424E-01 0.800E-01 0.800E-01
UADJ  0.000E+00 0.000E+00 0.000E+00 0.000E+00 0.000E+00 0.000E+00 0.000E+00 0.000E+00
TIPM  0.150E+00 0.150E+00 0.150E+00 0.150E+00 0.150E+00 0.150E+00 0.150E+00 0.150E+00
RHO   0.333E+00 0.333E+00 0.333E+00 0.333E+00 0.333E+00 0.333E+00 0.333E+00 0.333E+00
WHCL  0.350E-01 0.350E-01 0.350E-01 0.350E-01 0.350E-01 0.350E-01 0.350E-01 0.350E-01
DAYGM     0.000     0.000     0.000     0.000     0.000     0.000
flgev      2.00       1 = pan; 2 = Hargreaves; 3 = Priestley-Taylor
albed      1.00
allw       1.03      1.00      0.95      1.03      1.27      0.96      0.96
fpet       2.19      2.03      2.08      1.00      1.00      0.50      1.00
ftal       0.50      0.51      0.51      0.51      0.62      0.73      1.00
flint        1.        1.        1.        0.        0.        1.        0.
fcap       0.25      0.15      0.20      0.18      0.15      0.25      0.01
ffcap      0.10      0.13      0.10      0.12      0.10      0.10      0.01
spore      0.40      0.30      0.30      0.30      0.30      0.40      0.01
tempa       40.
tempa       50.
tempa      500.
tton         0.
lat.        54.
dif-m 10.2 12.3 12.1 12.3 14.3 14.2 13.8 14.0 13.1 10.6  8.2  9.3
humid 69.5 70.5 72.5 65.5 60.0 64.5 69.0 68.5 73.5 68.0 74.5 72.5
meanp 96.5 96.5 96.4 96.3 96.2 96.0 96.2 96.3 96.3 96.2 96.3 96.4
ti2    jan  feb  mar  apr  may  jun  jul  aug  sep  oct  nov  dec
h1    1.80 1.80 1.80 1.80 1.80 1.80 1.80 1.80 2.00 2.00 1.80 1.80
h2    1.30 1.30 1.30 1.30 1.30 1.30 1.30 1.30 2.50 2.50 1.30 1.30
h3    1.10 1.10 1.10 1.50 1.60 1.80 1.80 1.80 2.00 2.00 1.10 1.10
h4    0.01 0.01 0.01 0.01 0.01 0.01 0.01 0.01 0.01 0.01 0.01 0.01
h5    0.01 0.01 0.01 0.01 0.01 0.01 0.01 0.01 0.01 0.01 0.01 0.01
h6    0.05 0.05 0.05 0.05 0.20 0.20 0.20 0.20 0.20 0.05 0.05 0.05
h7    0.01 0.01 0.01 0.01 0.10 0.15 0.20 0.25 0.20 0.10 0.01 0.01
ti3       delta       low      high parameter
AK   -0.200E-01 0.400E+00 0.500E+02 0.420E+02
AK   -0.200E-01 0.400E-01 0.200E+02 0.126E+02
AK   -0.200E-01 0.400E-02 0.500E-01 0.270E+02
AK   -0.200E-01 0.400E-01 0.500E+01 0.500E+02
AK   -0.200E-01 0.400E-02 0.500E-01 0.500E+02
AK   -0.200E-01 0.400E-01 0.500E+01 0.200E+03
AKfs -0.200E-01 0.400E-02 0.500E+00 0.259E+02
```

```
AKfs -0.200E-01 0.400E-01 0.200E+02 0.125E+02
AKfs -0.200E-01 0.400E-02 0.500E-01 0.270E+02
AKfs -0.200E-01 0.400E-01 0.500E+01 0.200E+02
AKfs -0.200E-01 0.400E-02 0.500E-01 0.200E+02
AKfs -0.200E-01 0.400E-01 0.500E+01 0.200E+03
Re   -0.200E-01 0.500E-03 0.100E+00 0.314E-01
Re   -0.200E-01 0.500E-03 0.100E+00 0.286E-01
Re   -0.200E-01 0.500E-03 0.100E+00 0.275E-01
Re   -0.200E-01 0.500E-03 0.100E+00 0.275E-01
Re   -0.200E-01 0.500E-03 0.100E+00 0.171E-01
Re   -0.200E-01 0.500E-05 0.100E-01 0.327E-03
R3   -0.200E-01 0.100E+01 0.250E+02 0.300E+02
R3   -0.200E-01 0.100E+01 0.100E+02 0.300E+02
R3   -0.200E-01 0.100E+01 0.250E+02 0.300E+02
R3   -0.200E-01 0.100E+01 0.100E+02 0.920E+03
R3   -0.200E-01 0.100E+01 0.250E+02 0.920E+03
R3   -0.200E-01 0.100E+01 0.100E+02 0.500E+03
fpet -0.200E-01 0.100E+00 0.300E+01 0.219E+01
fpet -0.200E-01 0.100E+00 0.300E+01 0.203E+01
fpet -0.200E-01 0.100E+00 0.300E+01 0.208E+01
fpet -0.200E-01 0.100E+00 0.300E+01 0.100E+01
fpet -0.200E-01 0.100E+00 0.300E+01 0.100E+01
fpet -0.200E-01 0.100E+00 0.300E+01 0.500E+00
ftal -0.200E-01 0.100E+00 0.120E+01 0.500E+00
ftal -0.200E-01 0.100E+00 0.120E+01 0.510E+00
ftal -0.200E-01 0.100E+00 0.120E+01 0.510E+00
ftal -0.200E-01 0.100E+00 0.120E+01 0.510E+00
ftal -0.200E-01 0.100E+00 0.120E+01 0.620E+00
ftal -0.200E-01 0.100E+00 0.120E+01 0.730E+00
MF    0.500E-01 0.500E-01 0.250E+00 0.112E+00
MF    0.500E-01 0.500E-01 0.250E+00 0.112E+00
MF    0.500E-01 0.500E-01 0.250E+00 0.112E+00
MF    0.500E-01 0.500E-01 0.250E+00 0.112E+00
MF    0.500E-01 0.500E-01 0.250E+00 0.112E+00
MF    0.500E-01 0.500E-01 0.250E+00 0.944E-01
BASE  0.200E-02-0.200E+01 0.300E+01-0.548E+00
BASE  0.200E-02-0.200E+01 0.300E+01 0.200E+01
BASE  0.200E-02-0.200E+01 0.300E+01 0.200E+01
BASE  0.200E-02-0.200E+01 0.300E+01 0.200E+01
BASE  0.200E-02-0.200E+01 0.300E+01 0.200E+01
BASE  0.200E-02-0.200E+01 0.300E+01 0.200E+01
NMF  -0.100E-02-0.500E-01 0.500E+00 0.660E-01
NMF  -0.100E-02-0.500E-01 0.500E+00 0.137E+00
NMF  -0.100E-02-0.500E-01 0.500E+00 0.521E-01
NMF  -0.100E-02-0.500E-01 0.500E+00 0.102E-01
NMF  -0.100E-02-0.500E-01 0.500E+00 0.102E-01
NMF  -0.100E-02-0.500E-01 0.500E+00 0.424E-01
retn  0.200E-01 0.100E+01 0.500E+02 0.210E+02
retn  0.200E-01 0.100E+01 0.500E+02 0.220E+02
retn  0.200E-01 0.100E+01 0.500E+02 0.356E+02
retn  0.200E-01 0.100E+01 0.500E+02 0.200E+02
retn  0.200E-01 0.100E+01 0.500E+02 0.220E+02
retn -0.200E-01 0.100E+01 0.500E+02 0.100E+00
ak2   0.200E-01 0.100E-02 0.200E+00 0.186E+00
ak2   0.200E-01 0.100E-02 0.200E+00 0.186E+00
ak2   0.200E-01 0.100E-02 0.200E+00 0.173E+00
ak2   0.200E-01 0.100E-02 0.200E+00 0.144E+00
ak2   0.200E-01 0.100E-02 0.200E+00 0.186E+00
ak2  -0.200E-01 0.100E-02 0.200E+00 0.349E-09
ak2fs 0.200E-01 0.100E-02 0.200E+00 0.150E+00
ak2fs 0.200E-01 0.100E-02 0.200E+00 0.161E+00
ak2fs 0.200E-01 0.100E-02 0.200E+00 0.186E+00
ak2fs 0.200E-01 0.100E-02 0.200E+00 0.186E+00
ak2fs 0.200E-01 0.100E-02 0.200E+00 0.186E+00
ak2fs-0.200E-01 0.100E-02 0.200E+00 0.349E-09
lzf   0.200E-01 0.500E-05 0.500E-03 0.107E-04
lzf   0.200E-01 0.500E-05 0.500E-03 0.914E-05
lzf   0.200E-01 0.500E-05 0.500E-03 0.947E-05
lzf   0.200E-01 0.500E-05 0.500E-03 0.914E-05
lzf   0.200E-01 0.500E-05 0.500E-03 0.979E-05
pwr   0.200E-01 0.300E+00 0.250E+01 0.200E+01
```

```
pwr   0.200E-01 0.300E+00 0.250E+01 0.202E+01
pwr   0.200E-01 0.300E+00 0.250E+01 0.213E+01
pwr   0.200E-01 0.300E+00 0.250E+01 0.175E+01
pwr   0.200E-01 0.300E+00 0.250E+01 0.201E+01
a5   -0.100E-02 0.980E+00 0.999E+00 0.983E+00
R2    0.200E-01 0.100E+00 0.200E+01 0.139E+01
R2    0.200E-01 0.100E+00 0.200E+01 0.170E+01
R2    0.200E-01 0.100E+00 0.200E+01 0.170E+01
R2    0.200E-01 0.100E+00 0.200E+01 0.157E+01
R2    0.200E-01 0.100E+00 0.200E+01 0.170E+01
```

WATFLOOD FIFE MAP FILE

```
1    1   10  123   -2
     1000.151.5    0    2 1.00
 4313 4334  704  725

elevations
   0   0   0   0   0   0   0   0   0   0   0   0   0   0   0   0   0   0   0   0   0   0
   0   0   0   0 307   0 307   0   0   0   0 368 362 345 324 307 319   0   0   0   0   0
   0 313 307 309 308 325 336 337 383 411 389 366 342 329 323 322 326   0   0   0   0   0
   0 314 319 324 351 339 351 354 376 401 359 351 333 330 364 355 338   0   0   0   0   0
   0 373 332 331 339 354 370 376 377 391 369 366 336 334 352 377   0   0   0   0   0   0
   0 401 345 365 351 365 384 411 403 376 364 349 337 386 376 398 421 425 443 438 460   0
   0   0 381 385 383 380 407 421 403 384 373 354 344 372 391 407 396 400 421 432 443   0
   0 380 385 404 414 407 413 409 424 411 384 368 353 358 367 375 388 406 426 441 453   0
   0 307 370 393 409 397 394 401 421 413 403 376 364 390 399 380 387 403 423 435 449   0
   0   0 385 395 383 381 386 403 416 426 426 404 367 371 417 422 405 416 435 441   0   0
   0 365 369 381 368 373 391 406 427 429 429 409 396 384 396 416 433 441 448   0   0   0
   0 307 350 355 361 384 393 407 411 410 412 435 425 428 406 415 426 453   0   0   0   0
   0 377 353 356 358 364 367 397 387 394 403 414 427 440 423 434 448   0   0   0   0   0
   0 378 370 360 380 403 368 373 381 401 427 421 428 434 439   0   0   0   0   0   0   0
   0 403 371 361 362 398 410 379 386 392 410 421 428 448 457   0   0   0   0   0   0   0
   0 402 379 380 368 377 396 403 394 396 402 411 438 444   0   0   0   0   0   0   0   0
   0 414 405 386 379 380 386 390 404 408 415 416 428 445   0   0   0   0   0   0   0   0
   0   0 420 396 387 396 396 393 416 413 426 437 441 446   0   0   0   0   0   0   0   0
   0   0 425 411 393 395 400 407 413 432 442 438 451   0   0   0   0   0   0   0   0   0
   0   0   0 426 399 406 419 423 418 432 441 453   0   0   0   0   0   0   0   0   0   0
   0   0   0   0 401 402 434 434 427 438 448   0   0   0   0   0   0   0   0   0   0   0
   0   0   0   0   0   0   0   0   0   0   0   0   0   0   0   0   0   0   0   0   0   0

element areas
   0   0   0   0   0   0   0   0   0   0   0   0   0   0   0   0   0   0   0   0   0   0
   0   0   0   0   0   0   0   1   0   0   0   9  25   8  19   0   6   0   0   0   0   0
   0  23   0 133  29  91  69  80  47   8  22  90  96  92 123  97  26   0   0   0   0   0
   0  10  82  68  29  90  71 129 110  71 112 117 133 105  53 159  10   0   0   0   0   0
   0   2 112 138 131 146 107 104  51 124  83  85  60 125  96  52   0   0   0   0   0   0
   0   2  97  57 108 162 114  84 129 109  85 117 106  50 137  64  40  64   5  27   1   0
   0   0  32  40 117 113  65  46 161  84  98  90 123 139 101  73 124  99  88  87  13   0
   0  12  79  94  62  59  77 164  36  85 132  65 134 161 100  99  50  43  88  93  26   0
   0   0  98 127  50  70 105 118  36 108 123 105 111  34 106  93 133 158 104 118  17   0
   0   0  21  46 191 106 117 124 111  49  80  69 128 135  56  69 114 152  54  28   0   0
   0   1  60  49 126 126 101 150 147 118  72  78  98 132 111  85  74  38   3   0   0   0
   0   0  14  96 112  88  46  41  58  98  97  52 102  59 101 120  92   5   0   0   0   0
   0  35 225  19 135 141  83  69 157 114 121 131 102  48 148  32  19   0   0   0   0   0
   0  36  39 157  85  63 159 104 108  84  97  63 143 145  29   2   0   0   0   0   0   0
   0  17 119 102 131  57  34 185  34 141 104  69  90  53   5   0   0   0   0   0   0   0
   0  25  81 115 119  67 131  32 128  67 109 140  38  65   0   0   0   0   0   0   0   0
   0  11  53 138 108 137 166 129  91  37 145  92 127  62   0   0   0   0   0   0   0   0
   0   0  25  67 142  38  38 115 110 147 105  75  81  11   0   0   0   0   0   0   0   0
   0   0   8  88  97 135  63  87  90  90  55  91  16   0   0   0   0   0   0   0   0   0
   0   0   0  12 165  50 101  99 123  89 102   9   0   0   0   0   0   0   0   0   0   0
   0   0   0   0  64  50  22  42  94  97  71   0   0   0   0   0   0   0   0   0   0   0
   0   0   0   0   0   0   0   0   0   0   0   0   0   0   0   0   0   0   0   0   0   0
```

```
drainage direction
 0  0  0  0  0  0  0  0  0  0  0  0  0  0  0  0  0  0  0  0  0  0
 0  0  0  0  0  0  0  0  0  0  0  2  4  4  4  0  6  0  0  0  0  0
 0  2  0  2  8  6  8  6  6  4  2  2  2  2  2  8  8  0  0  0  0  0
 0  8  8  6  6  8  8  8  6  2  2  2  2  8  6  8  8  0  0  0  0  0
 0  2  8  8  6  6  6  8  8  2  8  2  2  8  6  6  0  0  0  0  0  0
 0  2  8  6  8  6  8  6  2  2  2  2  8  6  8  8  4  4  4  4  6  0
 0  0  8  8  8  7  6  2  2  8  8  8  8  4  4  4  4  6  6  6  6  0
 0  4  4  4  4  4  4  4  6  2  2  8  8  6  6  6  6  8  6  6  6  0
 0  0  6  6  6  2  4  6  4  2  8  2  8  4  8  8  6  6  6  6  6  0
 0  0  8  4  4  4  6  6  6  8  2  8  8  6  4  8  8  8  8  8  0  0
 0  4  4  6  4  6  6  6  6  4  4  8  8  8  6  4  4  8  8  0  0  0
 0  0  6  6  6  4  4  6  2  4  4  6  8  2  8  6  6  6  0  0  0  0
 0  2  8  8  6  6  6  6  4  6  6  6  6  4  8  6  8  0  0  0  0  0
 0  2  8  8  6  6  8  6  6  6  6  8  6  6  8  0  0  0  0  0  0  0
 0  2  2  8  6  4  2  8  8  6  4  4  6  4  6  0  0  0  0  0  0  0
 0  2  8  8  8  6  6  2  8  8  6  6  8  6  0  0  0  0  0  0  0  0
 0  8  8  2  8  8  6  6  8  6  8  8  6  6  0  0  0  0  0  0  0  0
 0  0  2  2  8  4  2  8  6  8  6  6  8  6  0  0  0  0  0  0  0  0
 0  0  2  8  8  6  8  6  6  8  8  8  8  0  0  0  0  0  0  0  0  0
 0  0  0  8  8  8  6  8  8  6  6  8  0  0  0  0  0  0  0  0  0  0
 0  0  0  0  8  6  8  8  8  6  6  0  0  0  0  0  0  0  0  0  0  0
 0  0  0  0  0  0  0  0  0  0  0  0  0  0  0  0  0  0  0  0  0  0

basin number
 0  0  0  0  0  0  0  0  0  0  0  0  0  0  0  0  0  0  0  0  0  0
 0  0  0  0  2  0  2  0  0  0  0  2  2  2  1  2  2  0  0  0  0  0
 0  2  2  2  2  2  2  2  2  2  2  2  2  1  1  1  2  0  0  0  0  0
 0  2  1  1  2  2  2  2  2  2  2  2  2  1  2  2  2  0  0  0  0  0
 0  2  2  1  2  2  2  2  2  2  2  2  1  1  2  2  0  0  0  0  0  0
 0  2  2  2  2  2  2  2  2  2  2  2  1  2  2  2  2  2  2  2  2  0
 0  0  2  2  2  2  2  2  2  2  2  2  1  2  2  2  2  2  2  2  2  0
 0  2  2  2  2  2  2  2  2  2  2  2  1  1  1  1  2  2  2  2  2  0
 0  2  2  2  2  2  2  2  2  2  2  2  1  2  2  2  2  2  2  2  2  0
 0  0  2  2  2  2  2  2  2  2  2  2  1  2  2  2  2  2  2  2  0  0
 0  2  2  2  1  1  2  2  2  2  2  2  2  2  2  2  2  2  2  0  0  0
 0  2  1  1  1  2  2  2  2  2  2  2  2  2  2  2  2  2  0  0  0  0
 0  2  1  1  1  1  1  2  1  1  2  2  2  2  2  2  2  0  0  0  0  0
 0  2  2  1  2  2  1  1  1  2  2  2  2  2  2  0  0  0  0  0  0  0
 0  2  2  1  1  2  2  2  1  1  2  2  2  2  2  0  0  0  0  0  0  0
 0  2  2  2  1  1  2  2  2  1  2  2  2  2  0  0  0  0  0  0  0  0
 0  2  2  2  1  1  1  1  2  2  2  2  2  2  0  0  0  0  0  0  0  0
 0  0  2  2  2  2  2  2  2  2  2  2  2  2  0  0  0  0  0  0  0  0
 0  0  2  2  2  2  2  2  2  2  2  2  2  0  0  0  0  0  0  0  0  0
 0  0  0  2  2  2  2  2  2  2  2  2  0  0  0  0  0  0  0  0  0  0
 0  0  0  0  2  2  2  2  2  2  2  0  0  0  0  0  0  0  0  0  0  0
 0  0  0  0  0  0  0  0  0  0  0  0  0  0  0  0  0  0  0  0  0  0

contour
 0  0  0  0  0  0  0  0  0  0  0  0  0  0  0  0  0  0  0  0  0  0
 0  0  0  0  1  0  3  0  0  0  0  3  3  2  1  1  2  0  0  0  0  0
 0  1  2  4  5  4  5  4  4  2  2  3  3  2  5  3  1  0  0  0  0  0
 0  3  2  3  4  4  5  5  4  2  2  2  3  5  5  4  3  0  0  0  0  0
 0  6  3  3  3  4  3  5  3  2  2  3  3  5  4  4  0  0  0  0  0  0
 0  5  4  3  3  3  3  3  2  4  3  2  4  3  4  3  4  5  6  5  2  0
 0  0  3  3  4  3  3  2  2  3  4  3  3  3  3  3  5  3  2  2  2  0
 0  4  3  3  3  4  2  2  3  2  3  3  3  3  4  3  4  2  2  2  2  0
 0  4  2  2  3  2  2  2  2  2  3  4  3  3  4  4  4  3  2  2  1  0
 0  0  2  2  2  3  2  2  2  1  3  3  4  3  3  4  3  4  3  2  0  0
 0  4  3  2  3  2  2  2  2  2  1  3  3  3  3  2  3  3  2  0  0  0
 0  3  3  3  2  2  2  3  3  3  2  2  5  3  3  3  3  2  0  0  0  0
 0  6  2  3  3  3  2  3  3  3  3  3  2  1  4  2  3  0  0  0  0  0
 0  5  4  2  2  4  3  3  2  3  2  2  2  1  2  0  0  0  0  0  0  0
 0  4  3  2  3  3  4  4  3  2  2  2  1  1  2  0  0  0  0  0  0  0
 0  5  3  3  2  4  4  2  3  4  3  3  2  1  0  0  0  0  0  0  0  0
 0  5  3  4  4  3  5  3  3  3  3  3  3  1  0  0  0  0  0  0  0  0
 0  0  1  4  4  4  5  4  3  3  1  1  1  1  0  0  0  0  0  0  0  0
 0  0  2  2  4  4  2  3  2  1  1  1  1  0  0  0  0  0  0  0  0  0
 0  0  0  2  3  3  2  3  3  1  1  1  0  0  0  0  0  0  0  0  0  0
 0  0  0  0  2  2  1  1  2  1  1  0  0  0  0  0  0  0  0  0  0  0
 0  0  0  0  0  0  0  0  0  0  0  0  0  0  0  0  0  0  0  0  0  0
```

```
no of channels
 0 0 0 0 0 0 0 0 0 0 0 0 0 0 0 0 0 0 0 0 0 0
 0 0 0 0 0 0 1 1 0 0 0 1 1 1 1 1 1 0 0 0 0 0
 0 1 2 1 1 1 1 1 3 2 3 1 1 1 1 1 2 0 0 0 0 0
 0 2 1 1 3 2 1 1 2 1 1 1 2 1 1 2 2 0 0 0 0 0
 0 2 1 1 1 1 1 1 1 1 1 2 1 1 1 1 0 0 0 0 0 0
 0 2 1 1 1 1 1 1 1 2 1 2 1 1 1 1 3 1 3 3 2 0
 0 0 3 4 1 2 2 2 2 1 1 1 1 1 1 2 1 1 1 1 2 0
 0 2 2 1 1 1 2 2 3 1 2 1 2 1 1 1 1 2 1 1 2 0
 0 2 1 1 1 1 1 1 2 1 2 1 1 2 2 1 1 1 1 1 2 0
 0 0 2 1 2 1 1 1 1 1 2 3 1 1 1 2 1 1 1 2 0 0
 0 1 1 1 1 1 1 1 1 1 1 1 1 1 1 2 1 2 2 0 0 0
 0 1 1 1 1 1 1 1 2 1 1 1 1 2 2 1 1 2 0 0 0 0
 0 2 1 2 1 1 1 1 1 1 1 1 1 3 1 2 3 0 0 0 0 0
 0 1 1 1 1 2 1 1 1 1 2 1 1 1 2 1 0 0 0 0 0 0
 0 1 1 1 1 1 2 1 2 1 1 1 1 1 2 0 0 0 0 0 0 0
 0 1 1 1 1 1 1 3 1 1 1 1 1 1 0 0 0 0 0 0 0 0
 0 2 3 1 1 1 1 1 1 1 1 1 1 3 0 0 0 0 0 0 0 0
 0 0 3 1 1 1 1 1 1 1 1 1 1 3 0 0 0 0 0 0 0 0
 0 0 2 1 1 1 1 1 1 1 2 1 3 0 0 0 0 0 0 0 0 0
 0 0 0 3 1 1 1 1 1 1 1 3 0 0 0 0 0 0 0 0 0 0
 0 0 0 0 1 2 2 2 1 1 3 0 0 0 0 0 0 0 0 0 0 0
 0 0 0 0 0 0 0 0 0 0 0 0 0 0 0 0 0 0 0 0 0 0

routing reach number
 0 0 0 0 0 0 0 0 0 0 0 0 0 0 0 0 0 0 0 0 0 0
 0 0 0 0 0 0 0 0 0 0 0 0 0 0 0 0 0 0 0 0 0 0
 0 0 0 0 0 0 0 0 0 0 0 0 0 0 0 0 0 0 0 0 0 0
 0 0 0 0 0 0 0 0 0 0 0 0 0 0 0 0 0 0 0 0 0 0
 0 0 0 0 0 0 0 0 0 0 0 0 0 0 0 0 0 0 0 0 0 0
 0 0 0 0 0 0 0 0 0 0 0 0 0 0 0 0 0 0 0 0 0 0
 0 0 0 0 0 0 0 0 0 0 0 0 0 0 0 0 0 0 0 0 0 0
 0 0 0 0 0 0 0 0 0 0 0 0 0 0 0 0 0 0 0 0 0 0
 0 0 0 0 0 0 0 0 0 0 0 0 0 0 0 0 0 0 0 0 0 0
 0 0 0 0 0 0 0 0 0 0 0 0 0 0 0 0 0 0 0 0 0 0
 0 0 0 0 0 0 0 0 0 0 0 0 0 0 0 0 0 0 0 0 0 0
 0 0 0 0 0 0 0 0 0 0 0 0 0 0 0 0 0 0 0 0 0 0
 0 0 0 0 0 0 0 0 0 0 0 0 0 0 0 0 0 0 0 0 0 0
 0 0 0 0 0 0 0 0 0 0 0 0 0 0 0 0 0 0 0 0 0 0
 0 0 0 0 0 0 0 0 0 0 0 0 0 0 0 0 0 0 0 0 0 0
 0 0 0 0 0 0 0 0 0 0 0 0 0 0 0 0 0 0 0 0 0 0
 0 0 0 0 0 0 0 0 0 0 0 0 0 0 0 0 0 0 0 0 0 0
 0 0 0 0 0 0 0 0 0 0 0 0 0 0 0 0 0 0 0 0 0 0
 0 0 0 0 0 0 0 0 0 0 0 0 0 0 0 0 0 0 0 0 0 0
 0 0 0 0 0 0 0 0 0 0 0 0 0 0 0 0 0 0 0 0 0 0
 0 0 0 0 0 0 0 0 0 0 0 0 0 0 0 0 0 0 0 0 0 0
 0 0 0 0 0 0 0 0 0 0 0 0 0 0 0 0 0 0 0 0 0 0

Landclass 1   Impervious
   0   0   0   0   0   0   0   0   0   0   0   0   0   0   0   0   0   0   0   0   0   0
   0   0   0   0   0   0   0   0   0   0   0   0   0   0   0   0   0   0   0   0   0   0
   0   0   0   0   0   0   0   0   0   0   0   0   0   0   0   0   0   0   0   0   0   0
   0   0   0   0   0   0   0   0   0   0   0   0   0   0   0   0   0   0   0   0   0   0
   0   0   0   0   0   0   0   0   0   0   0   0   0   0   0   0   0   0   0   0   0   0
   0   0   0   0   0   0   0   0   0   0   0   0   0   0   0   0   0   0   0   0   0   0
   0   0   0   0   0   0   0   0   0   0   0   0   0   0   0   0   0   0   0   0   0   0
   0   0   0   0   0   0   0   0   0   0   0   0   0   0   0   0   0   0   0   0   0   0
   0   0   0   0   0   0   0   0   0   0   0   0   0   0   0   0   0   0   0   0   0   0
   0   0   0   0   0   0   0   0   0   0   0   0   0   0   0   0   0   0   0   0   0   0
   0   0   0   0   0   0   0   0   0   0   0   0   0   0   0   0   0   0   0   0   0   0
   0   0   0   0   0   0   0   0   0   0   0   0   0   0   0   0   0   0   0   0   0   0
   0   0   0   0   0   0   0   0   0   0   0   0   0   0   0   0   0   0   0   0   0   0
   0   0   0   0   0   0   0   0   0   0   0   0   0   0   0   0   0   0   0   0   0   0
   0   0   0   0   0   0   0   0   0   0   0   0   0   0   0   0   0   0   0   0   0   0
   0   0   0   0   0   0   0   0   0   0   0   0   0   0   0   0   0   0   0   0   0   0
   0   0   0   0   0   0   0   0   0   0   0   0   0   0   0   0   0   0   0   0   0   0
   0   0   0   0   0   0   0   0   0   0   0   0   0   0   0   0   0   0   0   0   0   0
   0   0   0   0   0   0   0   0   0   0   0   0   0   0   0   0   0   0   0   0   0   0
   0   0   0   0   0   0   0   0   0   0   0   0   0   0   0   0   0   0   0   0   0   0
   0   0   0   0   0   0   0   0   0   0   0   0   0   0   0   0   0   0   0   0   0   0
   0   0   0   0   0   0   0   0   0   0   0   0   0   0   0   0   0   0   0   0   0   0
```

Landclass 2 Rangeland

0	0	0	0	0	0	0	0	0	0	0	0	0	0	0	0	0	0	0	0	0	0
0	100	100	100	100	100	100	100	100	100	100	100	100	100	100	100	100	100	100	100	100	0
0	100	89	94	88	94	88	84	93	99	100	95	80	95	86	89	92	94	100	100	100	0
0	100	89	71	85	79	93	82	85	100	100	94	84	79	74	92	97	92	100	100	100	0
0	100	98	79	84	83	100	91	92	100	98	73	88	76	84	91	93	89	99	100	100	0
0	100	88	85	88	96	93	97	98	89	93	89	71	88	90	94	95	85	99	100	100	0
0	100	95	94	93	96	98	100	97	78	79	79	71	96	99	99	99	100	100	100	100	0
0	100	99	99	97	100	100	100	100	95	88	90	87	87	91	76	65	99	100	100	100	0
0	100	94	98	99	99	98	96	100	98	98	100	92	96	75	86	80	94	100	100	100	0
0	100	100	100	100	99	88	100	100	100	100	100	94	93	100	100	97	95	100	100	100	0
0	100	86	100	98	88	98	98	100	100	100	100	98	74	95	100	100	100	100	100	100	0
0	100	91	100	86	77	83	92	98	100	100	100	100	100	82	96	100	100	100	100	100	0
0	100	94	83	74	82	94	95	100	92	98	99	100	100	100	100	100	100	100	100	100	0
0	100	87	90	89	65	67	86	84	96	100	100	100	100	100	100	95	100	100	100	100	0
0	100	100	94	75	90	76	86	92	91	100	100	100	99	100	98	81	96	100	100	100	0
0	100	94	93	78	92	100	98	96	98	94	100	100	100	100	100	99	90	99	100	100	0
0	100	100	97	83	86	89	98	97	99	99	98	100	100	99	98	96	100	100	100	100	0
0	100	100	100	91	100	75	84	99	95	97	100	100	100	93	81	92	99	100	100	100	0
0	100	100	100	98	99	99	98	100	100	100	100	100	100	99	99	98	94	100	100	100	0
0	100	100	100	100	100	100	100	100	100	100	100	100	100	100	100	100	100	100	100	100	0
0	100	100	100	100	100	100	100	100	100	100	100	100	100	100	100	100	100	100	100	100	0
0	0	0	0	0	0	0	0	0	0	0	0	0	0	0	0	0	0	0	0	0	0

Landclass 3 Agriculture

0	0	0	0	0	0	0	0	0	0	0	0	0	0	0	0	0	0	0	0	0	0
0	0	0	0	0	0	0	0	0	0	0	0	0	0	0	0	0	0	0	0	0	0
0	0	11	6	12	6	12	16	7	1	0	5	20	5	14	11	8	6	0	0	0	0
0	0	12	29	15	22	7	18	16	0	0	6	16	21	26	8	3	8	1	0	0	0
0	0	2	21	16	17	1	9	8	0	2	27	12	24	16	9	7	11	1	0	0	0
0	0	12	15	12	4	7	3	2	11	7	11	29	12	10	6	5	15	1	0	0	0
0	0	5	6	7	4	2	0	3	22	22	21	29	4	1	1	2	0	0	0	0	0
0	0	1	1	3	0	0	0	0	5	12	10	13	13	10	24	35	1	0	0	0	0
0	0	6	2	1	1	2	4	0	2	2	0	8	4	26	14	20	6	0	0	0	0
0	0	1	0	0	1	12	0	1	0	0	0	6	7	0	0	3	5	1	0	0	0
0	0	14	0	2	12	2	2	0	0	0	0	2	26	5	0	0	0	0	0	0	0
0	0	9	0	14	23	17	8	2	0	0	0	0	0	18	4	0	0	0	0	0	0
0	0	6	17	26	19	6	5	0	8	2	1	0	0	0	0	0	0	0	0	0	0
0	0	13	10	11	35	34	14	16	4	0	0	0	0	0	0	5	0	0	0	0	0
0	0	1	6	25	10	25	14	8	9	0	0	0	1	0	2	19	4	0	0	0	0
0	0	6	7	22	8	0	2	4	2	7	0	0	0	0	0	1	10	1	0	0	0
0	0	0	3	17	14	11	2	3	1	1	2	0	0	1	2	4	0	1	0	0	0
0	0	0	0	9	0	25	16	1	5	3	0	0	0	7	19	8	1	0	0	0	0
0	0	0	0	2	1	1	2	0	0	0	0	0	0	1	1	2	6	0	0	0	0
0	0	0	0	0	0	0	0	0	0	0	0	0	0	0	0	0	0	0	0	0	0
0	0	0	0	0	0	0	0	0	0	0	0	0	0	0	0	0	0	0	0	0	0
0	0	0	0	0	0	0	0	0	0	0	0	0	0	0	0	0	0	0	0	0	0

APPENDIX B

MAP UZS Comparison Plots and Hydrographs

Figure B.1: Measured Cumulative Water Content and Modelled Upper Zone Storage Claro and RFF2 (Grassland) Using Rain Gauge Precipitation Input

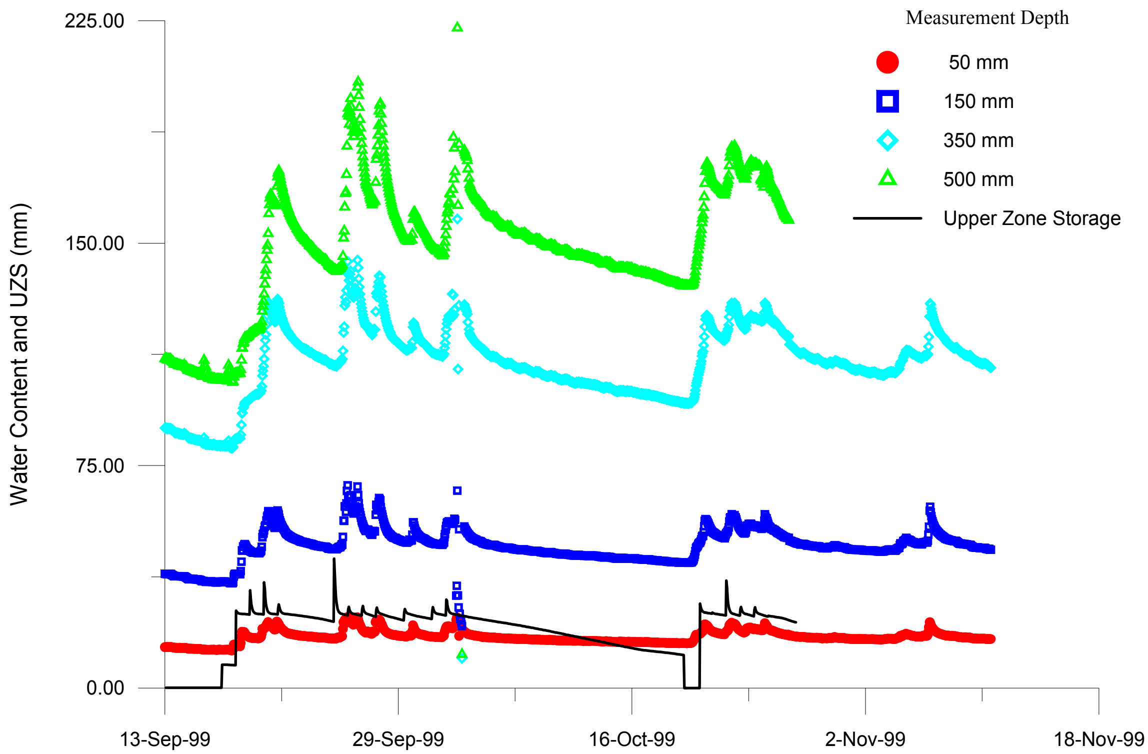

Figure B.2: Measured Cumulative Water Content and Modelled Upper Zone Storage Tower and RFF2 (Grassland) Using Rain Gauge Precipitation Input

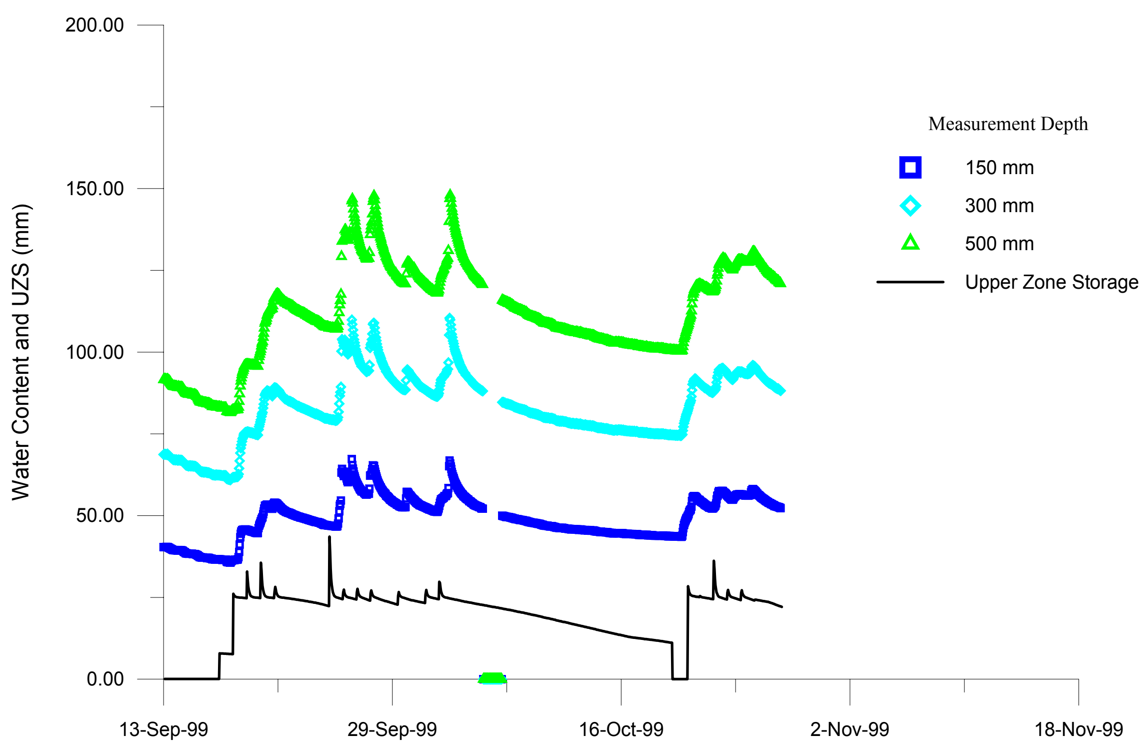

**Figure B.3: Measured Cumulative Water Content and Modelled Upper Zone Storage
Maruso and RFF2 (Grassland) Using Rain Gauge Precipitation Input**

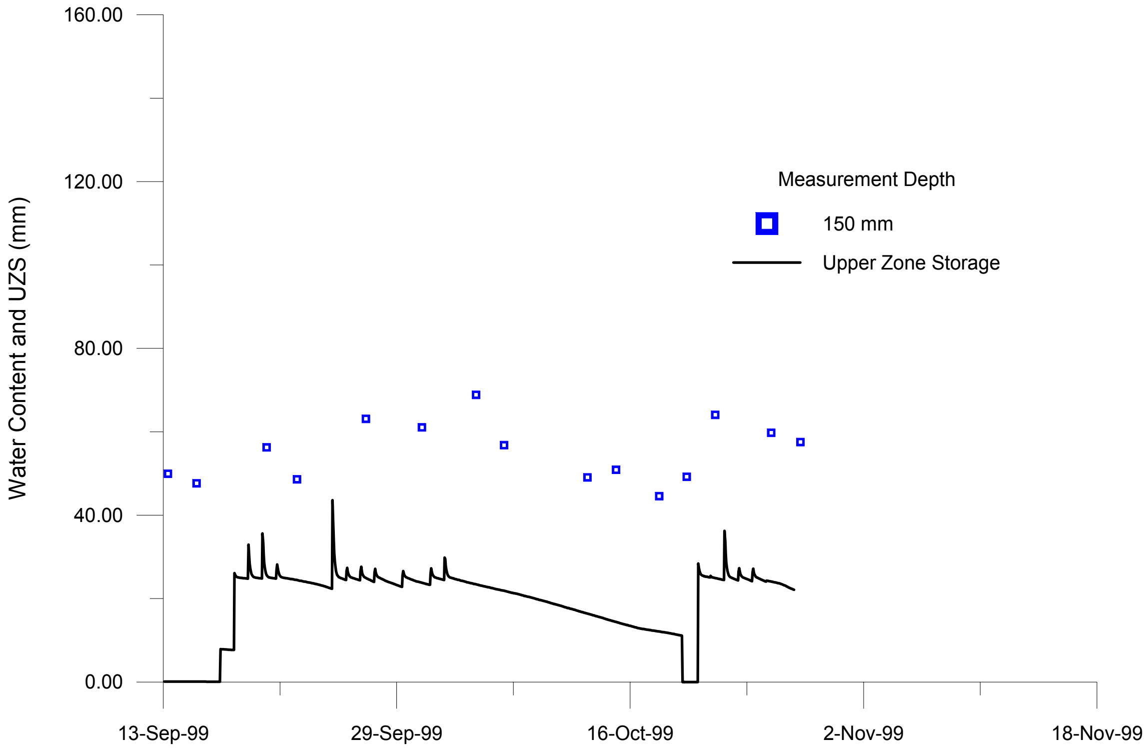

**Figure B.4: Measured Cumulative Water Content and Modelled Upper Zone Storage
Blenio and RFF2 (Grassland) Using Rain Gauge Precipitation Input**

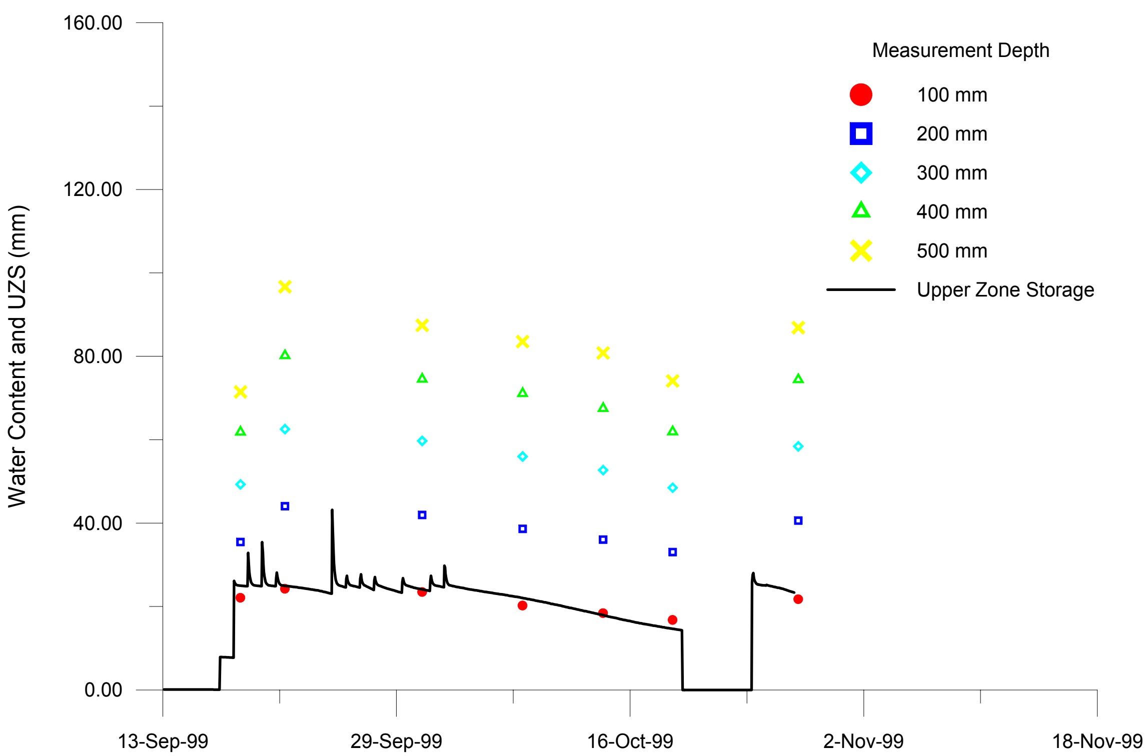

Figure B.5: Measured Cumulative Water Content and Modelled Upper Zone Storage Verzasca and RFF2 (Grassland) Using Rain Gauge Precipitation Input

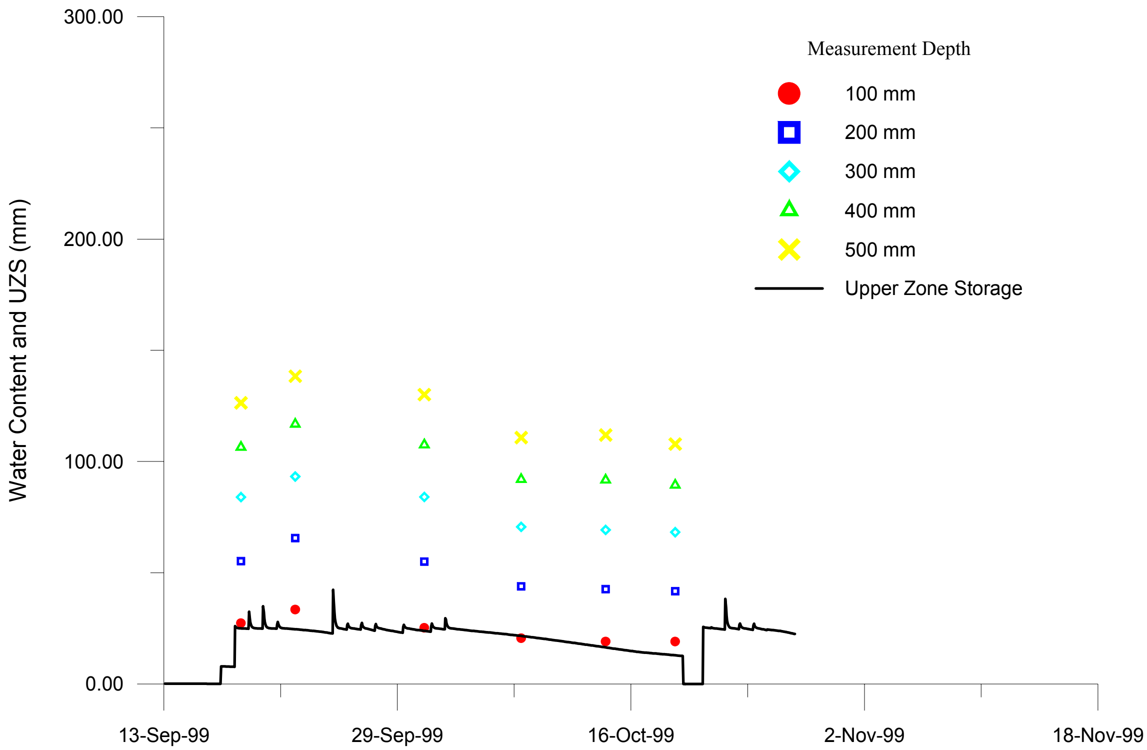

Figure B.6: Measured Cumulative Water Content and Modelled Upper Zone Storage Maggia and RFF2 (Grassland) Using Rain Gauge Precipitation Input

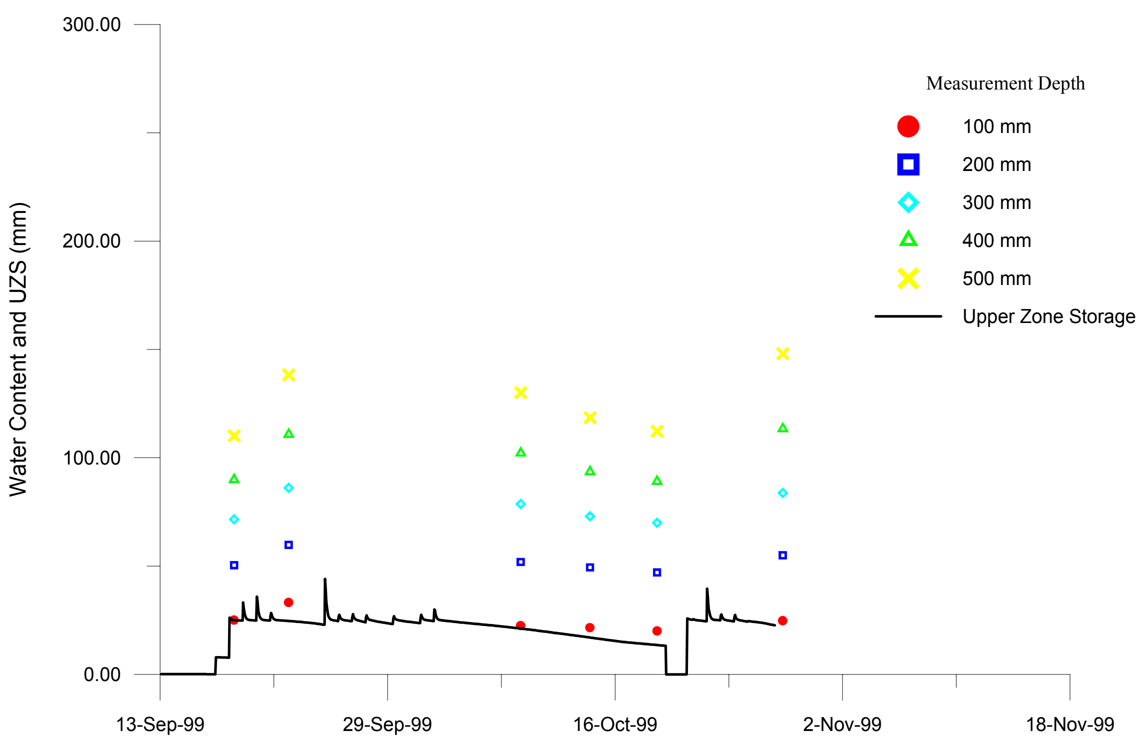

Figure B.7: Measured Cumulative Water Content and Modelled Upper Zone Storage Claro and RFF2 (Grassland) Using Radar Precipitation Input

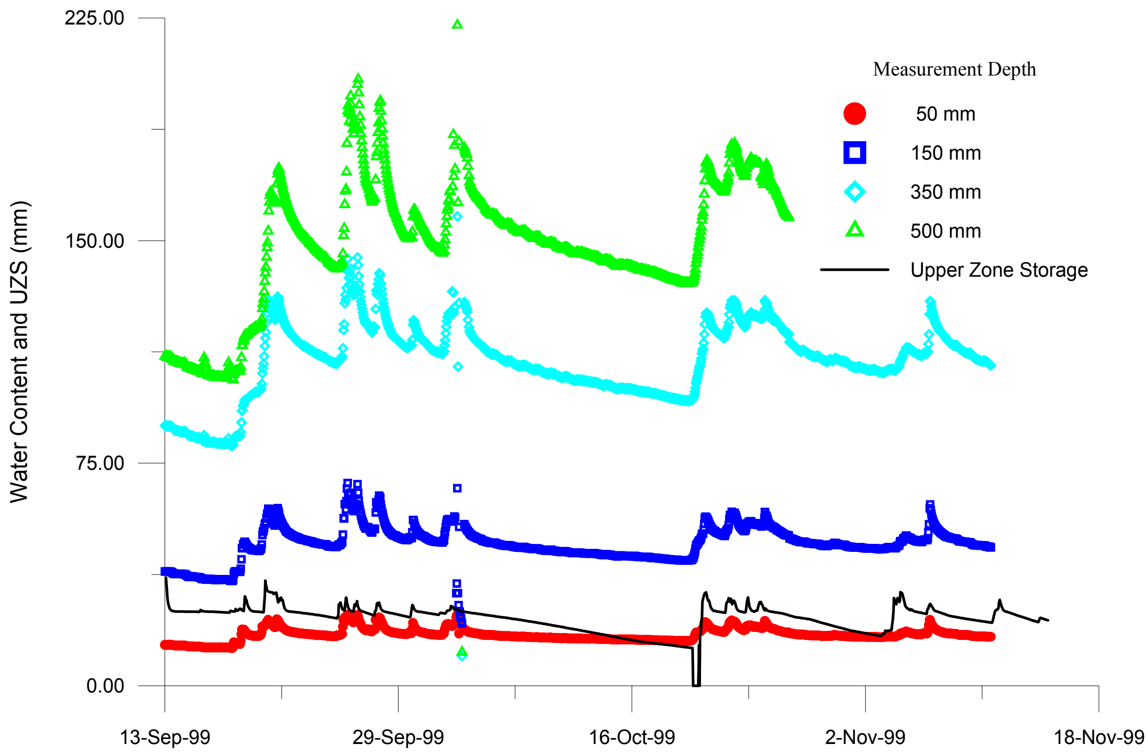

Figure B.8: Measured Cumulative Water Content and Modelled Upper Zone Storage Tower and RFF2 (Grassland) Using Radar Precipitation Input

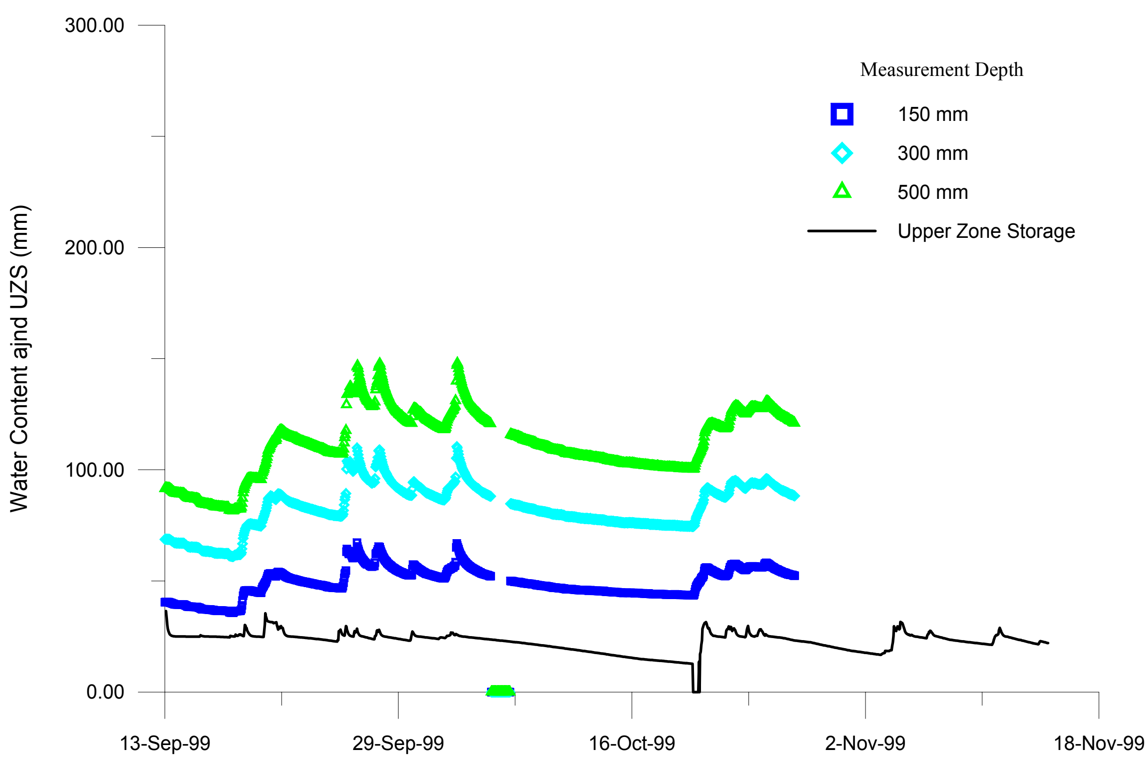

Figure B.9: Measured Cumulative Water Content and Modelled Upper Zone Storage Maruso and RFF2 (Grassland) Using Radar Precipitation Input

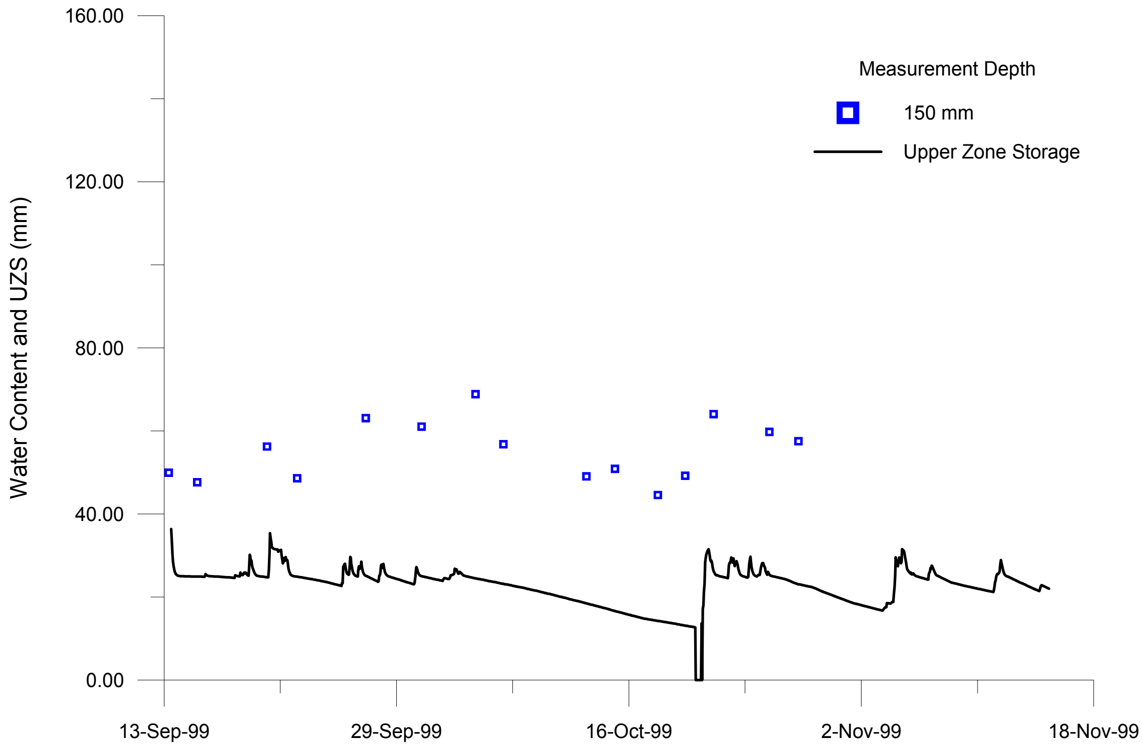

Figure B.10: Measured CumulativeWater Content and Modelled Upper Zone Storage Blenio and RFF2 (Grassland) Using Radar Precipitation Input

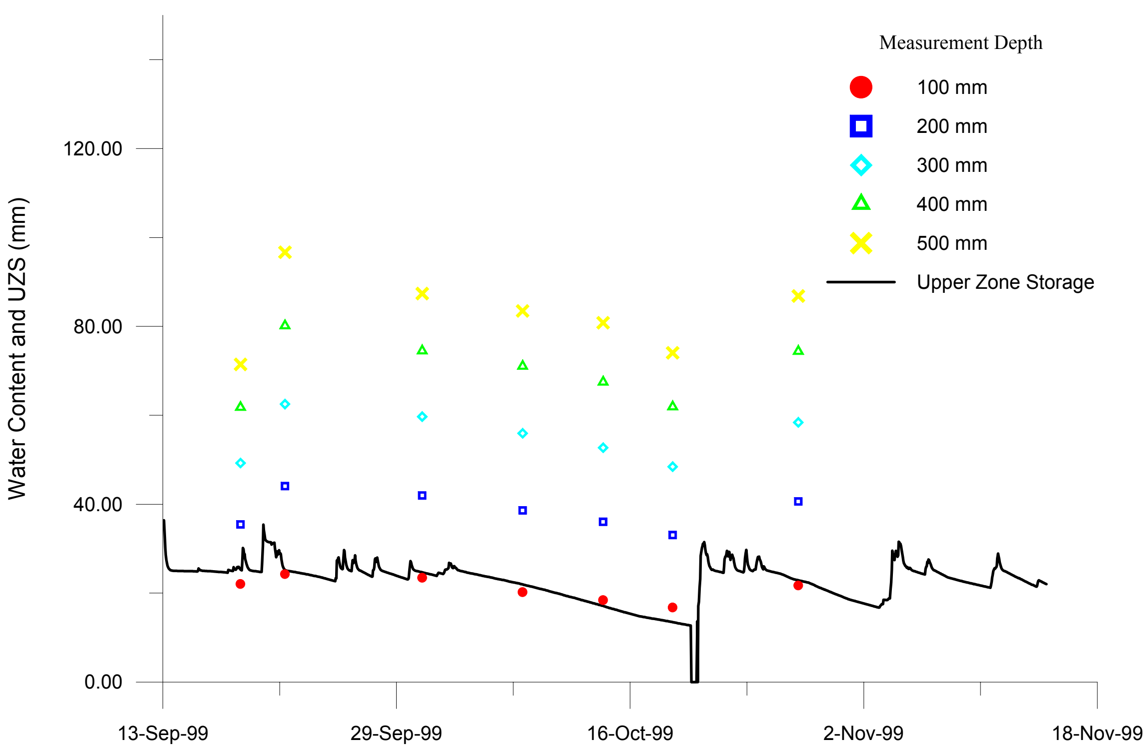

Figure B.11: Measured Cumulative Water Content and Modelled Upper Zone Storage Verzasca and RFF2 (Grassland) Using Radar Precipitation Input

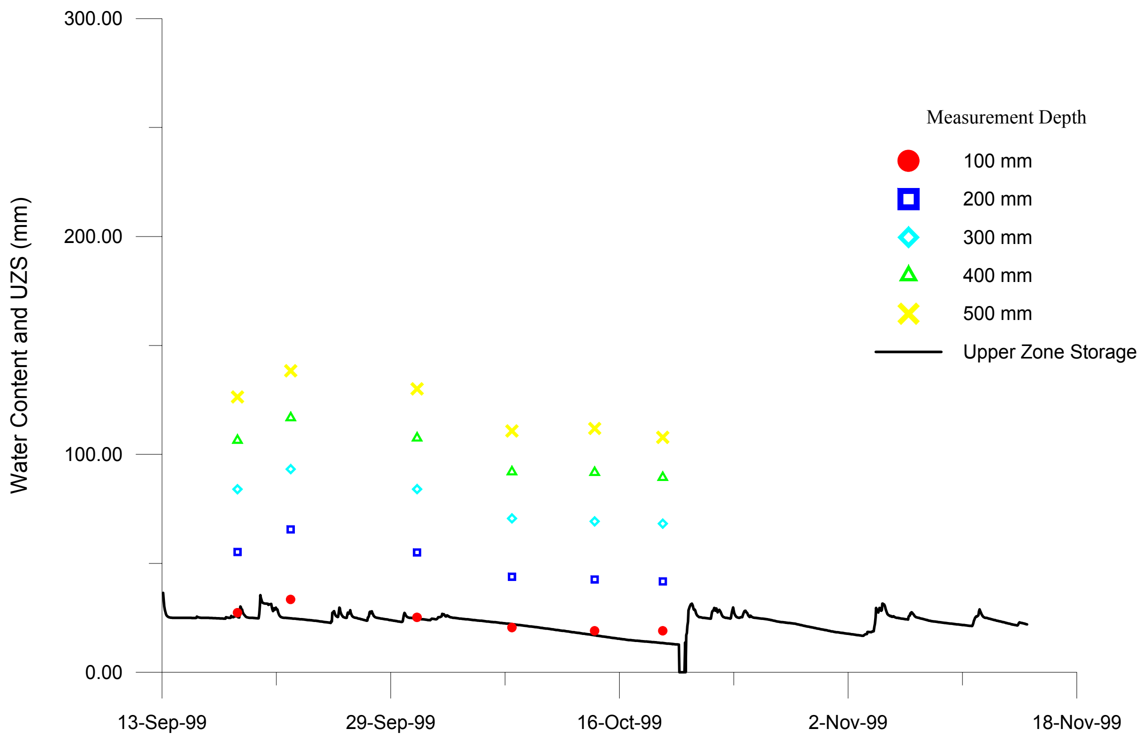

Figure B.12: Measured Cumulative Water Content and Modelled Upper Zone Storage Maggia and RFF2 (Grassland) Using Radar Precipitation Input

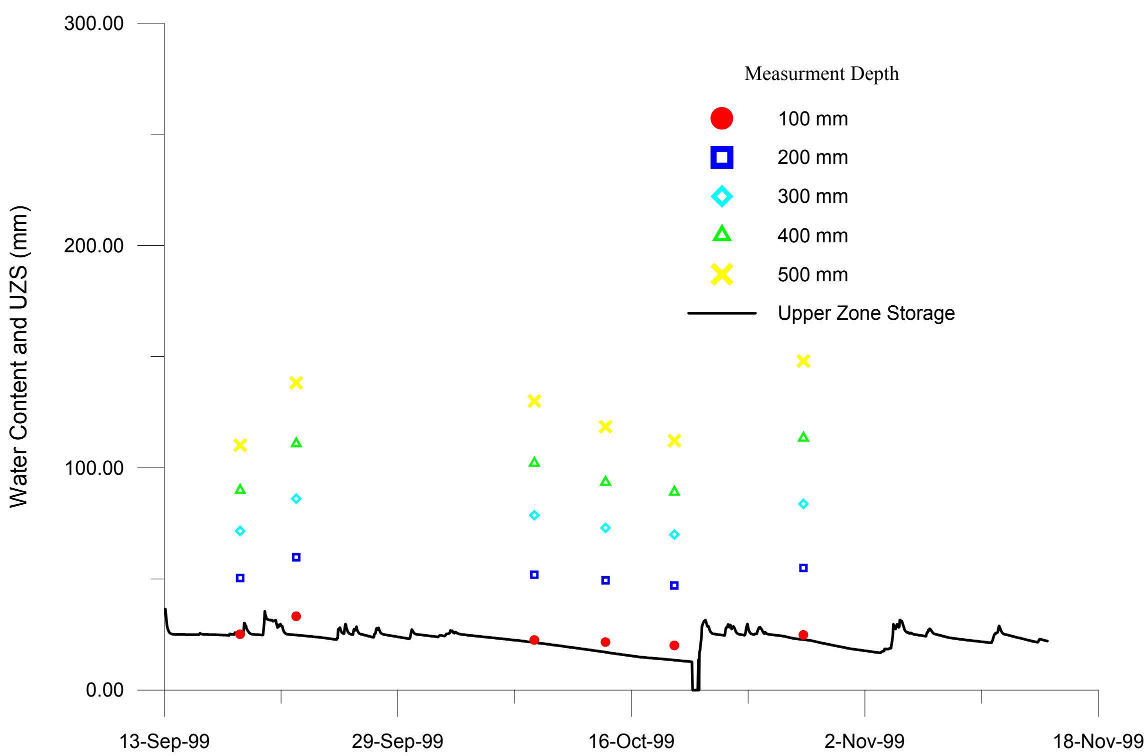

Figure B.13: Measured Cumulative Water Content and Modelled Upper Zone Storage Claro and RFF2 (Grassland) Using MC2 Precipitation Input

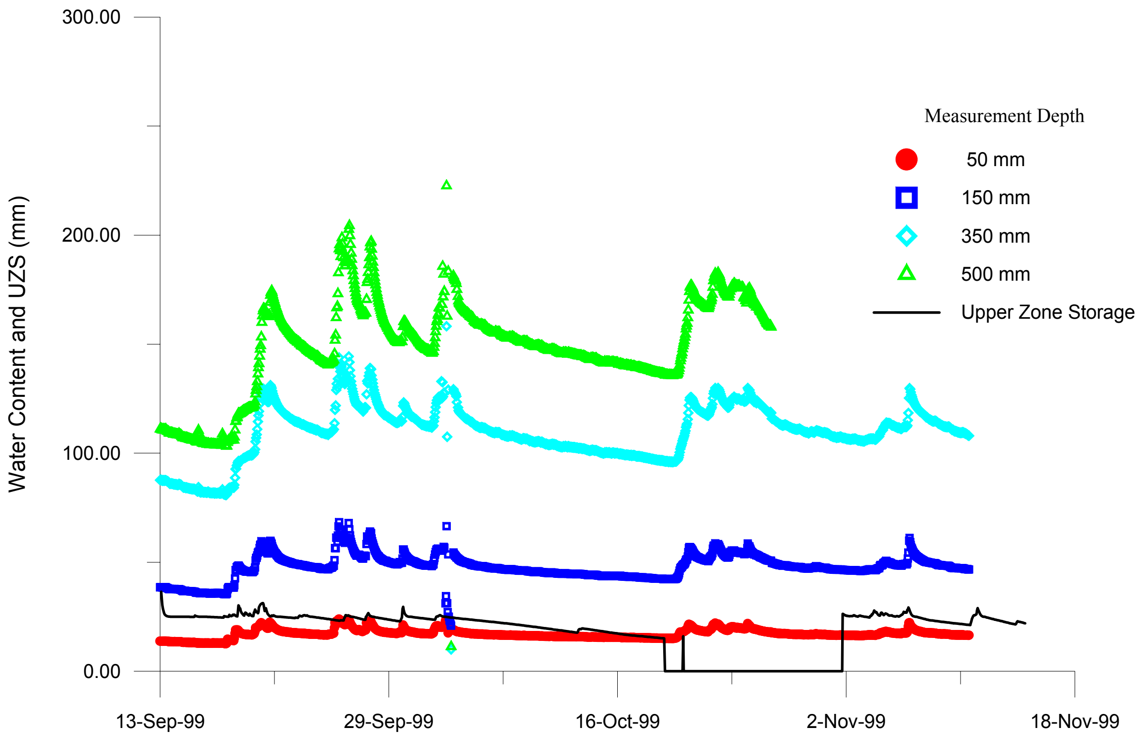

Figure B.14: Measured Cumulative Water Content and Modelled Upper Zone Storage Tower and RFF2 (Grassland) Using MC2 Precipitation Input

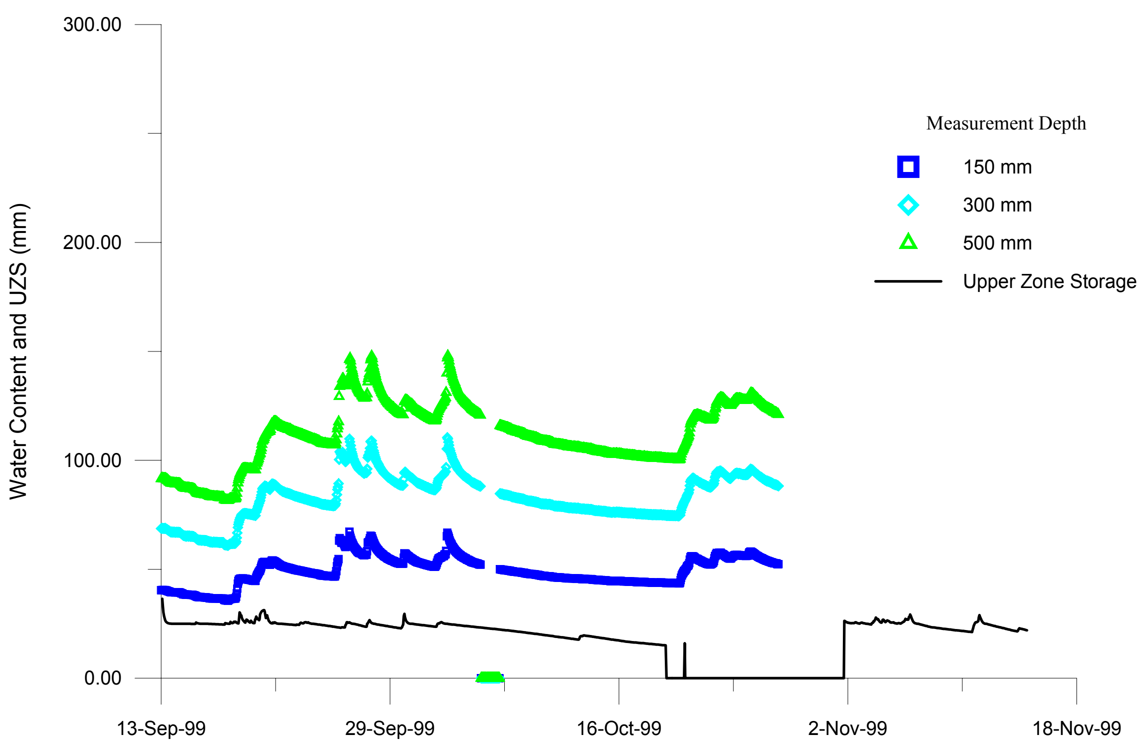

Figure B.15: Measured Cumulative Water Content and Modelled Upper Zone Storage Maruso and RFF2 (Grassland) Using MC2 Precipitation Input

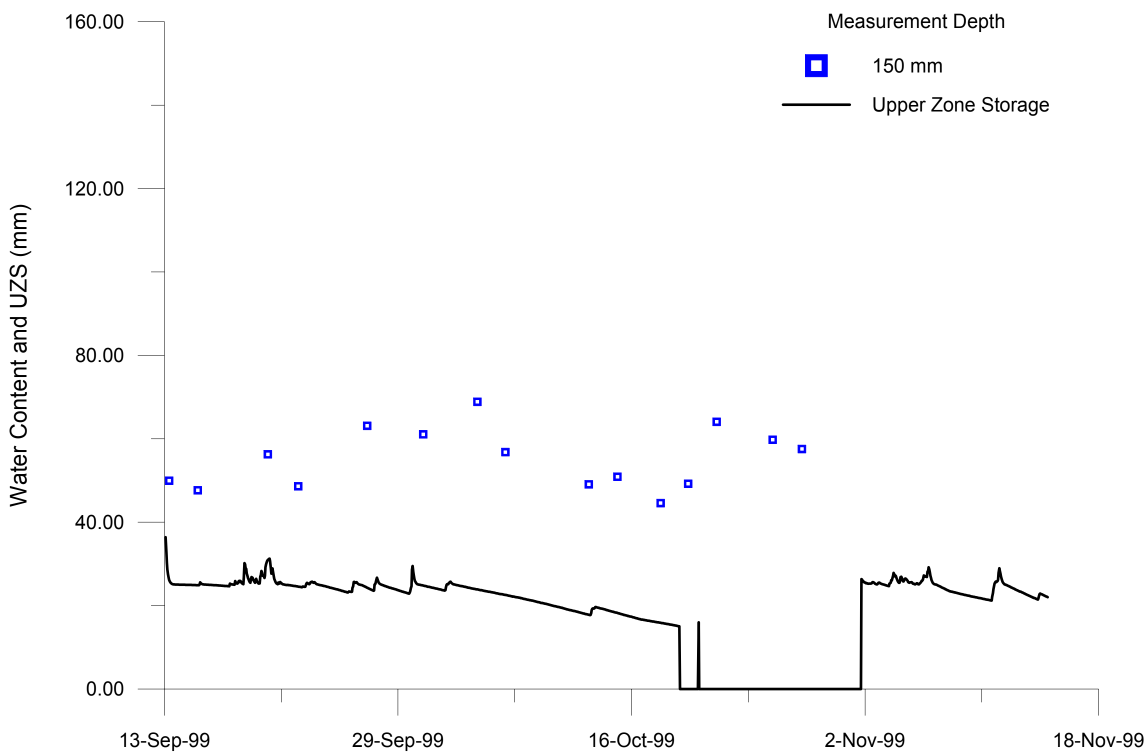

Figure B.16: Measured Cumulative Water Content and Modelled Upper Zone Storage Blenio and RFF2 (Grassland) Using MC2 Precipitation Input

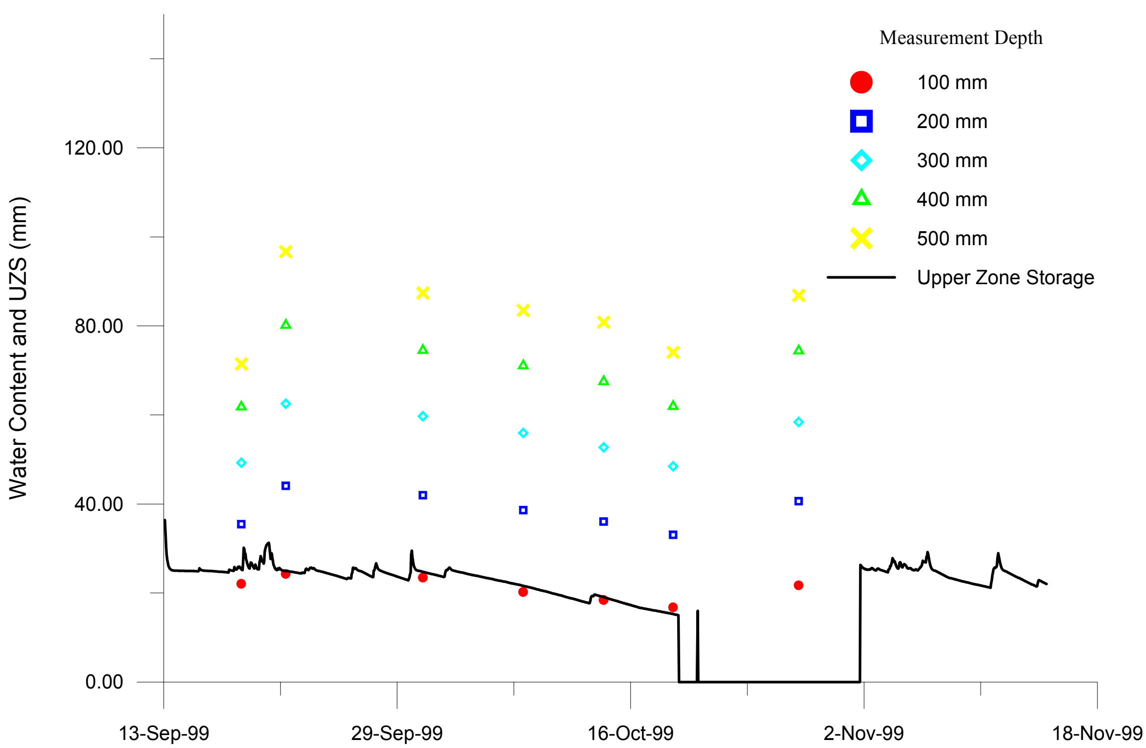

Figure B.17: Measured Cumulative Water Content and Modelled Upper Zone Storage Verzasca and RFF2 (Grassland) Using MC2 Precipitaion Input

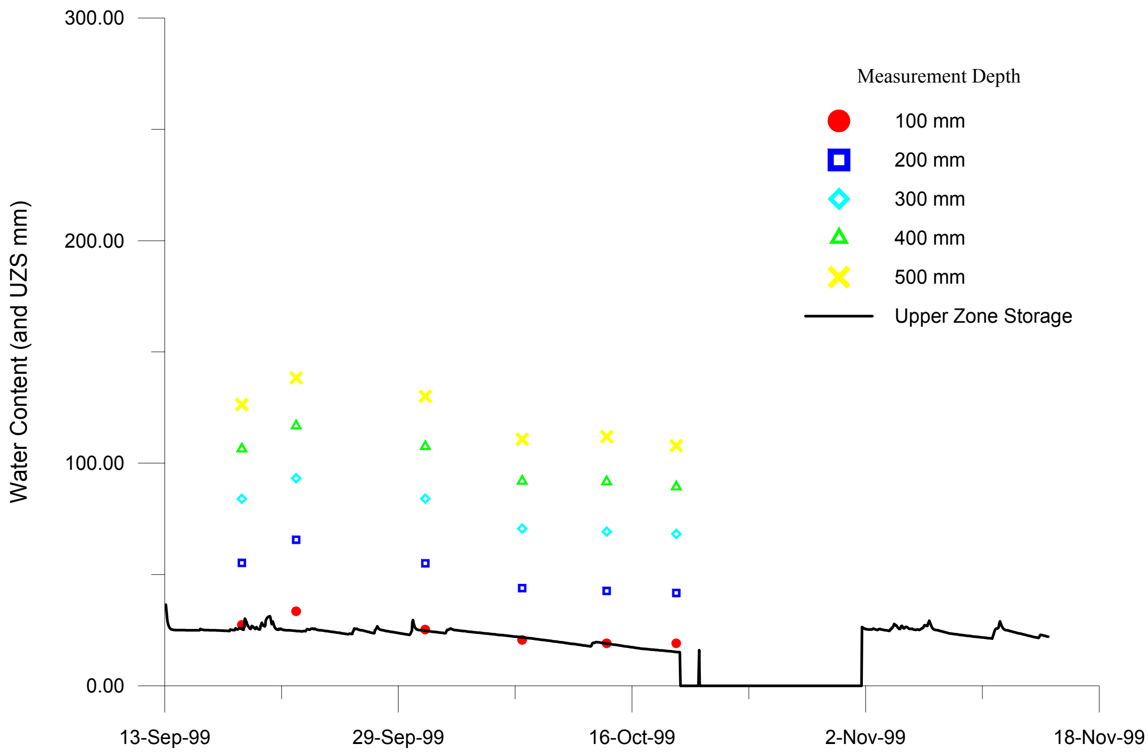

Figure B.18: Measured Cumulative Water Content and Modelled Upper Zone Storage Maggia and RFF2 (Grassland) Using MC2 Precipitation Input

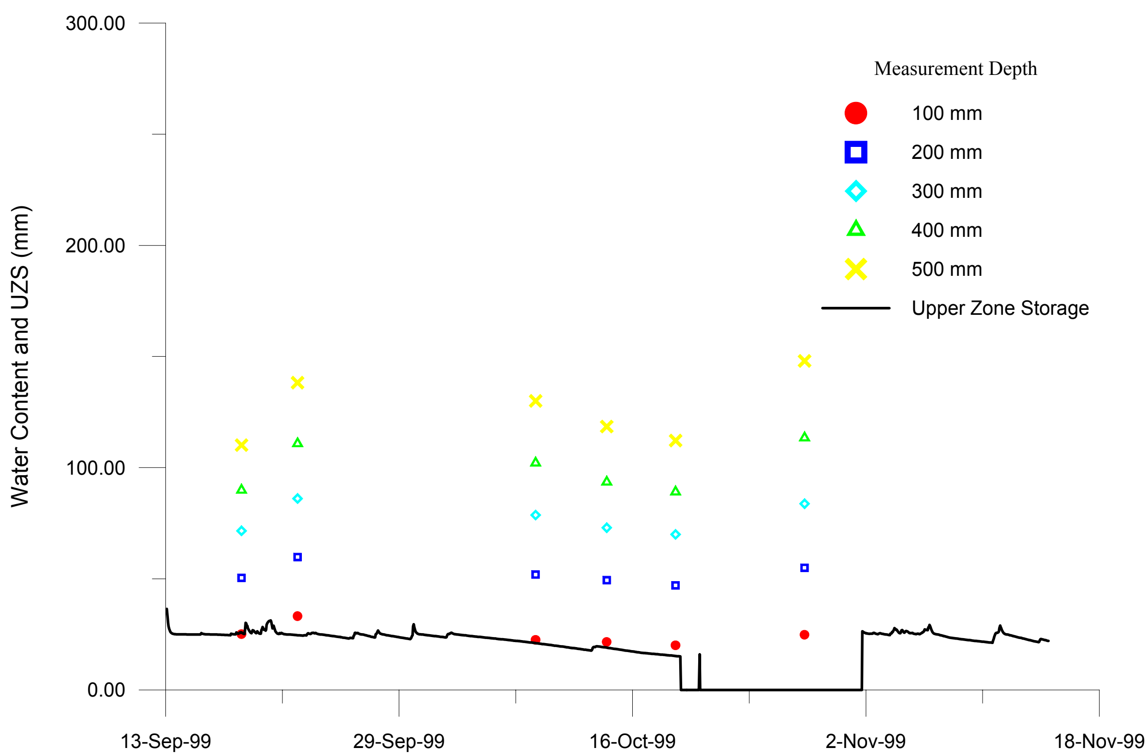

Figure B.19: Toce-Ticino Hydrographs with Rain Gauge Precipitation Input

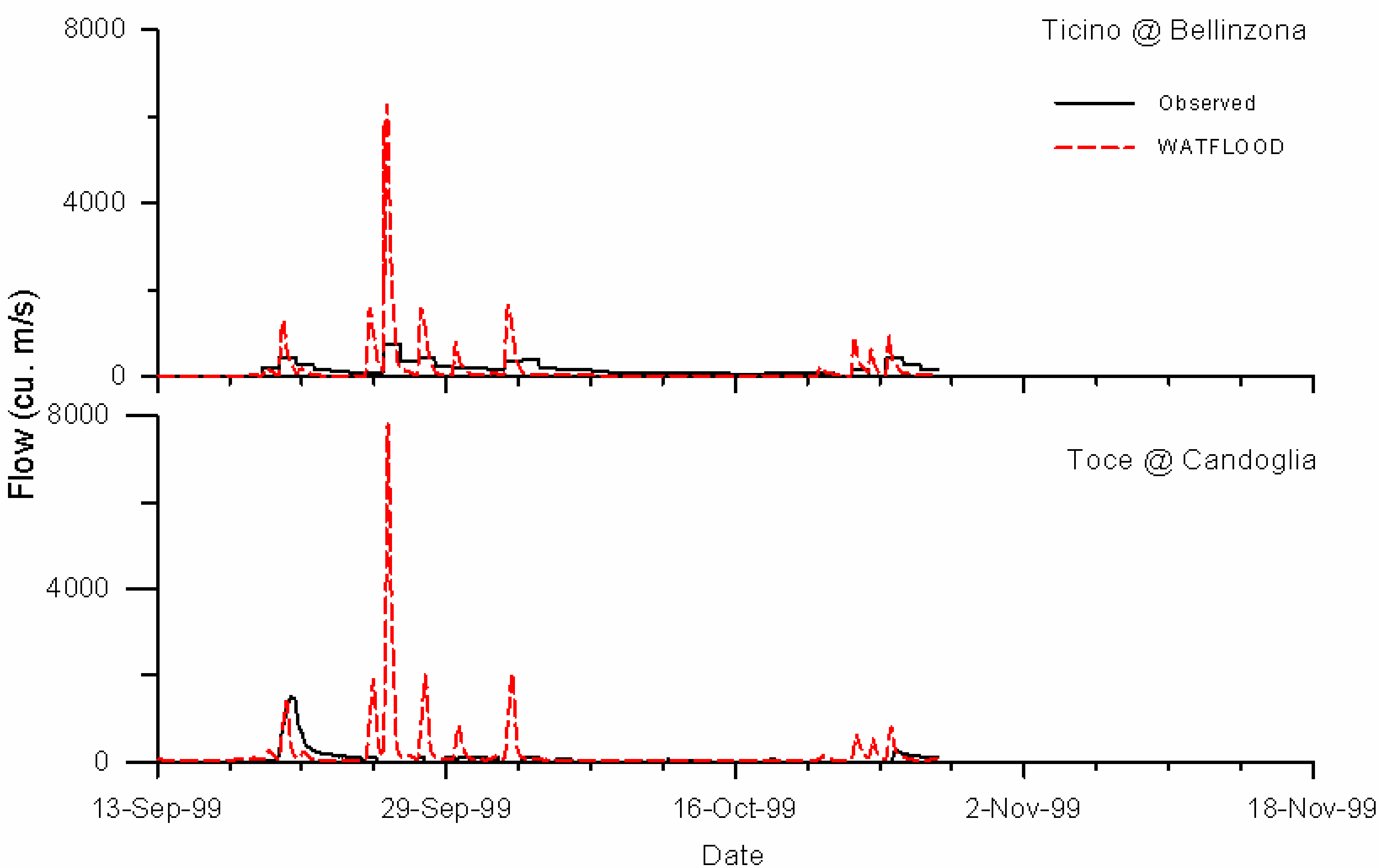

Figure B.20: Toce-Ticino Hydrographs with Radar Precipitation Input

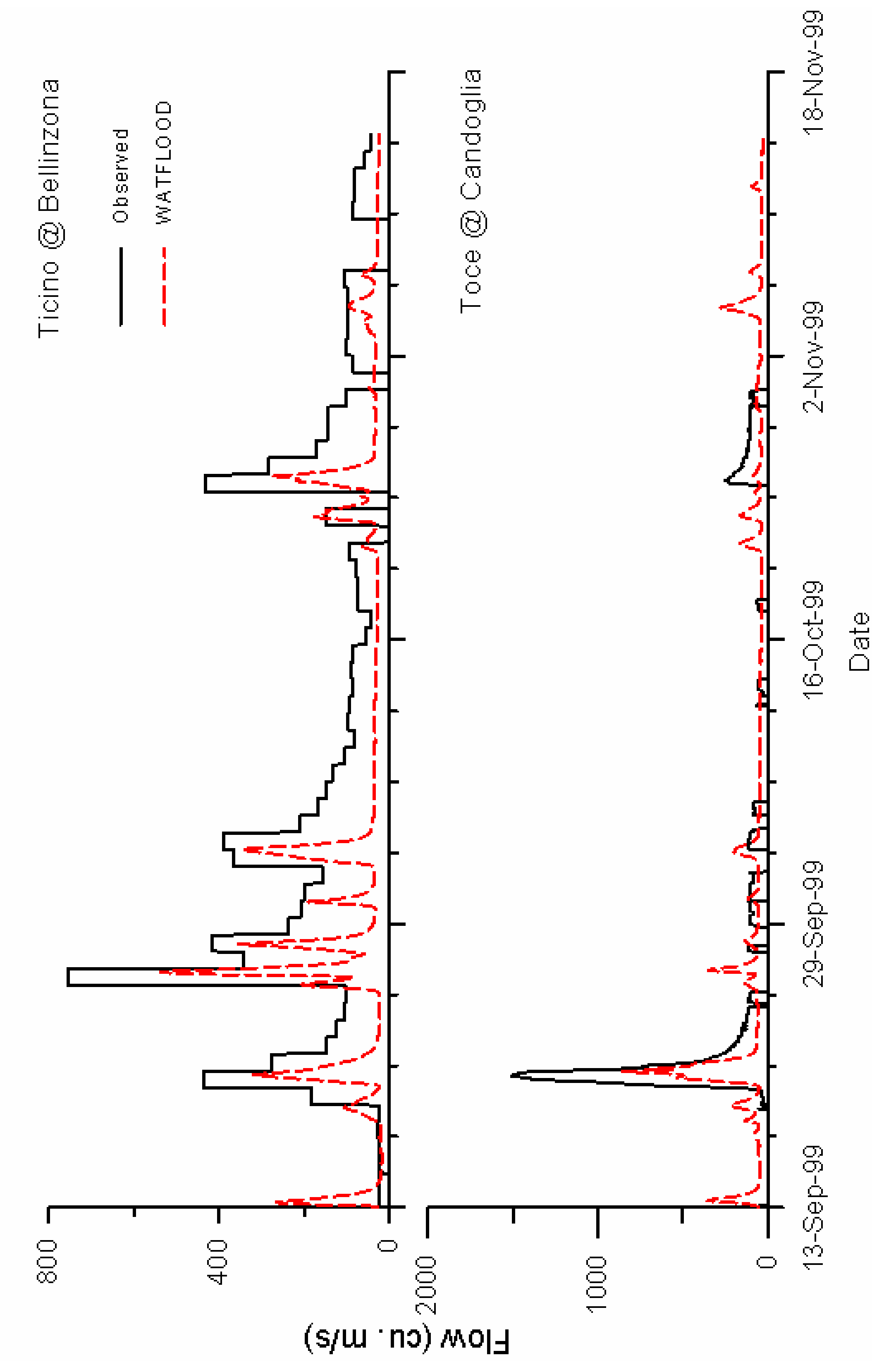

Figure B.21: Toce-Ticino Hydrographs with MC2 Precipitation Input

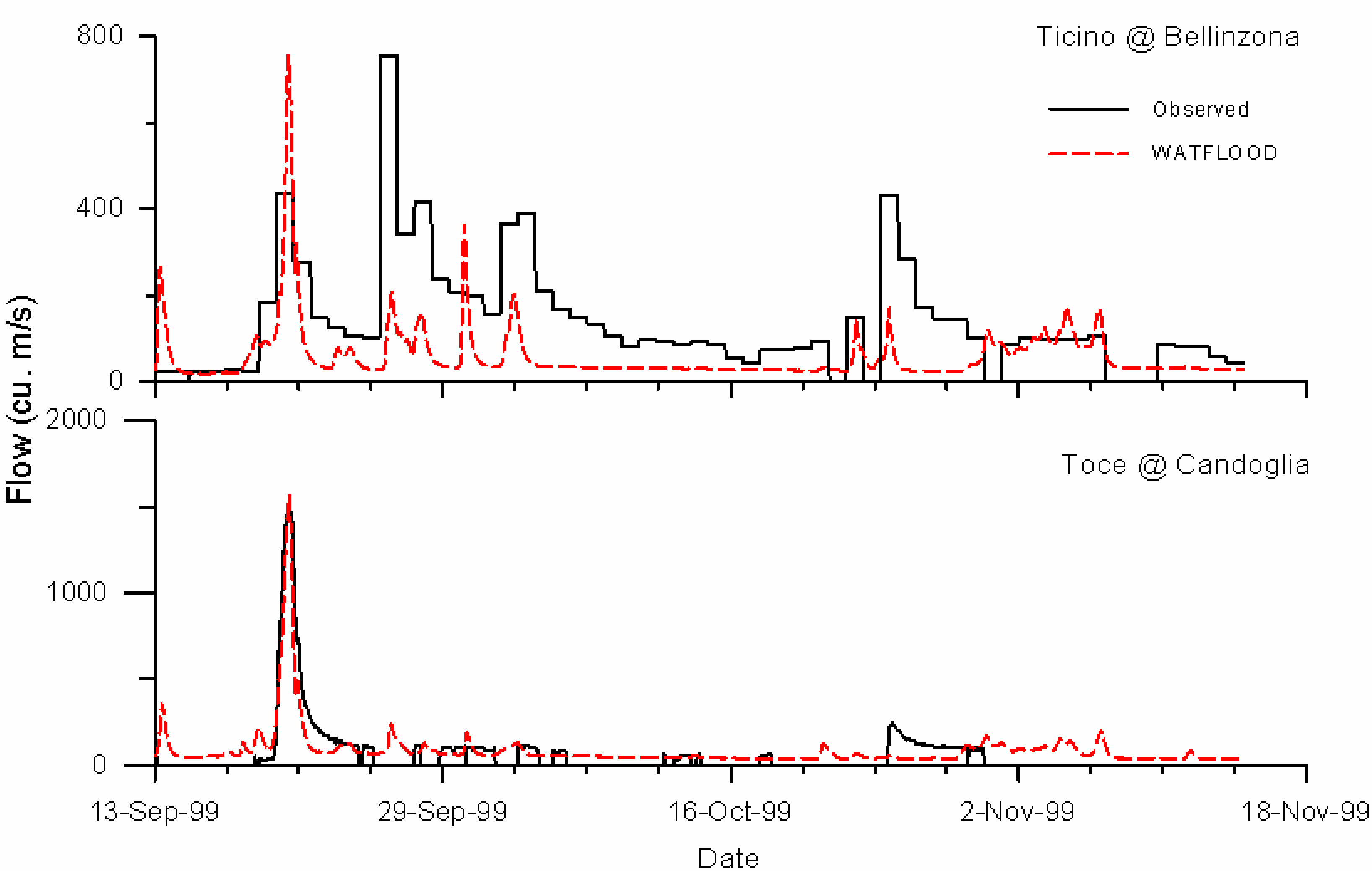

APPENDIX C

BOREAS UZS Comparison Plots and Hydrographs

Figure C.1: Measured Cumulative Water Content and Modelled Upper Zone Storage NSAOBS 1 and RFF 3 (Wet Forest)

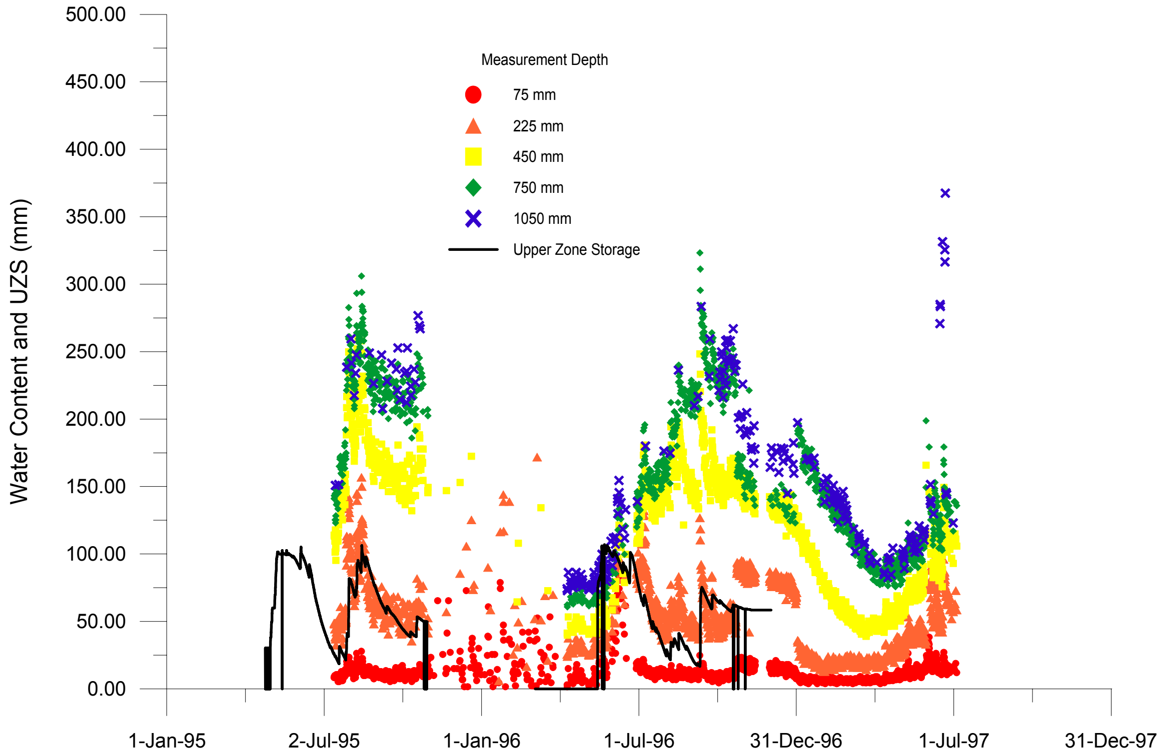

Figure C.2: Measured Cumulative Water Content and Modelled Upper Zone Storage NSAOBS 2 and RFF 3 (Wet Forest)

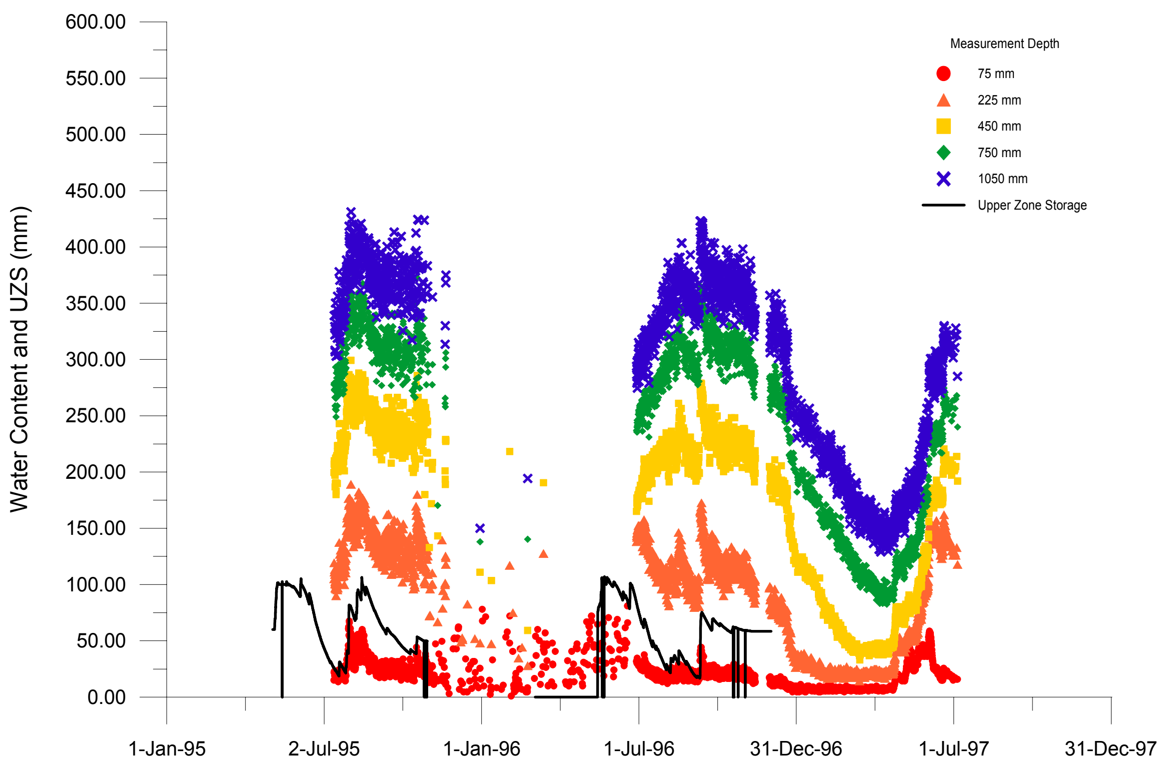

Figure C.3: Measured Cumulative Water Content and Modelled Upper Zone Storage NSAOBS 3 and RFF 3 (Wet Forest)

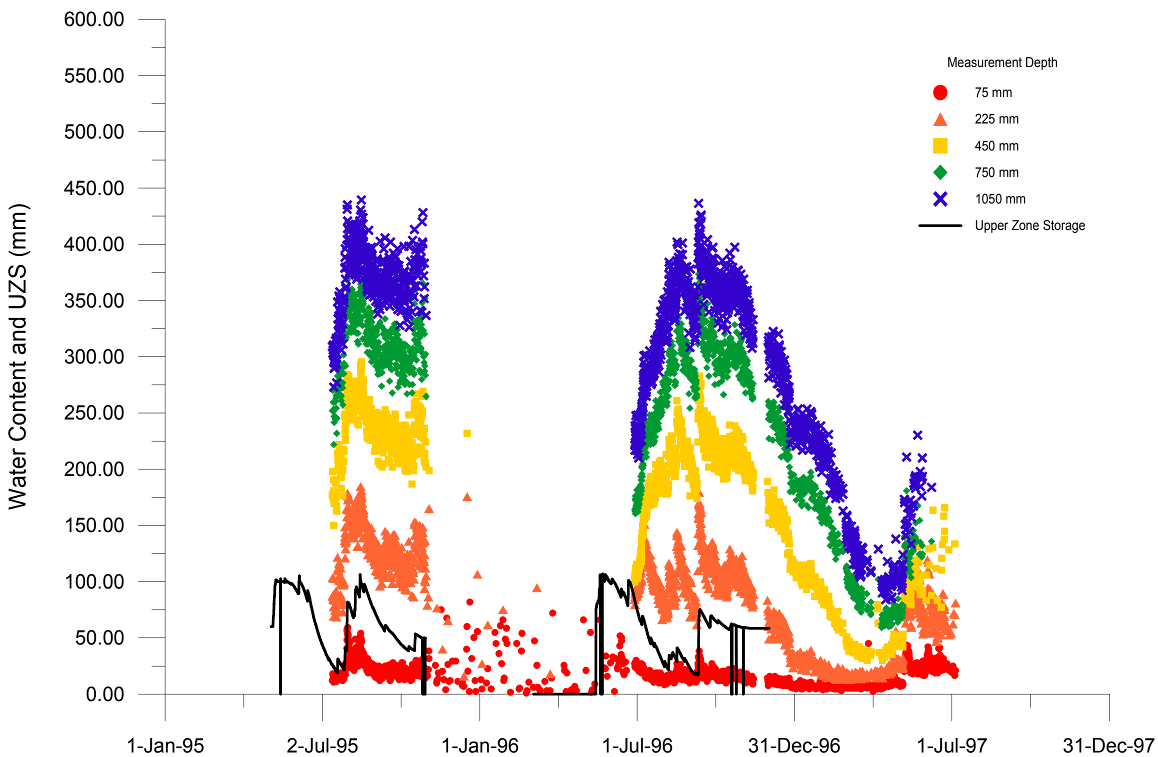

Figure C.4: Measured Cumulative Water Content and Modelled Upper Zone Storage NSAOBS 4 and RFF 3 (Wet Forest)

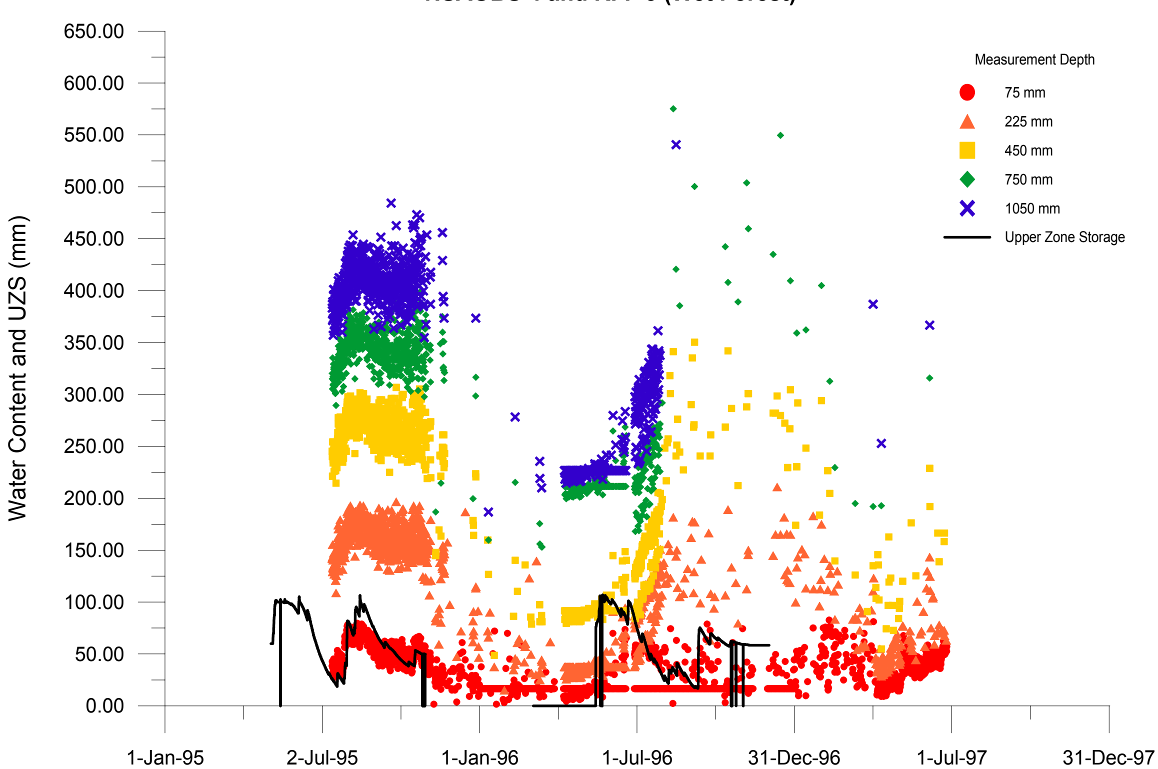

Figure C.5: Measured Cumulative Water Content and Modelled Upper Zone Storage NSAOBS 5 and RFF 3 (Wet Forest)

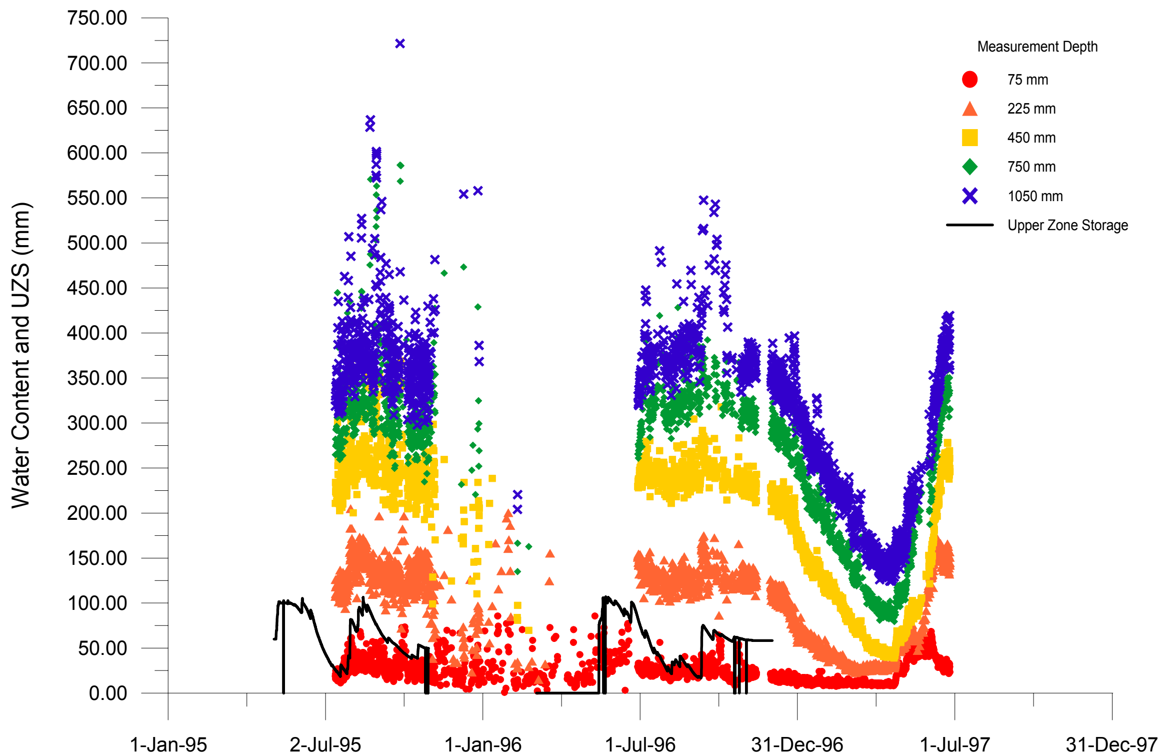

Figure C.6: Measured Cumulative Water Content and Modelled Upper Zone Storage NSAOBS 6 and RFF 3 (Wet Forest)

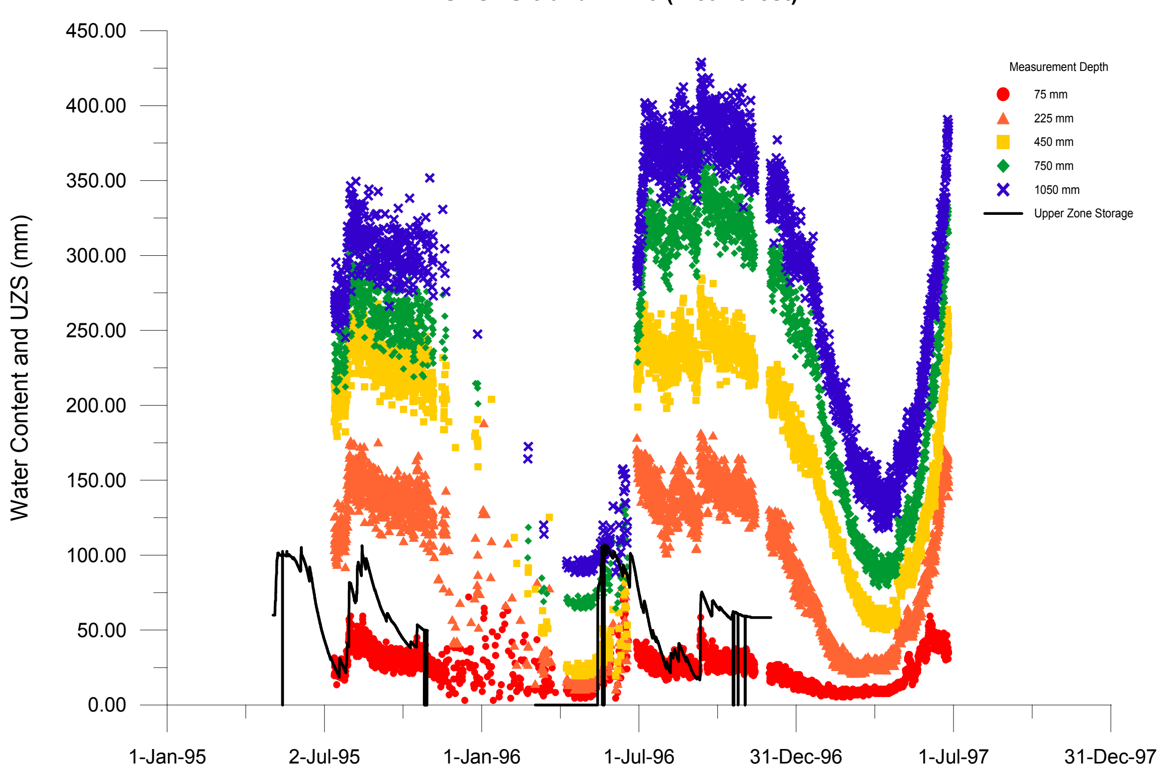

Figure C.7: Measured Cumulative Water Conten and Modelled Upper Zone Storage NSAOBS 7 and RFF 3 (Wet Forest)

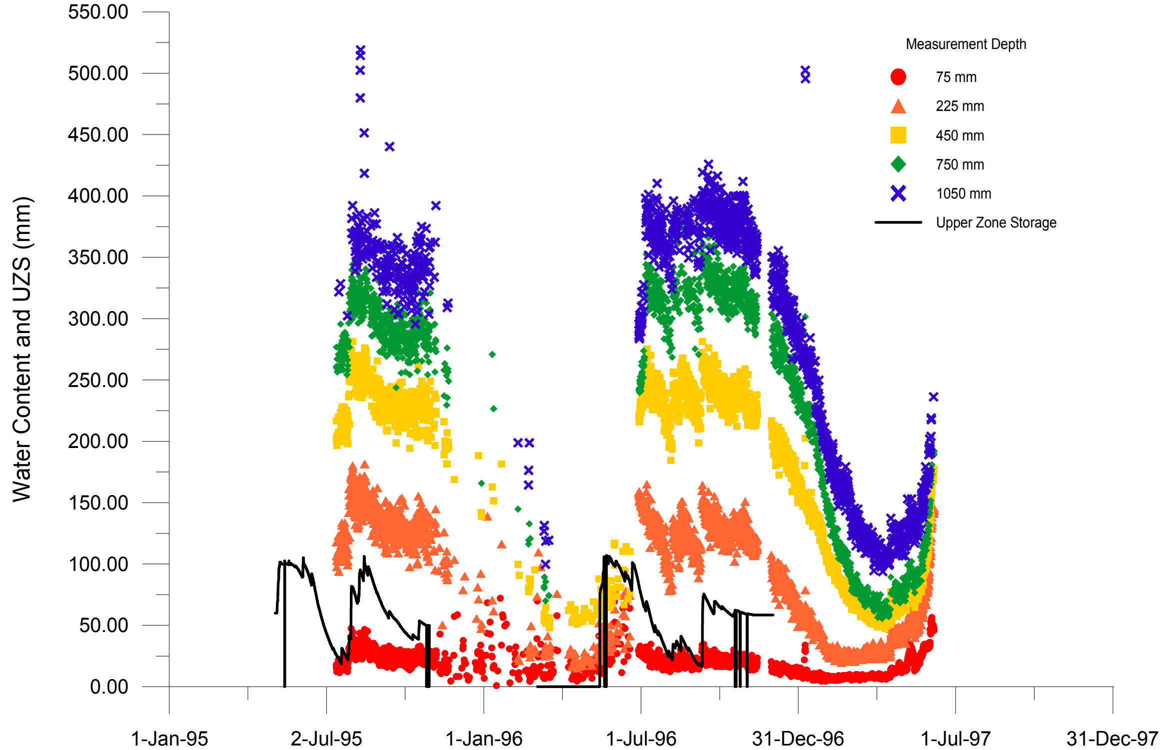

Figure C.8: Measured Cumulative Water Content and Modelled Upper Zone Storage NSAOBS 8 and RFF 3 (Wet Forest)

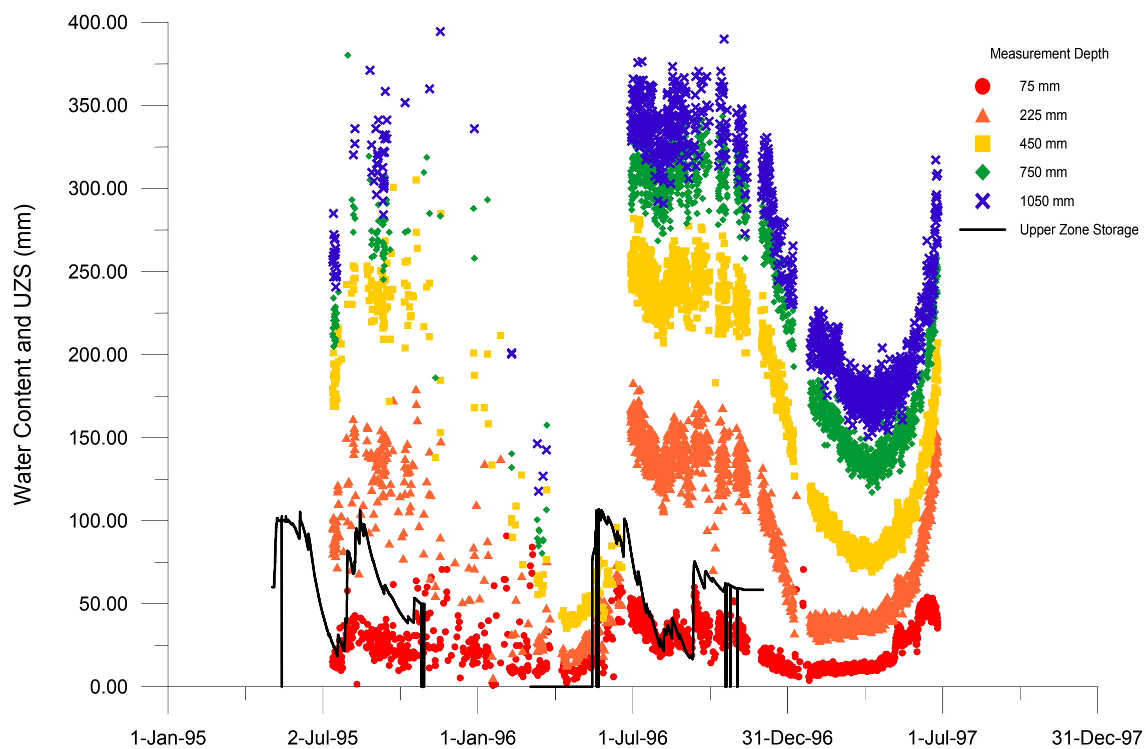

Figure C.9: Measured Cumulative Water Content and Modelled Upper Zone Storage NSAOJP 1 and RFF 2 (Dry Forest)

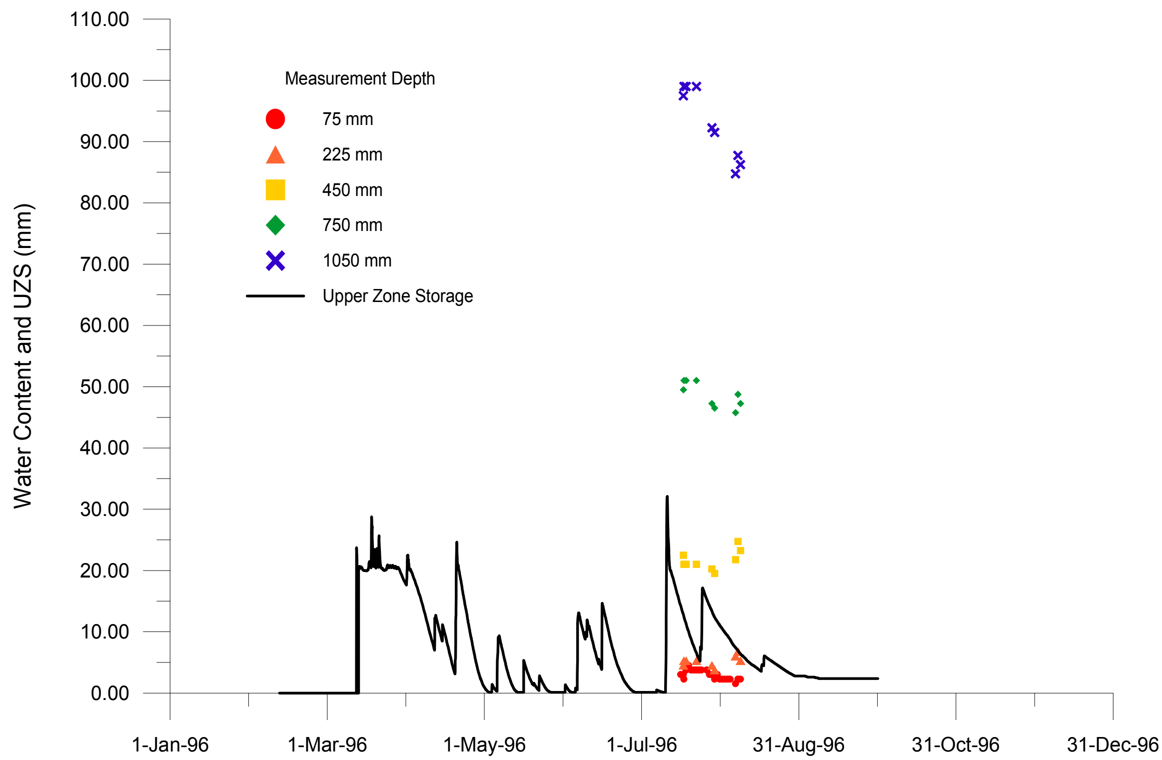

Figure C.10: Measured Cumulative Water Content and Modelled Upper Zone Storage NSAOJP 2 and RFF 2 (Dry Forest)

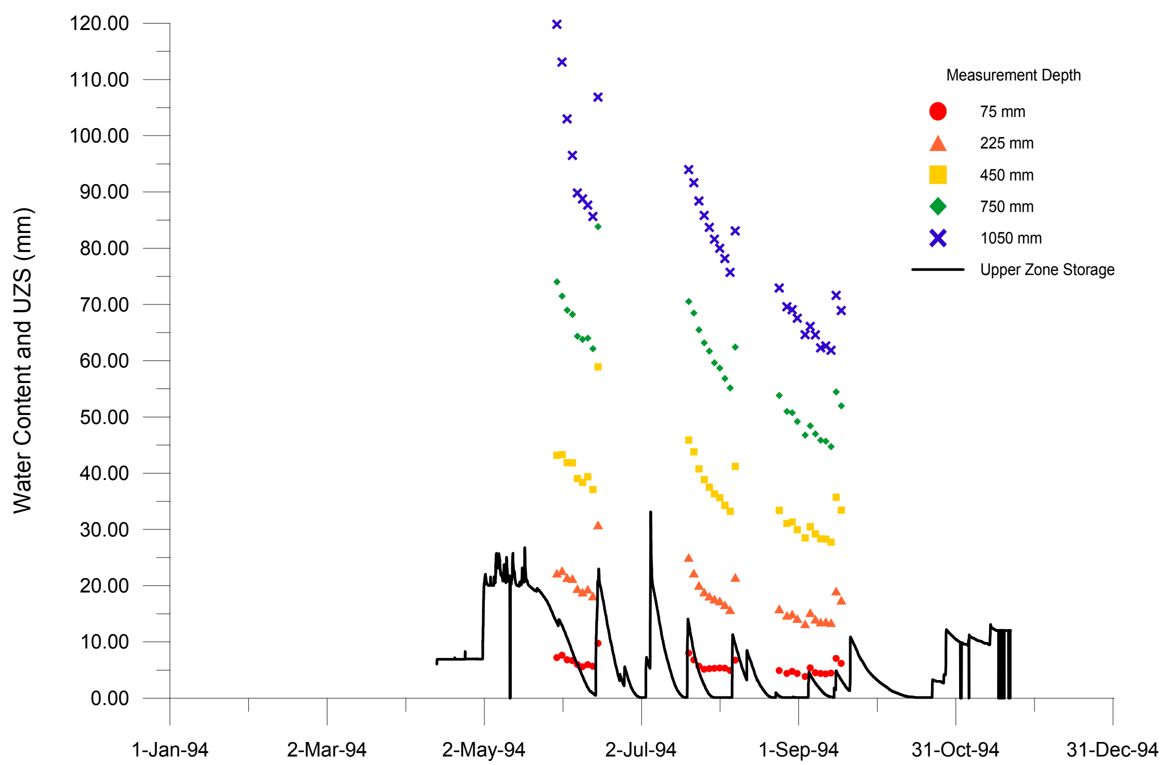

Figure C.11: Measured Cumulative Water Content and Modelled Upper Zone Storage NSAOJP 3 and RFF 2 (Dry Forest)

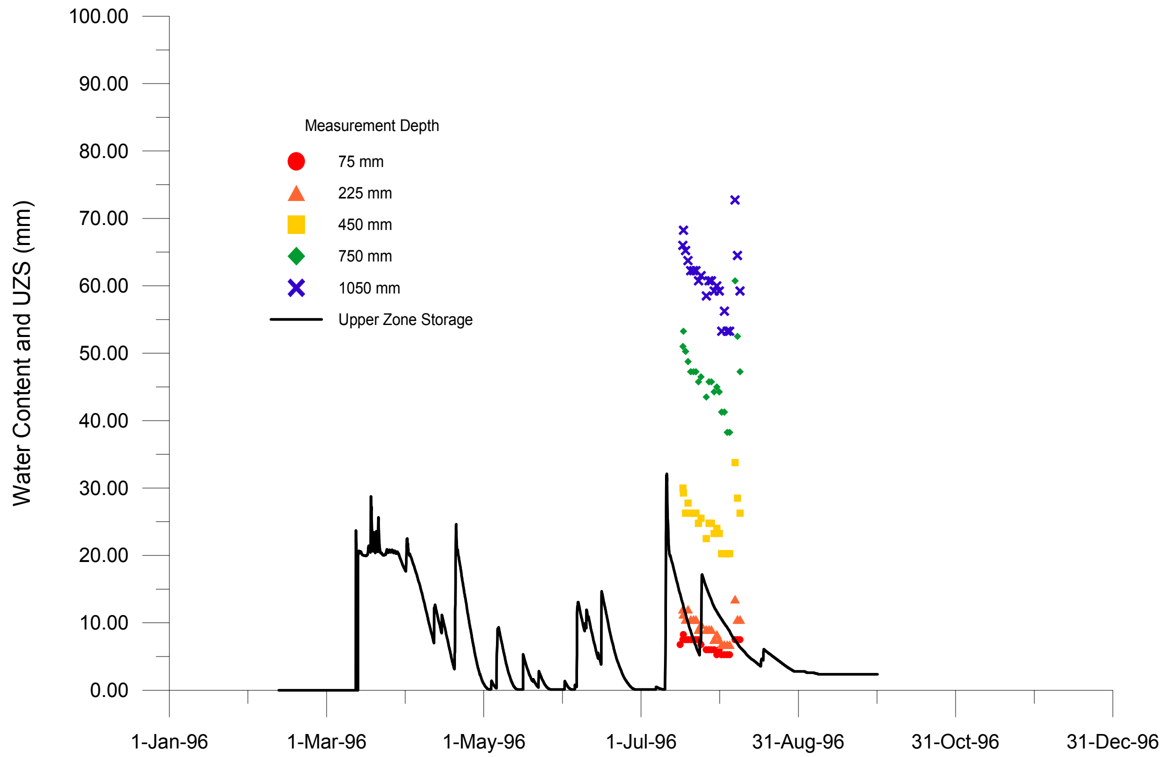

Figure C.12: Measured Cumulative Water Content and Modelled Upper Zone Storage NSAOJP 4 and RFF 2 (Dry Forest)

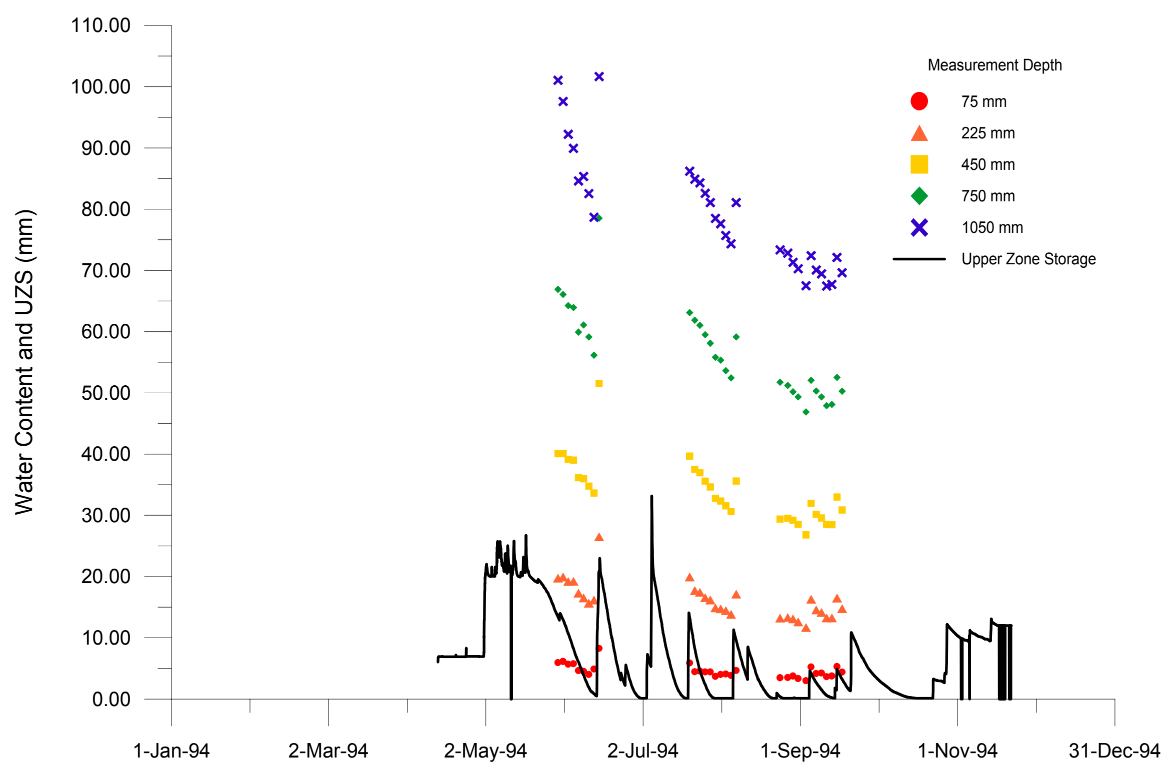

Figure C.13: Measured Cumulative Water Content and Modelled Upper Zone Storage NSAOJP 5 and RFF 2 (Dry Forest)

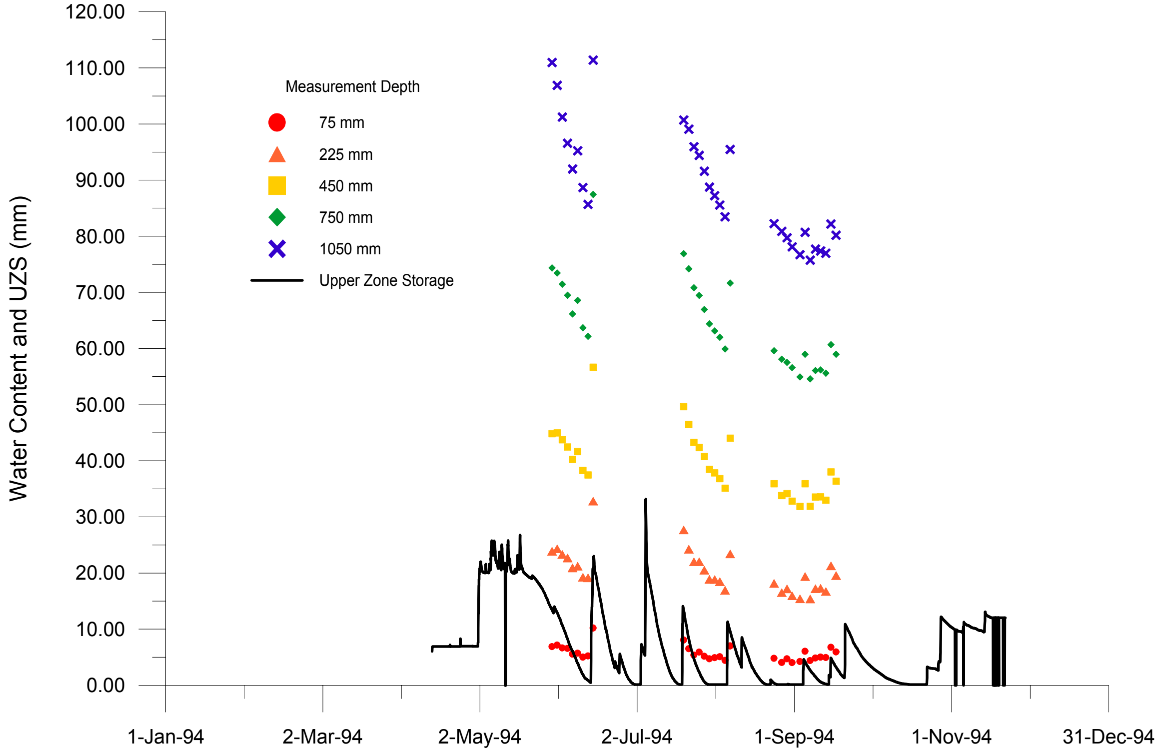

Figure C.14: Measured Cumulative Water Content and Modelled Upper Zone Storage NSAOJP 6 and RFF 2 (Dry Forest)

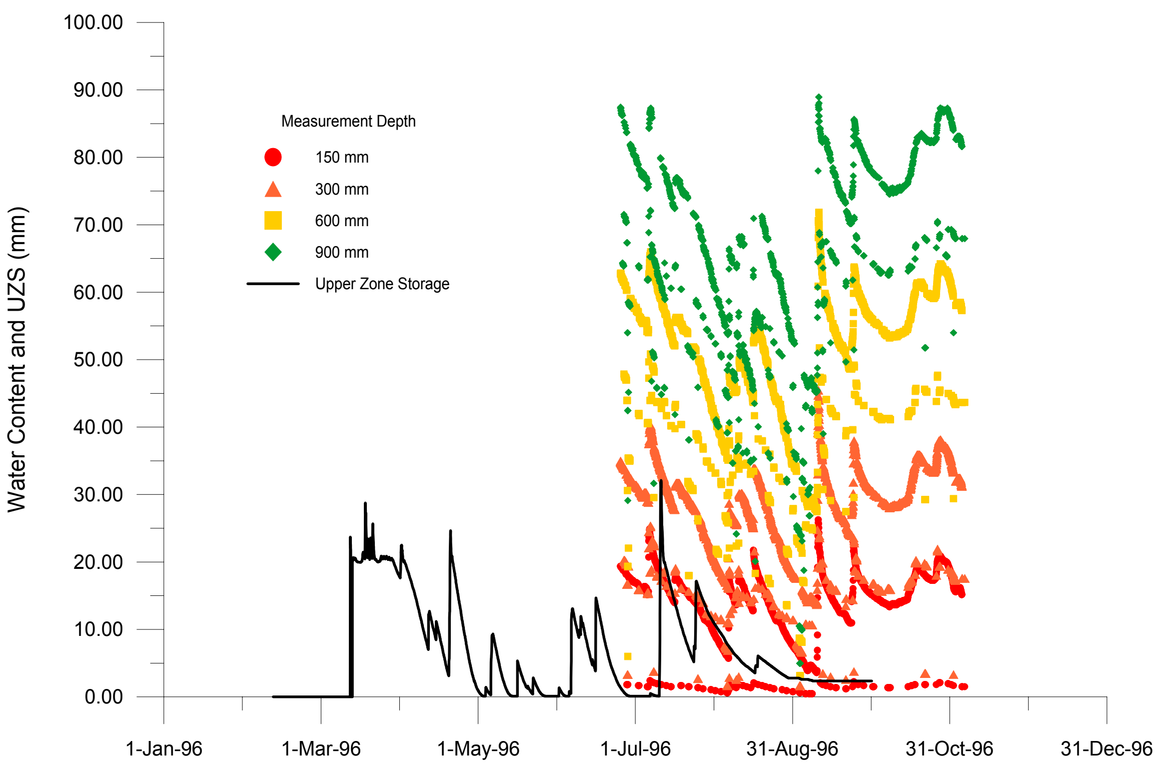

Figure C.15: Measured Cumulative Water Content and Modelled Upper Zone Storage
NSAOJP 7 and RFF 2 (Dry Forest)

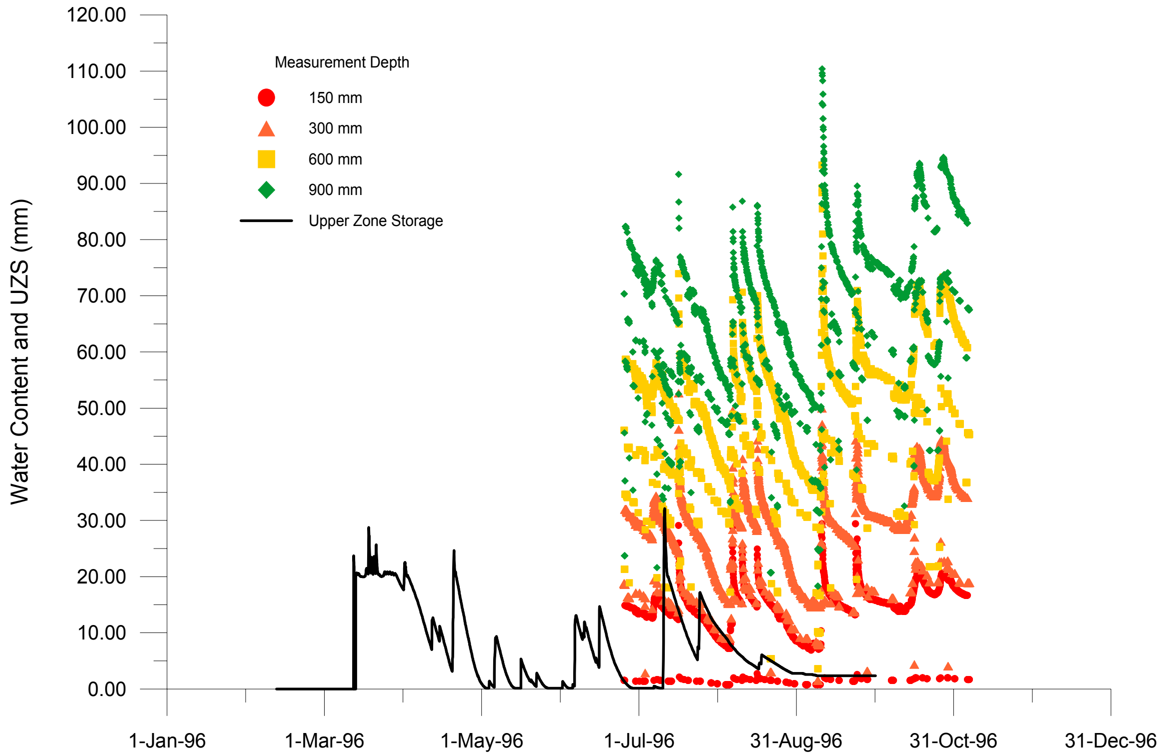

Figure C.16: Measured Cumulative Water Content and Modelled Upper Zone Storage
NSAYJP 1 and RFF 2 (Dry Forest)

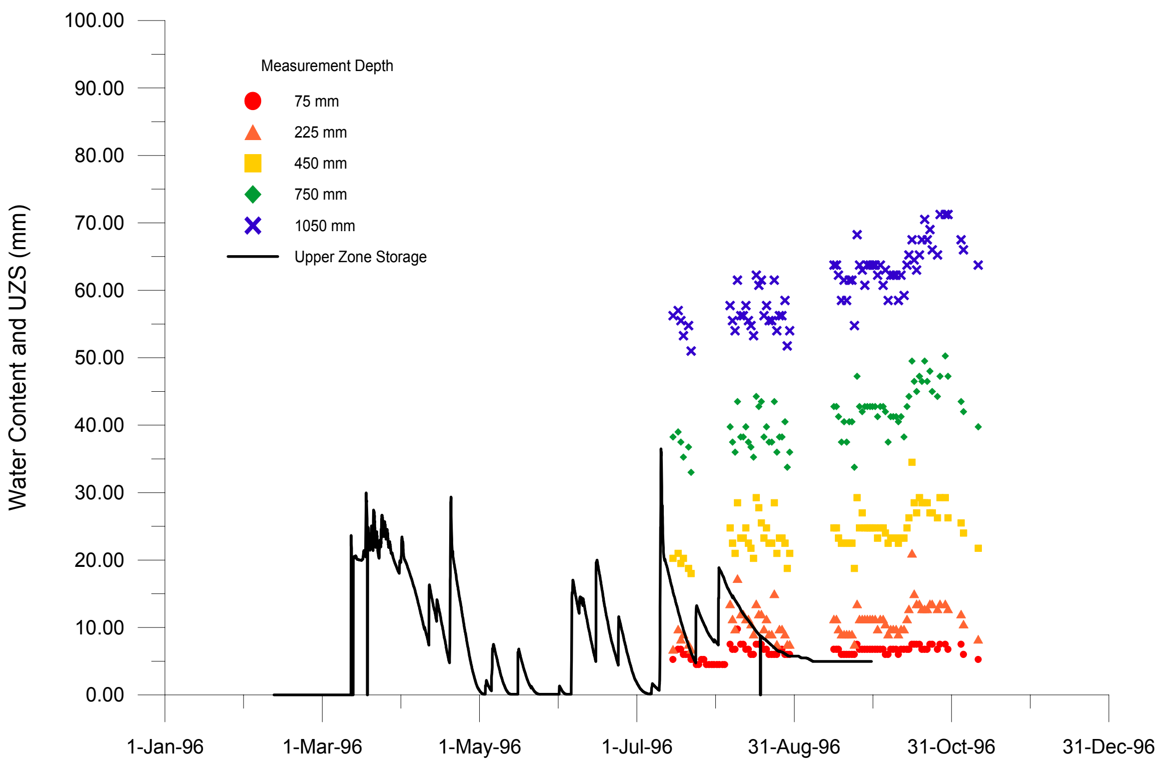

Figure C.17: Measured Cumulative Water Content and Modelled Upper Zone Storage NSAYJP 2 and RFF 2 (Dry Forest)

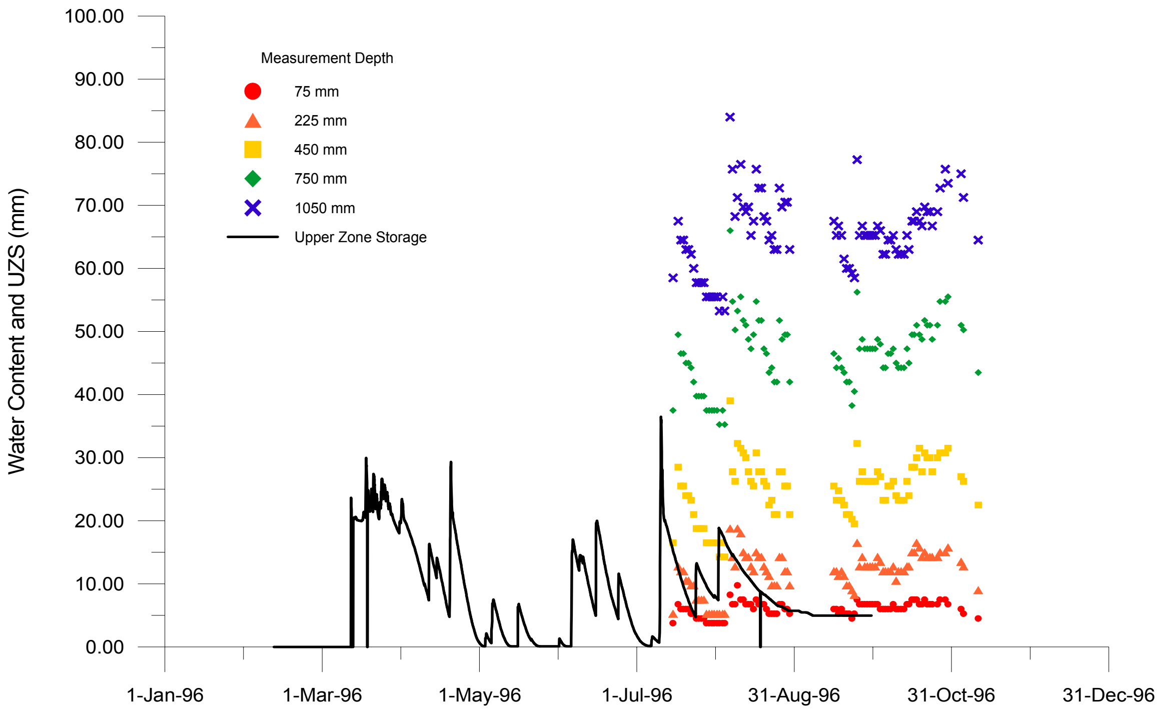

Figure C.18: Measured Cumulative Water Content and Modelled Upper Zone Storage NSAYJP 3 and RFF 2 (Dry Forest)

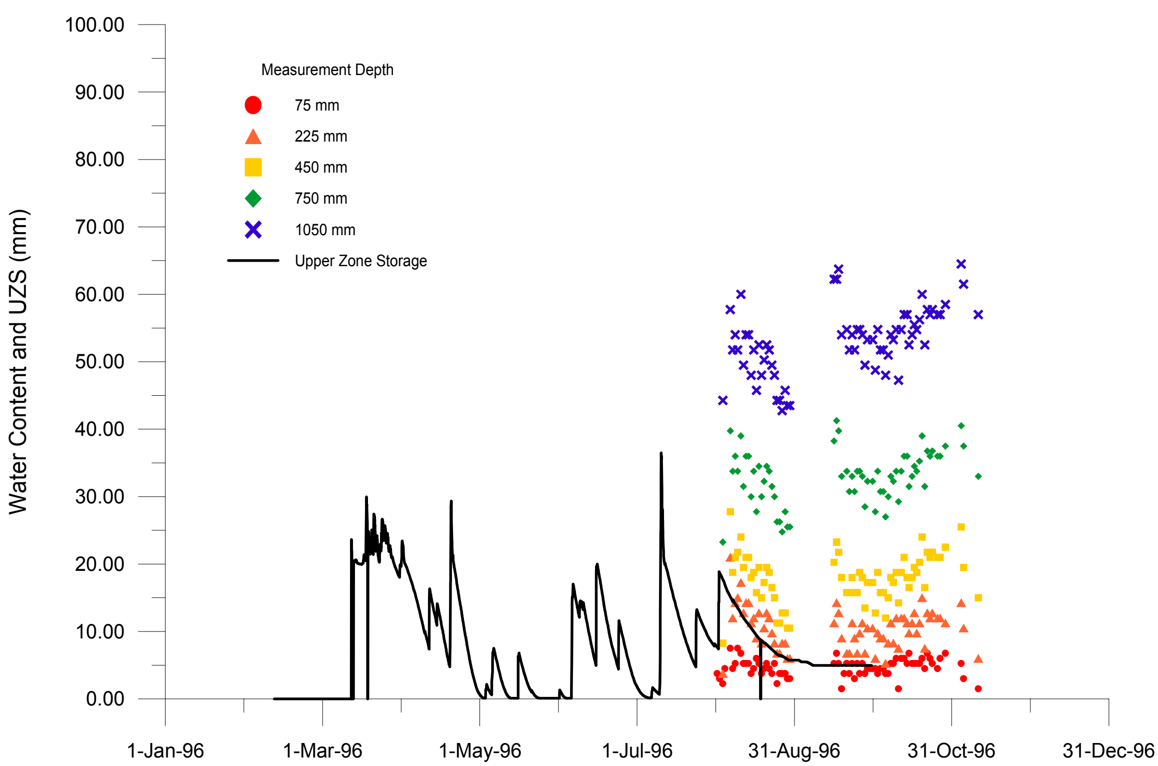

Figure C.19: Measured Cumulative Water Content and Modelled Upper Zone Storage NSAYJP 4 and RFF 2 (Dry Forest)

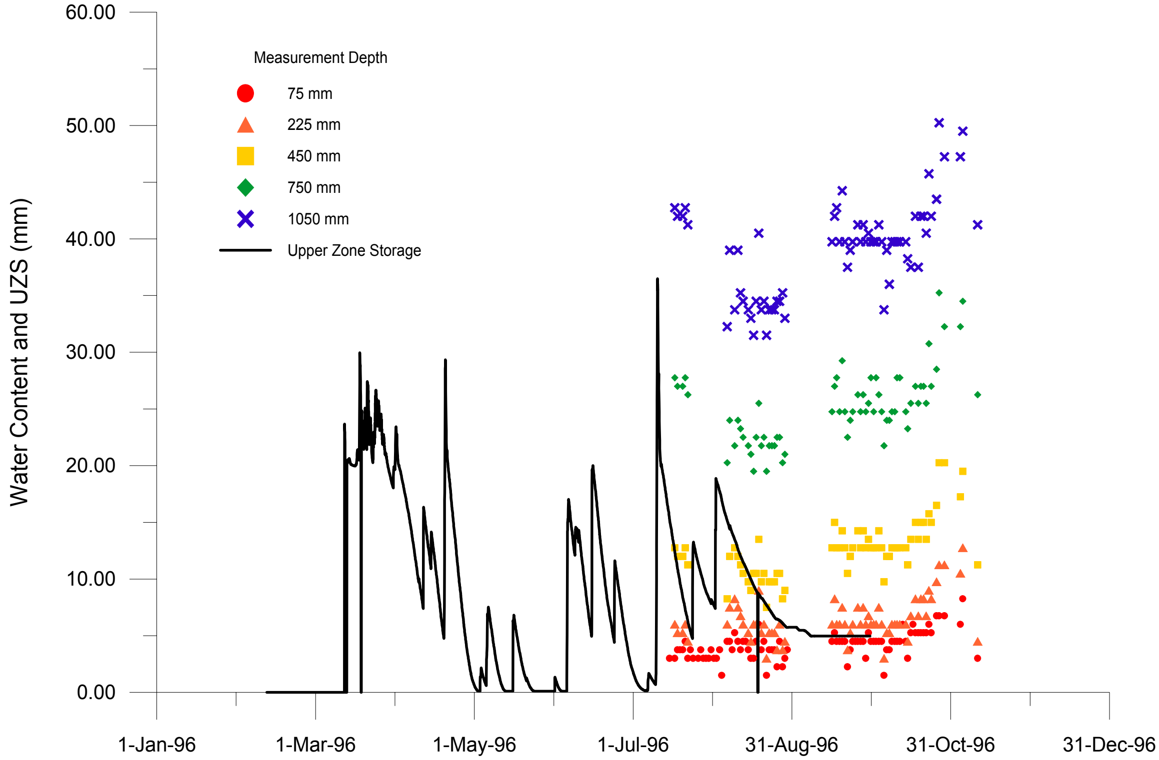

Figure C.20: Measured Cumulative Water Content and Modelled Upper Zone Storage NSAYJP 5 and RFF 2 (Dry Forest)

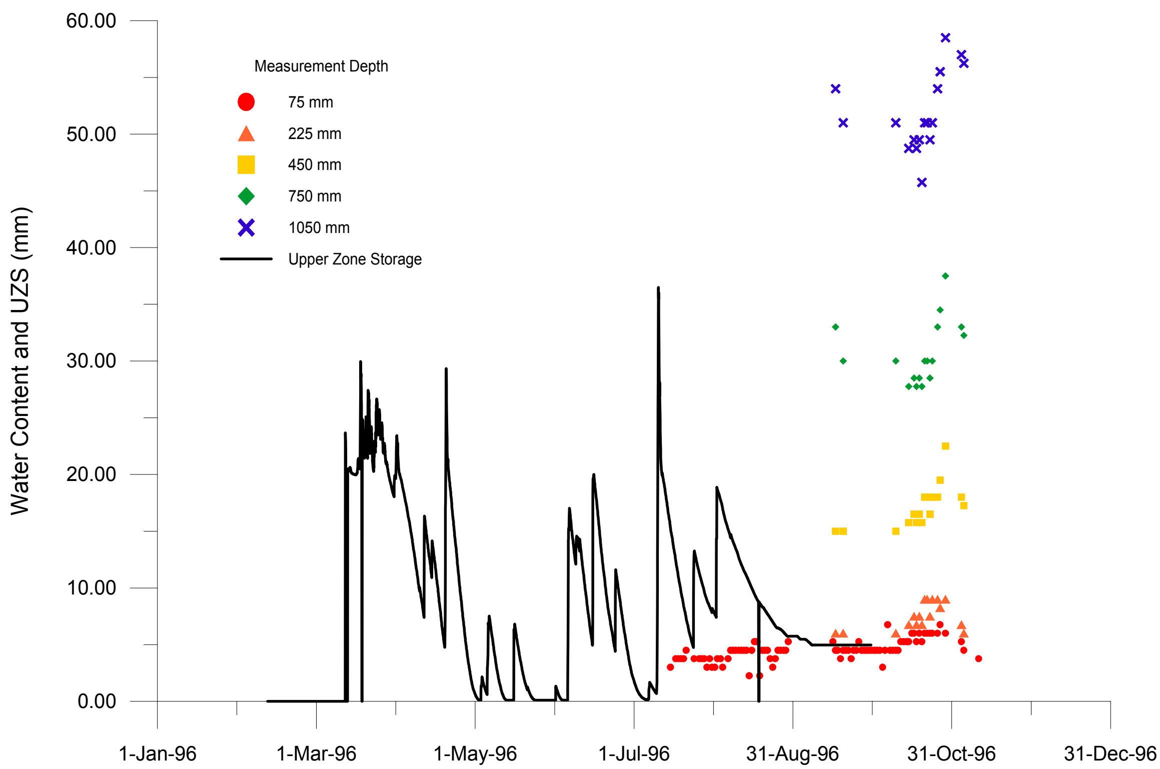

Figure C.21: Measured Cumulative Water Content and Modelled Upper Zone Storage
NSAYJP 6 and RFF 2 (Dry Forest)

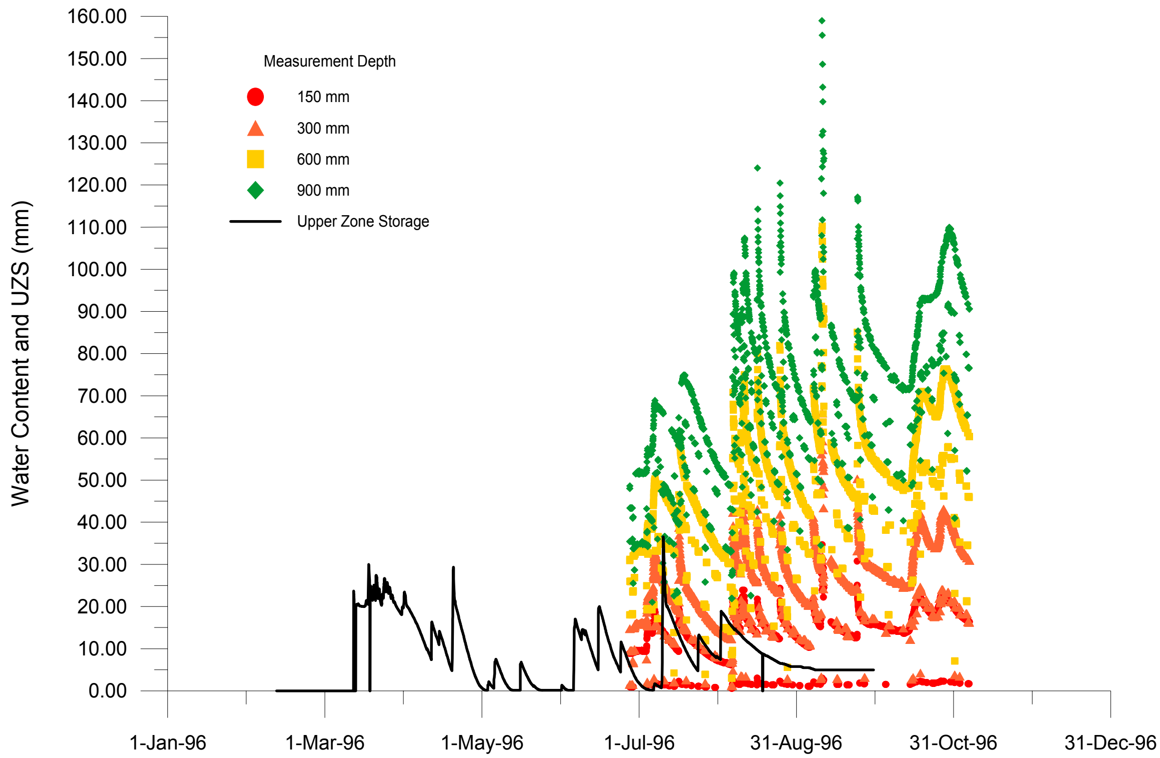

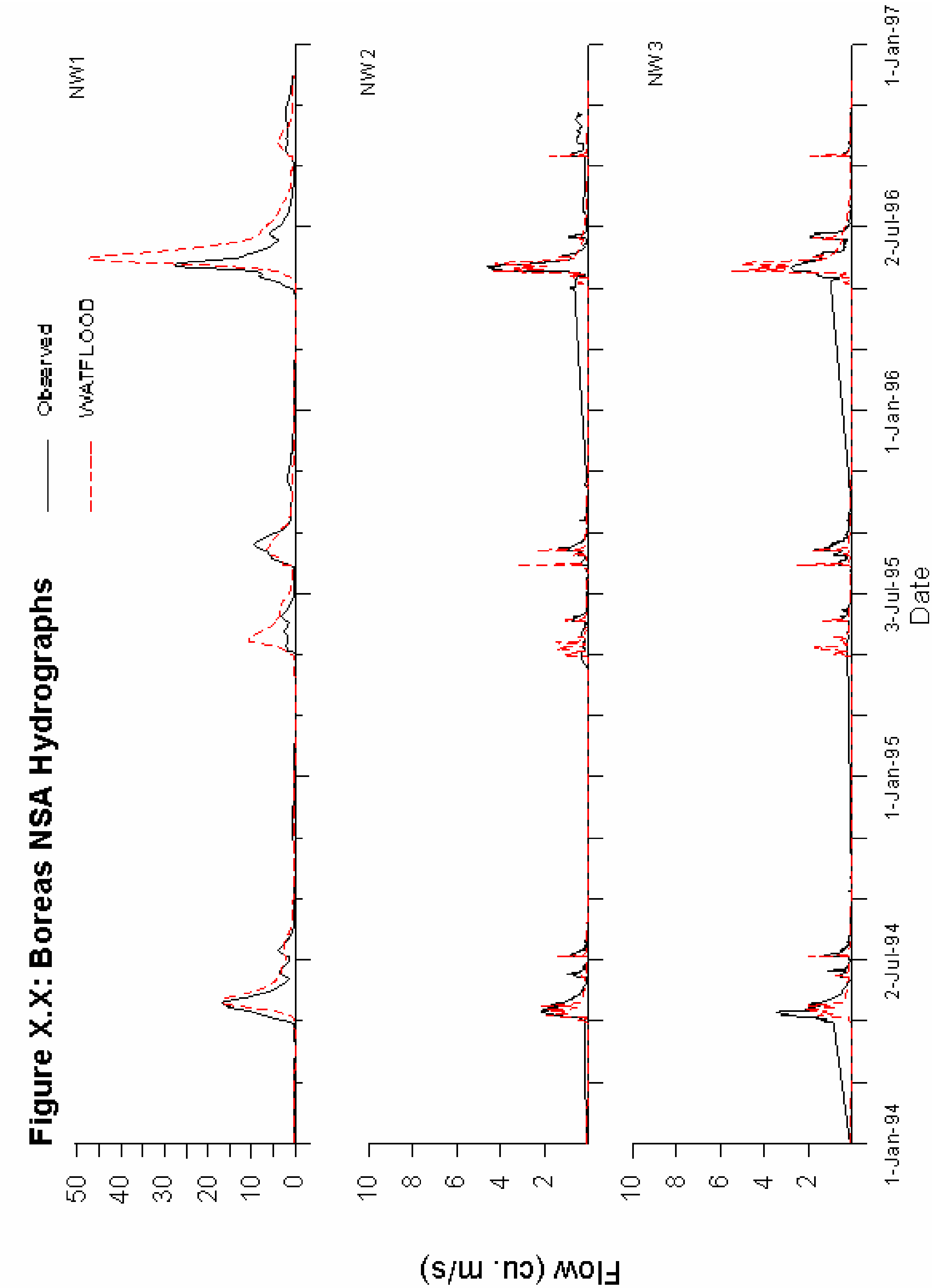
Figure X.X: Boreas NSA Hydrographs
Observed
WATFLOOD
NW1
NW2
NW3
50
40
30
20
10
0
10
8
6
4
2
10
8
6
4
2
Flow (cu. m/s)
1-Jan-94
2-Jul-94
1-Jan-95
3-Jul-95
1-Jan-96
2-Jul-96
1-Jan-97
Date

Figure C.23: Boreas NSA Hydrographs Using SSA Parameters

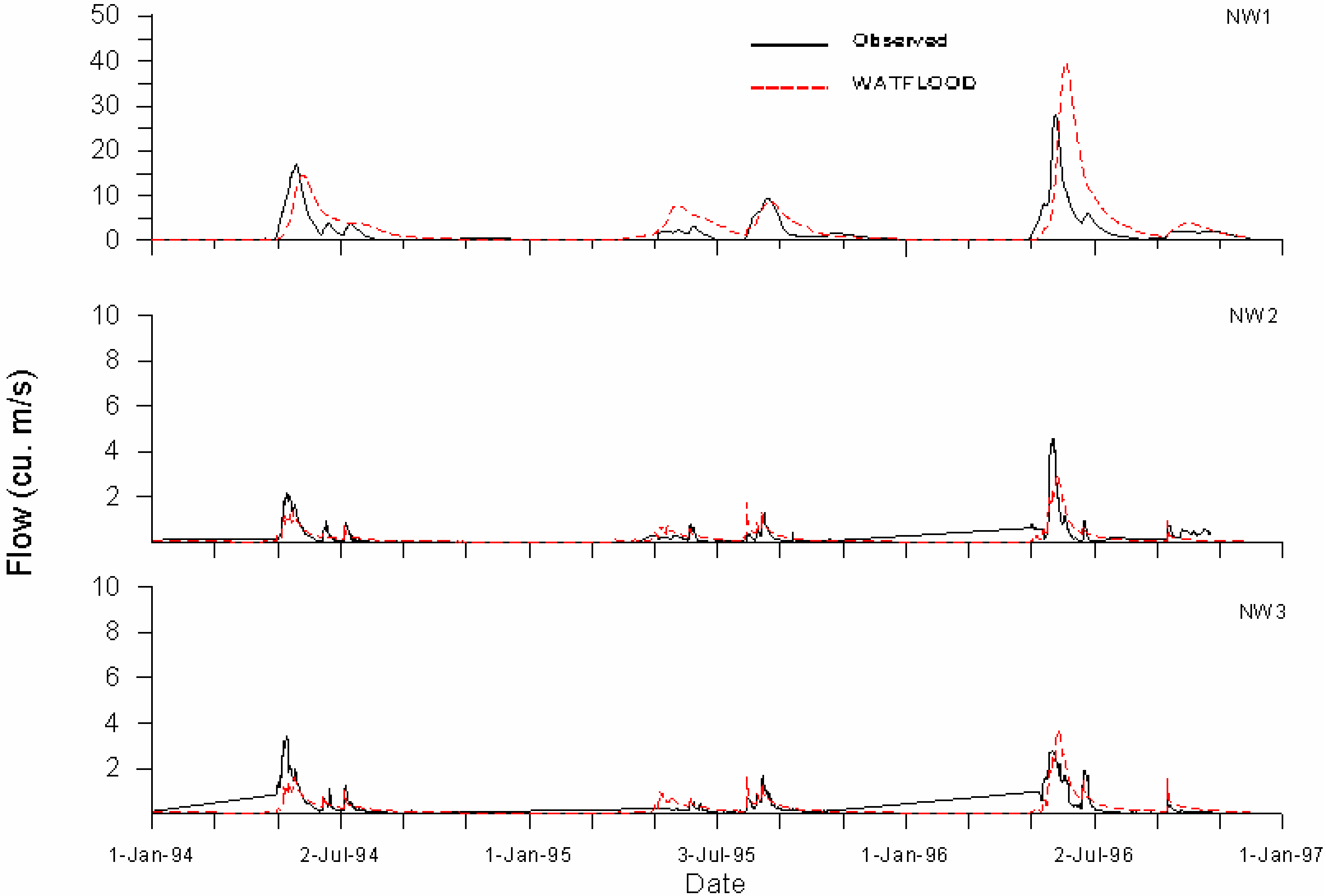

Figure C.24: Measured Cumulative Water Content and Modelled Upper Zone Storage SSAOBS 1-1 and RFF 6 (Wetland)

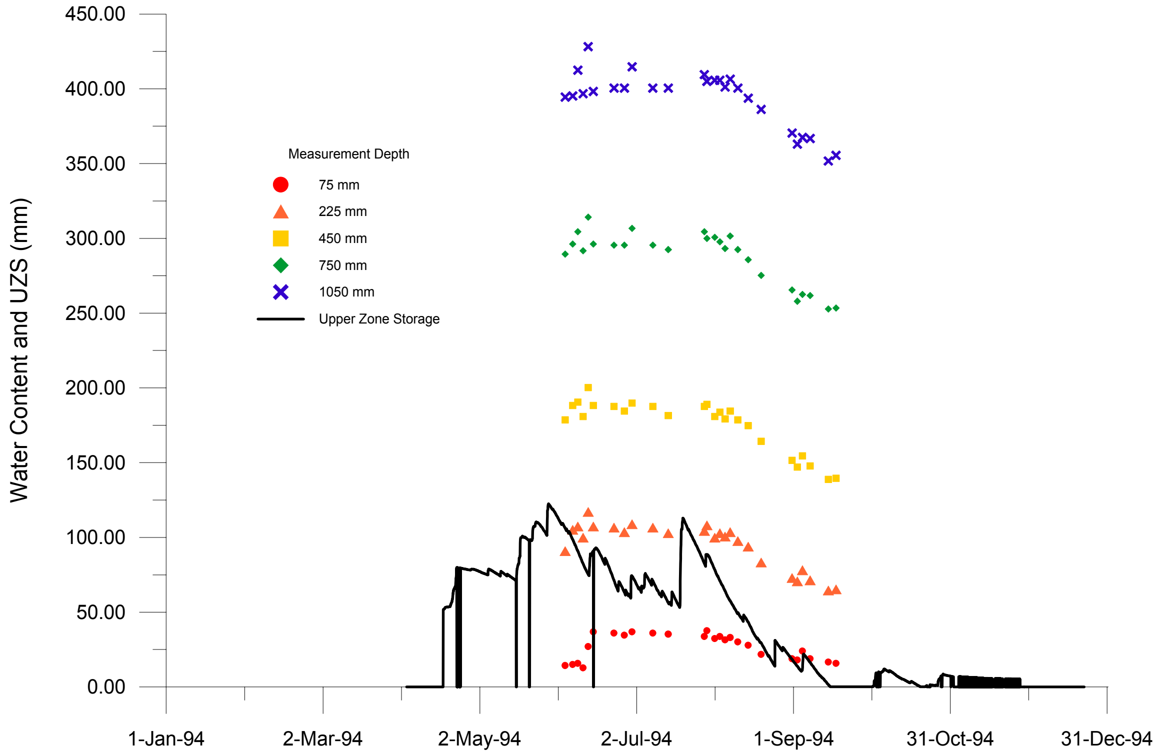

Figure C.25: Measured Cumulative Water Content and Modelled Upper Zone Storage SSAOBS 1-1 and RFF 6 (Wetland)

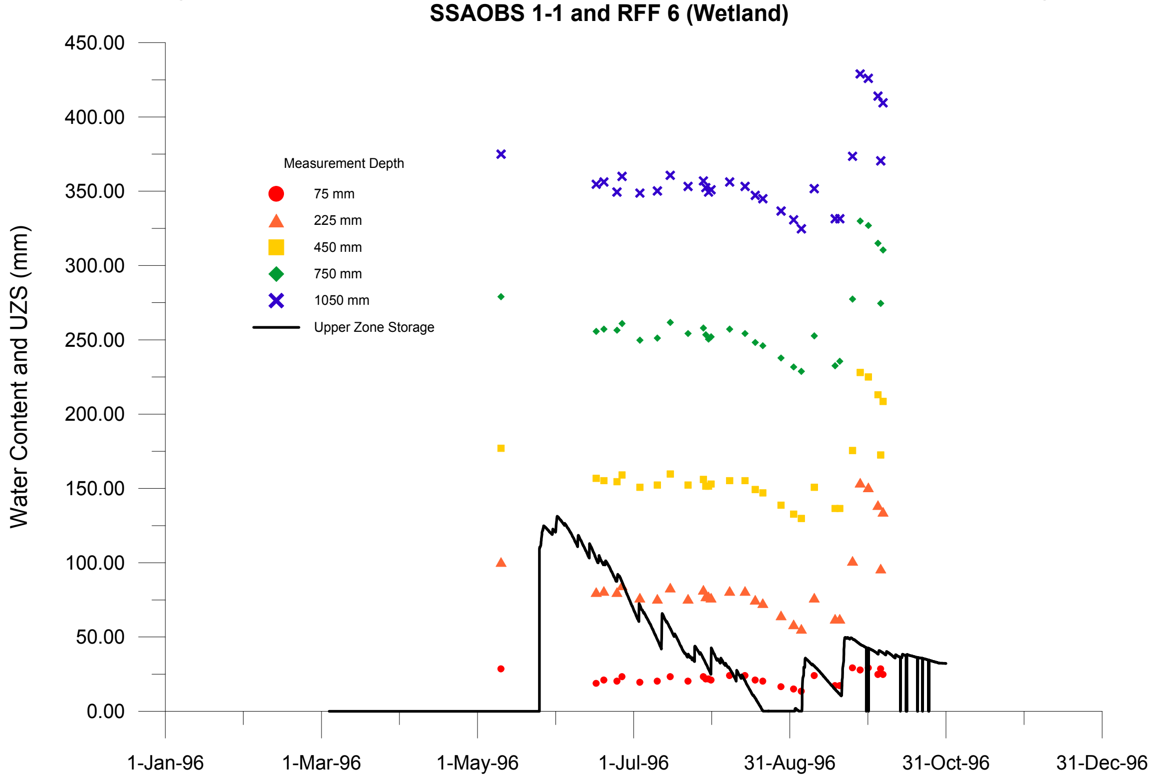

Figure C.26: Measured Cumulative Water Content and Modelled Upper Zone Storage SSAOBS 1-2 and RFF 6 (Wetland)

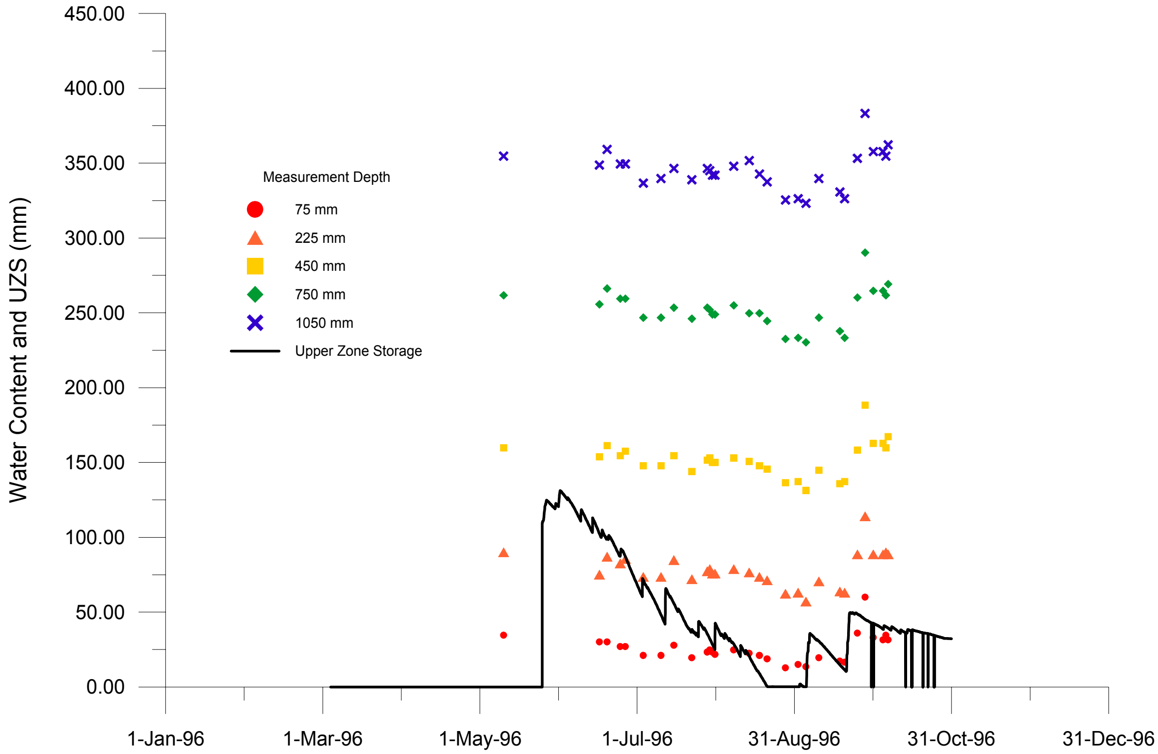

Figure C.27: Measured Cumulative Water Content and Modelled Upper Zone Storage SSAOBS 1-3 and RFF 6 (Wetland)

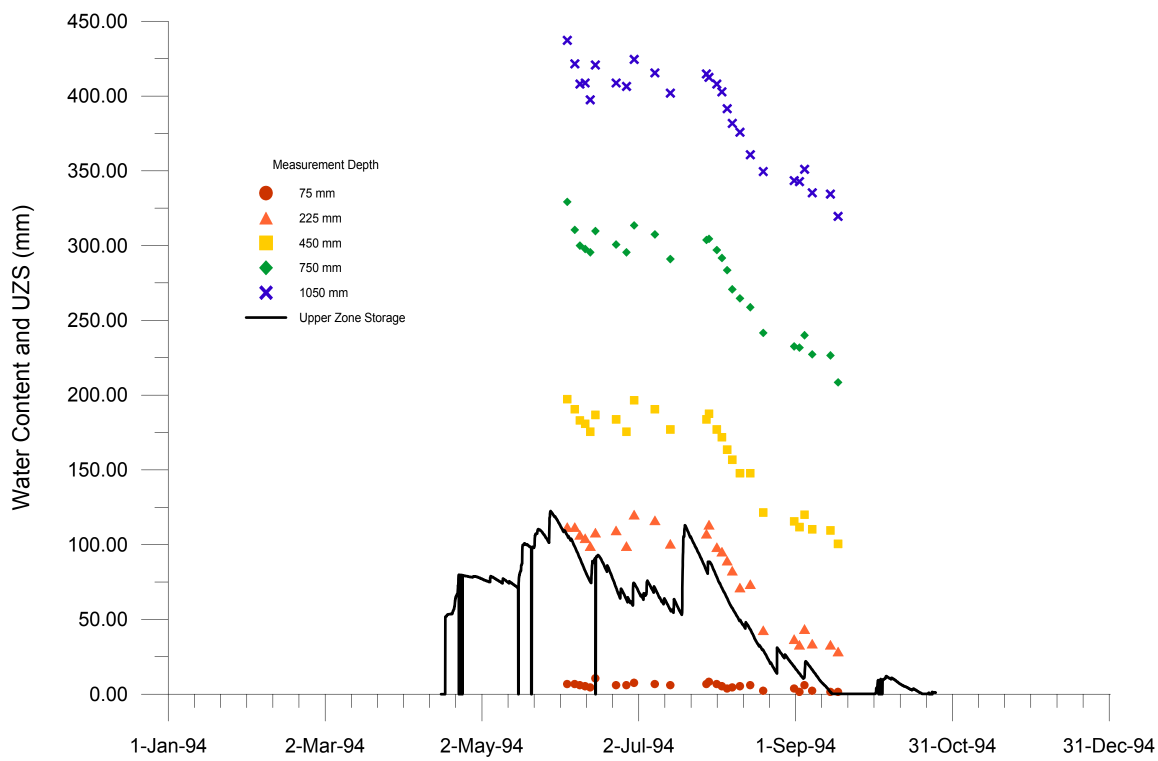

Figure C.30: Measured Cumulative Water Content and Modelled Upper Zone Storage SSAOBS 2-1 and RFF 6 (Wetland)

Figure C.28: Measured Cumulative Water Content and Modelled Upper Zone Storage SSAOBS 1-4 and RFF 6 (Wetland)

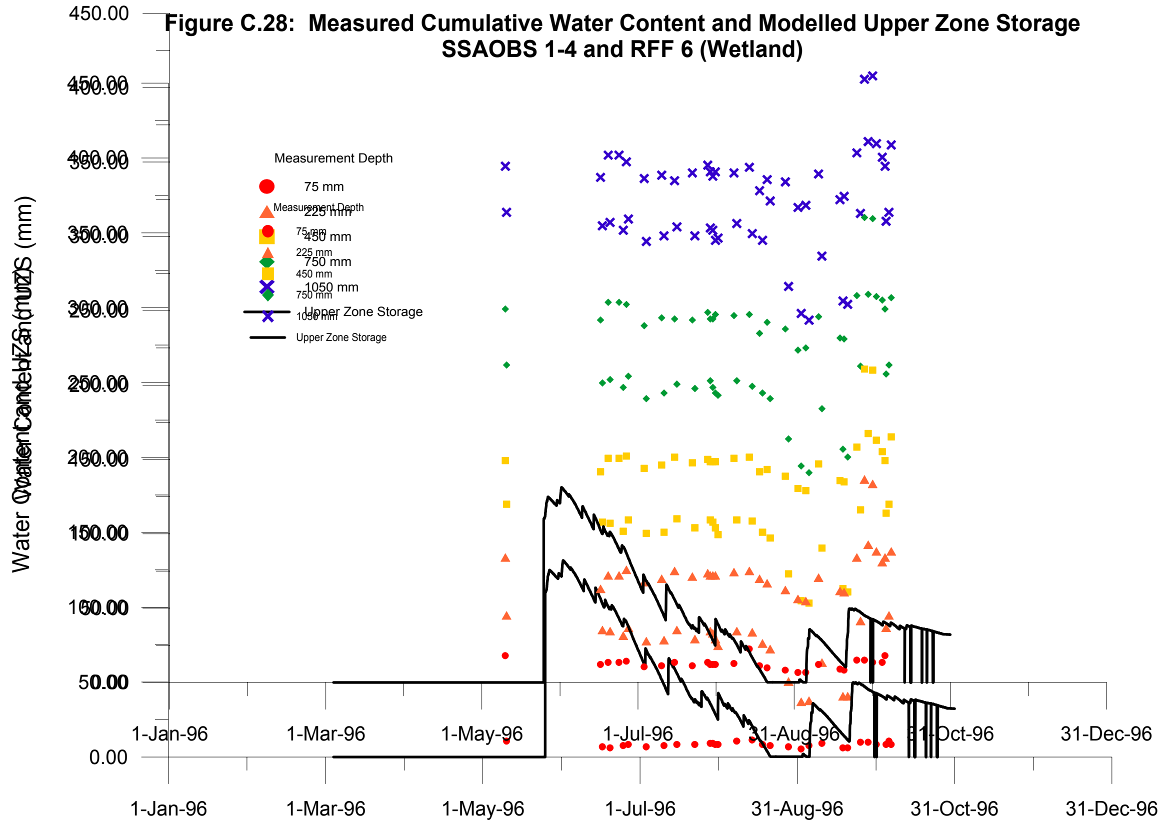

Figure C.29: Measured Cumulative Water Content and Modelled Upper Zone Storage SSAOBS 1-5 and RFF 6 (Wetland)

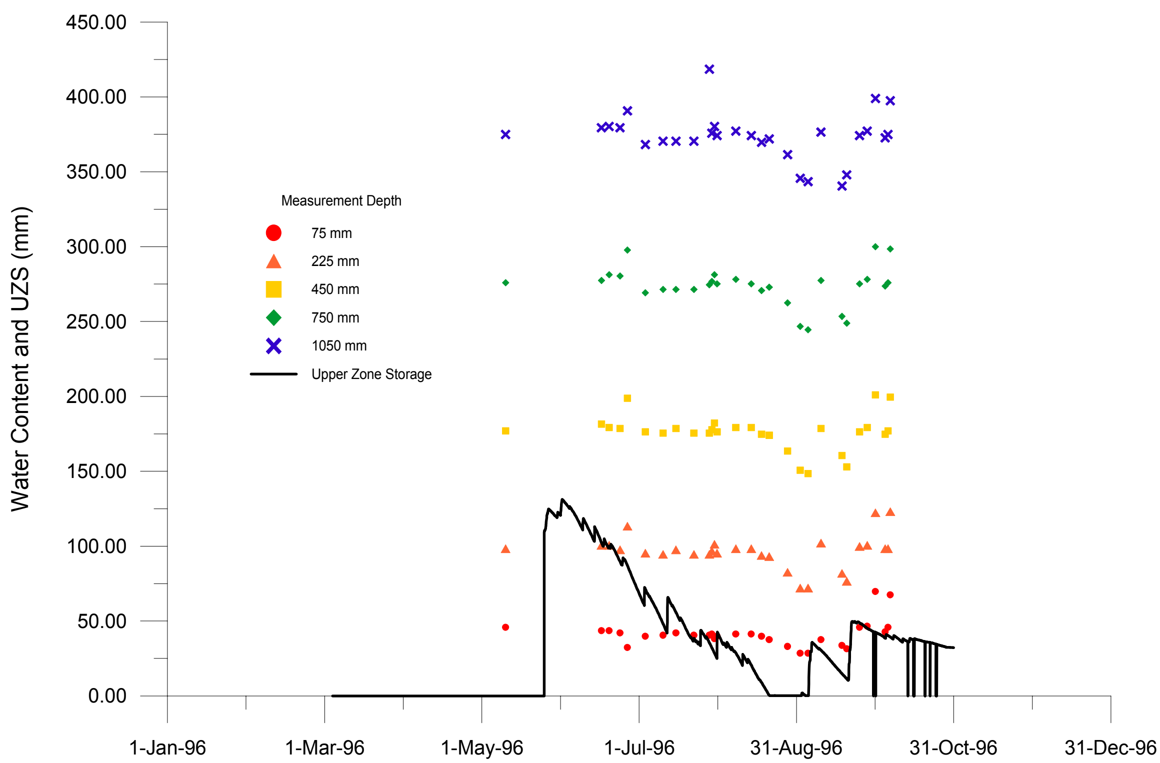

Figure C.31: Measured Cumulative Water Content and Modelled Upper Zone Storage
SSAOBS 2-3 and RFF 6 (Wetland)

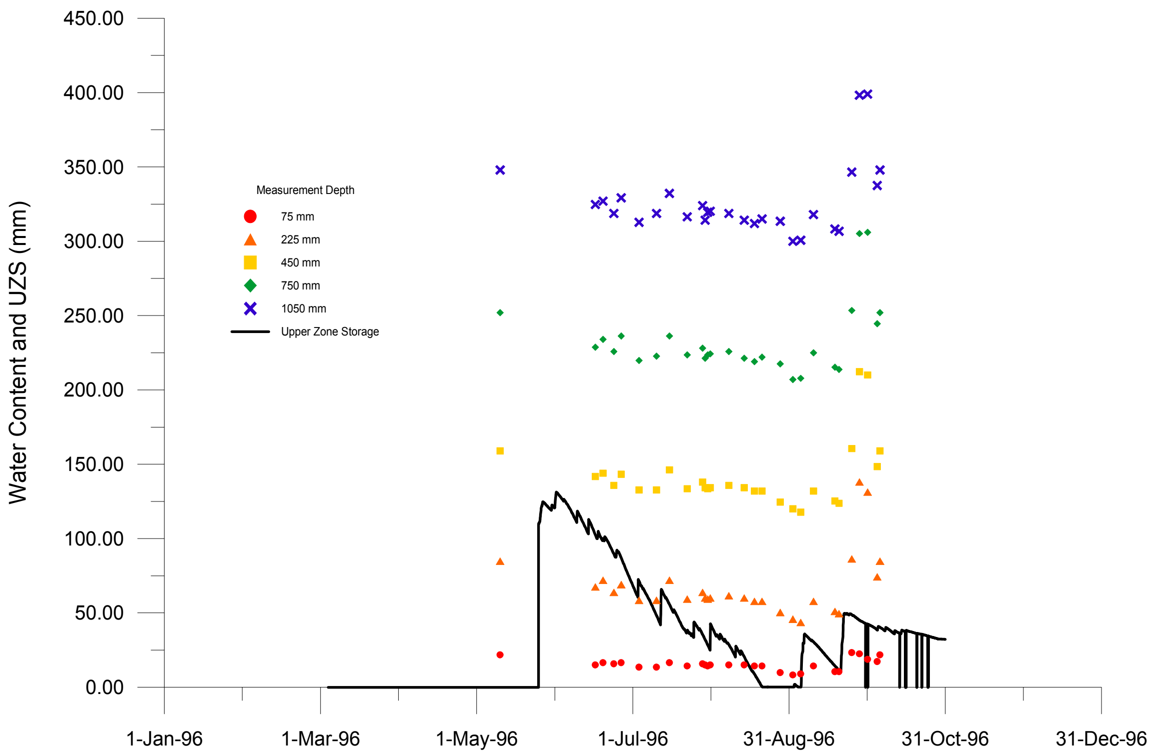

Figure C.32: Measured Cumulative Water Content and Modelled Upper Zone Storage SSAOBS 2-4 and RFF 6 (Wetland)

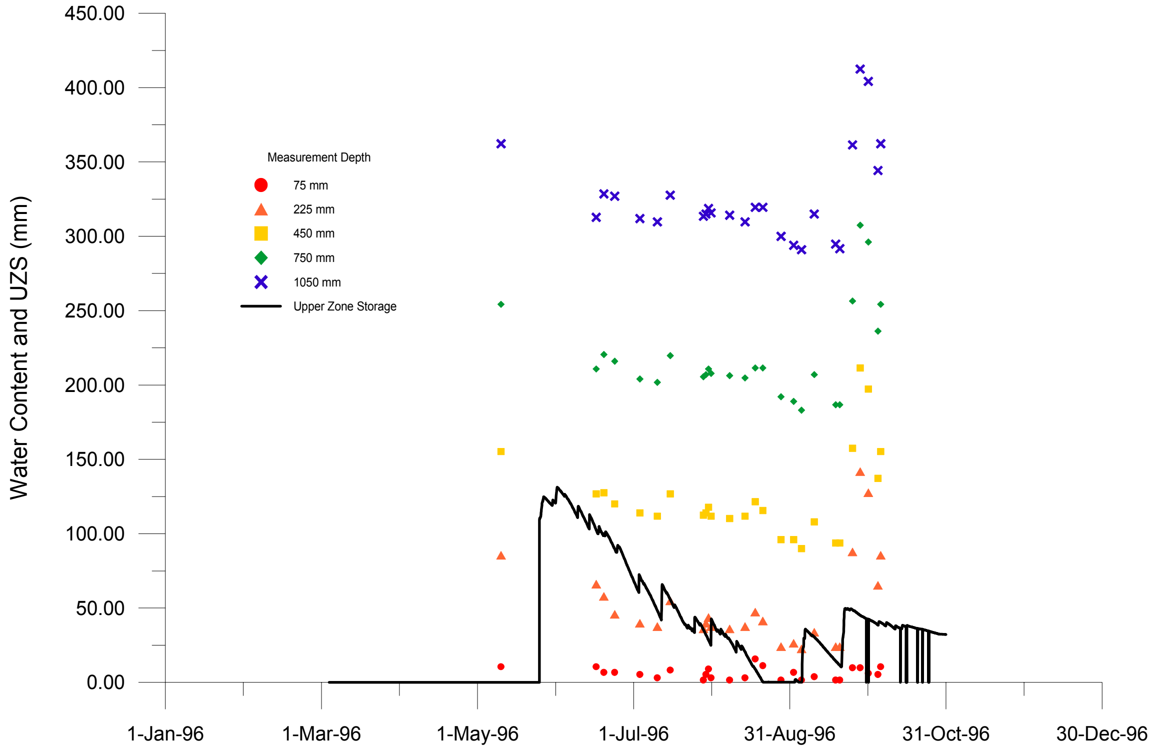

Figure C.33: Measured Cumulative Water Content and Modelled Upper Zone Storage SSAOBS 2-5 and RFF 6 (Wetland)

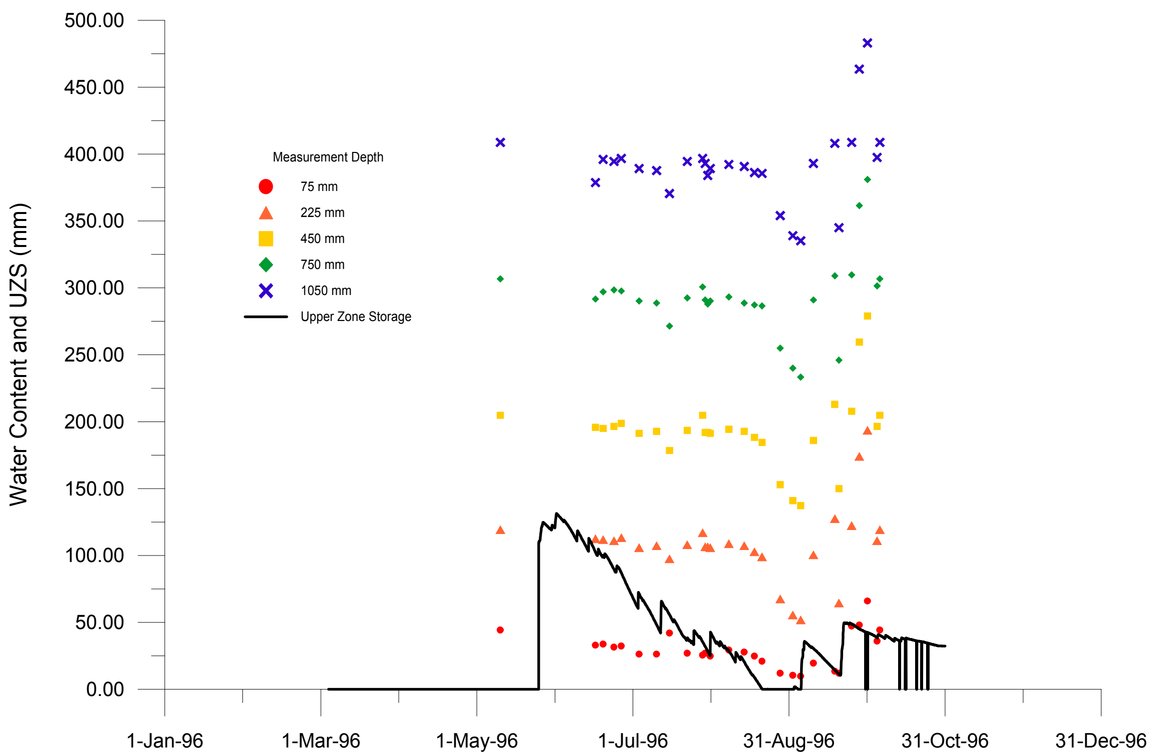

Figure C.34: Measured Cumulative Water Content and Modelled Upper Zone Storage SSAOJP 1 and RFF 2 (Dry Conifer)

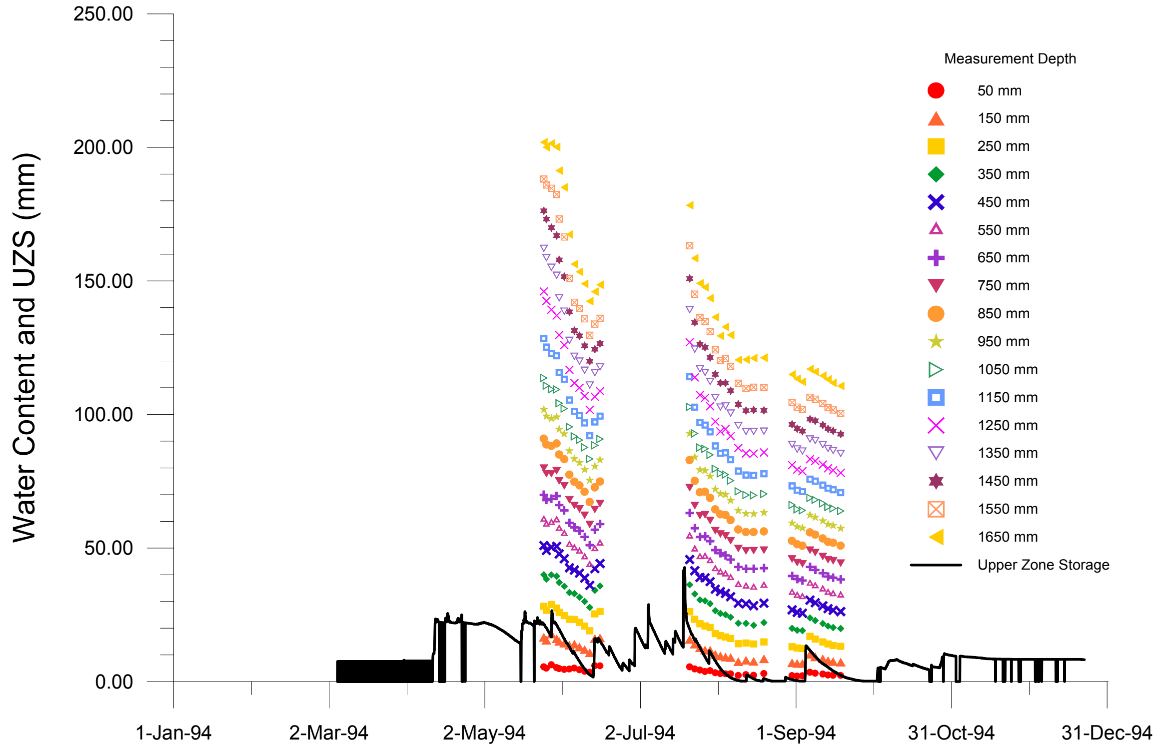

Figure C.35: Measured Cumulative Water Content and Modelled Upper Zone Storage SSAOJP 2 and RFF 2 (Dry Conifer)

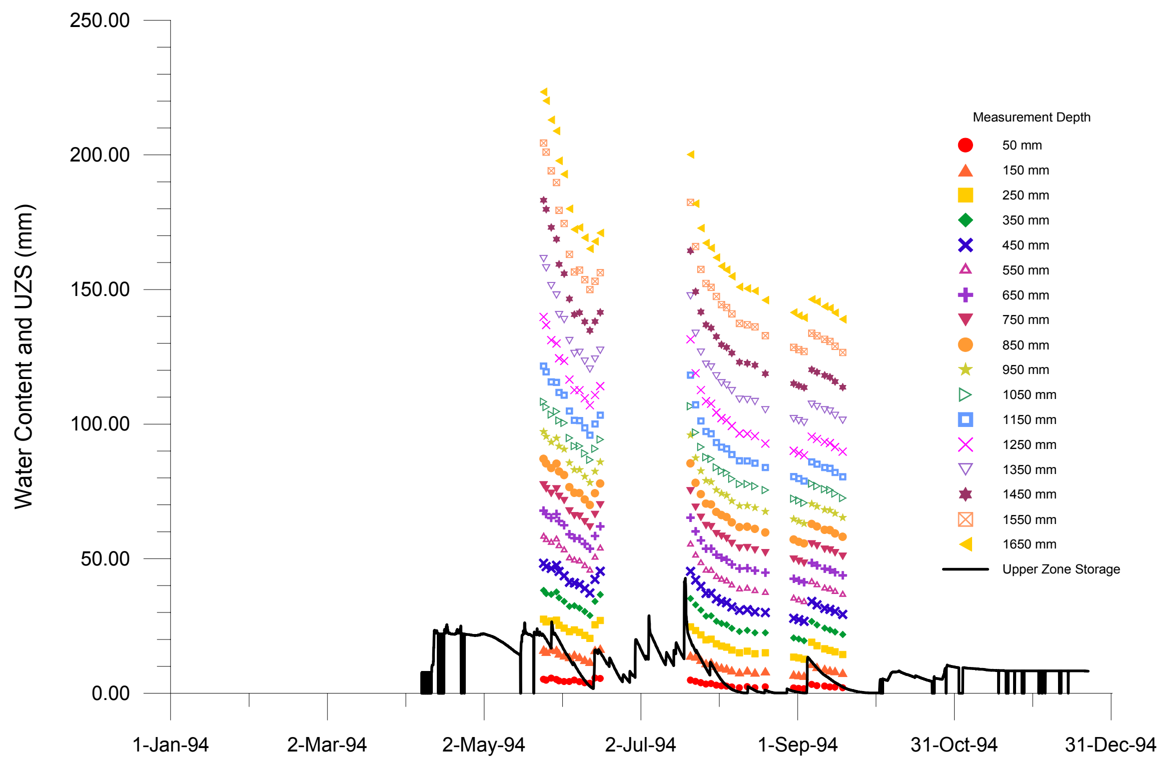

Figure C.36: Measured Cumulative Water Content and Modelled Upper Zone Storage
SSAOJP 3 and RFF 2 (Dry Conifer)

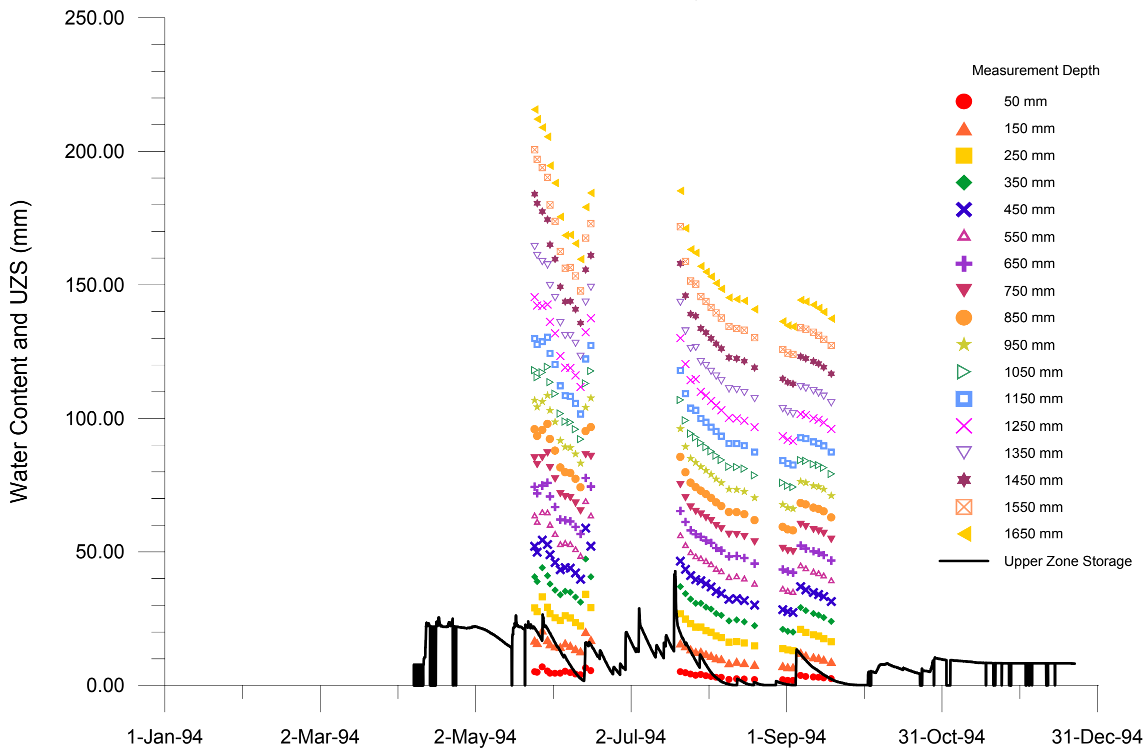

Figure C.37: Measured Cumulative Water Content and Modelled Upper Zone Storage
SSAOJP 4 and RFF 2 (Dry Conifer)

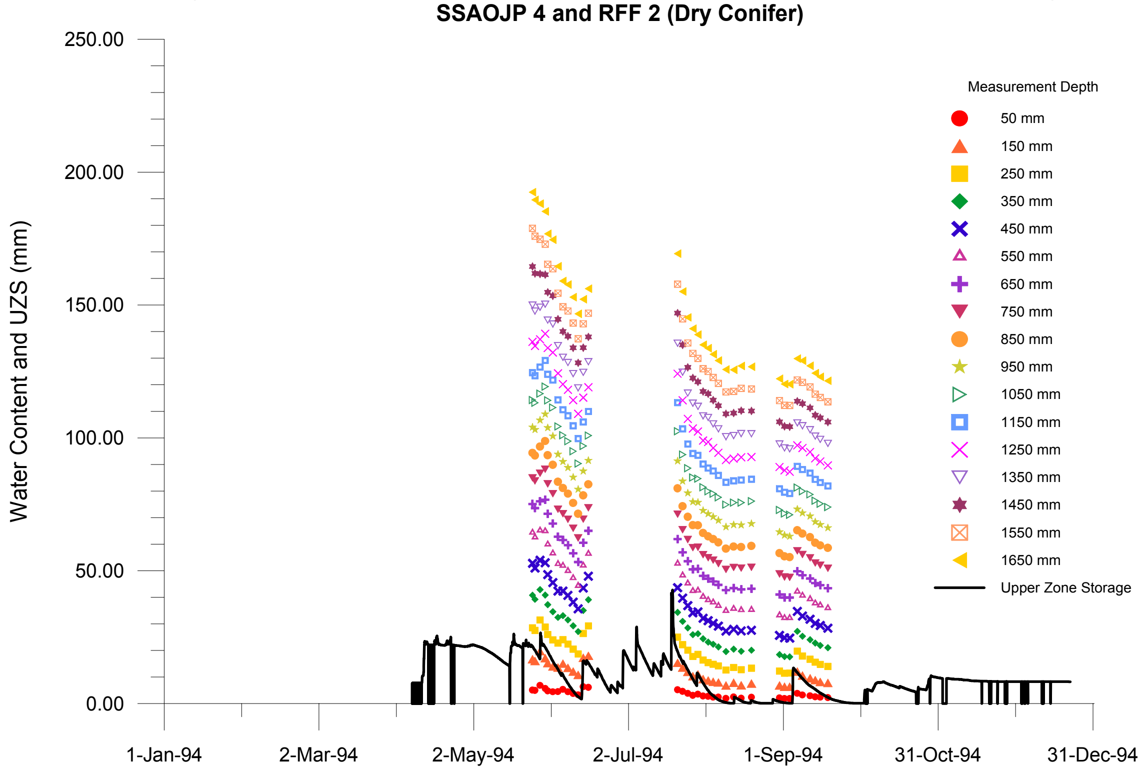

Figure C.38: Measured Cumulative Water Content and Modelled Upper Zone Storage
SSAOJP 5 and RFF 2 (Dry Conifer)

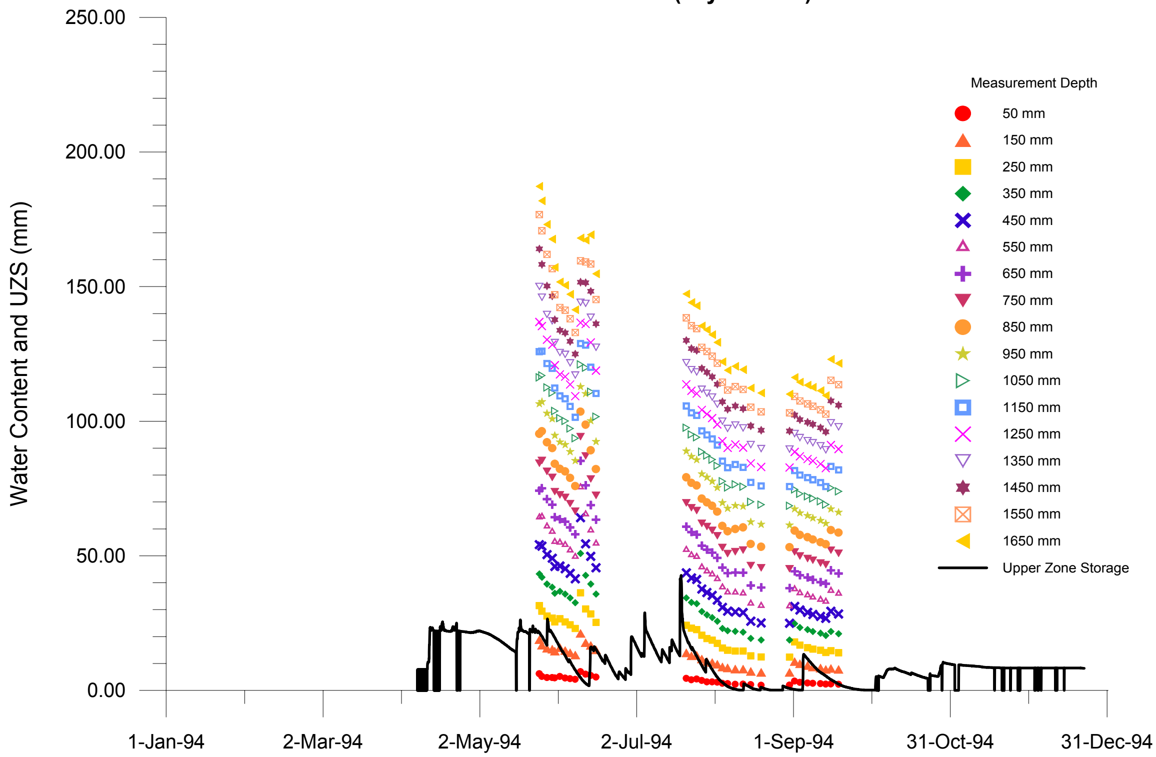

Figure C.39: Measured Cumulative Water Content and Modelled Upper Zone Storage
SSAYJP 1 and RFF 2 (Dry Conifer)

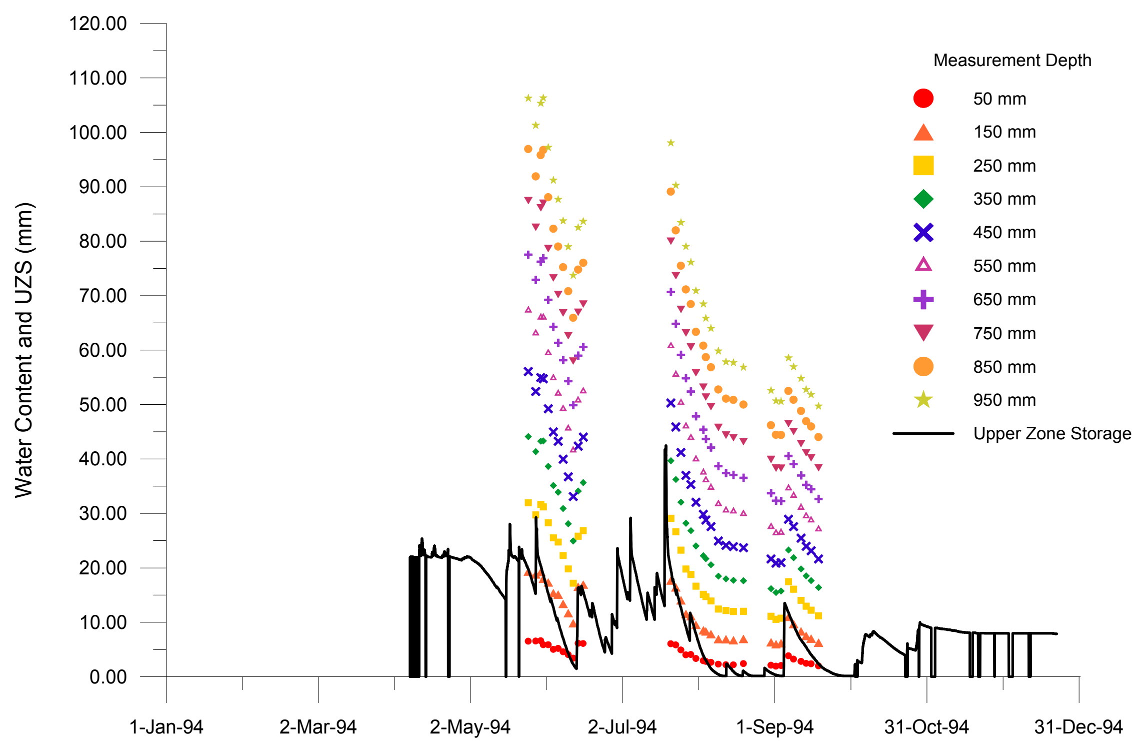

Figure C.40: Measured Cumulative Water Content and Modelled Upper Zone Storage SSAYJP 2 and RFF 2 (Dry Conifer)

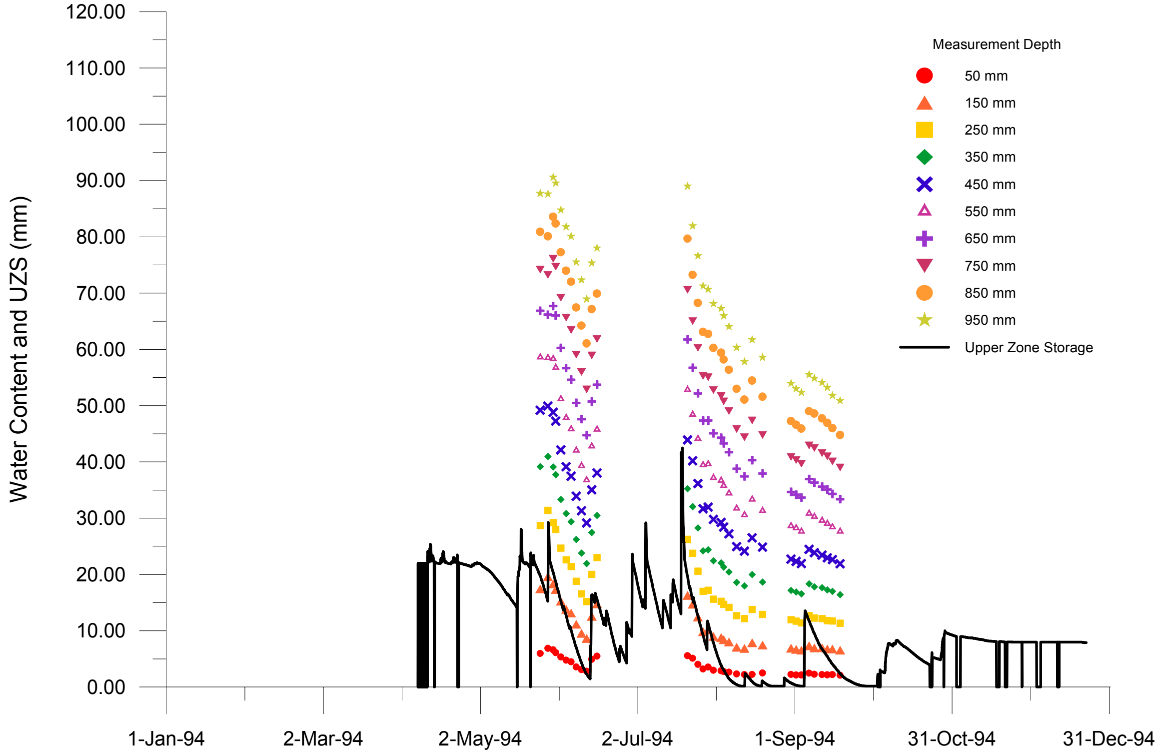

Figure C.41: Measured Cumulative Water Content and Modelled Upper Zone Storage SSAYJP 3 and RFF 2 (Dry Conifer)

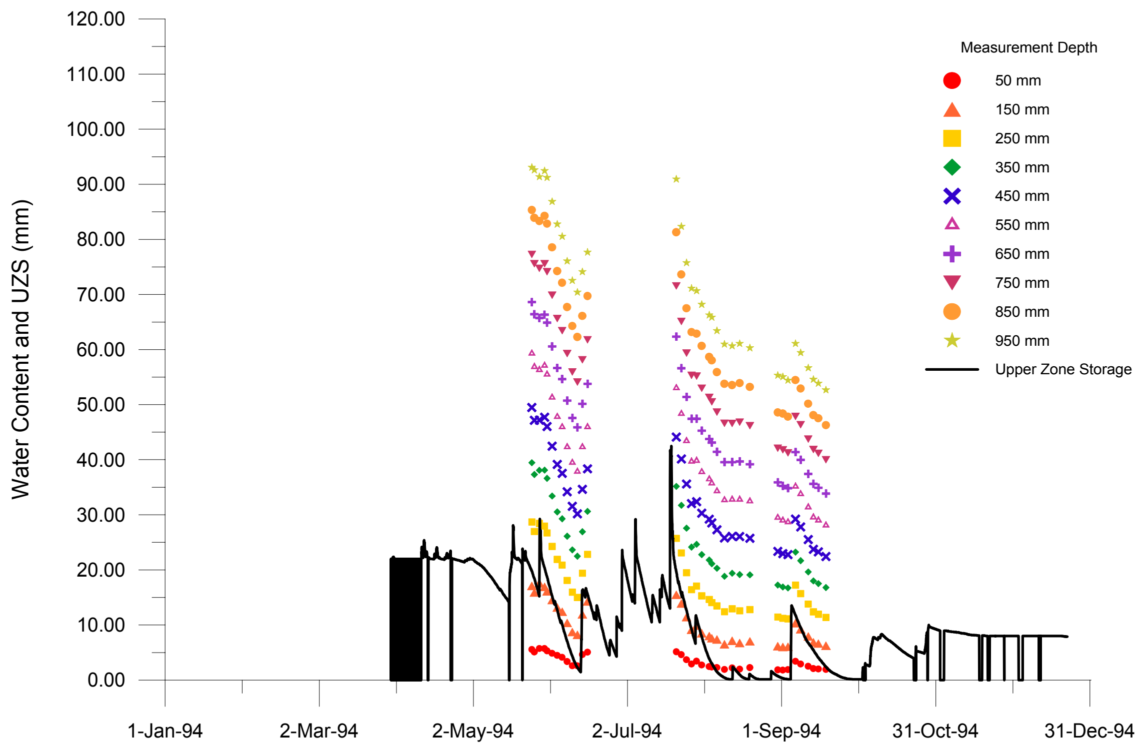

Figure C.42: Measured Cumulative Water Content and Modelled Upper Zone Storage
SSAYJP 4 and RFF 2 (Dry Conifer)

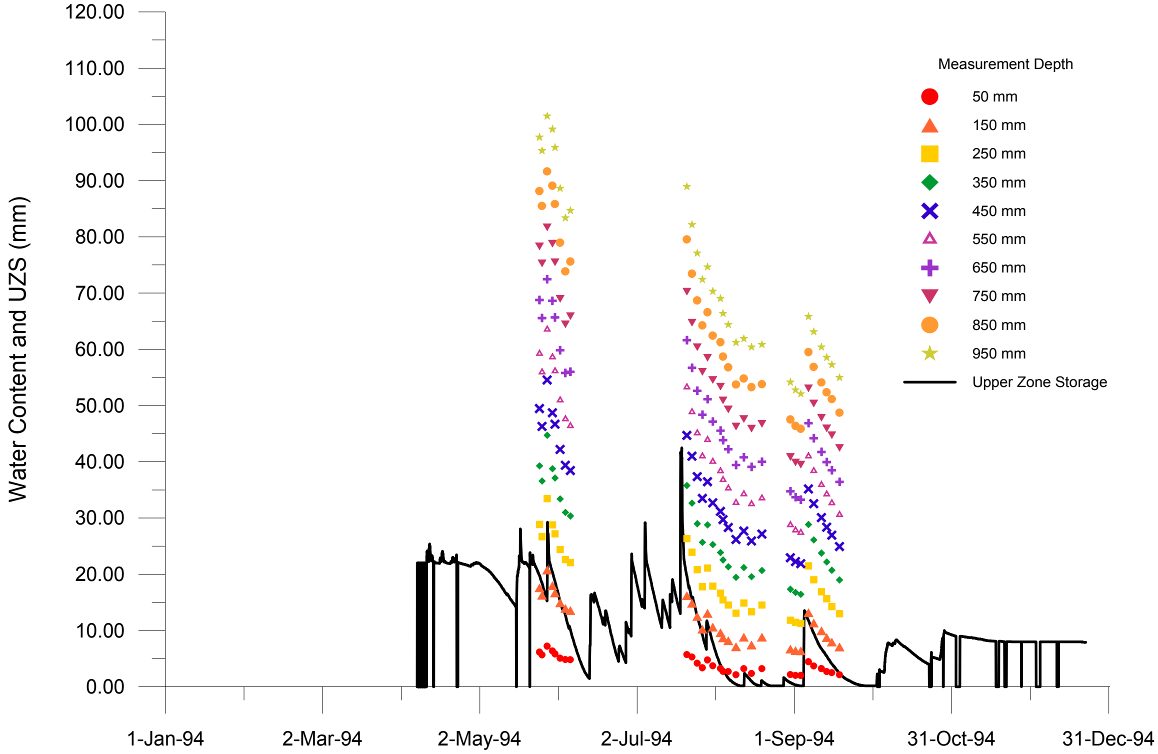

Figure C.43: Measured Cumulative Water Content and Modelled Upper Zone Storage
SSAYJP 5 and RFF 2 (Dry Conifer)

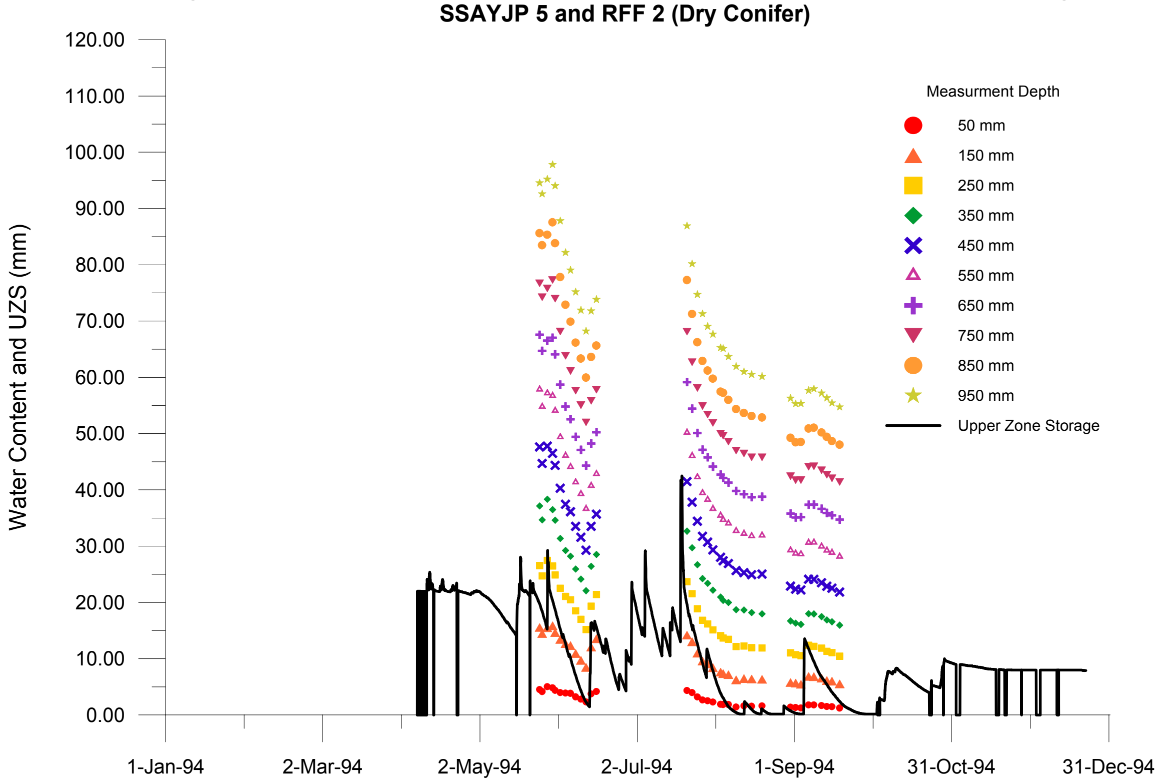

Figure C.44: Measured Cumulative Water Content and Modelled Upper Zone Storage SSAYJP 6 and RFF 1 (Conifer)

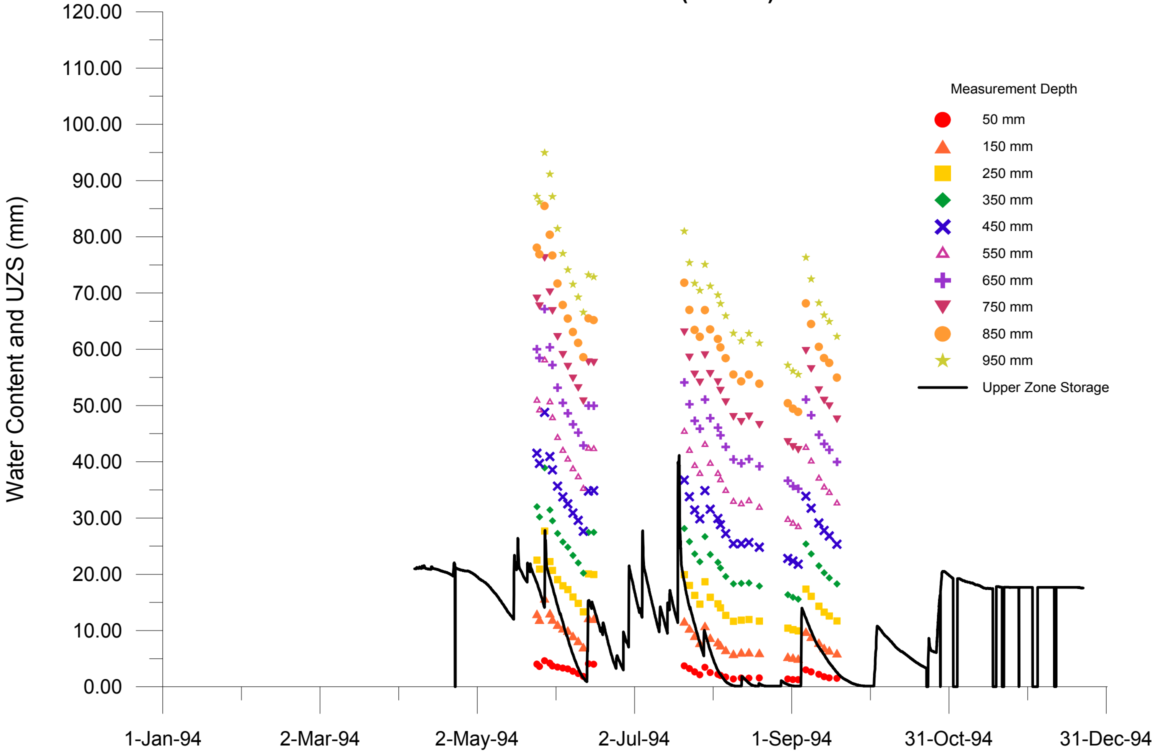

Figure C.45: BOREAS SSA Hydrographs

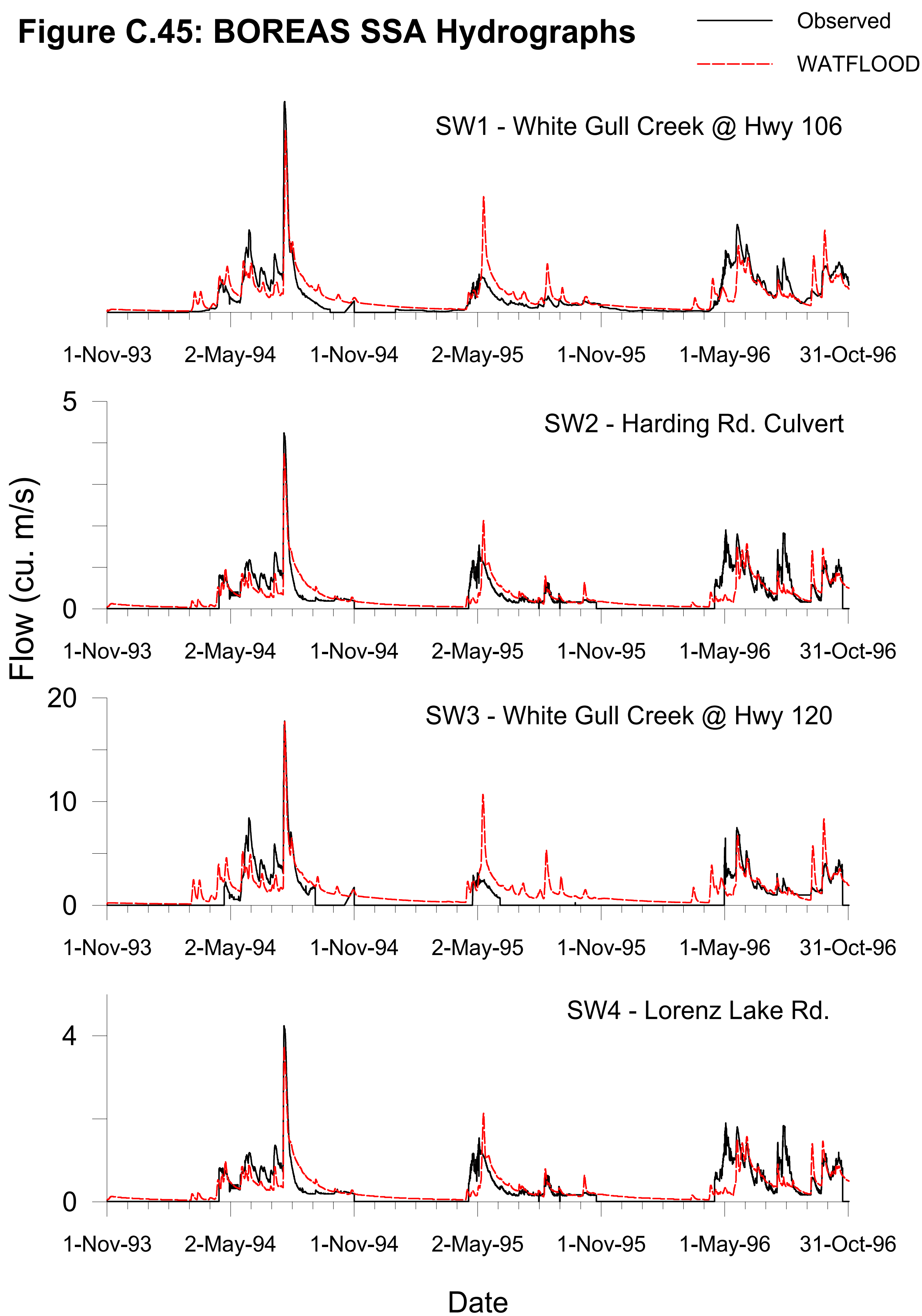

APPENDIX D

FIFE UZS Comparison Plots and Hydrographs

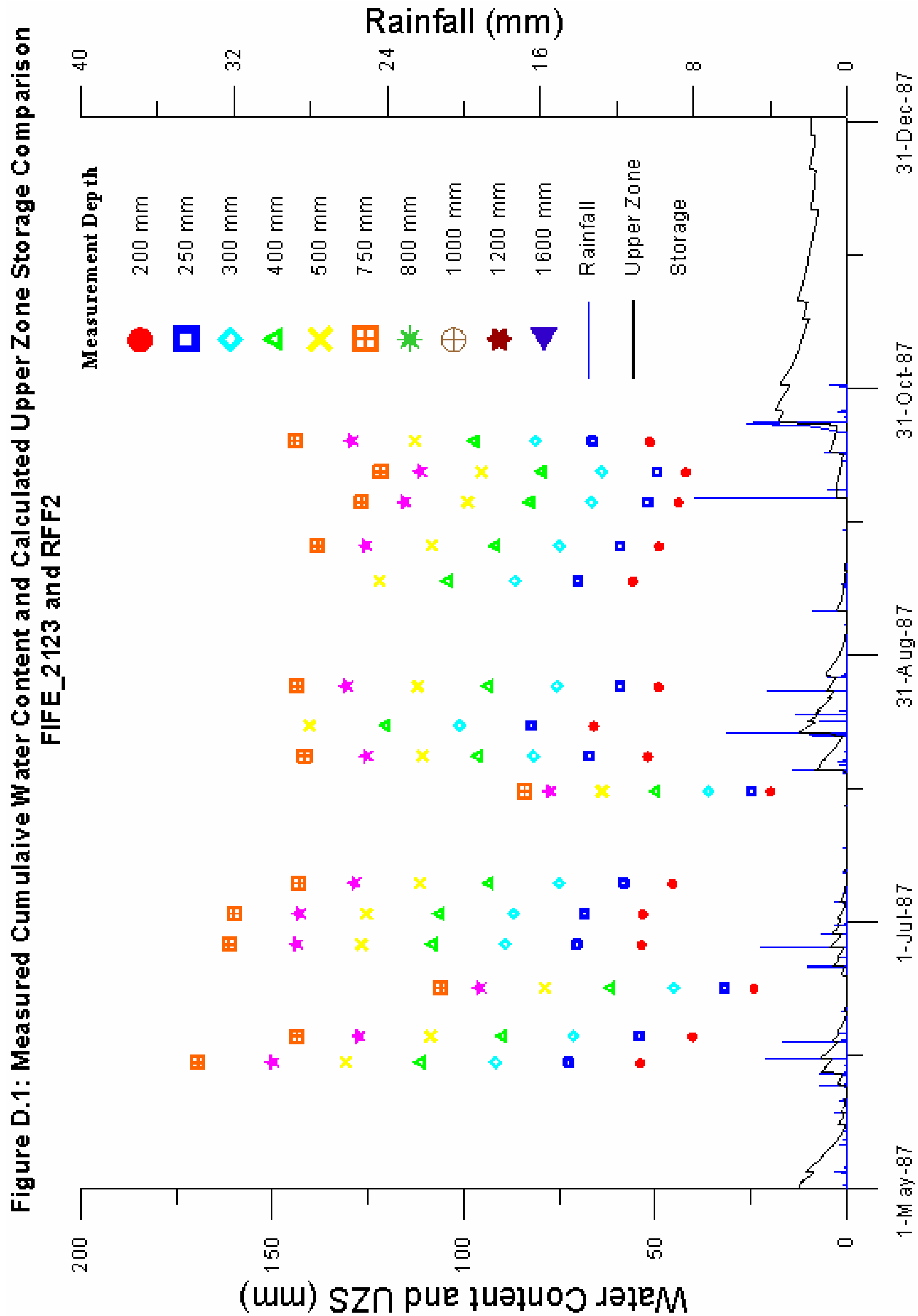

Figure D.1: Measured Cumulaive Water Content and Calculated Upper Zone Storage Comparison
FIFE_2123 and RFF2

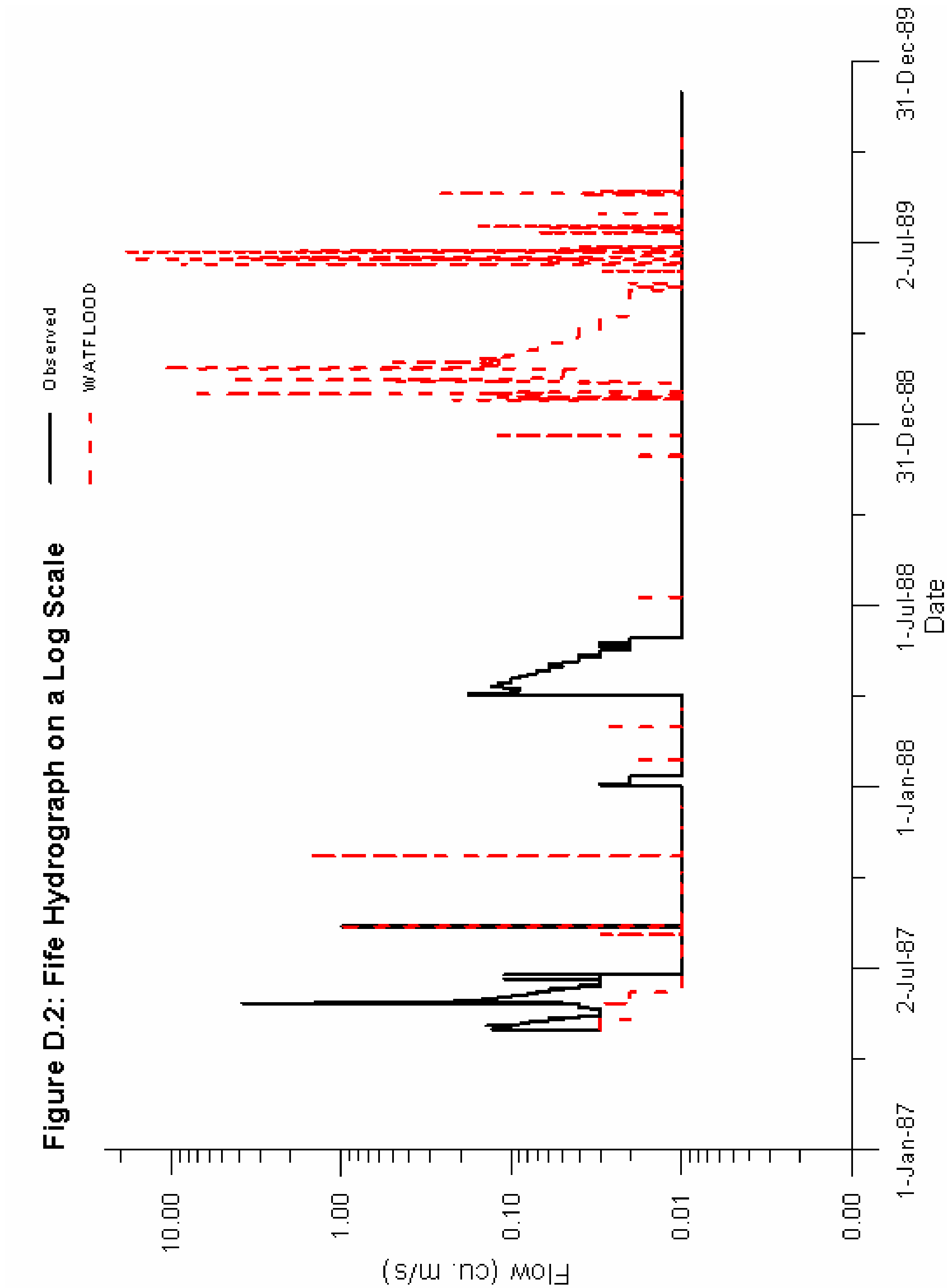
Figure D.2: Fife Hydrograph on a Log Scale
Observed
WATFLOOD
Flow (cu. m/s)
10.00
1.00
0.10
0.01
0.00
1-Jan-87
2-Jul-87
1-Jan-88
1-Jul-88
31-Dec-88
2-Jul-89
31-Dec-89
Date

APPENDIX E

Soil Moisture Content Range Plots for Active Upper Zone Estimation

Figure E.1: Soil Moisture Content Range
CLARO

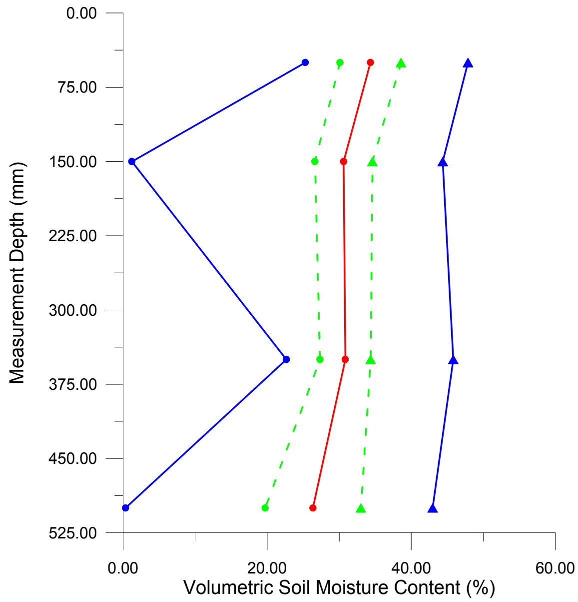

Figure E.2: Soil Moisture Content Range
TOWER

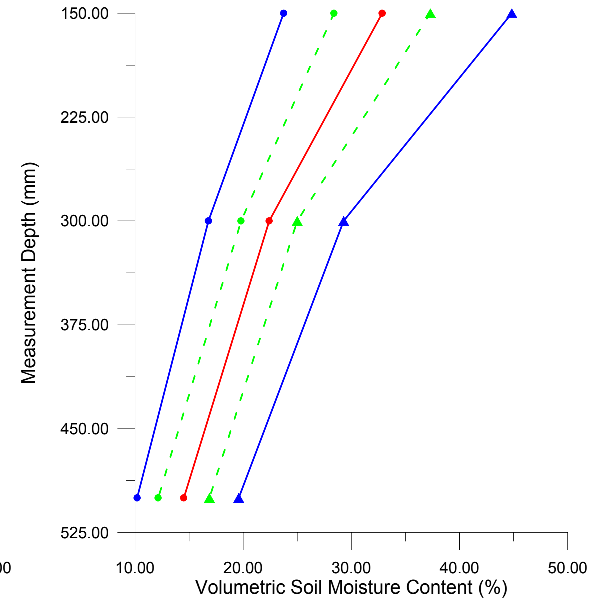

Figure E.3: Soil Moisture Content Range
BLENIO

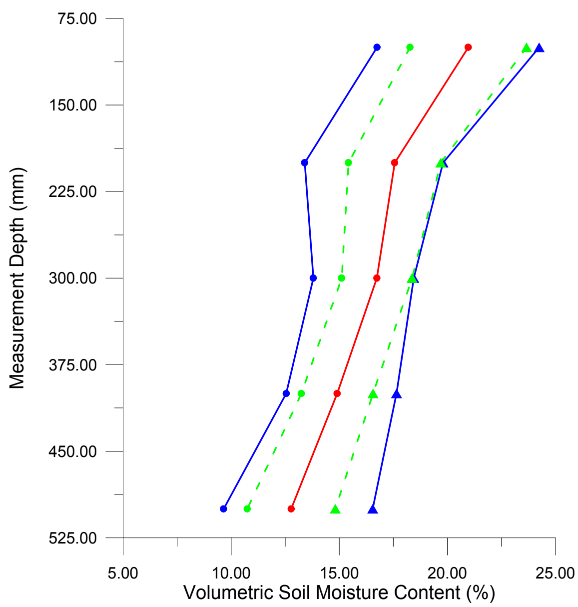

Figure E.4: Soil Moisture Content Range
VERZASCA

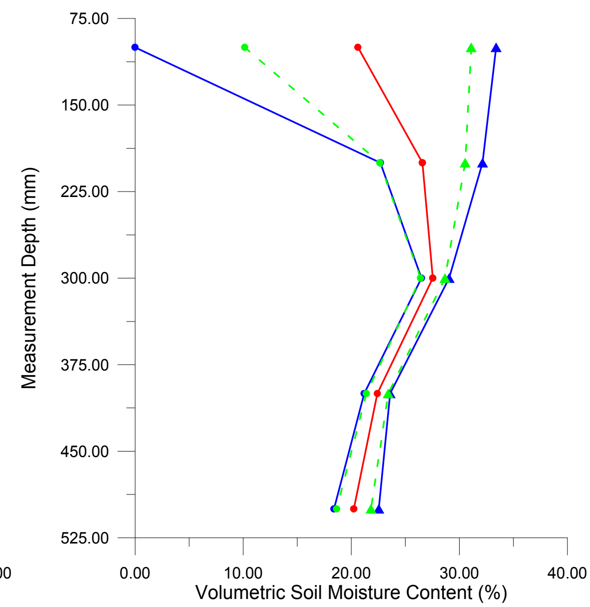

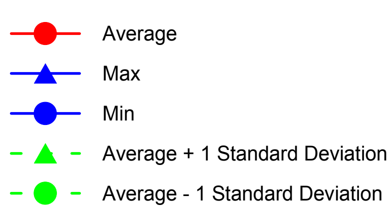

Figure E.5: Soil Moisture Content Range
MAGGIA

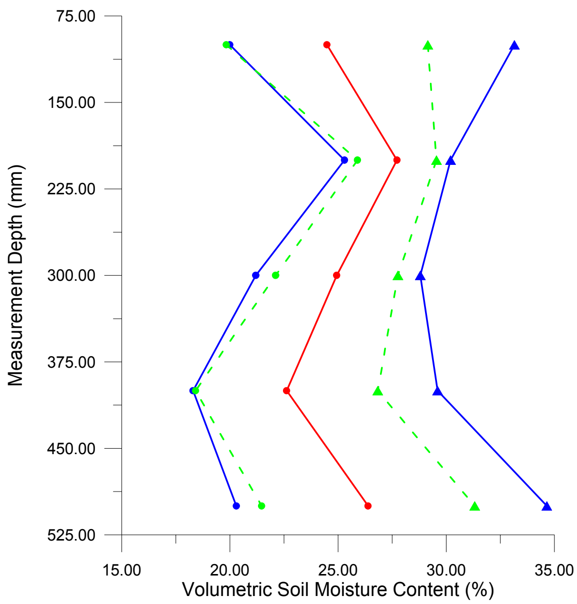

Figure E.6: Soil Moisture Content Range
NSAOBS 1

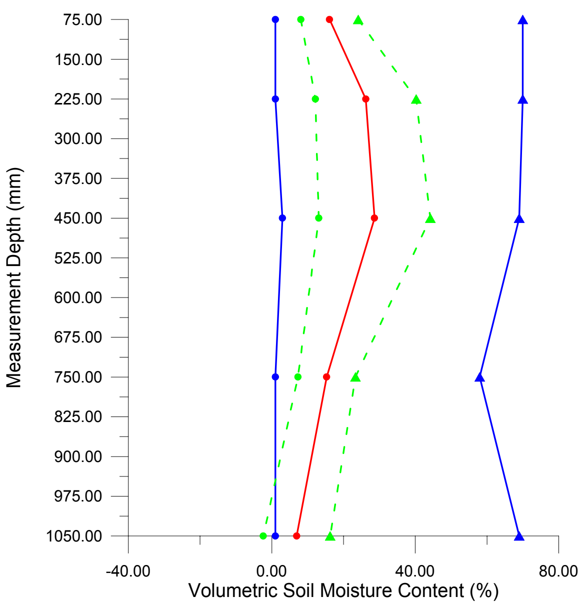

Figure E.7: Soil Moisture Content Range
NSAOBS 2

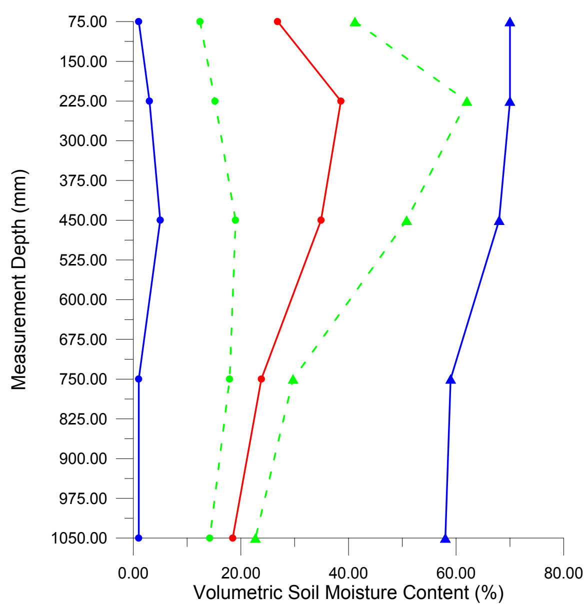

Figure E.8: Soil Moisture Content Range
NSAOBS 3

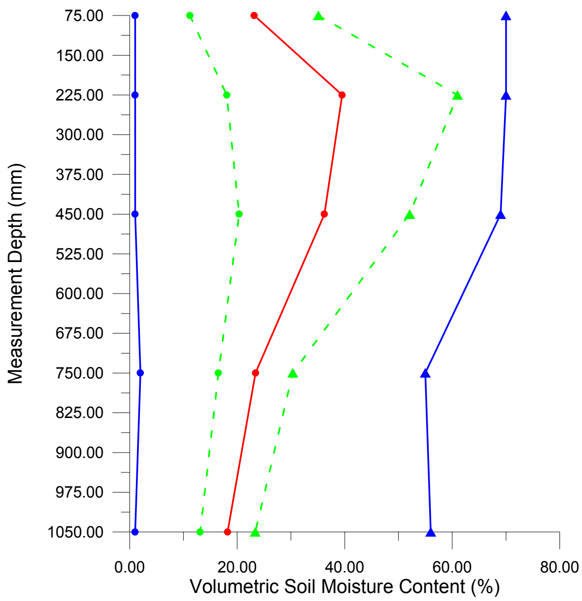

Figure E.9: Soil Moisture Content Range
NSAOBS 4

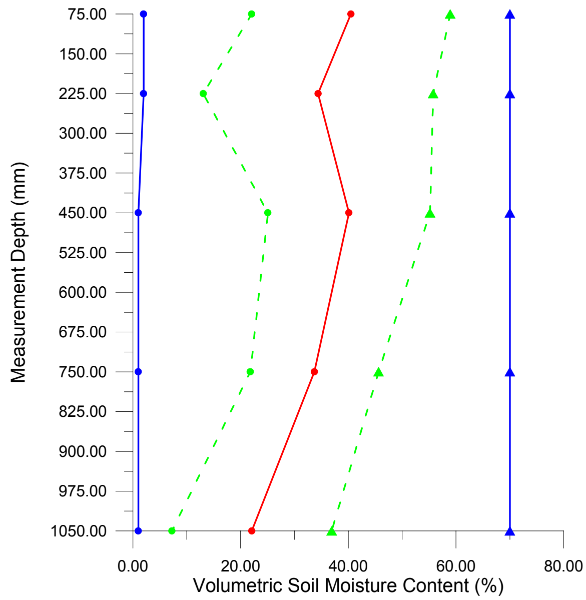

Figure E.10: Soil Moisture Content Range
NSAOBS 5

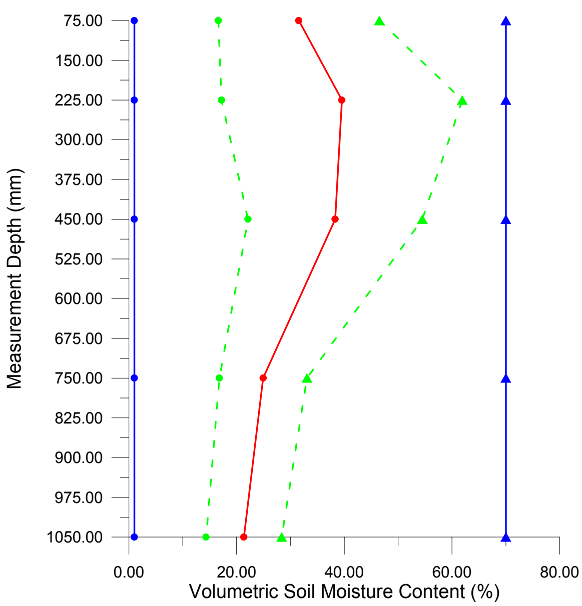

Figure E.11: Soil Moisture Content Range
NSAOBS 6

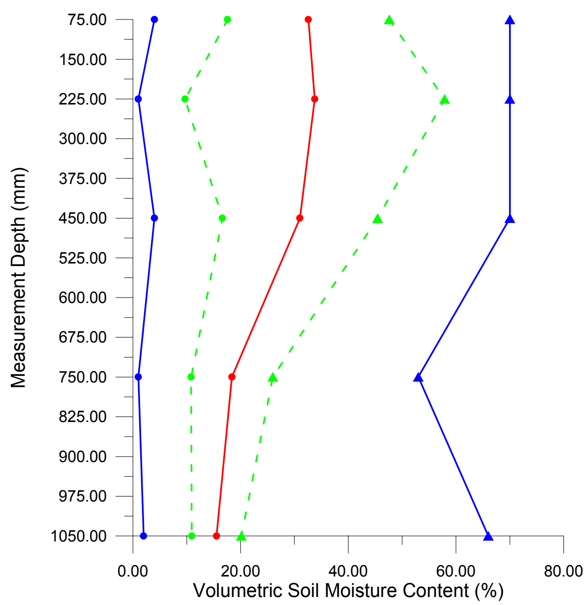

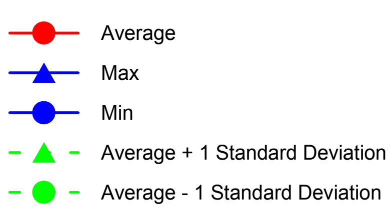

Figure E.12: Soil Moisture Content Range
NSAOBS 7

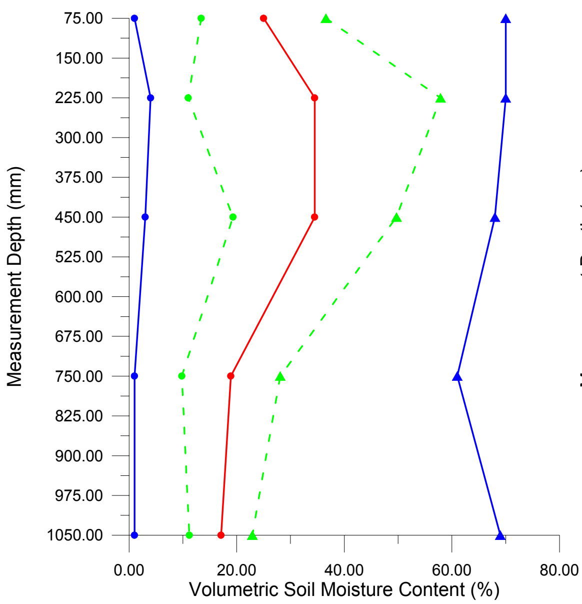

Figure E.13: Soil Moisture Content Range
NSAOBS 8

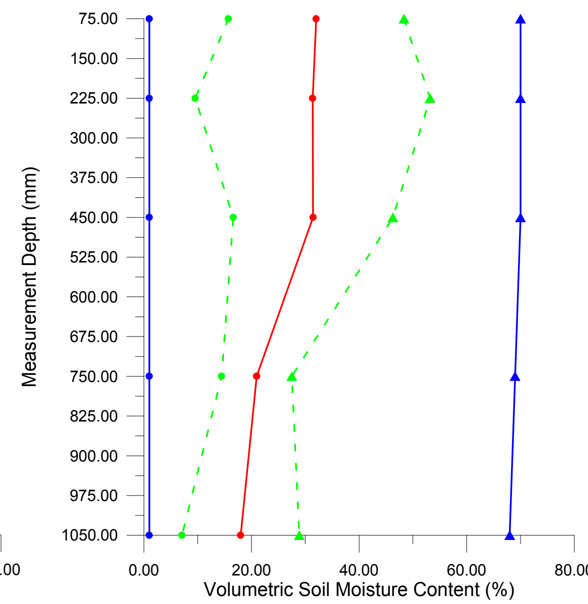

FigureE.14: Soil Moisture Content Range
NSAOJP 1

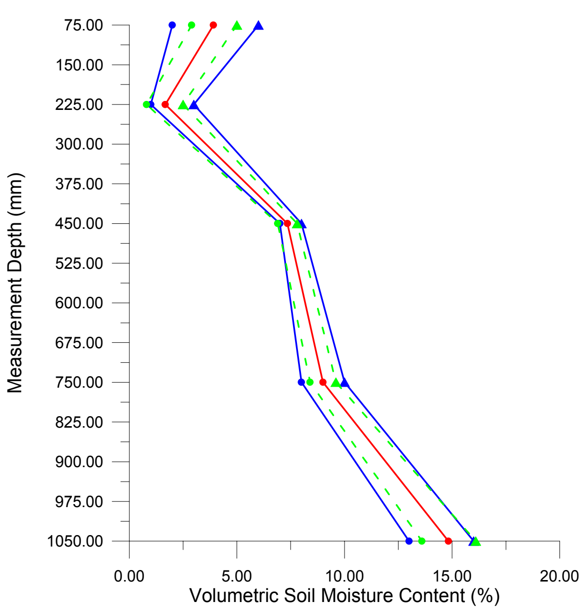

Figure E.15: Soil Moisture Content Range
NSAOJP 2

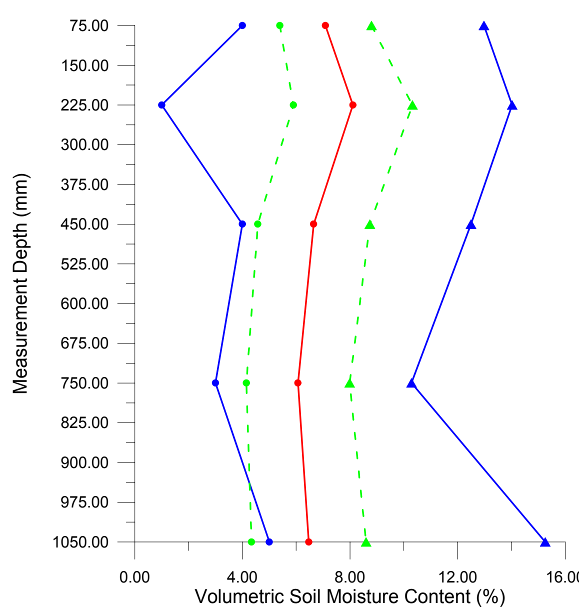

Figure E.16: Soil Moisture Content Range
NSAOJP 3

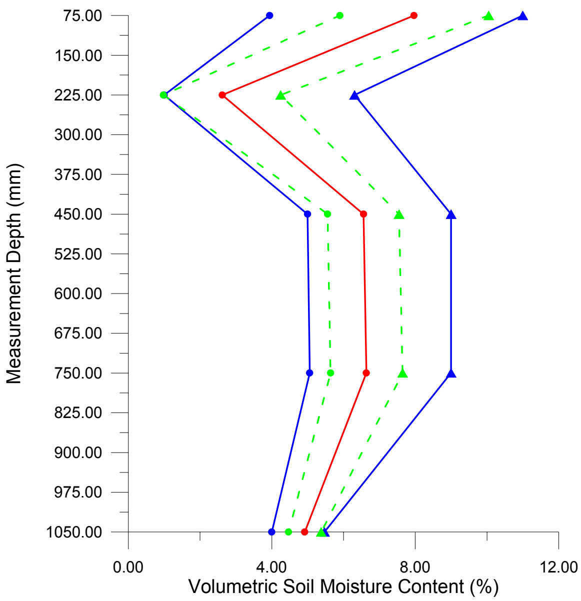

Figure E.17: Soil Moisture Content Range
NSAOJP 4

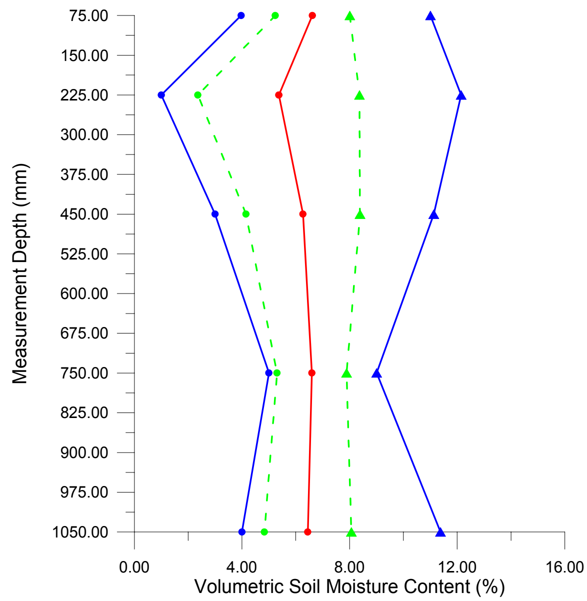

Figure E.18: Soil Moisture Content Range
NSAOJP 5

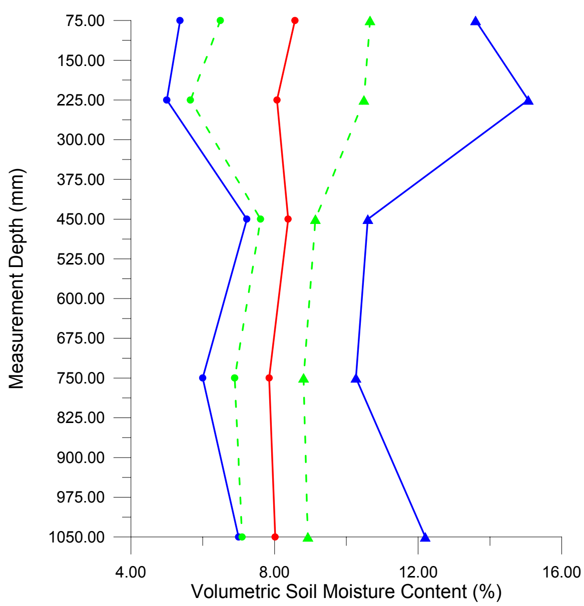

Figure E.19: Soil Moisture Content Range
NSAOJP 6

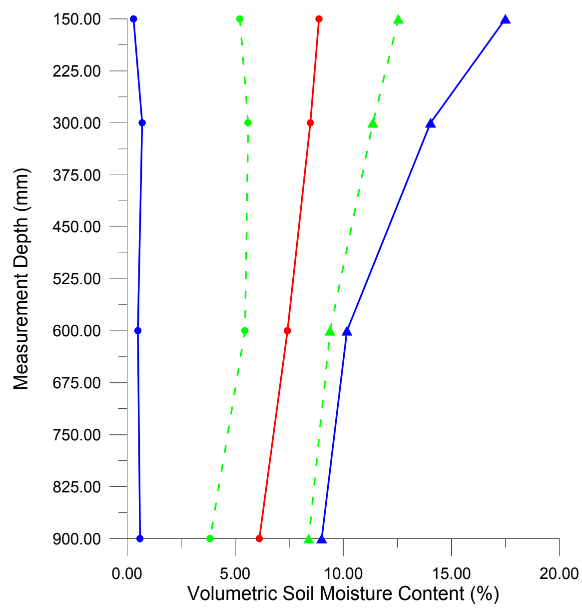

Figure E.20: Soil Moisture Content Range
NSAOJP 7

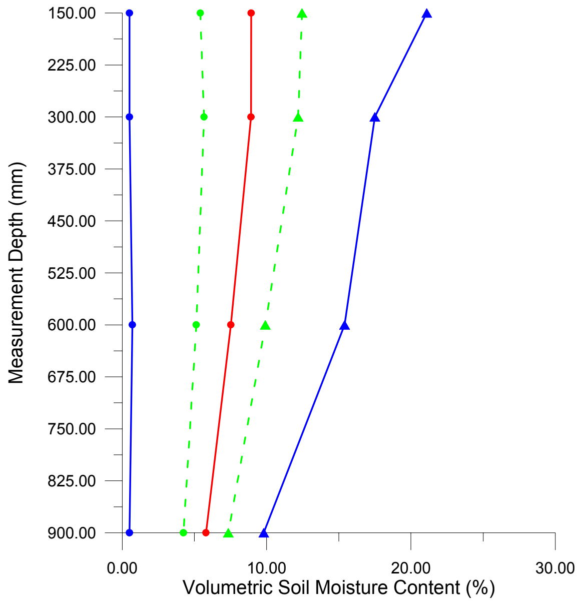

Figure E.21: Soil Moisture Content Range
NSAYJP 1

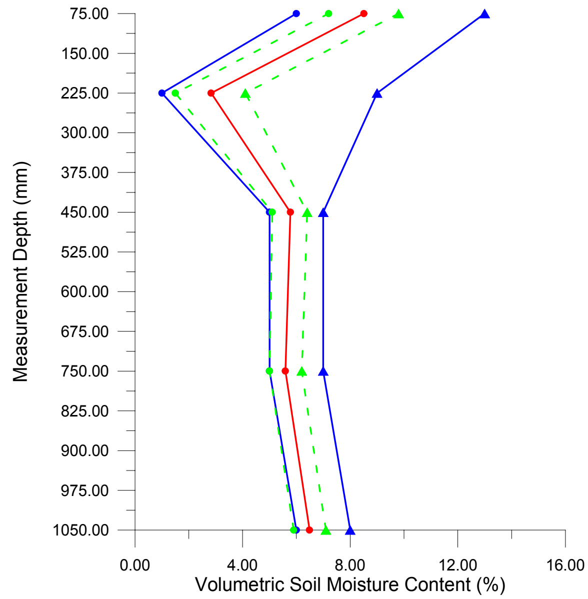

Figure E.22: Soil Moisture Content Range
NSAYJP 2

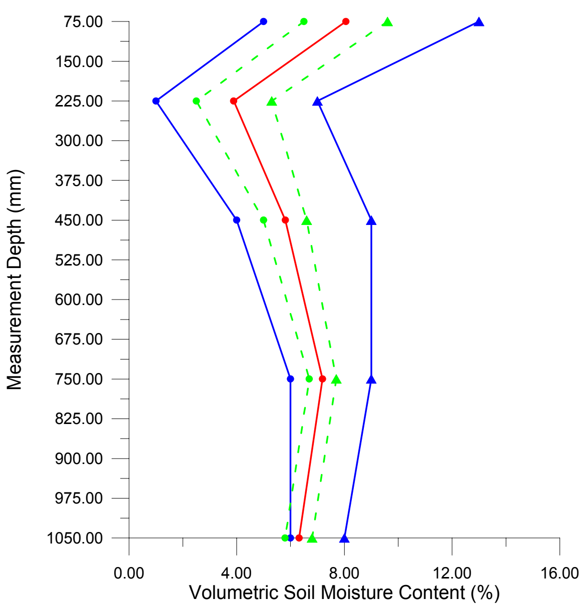

Figure E.23: Soil Moisture Content Range
NSAYJP 3

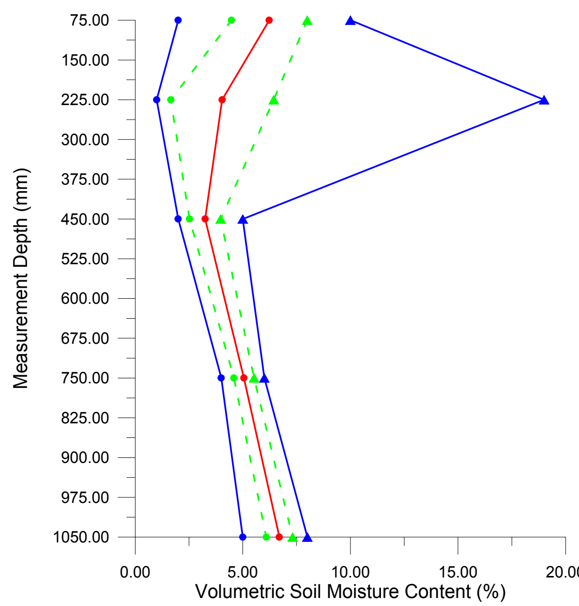

Figure E.24: Soil Moisture Content Range
NSAYJP 4

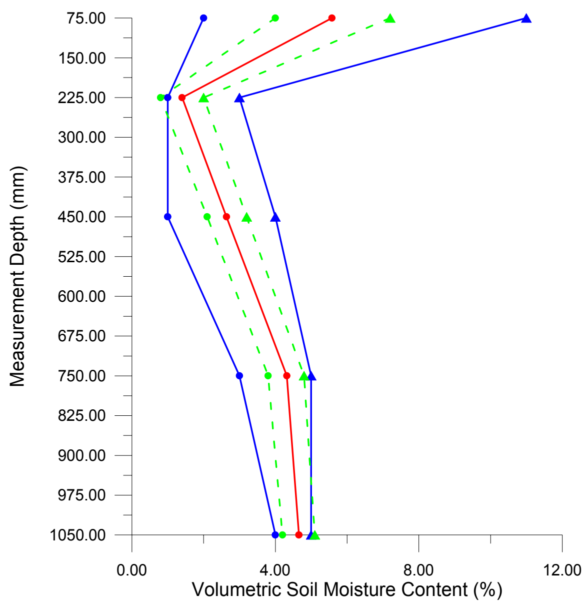

Figure E.25: Soil Moisture Content Range
NSAYJP 5

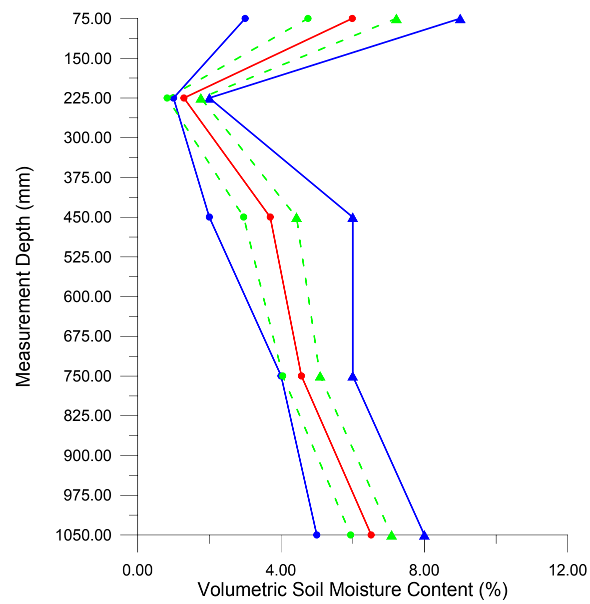

Figure E.26: Soil Moisture Content Range
NSAYJP 6

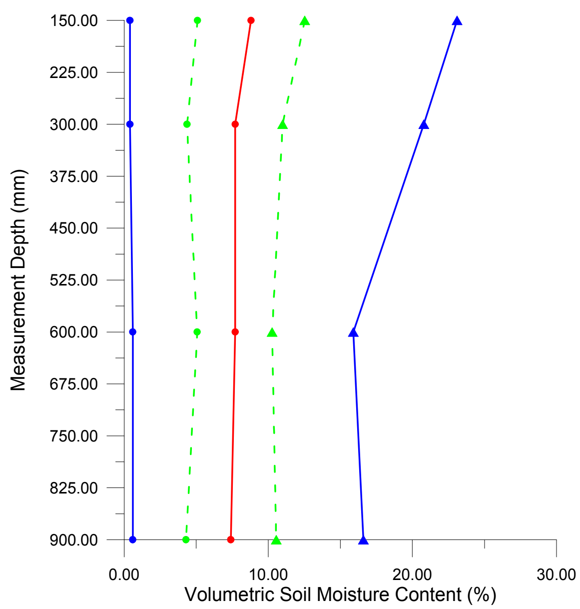

Figure E.27: Soil Moisture Content Range
NSAYJP 7

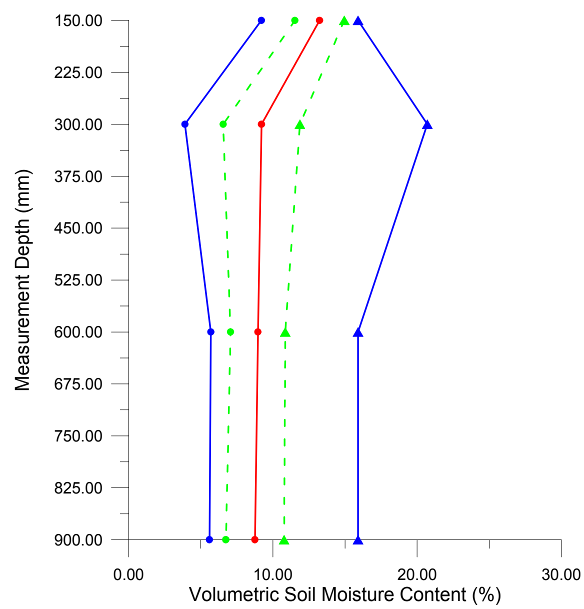

Figure E.28: Soil Moisture Content Range
SSAOBS 1_1

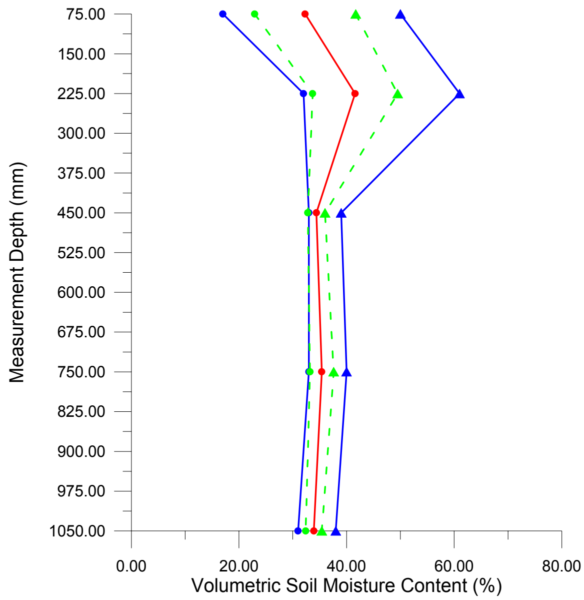

Figure E.29: Soil Moisture Content Range
SSAOBS 1_2

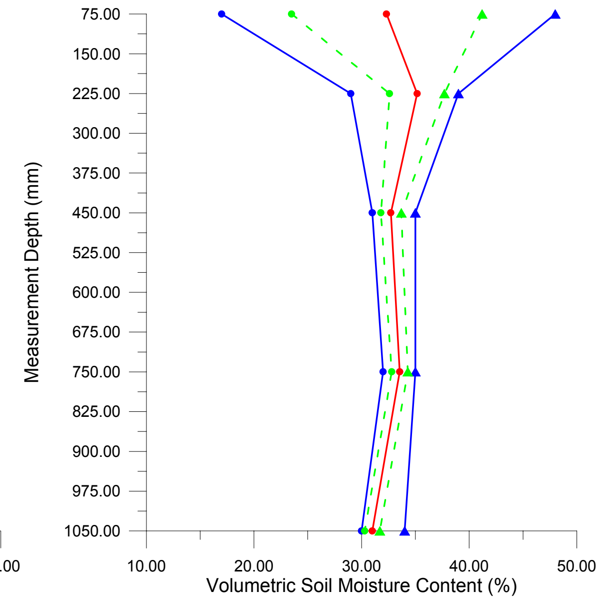

Figure E.30: Soil Moisture Content Range
SSAOBS 1_3

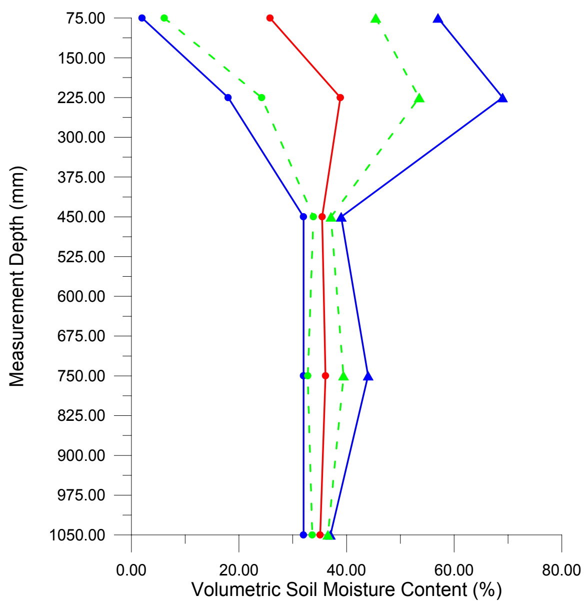

Figure E.31: Soil Moisture Content Range
SSAOBS 1_4

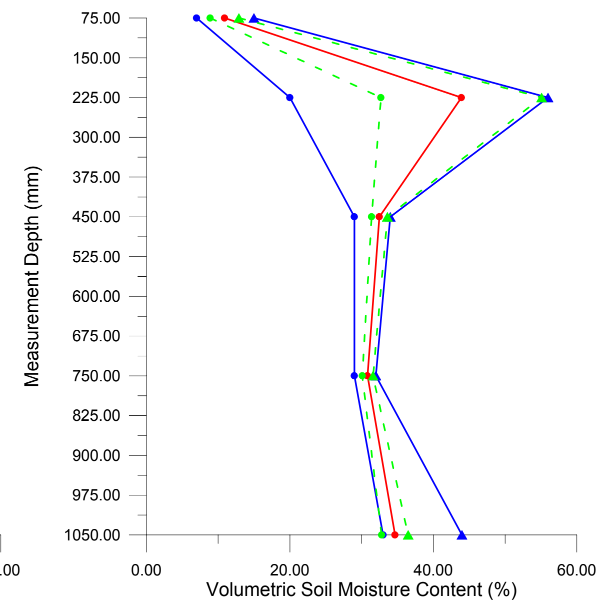

Figure E.32: Soil Moisture Content Range
SSAOBS 1_5

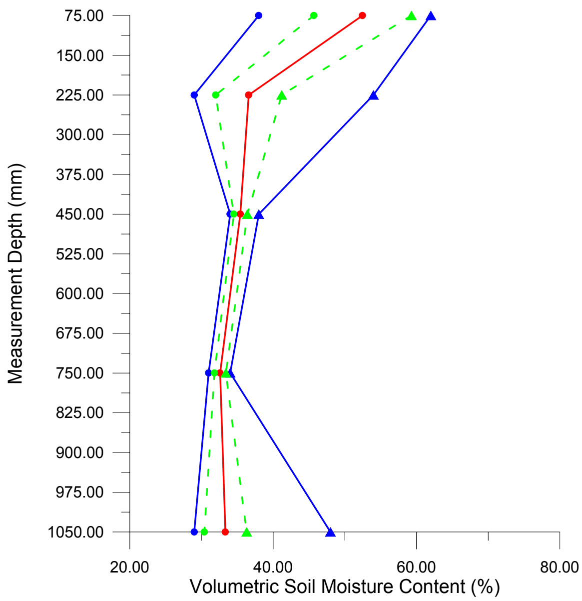

Figure E.33: Soil Moisture Content Range
SSAOBS 2_1

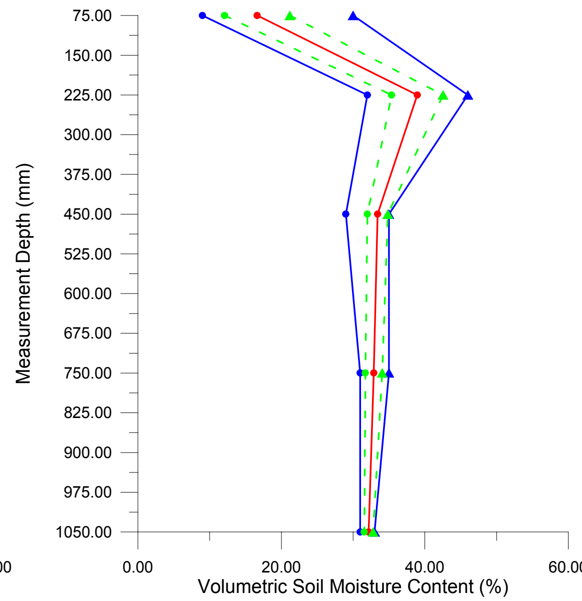

Figure E.34: Soil Moisture Content Range
SSAOBS 2_3

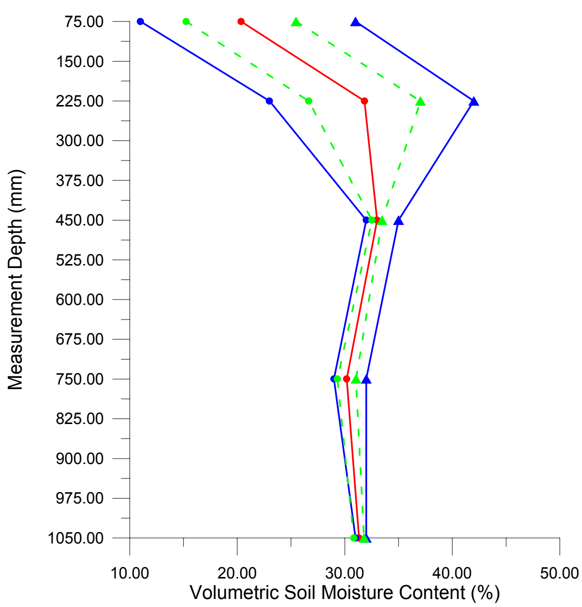

Figure E.35: Soil Moisture Content Range
SSAOBS 2_4

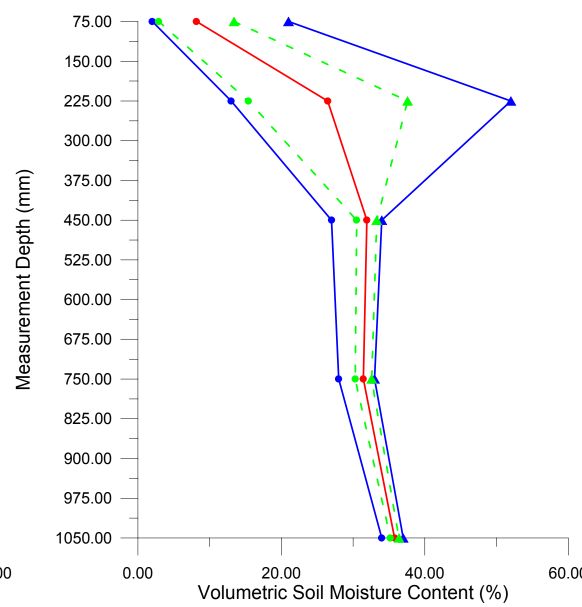

Figure E.36: Soil Moisture Content Range
SSAOBS 2_5

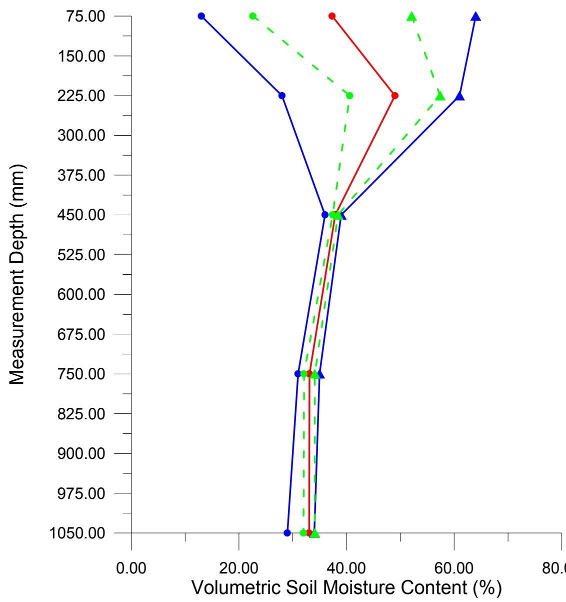

Figure E.37: Soil Moisture Content Range
SSAOJP 1

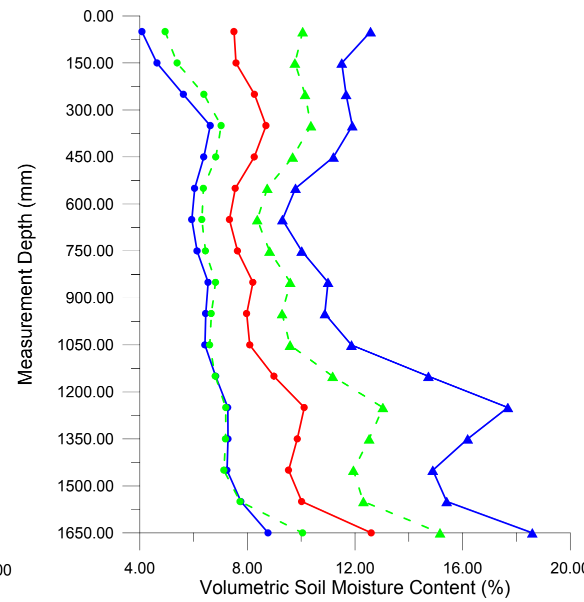

Figure E.38: Soil Moisture Content Range
SSAOJP 2

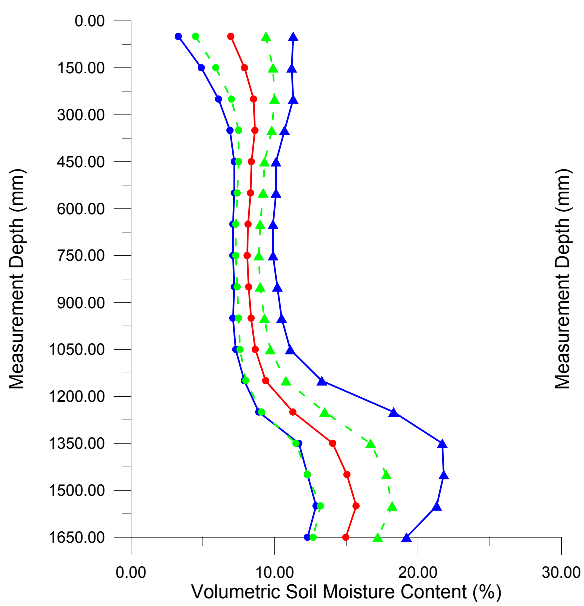

Figure E.39: Soil Moisture Content Range
SSAOJP 3

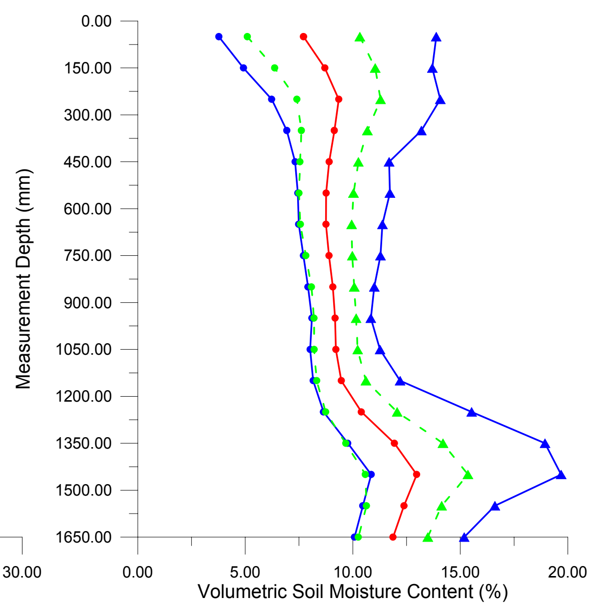

Figure E.40: Soil Moisture Content Range
SSAOJP 4

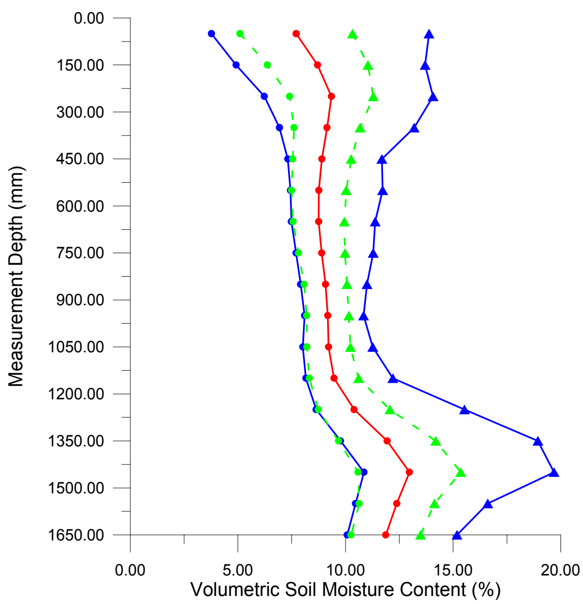

Figure E.41: Soil Moisture Content Range
SSAOJP 5

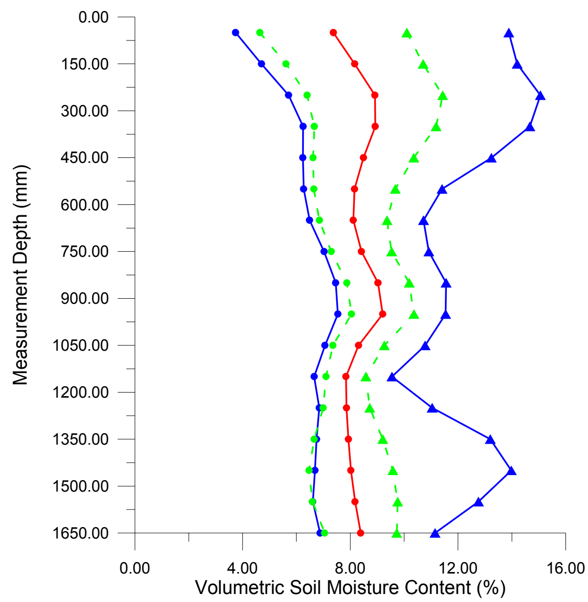

Figure E.42: Soil Moisture Content Range
SSAYJP 1

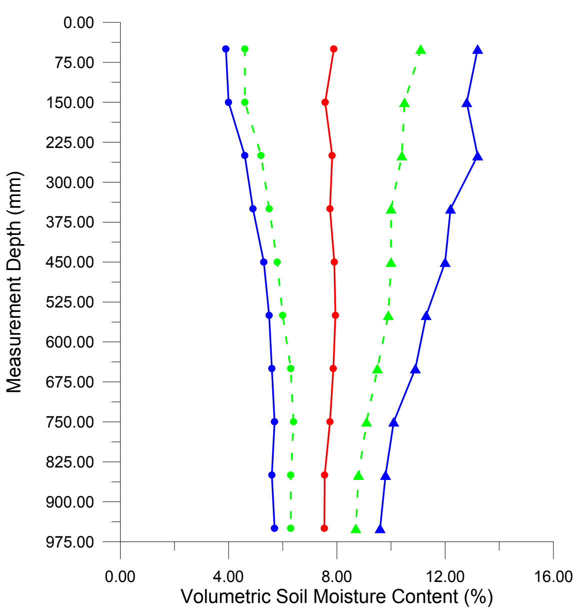

Figure E.43: Soil Moisture Content Range
SSAYJP 2

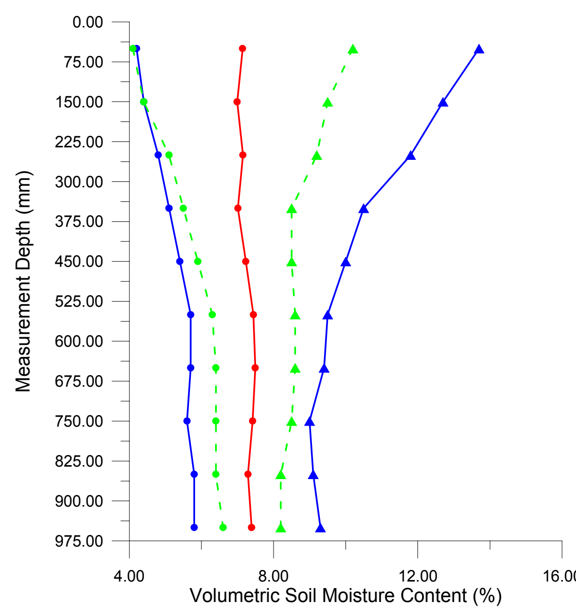

Figure E.44: Soil Moisture Content Range
SSAYJP 3

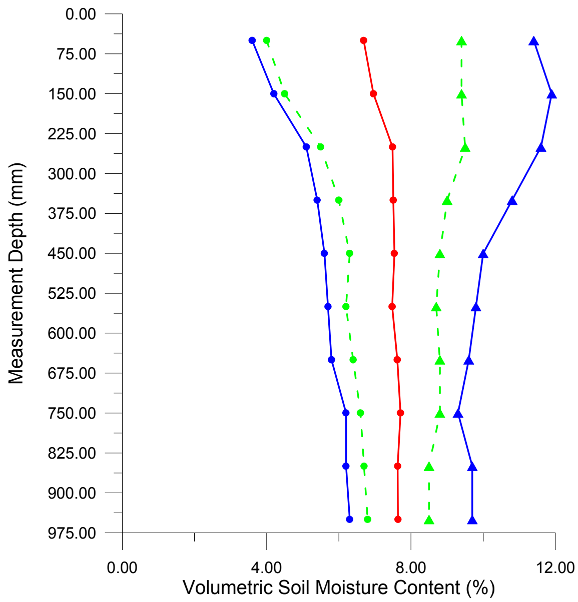

Figure E.45: Soil Moisture Content Range
SSAYJP 4

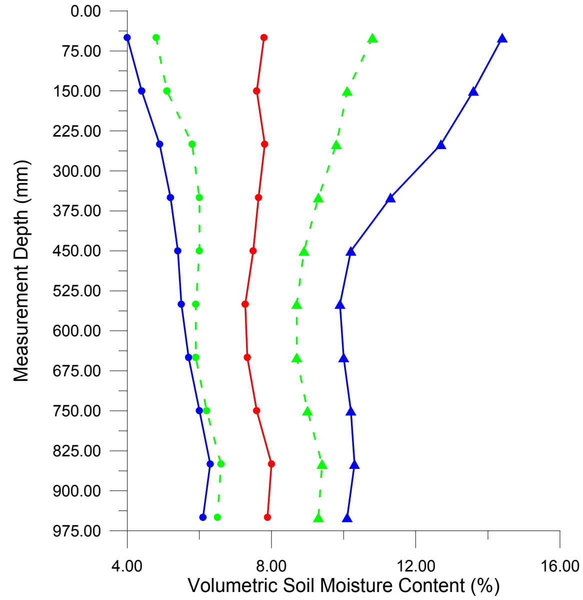

Figure E.46: Soil Moisture Content Range
SSAYJP 5

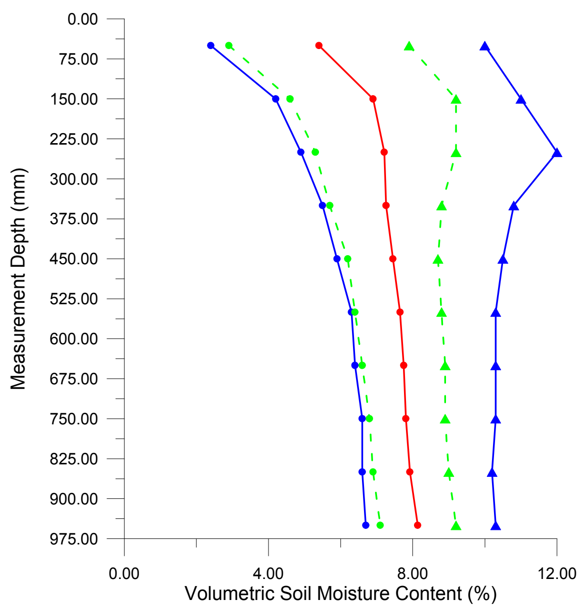

Figure E.47: Soil Moisture Content Range
SSAYJP 6